POLITECHNIKA GDAŃSKA

Imię i nazwisko autora rozprawy: Joanna Sypniewska
Dyscyplina naukowa: inżynieria materiałowa

ROZPRAWA DOKTORSKA

Tytuł rozprawy w języku polskim: Wpływ obróbki laserowej biostopów tytanu i zastosowanie dodatków na wybrane właściwości funkcjonalne

Tytuł rozprawy w języku angielskim: Influence of laser machining of titanium bioalloys and the use of additives on some functional properties

Promotor *podpis*	Drugi promotor Nie dotyczy *podpis*
Prof.dr hab. inż. Marek Szkdodo	<Tytuł, stopień, imię i nazwisko>
Promotor pomocniczy *podpis*	Kopromotor Nie dotyczy *podpis*
Dr inż. Beata Majkowska Marzec	<Tytuł, stopień, imię i nazwisko>

Gdańsk, rok 2025

POLITECHNIKA GDAŃSKA

OŚWIADCZENIE

Autor rozprawy doktorskiej: Joanna Sypniewska

Ja, niżej podpisany(a), oświadczam, iż jestem świadomy(a), że zgodnie z przepisem art. 27 ust. 1 i 2 ustawy z dnia 4 lutego 1994 r. o prawie autorskim i prawach pokrewnych (t.j. Dz.U. z 2021 poz. 1062), uczelnia może korzystać z mojej rozprawy doktorskiej zatytułowanej:
Wpływ obróbki laserowej biostopów tytanu i zastosowanie dodatków na wybrane właściwości funkcjonalne

do prowadzenia badań naukowych lub w celach dydaktycznych.[1]

Świadomy(a) odpowiedzialności karnej z tytułu naruszenia przepisów ustawy z dnia 4 lutego 1994 r. o prawie autorskim i prawach pokrewnych i konsekwencji dyscyplinarnych określonych w ustawie Prawo o szkolnictwie wyższym i nauce (Dz.U.2021.478 t.j.), a także odpowiedzialności cywilno- prawnej oświadczam, że przedkładana rozprawa doktorska została napisana przeze mnie samodzielnie.

Oświadczam, że treść rozprawy opracowana została na podstawie wyników badań prowadzonych pod kierunkiem i w ścisłej współpracy z promotorem prof. dr hab. inż. Marek Szkodo, promotorem pomocniczym dr inż. Beata Majkowska-Marzec.

Niniejsza rozprawa doktorska nie była wcześniej podstawą żadnej innej urzędowej procedury związanej z nadaniem stopnia doktora.

Wszystkie informacje umieszczone w ww. rozprawie uzyskane ze źródeł pisanych i elektronicznych, zostały udokumentowane w wykazie literatury odpowiednimi odnośnikami, zgodnie z przepisem art. 34 ustawy o prawie autorskim i prawach pokrewnych.

Potwierdzam zgodność niniejszej wersji pracy doktorskiej z załączoną wersją elektroniczną.

Gdańsk, dnia ....

podpis doktoranta

Ja, niżej podpisany(a), nie wyrażam zgody na umieszczenie ww. rozprawy doktorskiej w wersji elektronicznej w otwartym, cyfrowym repozytorium instytucjonalnym Politechniki Gdańskiej

Gdańsk, dnia ....

podpis doktoranta

[1] Art. 27. 1. Instytucje oświatowe oraz podmioty, o których mowa w art. 7 ust. 1 pkt 1, 2 i 4–8 ustawy z dnia 20 lipca 2018 r. – Prawo o szkolnictwie wyższym i nauce, mogą na potrzeby zilustrowania treści przekazywanych w celach dydaktycznych lub w celu prowadzenia działalności naukowej korzystać z rozpowszechnionych utworów w oryginale i w tłumaczeniu oraz zwielokrotniać w tym celu rozpowszechnione drobne utwory lub fragmenty większych utworów.
2. W przypadku publicznego udostępniania utworów w taki sposób, aby każdy mógł mieć do nich dostęp w miejscu i czasie przez siebie wybranym korzystanie, o którym mowa w ust. 1, jest dozwolone wyłącznie dla ograniczonego kręgu osób uczących się, nauczających lub prowadzących badania naukowe, zidentyfikowanych przez podmioty wymienione w ust.1.

OPIS ROZPRAWY DOKTORSKIEJ

Autor rozprawy doktorskiej: Joanna Sypniewska

Tytuł rozprawy doktorskiej w języku polskim: Wpływ obróbki laserowej biostopów tytanu i zastosowanie dodatków na wybrane właściwości funkcjonalne

Tytuł rozprawy w języku angielskim: Influence of laser machining of titanium bioalloys and the use of additives on some functional properties

Język rozprawy doktorskiej: polski

Promotor rozprawy doktorskiej: prof. dr hab. inż. Marek Szkodo

Promotor pomocniczy rozprawy doktorskiej: dr inż. Beata Majkowska-Marzec

Data obrony: -

Słowa kluczowe rozprawy doktorskiej w języku polskim: stopy tytanu, warstwy ceramiczne, modyfikacja laserowa, micro-arc oxidation, mikrostruktura, topografia powierzchni, badania biologiczne

Słowa kluczowe rozprawy doktorskiej w języku angielskim: titanium alloys, ceramic coatings, laser modification, micro-arc oxidation, microstructure, surface topography, biological studies

Streszczenie rozprawy w języku polskim: Celem rozprawy była ocena wpływu hybrydowej modyfikacji powierzchni biostopów tytanu (Ti13Nb13Zr i Ti6Al4V), łączącej obróbkę laserową Nd:YAG oraz mikrołukowe utlenianie (MAO), na ich wybrane właściwości funkcjonalne. Przeprowadzono badania morfologii, mikrostruktury, składu chemicznego, odporności korozyjnej oraz właściwości biologicznych w kontekście zastosowań implantologicznych. W pracy zaprojektowano nowe układy elektrolitów zawierające jony wapnia, sodu i cynku oraz cząsteczki hydroksyapatytu, umożliwiające inkorporację bioaktywnych dodatków do warstw ceramicznych. Wykazano, że modyfikacja hybrydowa poprawia odporność na korozję, zwiększa biozgodność i sprzyja osteointegracji. Stwierdzono, że odpowiednio dobrane parametry procesów prowadzą do uzyskania powierzchni o korzystnych właściwościach fizykochemicznych i biologicznych. Wyniki badań potwierdzają zasadność zastosowania kombinacji laser–MAO jako efektywnej techniki inżynierii powierzchniowej biomateriałów tytanowych. Proponowana metoda może przyczynić się do rozwoju nowoczesnych implantów o zwiększonej trwałości i lepszej

integracji z tkanką kostną.

Streszczenie rozprawy w języku angielskim: The dissertation aimed to evaluate the effect of hybrid surface modification of titanium bioalloys (Ti13Nb13Zr and Ti6Al4V), combining Nd:YAG laser treatment and micro-arc oxidation (MAO), on their selected functional properties. The research included analyses of morphology, microstructure, chemical composition, corrosion resistance, and biological properties in the context of implantology applications. Novel electrolyte systems were designed, containing calcium, sodium, and zinc ions as well as hydroxyapatite, enabling the incorporation of bioactive additives into the ceramic coatings. It was demonstrated that the hybrid modification enhances corrosion resistance, increases biocompatibility, and supports osseointegration. The results showed that properly selected process parameters lead to surfaces with favorable physicochemical and biological characteristics. The findings confirm the relevance of applying the laser–MAO combination as an effective surface engineering technique for titanium biomaterials. The proposed method may contribute to the development of modern implants with improved durability and enhanced integration with bone tissue.

ROZPRAWA DOKTORSKA

Wpływ obróbki laserowej biostopów tytanu i zastosowanie dodatków na wybrane właściwości funkcjonalne

mgr inż. Joanna Sypniewska

Promotor: prof. dr hab. inż. Marek Szkodo

Promotor pomocniczy: dr inż. Beata Majkowska-Marzec

Gdańsk, 2025

Podziękowania

Dziękuje Profesorowi dr hab. inż. Markowi Szkodo – mojemu Promotorowi – za opiekę naukową, wsparcie merytoryczne i cenne wskazówki.

Wyrazy wdzięczności kieruję również do dr inż. Beaty Majkowskiej-Marzec, Promotor pomocniczej, za zaangażowanie, dostępność i pomoc zarówno podczas badań, jak i prac nad publikacjami.

Dziękuję koleżankom i kolegom z Instytutu Technologii Maszyn i Materiałów, Wydziału Inżynierii Mechanicznej i Okrętownictwa Politechniki Gdańskiej za współpracę, pomoc w laboratorium i życzliwą atmosferę, która towarzyszyła mi na co dzień.

Ogromne podziękowania chciałabym złożyć Juan Pablo Hernán Fernández za pomoc podczas wykonywania badań i wsparcie merytoryczne przy realizacji publikacji naukowych.

Szczególne podziękowania kieruję do moich Rodziców za ich nieustające wsparcie, cierpliwość i wiarę w moje możliwości.

Dziękuję również bliskim znajomym za motywację, zrozumienie i obecność w trudnych momentach – Wasze wsparcie miało dla mnie ogromne znaczenie.

Przygotowana rozprawa doktorska stanowi przewodnik po artykułach naukowych w ramach jednotematycznego cyklu publikacji.

Spis treści

WYKAZ NAJWAŻNIEJSZYCH OZNACZEŃ I SKRÓTÓW

AFM – mikroskopia sił atomowych (ang. *atomic force microscopy*)

ANOVA – analiza wariancji (ang. *Analysis of Variance*)

DC – prąd stały, zasilanie (ang. *direct current*)

E – moduł Younga, [GPa]

E_{corr} – potencjał korozyjny, [V]

EDX – spektroskopia rentgenowska z dyspersją energii (ang. *energy dispersive X-ray spectroscopy*)

EIS – elektrochemiczna spektroskopia impedancyjna (ang. *electrochemical impedance spectroscopy*)

FTIR – spektroskopia w podczerwieni z transformacją Fouriera (ang. *Fourier-transform infrared spectroscopy*)

H – twardość, [GPa]

j_{corr} – gęstość prądu korozyjnego, [A/cm^2]

Lc – siła krytyczna, [N]

Lf – krytyczna siła tarcia, [N]

MAO – mikrołukowe utlenianie (ang. *micro-arc oxidation*)

Nd:YAG – laser neodymowo-jagowy (ang. *Neodymium-doped Yttrium Aluminum Garnet laser*)

OCP – potencjał obwodu otwartego (ang. *open circuit potential*), [V]

PBS – roztwór buforowy fosforanowy (ang. *phosphate-buffered saline*)

PEO – plazmowe ultenianie elektrolityczne (*ang. plasma electrolitic oxidation*)

Ra – średnia chropowatość (ang. *roughness average*) [µm]

Rp – maksymalna wysokość profilu (ang. *maximum profile peak height*) [µm]

Sa – średnie arytmetyczne odchylenie chropowatości, (ang. *Arithmetical mean height)* [µm]

SBF – roztwór symulujący płyny ustrojowe człowieka (ang. *simulated body fluid*)

SEM – skaningowa mikroskopia elektronowa (ang. *scanning electron microscopy*)

Wt – całkowita falistość (ang. *total waviness)* [μm]

XRD – dyfrakcja rentgenowska (ang. *X-ray diffraction*)

θ – kąt zwilżania [°]

STRESZCZENIE I SŁOWA KLUCZOWE

Rozprawa doktorska poświęcona została opracowaniu oraz ocenie skuteczności hybrydowej modyfikacji powierzchniowej biostopów tytanu, ze szczególnym uwzględnieniem wpływu obróbki laserowej oraz techniki mikrołukowego utleniania (MAO) na właściwości funkcjonalne materiałów implantacyjnych. Praca koncentruje się na dwóch stopach: nowoczesnym Ti13Nb13Zr oraz szeroko stosowanym komercyjnie Ti6Al4V.

Podstawą pracy jest rosnące zapotrzebowanie na nowoczesne, trwałe i biozgodne implanty ortopedyczne oraz stomatologiczne. Współczesna implantologia wymaga materiałów, które nie tylko wykazują odpowiednią wytrzymałość mechaniczną i odporność korozyjną, ale również wspierają procesy osteointegracji i ograniczają ryzyko reakcji zapalnych. Tytan i jego stopy, choć powszechnie stosowane, mają ograniczoną odporność na ścieranie i korozję w agresywnym środowisku fizjologicznym. Wobec tego opracowanie skutecznych metod inżynierii powierzchni nabiera kluczowego znaczenia.

W rozprawie zaproponowano hybrydową metodę modyfikacji powierzchni, polegającą na wstępnej obróbce laserowej z użyciem lasera Nd:YAG oraz następczym wytwarzaniu ceramicznych warstw tlenkowych w procesie MAO. Modyfikacja laserowa umożliwia kontrolowane przetapianie powierzchni, poprawiając jej topografię, morfologię i właściwości mechaniczne. Z kolei proces MAO pozwala na uzyskanie porowatych, biozgodnych warstw ceramicznych, które można wzbogacić o bioaktywne jony takie jak Ca^{2+}, Na^{+}, Zn^{2+} oraz cząsteczki hydroksyapatytu.

W ramach badań przeprowadzono analizę wpływu różnych kombinacji parametrów modyfikacji (kolejność procesów, skład elektrolitów, moc lasera) na strukturę, topografię i właściwości chemiczne uzyskanych powierzchni. Szczególny nacisk położono na ocenę odporności korozyjnej (OCP, EIS), właściwości biologicznych (zwilżalność, testy z komórkami śródbłonka) oraz charakterystyki powierzchni (SEM, EDS, XRD, FTIR, XPS).

Wyniki potwierdziły, że zastosowanie modyfikacji hybrydowej prowadzi do znacznego polepszenia właściwości użytkowych biostopów tytanu. Uzyskane warstwy wykazywały wysoką jednorodność, dużą porowatość korzystną dla adhezji komórek, a także lepszą odporność korozyjną w porównaniu z próbkami modyfikowanymi pojedynczo. Wykazano, że odpowiednio dobrany skład elektrolitu umożliwia kontrolowane wprowadzenie bioaktywnych jonów, co bezpośrednio przekłada się na

poprawę biozgodności i potencjał osteointegracyjny materiału.

Przeprowadzone badania dowodzą, że technika laser–MAO stanowi obiecującą metodę modyfikacji powierzchniowej biomateriałów tytanowych i może być z powodzeniem zastosowana w projektowaniu nowej generacji implantów o zwiększonej trwałości, odporności biologicznej i funkcjonalnej personalizacji powierzchni.

Słowa kluczowe: stopy tytanu, warstwy ceramiczne, modyfikacja laserowa, utlenianie mikrołukowe, mikrostruktura, topografia powierzchni, badania biologiczne

ABSTRACT AND KEYWORDS

This doctoral dissertation focuses on the development and evaluation of a hybrid surface modification method for titanium bioalloys, specifically examining the effects of laser treatment and micro-arc oxidation (MAO) on selected functional properties of implant materials. The study involves two titanium alloys: the modern Ti13Nb13Zr and the widely used commercial Ti6Al4V.

The research is motivated by the growing demand for advanced, durable, and biocompatible orthopedic and dental implants. Modern implantology requires materials that offer not only mechanical strength and corrosion resistance but also promote osteointegration and minimize inflammatory responses. Titanium and its alloys, although commonly used, exhibit limited wear and corrosion resistance in aggressive physiological environments. Therefore, the development of effective surface engineering strategies is of critical importance.

A hybrid surface modification approach was proposed, combining initial laser treatment using a Nd:YAG laser with subsequent deposition of oxide ceramic layers via the MAO process. Laser treatment enables controlled remelting of the surface, improving topography, morphology, and mechanical performance. MAO, in turn, allows the formation of porous, biocompatible ceramic coatings that can be enriched with bioactive ions such as Ca^{2+}, Na^{+}, Zn^{2+}, and hydroxyapatite particles.

The study investigated how different combinations of process parameters (order of modification, electrolyte composition, laser power) influence the structure, surface topography, and chemical properties of the modified surfaces. Emphasis was placed on evaluating corrosion resistance (OCP, EIS), biological performance (wettability, endothelial cell response), and surface characteristics (SEM, EDS, XRD, FTIR, XPS).

The results confirmed that hybrid modification significantly enhances the functional properties of titanium bioalloys. The resulting layers exhibited high uniformity, beneficial porosity for cell adhesion, and improved corrosion resistance compared to samples modified with a single technique. The tailored electrolyte compositions enabled controlled incorporation of bioactive ions, directly contributing to enhanced biocompatibility and osteointegration potential.

Overall, the findings demonstrate that the laser–MAO hybrid technique is a promising surface modification strategy for titanium-based biomaterials, offering potential for the development of next-generation implants with improved durability,

biological performance, and application-specific surface customization.

Key words: titanium alloys, ceramic coatings, laser modification, micro-arc oxidation, microstructure, surface topography, biological studies

WYKAZ PUBLIKACJI BĘDĄCYCH PODSTAWĄ ROZPRAWY DOKTORSKIEJ .

[JS1] Sypniewska J.,Szkodo M.; *Influence of Laser Modification on the Surface Character of Biomaterials: Titanium and Its Alloys - A Review,* Coatings, (2022), doi.org/10.3390/coatings12101371 **(IF: 3.4; 100 pkt na liście MNiSW)**

[JS2] J.Sypniewska, M.Szkodo, B. Majkowska-Marzec, A. Mielewczyk-Gryń; *Effect of hybrid modification by ceramic layer formation in MAO process and laser remelting on the structure of titanium bio-alloy Ti13Nb13Zr*; Ceramics international, (2023) doi.org/10.1016/j.ceramint.2023.02.018 **(IF: 5.1, 100 pkt na liście MNiSW)**

[JS3]Sypniewska J., Szkodo M., Majkowska-Marzec B., Mielewczyk-Gryń A.; *Exploring the composition and corrosion resistance in hybrid-modified Ti13Nb13Zr alloy*. MRS Communications (2024); doi.org/10.1557/s43579-024-00663-z **(IF: 1.8; 100 pkt na liście MNiSW)**

[JS4] Sypniewska, J., Szkodo, M., Majkowska-Marzec, B. Pawłowski Ł., Mirowska A., Ryl J., Mielwczyk-Gryń A., Gaweł Ł. Campos E.M., Fernández Hernán J.P., *Hybrid laser-micro-arc oxidation techniques for enhanced biocompatibility and surface modification of Ti13Nb13Zr alloy in biomedical applications*. Applied Surface Science (2024); doi.org/10.1016/j.apsusc.2025.163136 **(IF: 6.3, 140 pkt na liście MNiSW)**

[JS5] Sypniewska J., Szkodo M., Majkowska-Marzec B., Pawłowski Ł., Martinez-Campos E., Fernández Hernán J.P.; *Influence of hybrid modification on functional properties of a commercial bio-titanium alloy Ti6Al4V**; Materials Letters (2025)

***Artykuł w trakcie recenzji w czasopiśmie Materials Letters (IF: , 70 pkt na liście MNiSW)**

DOROBEK NAUKOWY I ORGANIZACYJNY DOKTORANTA

Wskaźniki bibliometryczne

1. Google Scholar

   Liczba cytowań: 44

   Indeks Hirscha 3

2. Scopus

   Liczba cytowań: 27

   Liczba cytowań bez autocytowań: 23

   Indeks Hirscha 2

3. Web of Science:

   Liczby cytowań: 37

   Liczba cytowani bez autocytowań: 29

   Indeks Hirscha: 3

4. Recenzowane artykuły

   Ceramics International (MNiSW 100pkt.) - **6**

   Journal of Vacuum Science and Technology (MNiSW 70pkt.) – **1**

Publikacje

1. Sypniewska, J., Szkodo, M., Majkowska-Marzec, B., Pawłowski, Ł., Miwska, A., Ryl, J., Mielewczyk-Gryń, A., Gaweł, Ł., Campos, E. M., & Fernández Hernán, J. P. (2024). Hybrid laser-micro-arc oxidation techniques for enhanced biocompatibility and surface modification of Ti13Nb13Zr alloy in biomedical applications. Applied Surface Science, 698, 163136. https://doi.org/10.1016/j.apsusc.2025.163136
2. Sypniewska, J., Szkodo, M., Majkowska-Marzec, B., & Mielewczyk-Gryń, A. (2024). Exploring the composition and corrosion resistance in hybrid-modified Ti13Nb13Zr alloy. MRS Communications. https://doi.org/10.1557/s43579-024-00663-z
3. Majkowska-Marzec, B., Staszewski, K., & Sypniewska, J. (2023). Effect of pulse laser treatment at different process variables on mechanical behavior of carbon nanotubes electrophoretically deposited on titanium alloy. Acta of Bioengineering and Biomechanics, 25(2), 157–168. https://doi.org/10.37190/abb-02324-2023-02
4. Sypniewska, J., Szkodo, M., Majkowska-Marzec, B., & Mielewczyk-Gryń, A. (2023). Effect of hybrid modification by ceramic layer formation in MAO process and laser remelting on the structure of titanium bio-alloy Ti13Nb13Zr. Ceramics International. https://doi.org/10.1016/j.ceramint.2023.02.018

5. Sypniewska, J., & Szkodo, M. (2022). Influence of laser modification on the surface character of biomaterials: Titanium and its alloys—A review. Coatings, 12(10), 1371. https://doi.org/10.3390/coatings12101371

6. Majkowska-Marzec, B., & Sypniewska, J. (2021). Microstructure and mechanical properties of laser surface-treated Ti13Nb13Zr alloy with MWCNTs coatings. Advances in Materials Science, 21, 5–18. https://doi.org/10.2478/adms-2021-0021

Wystąpienia konferencyjne

1. 16-18.10.2024, 4th BioMaH Biennial International Conference, Biomatreials and Novel Technologies for Healthcare, Rome, Italy; Rodzaj udziału: czynny, prezentacja ustna. Tytuł wystąpienia: Influence of hybrid modification (laser Nd:YAG-MAO) on selected properties of Ti13Nb13Zr Autor: Joanna Sypniewska
2. 22-24.05.2024, VI Konferencja IMPLANTY, Gdańsk, Polska; Rodzaj udziału: Plakat; Tytuł plakatu: Wpływ procesu micro-arc oxidation i modyfikacji laserowej na wybrane właściwości stopu tytanu Ti13Nb13Zr. Autor: Joanna Sypniewska
3. 17-20th August 2023, conference Materials, methods & Technologies; Science and Education Foundation, Burgas, Bulgaria, Rodzaj udziału: czynny, prezentacja ustna.Tytuł: Effect of hybrid modification of titanium alloy on corrosion properties and chemical composition of the layers. Autor: Joanna Sypniewska
4. 27-28th March 2023, International Conference on Materials;Science and Engineering; Paris, France. Rodzaj udziału: plakat Tytuł: Surface structure properties of Ti13Nb13Zr titanium alloy subjected to laser modification and MAO proces. Autor: Joanna Sypniewska
5. 19-22th August 2022, conference Materials, methods & Technologies; Science and Education Foundation, Burgas, Bulgaria, Rodzaj udziału: czynny, prezentacja ustna. Title: Influence of laser modification of titanium alloy Ti13Nb13Zr on material structure and selected properties.Autor: Joanna Sypniewska

Projekty

1. Członek projektu; 2024-2025, Uranium Supporting Cooperation With High Schools 2024, IDUB Politechnika Gdańska

   Tytuł: Techniki inżynierii powierzchni i metody badań biomateriałów

   Szkoła: I Liceum ogólnokształcące w Bytowie; Liceum Ogólnokształcące w Makowie Mazowieckim

Kierownik projektu: dr inż. Beata Majkowska-Marzec

Obowiązki: Organizowanie i prowadzenie zajęć dla uczniów oraz koordynacja zakupów i przetargów w ramach projektu.Staże naukowo-badawcze i szkoleniowe

2. Uczestnik projektu; 2023-2024, Uranium Supporting Cooperation With High Schools 2024, IDUB Politechnika Gdańska

Tytuł: Inżynieria powierzchni biomateriałów

Szkoła: Liceum Ogólnokształcące w Makowie Mazowieckim

Kierownik projektu: dr inż. Beata Majkowska-Marzec

Obowiązki: Organizowanie i prowadzenie zajęć dla uczniów oraz koordynacja zakupów i przetargów w ramach projektu.

Wyjazdy szkoleniowe i naukowe

1. PROM NAVA 2025

02.-06.06.2025 Badania wykonywane na:

Universidad Complutense de Madrid, Hiszpania

- Universidad Rey Juan Carlos, kampus w Móstoles, Hiszpania

Badania prowadzone w ramach badań wstępnych łączenia różnych technik modyfikacji powierzchni oraz przeprowadzenie analizy wyników na potrzeby publikacji naukowej.

2. Erasmus + 2025

13-17.01.2025 Szkolenie realizowane na:

- Universidad Complutense de Madryt, Hiszpania
- Universidad Rey Juan Carlos, Kampus w Móstoles, Hiszpania

Szkolenia z zakresu**:**

- badań korozyjnych (test EIS, testy zanurzeniowe i testy degradacyjne)
- badań aktywności komórek ludzkich

3. Erasmus+ 2024

08.–12.07.2024 Szkolenie realizowane na:

- Universidad Complutense de Madryt, Hiszpania
- Universidad Rey Juan Carlos, Kampus w Móstoles, Hiszpania

Szkolenia z zakresu:

- badań korozyjnych (testy z użyciem krzywych potencjodynamicznych, test EIS, testy zanurzeniowe i testy degradacyjne)
- podstawowych metod badań komórkowych.

Działalność organizacyjna

1. **Politechnika Gdańska**
   Członek Rady Wydziału Inżynierii Mechanicznej i Okrętownictwa
   październik 2023 – obecnie
2. **Politechnika Gdańska**
   Organizator warsztatów w ramach programu „Politechnika wielu pokoleń” w 2024 roku

Szkolenia i certyfikaty

1. **Certyfikat USL Tuttnauer Autoklaw**
   Politechnika Gdańska
   05.02.2025
2. **Certyfikat TotalMedica**
   Szkolenie z pierwszej pomocy
   11.06.2024
3. **Certyfikat Zwick/Roell**
   Maszyna Zwić 5kN Prolin, oprogramowanie testXpertIII oraz norma
   2006/42/EG 28–30.03.2023
4. **Certyfikat z języka angielskiego B2 – ACERT**
   Centrum Języków Obcych, Politechnika Gdańska
   22.06.2021 | Nr PG/46/2021
5. **Prawo medyczne**
   Szkoła Doktorska, Politechnika Bydgoska
   22.02.2020 | Nr KRD/ZP.BoN/C465
6. **AUTODESK INVENTOR – Poziom I**
   Procad Poznań
   27.07.2018

1. WPROWADZENIE

1.1. Społeczne aspekty rozwoju materiałów biomedycznych

W dziedzinie implantów stomatologicznych podkreśla się ich znaczenie przede wszystkim z powodów medycznych, ale również estetycznych – odbudowa ubytków z wykorzystaniem implantów umożliwia trwalszą rekonstrukcję oraz poprawę wyglądu pacjenta [1].
Obszar implantów ortopedycznych doświadcza obecnie znaczącego wzrostu zapotrzebowania, co wynika głównie z dwóch kluczowych czynników: rosnącej liczby osób starszych oraz jednoczesnego wzrostu aktywności fizycznej w różnych grupach wiekowych [2,3]. To współwystępowanie zjawisk spowodowało zapotrzebowanie na implanty ortopedyczne, co w istotny sposób zmienia krajobraz opieki zdrowotnej. Wraz ze starzeniem się populacji światowej obserwuje się przesunięcie demograficzne – coraz większy odsetek ludzi osiąga wiek senioralny. Grupa ta jest bardziej podatna na problemy układu mięśniowo-szkieletowego i choroby zwyrodnieniowe, takie jak choroba zwyrodnieniowa stawów czy złamania, które wymagają interwencji z zastosowaniem implantów ortopedycznych.

Współcześnie ludzie pozostają aktywni fizycznie znacznie dłużej niż jeszcze w poprzednim stuleciu. Według raportu Głównego Urzędu Statystycznego coraz więcej osób starszych (w wieku 60 lat i więcej) spędza aktywnie czas wolny: jeżdżąc na rowerze, spacerując, biegając, grając w piłkę nożną, chodząc na siłownię czy uprawiając fitness [4]. Statystyki Narodowego Funduszu Zdrowia (NFZ) pokazują, że z roku na rok przeprowadza się coraz więcej operacji z zastosowaniem endoprotezoplastyki stawów – najczęściej biodrowych i kolanowych. Donoszono, że od 500 do 700 zabiegów endoplastyki dotyczyło wymiany wcześniej wszczepionego implantu [5]. Tak duża liczba reoperacji stanowi poważny problem w kontekście wytwarzania trwałego implantu, który spełnia zarówno wymagania medyczne, jak i oczekiwania pacjentów.

Reoperacje są przede wszystkim związane z faktem, że każdy implant ma określony czas, przez jaki może przebywać w organizmie, jednak wiele z nich wynika także z przedwczesnego uszkodzenia implantu na skutek środowiska biologicznego organizmu, obciążeń mechanicznych, a także reakcji alergicznych spowodowanych produktami korozji. To z kolei otwiera drogę do rozwoju implantów o ulepszonych właściwościach.

Osseointegracja, czyli podstawowy proces łączenia się kości z implantem, jest rozumiana jako proces bezcementowego zakotwiczenia i integracji implantu z kością [6]. Proces ten jest w znacznym stopniu uzależniony od właściwości powierzchni implantu. Modyfikacja powierzchni implantów w celu poprawy osteointegracji cieszy się coraz większym zainteresowaniem w nowoczesnej ortopedii. Wskazuje się na dwa czynniki mające wpływ na osteointegrację. Pierwsze to czynniki środowiskowe, związane z obciążeniami implantu, właściwościami kości pacjenta oraz jego chorobami. Ważnym czynnikiem środowiskowym jest również koncentracja i jakość komórek kościotwórczych. Drugim istotnym czynnikiem, często wskazywanym w literaturze, są właściwości samego implantu – jego sposób wytworzenia, materiał, z którego jest wykonany, powłoka powierzchniowa oraz jego struktura makro-, mikro- i nanometryczna [7].

Dużą wagę przywiązuje się do wyboru odpowiedniego materiału na implant. Obecnie dużą popularnością cieszą się implanty wykonane z tytanu lub jego stopów [8], które wykazują dobrą odporność na korozję, doskonałe właściwości mechaniczne i wysoką biokompatybilność [9,10]. Jednym z nielicznych mankamentów tytanu i jego stopów jest ich niska odporność na ścieranie i zużycie [11]

1.2. Uzasadnienie innowacyjności przedstawionej modyfikacji

W pracy pod tytułem „Wpływ obróbki laserowej i zastosowanie dodatków na wybrane właściwości funkcjonalne biostopów tytanu” na potrzeby realizacji jej celów zastosowano hybrydową, podwójną modyfikację. Zaproponowano połączenie dwóch technik: modyfikacji laserowej przy wykorzystaniu lasera Nd:YAG oraz techniki osadzania mikrołukowego (MAO – micro-arc oxidation), podczas której możliwe jest wytworzenie ceramicznej warstwy tlenkowej.

Zdecydowano się na zastosowanie podwójnej modyfikacji ze względu na możliwości, które daje taka metoda obróbki. Stanowi ona perspektywę do łączenia zalet obu technik, co pozwala na uzyskanie materiału o lepszych własnościach funkcjonalnych niż przy zastosowaniu klasycznej pojedynczej modyfikacji. Proces laserowej modyfikacji jest procesem powtarzalnym z możliwością kontrolowania wszystkich parametrów i zaprojektowania procesu tak, żeby uzyskać materiał o określonej chropowatości, odpowiednio rozwiniętej morfologii powierzchni, poprawionych własnościach mechanicznych i zwiększonej odporności na korozję. Natomiast utlenianie mikrołukowe MAO pozwala na wytworzenie biozgodnej warstwy ceramicznej wzbogaconej o jony, które stanowią aktywator do procesów kostnych, nadając własności antybakteryjne zmodyfikowanemu materiałowi, a dodatkowa ceramiczna warstwa MAO charakteryzuje się rozbudowaną, porowatą morfologią powierzchni co propaguje proliferację komórek.

Na podstawie przeglądu literaturowego stwierdzono, że temat modyfikacji hybrydowej w przedstawionej konfiguracji powyższych dwóch technik jest niecałkowicie zbadany i możliwe jest wprowadzenie innowacyjnego sposobu modyfikacji powierzchni bio-stopów tytanu do zastosowań biomedycznych, który pozwoli na uzyskanie materiału spełniającego szereg rygorystycznych wymagań stawianym biomateriałom oraz będzie on dawał możliwość personalizacji w zależności od wymagań jednostkowych.

W kontekście stopów tytanu istotne jest doskonalenie konkretnych właściwości, ponieważ niedostateczna odporność na zużycie i odporności na korozję stanowi poważne ograniczenie w wielu zastosowaniach. Wyniki badań literaturowych jednoznacznie wskazują, że zastosowanie modyfikacji powierzchni przy użyciu lasera jest prostą, a zarazem bardzo skuteczną metodą poprawy odporności na zużycie i korozję takich materiałów [12,13].

Modyfikacja laserowa poprawia odporność korozyjną powierzchni, co może być odpowiedzią na obniżoną odporność lokalną powłok uzyskiwanych metodą mikrołukowej oksydacji (MAO). Metoda MAO charakteryzuje się możliwością wytwarzania powłok poprzez wprowadzanie jonów z elektrolitu, w którym przebiega proces. Przewagą mikrołukowej oksydacji nad innymi metodami nanoszenia powłok na materiały implantacyjne jest prostota techniki [14], przy jednoczesnym uzyskiwaniu jednolitej powłoki o wysokiej porowatości [15]. Dodatkową zaletą tej metody jest możliwość wbudowywania jonów z elektrolitu w modyfikowany materiał, co przekłada się na zwiększoną biozgodność. W trakcie modyfikacji powierzchni materiałów implantacyjnych możliwe jest wprowadzenie takich pierwiastków jak: potas, wapń, cynk (jony budulcowe kości), a także srebro, które wykazuje właściwości antybakteryjne [16–18].

1.3. Uzasadnienie wyboru stopu tytanu do badań

Obecnie tytan i jego stopy wzbudzają ogromne zainteresowanie w różnych gałęziach przemysłu, przede wszystkim ze względu na ich niską gęstość. Ta wyjątkowo interesująca konfiguracja materiałów zyskała szerokie uznanie, zwłaszcza w produkcji komponentów do motocykli i samochodów sportowych, gdzie redukcja masy stanowi główny priorytet [19,20]. W przemyśle lotniczym stopy tytanu są trzecią najczęściej stosowaną grupą materiałów po stopach niklu. Ich popularność wynika nie tylko z niskiej gęstości, ale również z wyjątkowej odporności na korozję oraz zdolności do pracy w wysokich temperaturach, jak ma to miejsce w przypadku stopów α i α+β [21,22]. Jednak to właśnie w dziedzinie zastosowań medycznych, a w szczególności w implantologii, tytan i jego stopy przyciągają szczególną uwagę [23,24]. W stomatologii stopy tytanu są powszechnie stosowane do produkcji koron i mostów dentystycznych ze względu na zmniejszone ryzyko reakcji alergicznych oraz pozytywny wpływ na proces osteointegracji [25,26].

Główną zaletą tytanu i jego stopów jest ich znakomita odporność korozyjna, przewyższająca nawet stale nierdzewne oraz stopy kobaltu i chromu, co czyni je idealnym wyborem do implantów umieszczanych w środowisku organizmu [27–29]. Badania potwierdzają, że tytan wykazuje minimalny wpływ na organizm człowieka i jest uznawany za biokompatybilny materiał, podobnie jak jego stopy [30].

Stopy Ti6Al4V oraz Ti13Nb13Zr znajdują zastosowanie w inżynierii tkankowej [31]. Stop Ti6Al4V jest stopem komercyjnie stosowanym w implantologii, charakteryzuje się dobrą odpornością na korozję, niską gęstością i wysoką wytrzymałością właściwą [32]. Jednakże stopy zawierające aluminium wykazują wyższą toksyczność niż stop Ti13Nb13Zr [33]. Zarówno aluminium, jak i wanad w większych stężeniach mogą powodować problemy neurologiczne. Wykazano, że jony wanadu wywołują reakcje cytotoksyczne, a jony glinu (aluminium) przyczyniają się do zmiękczenia kości [33]. Nowym stopem, nad którego komercyjnym zastosowaniem wciąż trwają badania jest stop tytanu Ti13Nb13Zr charakteryzujący się bardzo dobrymi właściwościami osteointegracyjnymi, modułem Younga zbliżonym do kości oraz dobrymi właściwościami mechanicznymi. Zaleca się jego stosowanie głównie w endoprotezach stawu biodrowego i kolanowego [34].

1.4. Modyfikacja laserowa

Modyfikacja laserowa umożliwia uzyskanie chropowatej powierzchni, co jest szczególnie cenne w implantologii, ponieważ komórki kostne bardzo dobrze rosną na tego typu podłożu, co przekłada się na poprawę właściwości mechanicznych układu implant–kość [35,36]. Dodatkowo jako zalety tej metody podkreśla się precyzję, elastyczność i możliwość kontrolowania parametrów lasera Nd:YAG, powtarzalność procesu oraz małą strefę wpływu ciepła powstającą w wyniku modyfikacji [37]. Ze względu na wysoki poziom zaawansowania technologicznego tego procesu, możliwe jest również jego przeprowadzanie w sposób autonomiczny, bez bezpośredniej ingerencji człowieka, co zmniejsza ryzyko niepożądanych skutków dla organizmu [38].

Właściwości mechaniczne materiałów, jak również lepsze wiązanie implantu z kością [34], stanowią kluczowe czynniki decydujące o skuteczności zastosowania materiałów w implantologii. Z aktualnej literatury wynika, że obróbka laserowa powierzchni stopów tytanu prowadzi do zwiększenia chropowatości powierzchni, co bezpośrednio wiąże się ze wzrostem jej zwilżalności, co z kolei jest korzystne dla procesu osteointegracji [36,39,40].

Ponadto modyfikacja laserowa zwiększa odporność materiałów na zużycie i korozję, a także podnosi ich twardość, oferując perspektywę uzyskania materiału, który może wytrzymywać większe obciążenia przez dłuższy czas i nie uwalnia niebezpiecznych jonów, takich jak te powstające w wyniku degradacji materiału

Aspekt modyfikacji laserowej został szeroko omówiony w pracy [JS1]

1.5. Technika wytwarzania warstwy ceramicznej – MAO

Mikro-łukowa oksydacja, znana również jako plazmowa oksydacja elektrolityczna (PEO) [41], to technika, która wykorzystując mikro-wyładowania na powierzchni materiału, pozwala na wbudowanie w strukturę powłoki pierwiastków obecnych w roztworze elektrolitu, w którym prowadzony jest proces. Jednocześnie prowadzi to do powstania powłoki ceramicznej na powierzchni materiału [15]. Metoda umożliwia uzyskiwanie ceramicznych powłok zawierających starannie dobrane dodatki zawarte w środowisku elektrolitycznym. Początkowo wykorzystywana głównie dla podłoży magnezowych [42], zyskuje coraz większą popularność również w przypadku stopów tytanu [41].

Proces ten umożliwia poprawę biozgodności powierzchni dzięki zdolności do wprowadzania jonów, które są m.in. składnikami ludzkiej tkanki kostnej lub aktywują proces osteointegracji. Mikro-łukowa oksydacja zwiększa również porowatość powierzchni, co przyspiesza osteointegrację, a także poprawia twardość i odporność na zużycie materiału. W porównaniu do metody osadzania elektroforetycznego MAO zapewnia również lepszą adhezję powłoki do zmodyfikowanej powierzchni. Badania wskazują, że MAO może być stosowana do wbudowywania jonów w strukturę tlenkową powierzchni tytanu, co poprawia jej biozgodność. Niemniej jednak literatura wskazuje na możliwe obniżenie odporności powłok MAO na korozję erozyjną, dlatego zaleca się dodatkowe pokrycie powierzchni polimerem lub warstwą zawierającą sole wapnia i fosforu [27]. W literaturze [28] podkreśla się, że silne połączenia implant–kość są wspomagane przez obecność wapnia i jego fosforanów. Krytycznie istotnym aspektem projektowania modyfikacji z wykorzystaniem techniki MAO jest odpowiedni dobór składu elektrolitu do konkretnego zastosowania. W publikacjach wspomina się o zastosowaniu elektrolitów zawierających pierwiastki takie jak Ag (srebro), Zn (cynk), Au (złoto), Cu (miedź), Ca (wapń), P (fosfor) [29,42].

1.6. Biododatki

1.6.1. Sód, wapń i fosfor

Wskazuje się, że niektóre jony powodują wytwarzanie apatytów na powierzchni materiałów zanurzonych w symulowanych płynach ustrojowych (PBS) [43]. Jony sodu jako dodatek do materiałów tytanowych stosuje się właśnie w celu zwiększenia integracji hydroksyapatytu a w połączeniu z jonami wapnia poprawia on osseointegrację [44]. Ponadto udowodniono już w 2005 roku, że obecność jonów sodu może pozytywnie wpływać na odporność korozyjną materiałów tytanowych [45], a także poprawia bioaktywność i nie organicza biokompatybilności [43].

Wapń jest podstawowym elementem budulcowym kości, jego dodatek w materiałach tytanowych sprzyja tworzeniu bioaktywnej warstwy, wspomagając integrację implantu z tkanką kostną. Literatura stanowi, że jony Ca2+ zwiększają liczbę kontaktów komórkowych w obszarze kości, prowadząc do zwiększenia gęstości kości, stymuluje to kość do zwiększenia regeneracji po wszczepieniu implantu. Wskazuje się, że jest kluczowy dla integracji śród kostnej w praktyce klinicznej [46]. Jony wapnia razem z jonami fosforu tworzą kombinację, która określana jest jako wzajemnie współmobilizująca się, co w efekcie daje zwiększenie osteokonduktywności materiałów tytanowych, a także poprawę proliferacji komórek [47].

1.6.2. Hydroksyapatyt

Hydroksyapatyt stanowi rodzaj fosforanu wapnia, który jest szeroko wykorzystywany
w inżynierii tkankowej. Wykazuje się wysoką biokompatybilnością względem organizmu ludzkiego oraz charakteryzuje się wysoką bioaktywnością z komórkami kostnymi. Wykazano także, że hydroksyapatyt odgrywa bardzo dużą rolę w sygnalizacji kostnej na poziomie molekularnej [48]. Poza dobrymi własnościami biologicznymi wskazuje się, że omawiany związek wpływa korzystnie na odporność na korozję materiałów, do których jest wprowadzany [49,50].

1.6.3. Cynk

Cynk w organizmie jest pierwiastkiem, który występuje w znikomych ilościach, ale biologicznie pełni szereg ważnych ról. Wpływa między innymi na mineralizację, aktywność hormonalną, a jego niedobór może powodować opóźniony rozwój kości a także w późniejszych latach szybsze wystąpienie osteoporozy [51]. Literatura wskazuje, że podejmowane są próby wzbogacania materiałów biomedycznych jonami Zn^{2+} w celu poprawy własności mechanicznych, zwiększenia adhezji i proliferacji komórek [51,52]. Obecność jonów cynku wpływa na regulowanie szlaków biologicznych odpowiadających za przebudowę tkanki kostnej a także zwiększa biokompatybilność materiałów tytanowych [53]. Dla nanotlenku cynku wprowadzanego do materiałów tytanowych wykazuje się poprawę własności odporności na korozję oraz własności antybakteryjnych [54]. Cynk na powierzchni biomateriałów występuje bardzo często w postaci tlenku cynku, związek ten ma własności hydrofobowe, co pozwala na zmianę w kontrolowany sposób charakteru zwilżalności powierzchni [55].

1.7. Hybrydowa modyfikacja w literaturze

Przegląd aktualnej literatury dostarczył informacji na temat modyfikacji hybrydowych obejmujących wstępną obróbkę laserową, po której następował proces mikrołukowej oksydacji . Wyniki tych badań pokazują, że tego typu modyfikacja [14,27,28,56] hybrydowa umożliwia redukcję parametru chropowatości powierzchni w porównaniu z powłokami uzyskiwanymi wyłącznie za pomocą procesu MAO. Ponadto uzyskano powłoki o lepszej mikrostrukturze, bardziej jednorodnej i z mniejszą liczbą pęknięć w porównaniu z próbkami pokrywanymi jedynie ceramiczną powłoką w wyniku mikrołukowej oksydacji [28]. W literaturze wskazano również na poprawę właściwości mechanicznych, odporności korozyjnej i właściwości tribologicznych. Podkreślono także, że ulepszona struktura materiału dzięki modyfikacji laserowej skutkowała zwiększeniem energii powierzchniowej, co prowadziło do zwiększenia liczby wyładowań pojawiających się w trakcie procesu MAO. Zaprezentowane wyniki stanowią podstawę do słuszności założeń eksperymentalnych przyjętych w niniejszym projekcie. Ze względu na ograniczoną liczbę badań dotyczących tego typu modyfikacji hybrydowej zasugerowano, że dalsze badania powinny zostać rozszerzone i obejmować dokładną analizę makro-, mikro- i nanostruktury uzyskanych powierzchni oraz badania przemieszczeń i naprężeń w osnowie materiału. Jak wykazano na podstawie zgromadzonej literatury, powłoki MAO charakteryzują się dużą chropowatością, podatnością na pękanie oraz ograniczoną odpornością korozyjną [57]. Wskazane jest zatem przeprowadzenie modyfikacji polegającej na pierwotnym wytworzeniu powłoki MAO, a następnie jej dalszej obróbce przy użyciu wiązki energetycznej (np. lasera) w celu ujednorodnienia powłoki uzyskanej w procesie MAO. Z kolei zastosowanie modyfikacji laserowej poprzez przetapianie warstwy ceramicznej MAO może służyć przemieszczeniu wcześniej wprowadzonych jonów ku powierzchni, co stanowi próbę dalszego zwiększenia osteointegracji oraz biozgodności materiału

2. TEZA, CELE I ZAKRES PRACY

Teza przyjęta w pracy „Wpływ obróbki laserowej biostopów tytanu i zastosowanie dodatków na wybrane właściwości funkcjonalne" stanowi, że możliwe jest wytworzenie rozwiniętej morfologicznie powierzchni przy wykorzystaniu podwójnej modyfikacji przy użyciu techniki laserowej i techniki osadzania mikrołukowego, która poprawi odporność na korozje materiału, zapewni odpowiednie parametry chropowatości i zwilżalności powierzchni oraz dodatkowo możliwe będzie kontrolowane wzbogacenie materiału w jony bioaktywne, co spowoduje pozytywną odpowiedź komórkową.

Celem naukowym pierwszorzędnym było sprawdzenie możliwości przeprowadzenia podwójnej modyfikacji z wykorzystaniem dwóch technik, pierwszej modyfikacji wiązką lasera Nd:YAG, drugiej techniki mikrołukowego wytwarzania warstwy ceramicznej na biostopach tytanu. Kolejny cel naukowy stanowił o określeniu wpływu kombinowanej obróbki powierzchniowej, obejmującej modyfikację laserową oraz proces mikrołukowego utleniania (MAO), z zastosowaniem dodatków pierwiastków bioaktywnych, na strukturę, topografię i właściwości funkcjonalne biostopów tytanu. Badania miały na celu wykazanie, że odpowiednio dobrane parametry procesów prowadzą do poprawy odporności korozyjnej, zwiększenia biozgodności i modyfikacji właściwości powierzchni w kontekście ich zastosowania w implantologii.

Celem użytkowym pracy było opracowanie metody podwójnej modyfikacji powierzchni biostopów tytanu, umożliwiającej uzyskanie warstw wierzchnich o wysokiej odporności korozyjnej i korzystnych właściwościach biologicznych (zwilżalność, chropowatość, bioaktywność), które mogą znaleźć zastosowanie w produkcji nowoczesnych implantów o zwiększonej trwałości i lepszej integracji z tkankami.

Zakres pracy doktorskiej obejmował

- Przegląd literatury w zakresie modyfikacji laserowej materiałów tytanowych [JS1]
- Ocenę słuszności wykonywania podwójnej modyfikacji w różnych kombinacjach kolejności wykorzystania technik modyfikacji laserowej oraz wytwarzania warstwy ceramicznej techniką MAO, a także ocena

wpływu modyfikacji na własności stopu tytanu Ti13Nb13Zr [JS2]

- Wybór parametrów prowadzenia procesu modyfikacji laserowej laserem Nd:YAG dla modyfikacji materiału Ti13Nb13Zr [JS2]
- Przeprowadzenie badania składu chemicznego oraz odporności na korozję jako badania wstępne dla dwóch kombinacji modyfikacji stopu tytanu Ti13Nb13Zr [JS3]
- Zaprojektowanie nowego składu elektrolitu, zawierającego hydrkosyapatyt,
  do wytworzenia warstw ceramicznych na zmodyfikowanej laserowo powierzchni stopu Ti13Nb13Zr [JS4]
- Przeprowadzenie szczegółowych badań składu chemicznego (badania EDS, XPS), badań mikrostruktury powierzchni (SEM, badania profilograficznne), badań odporności na korozję połączone z testami zanurzeniowymi oraz badań odpowiedzi komórkowej, ludzkich komórek śródbłonka. [JS4]
- Przeprowadzenie badań na komercyjnie używanym stopie tytanu Ti6Al4V w zakresie modyfikacji podwójnej w jednej kombinacji laser Nd:YAG-MAO. [JS5]
- Przeprowadzenie badań wstępnych w zakresie oceny wpływu modyfikacji laserowej na stop (badania przekroju poprzecznego), ocena morfologii powierzchni (SEM), składu chemicznego (EDS), podstawowych badań biologicznych oraz badań własności elektrochemicznej (EIS podczas testu zanurzeniowego). [JS5]

3. METODYKA PROWADZONYCH BADAŃ

3.1. Przygotowanie próbek i podłoża

Próbki do badań w ramach pracy doktorskiej na podstawie cyklu publikacji [JS1-JS5] zostały przygotowane poprzez wycięcie okrągłych próbek z prętów stopu tytanu Ti13Nb13Zr (Bibus Metals, Poznań, Polska [skład tab.1] oraz JIANGSU GANGYA METAL PRODUCTS LIMITED, Chiny), oraz stopu Ti6Al4V (JIANGSU GANGYA METAL PRODUCTS LIMITED, Chiny [skład tab.2]). Próbki miały średnicę od 12 do 19 mm oraz wysokość 5mm.

Tabela 1. Skład chemiczny stopu tytanu Ti13Nb13Zr [JS2-JS3]

Element	Ti	Nb	Zr	O	N	Fe	C	H
Wt. [%]	71.38	14	13.5	0.016	0.05	0.25	0,8	0.015

Tabela 2. Skład chemiczny stopu tytanu Ti6Al4V

Element	Ti	Al	V	Fe	O	C	N	H
Wt. [%]	89.18	6.40	4.05	0.16	0.185	0.01	0.005	0.0035

Przed przystąpieniem do modyfikacji próbki były szlifowane z dwóch stron. Obróbkę mechaniczną przeprowadzono przy użyciu szlifierko-polerki (Saphir 330, Czechy) oraz papierów ściernych o gradacjach od 60 do 2000. W publikacjach [JS2–JS3, JS5] próbki były szlifowane do gradacji 1200, natomiast w [JS4] do 2000.

Po szlifowaniu próbki były każdorazowo oczyszczane: najpierw w wodzie destylowanej (Destylarka Hydrolab, Polska) przez 10 minut, a następnie w izopropanolu (99,9%, POCH S.A., Polska), również przez 10 minut. Po etapie oczyszczania, zarówno przed modyfikacją laserową Nd:YAG, jak i procesem mikrołukowego utleniania, próbki były osuszane sprężonym powietrzem.

3.2. Modyfikacja laserowa stopów tytanu

Jedną z przeprowadzonych modyfikacji biostopów tytanu była modyfikacja laserowa z użyciem lasera Nd:YAG (TruLaser Station 5004, TRUMPF, Niemcy) w obecności technicznego argonu (99,99% czystości, Air Liquide, Polska), co miało na celu ograniczenie procesu utleniania materiału.

Podczas modyfikacji laserowej kontrolowano jeden parametr – moc lasera [W], natomiast parametry takie jak posuw lasera [%], czas trwania impulsu [ms] oraz częstotliwość [Hz] były utrzymywane na stałym poziomie. W publikacjach [JS2–JS3] zastosowano moce lasera 1000 oraz 1500 W, posuw ustalono – na podstawie wcześniejszych badań – na poziomie 60% maksymalnych mozliwości lasera (6 mm/s), czas trwania impulsu wynosił 2,25 ms, a częstotliwość 25 Hz.

W pozostałych publikacjach [JS4–JS5] ustalono optymalną moc lasera na poziomie 1000 W, natomiast pozostałe parametry pozostały bez zmian – zarówno dla dalszych modyfikacji stopu Ti13Nb13Zr, jak i Ti6Al4V.

Podczas modyfikacji wykorzystywano program sterowania wiązką lasera, dedykowany dla próbek o określonej średnicy, tak aby zapewnić jednorodne przetapianie całej powierzchni modyfikowanego materiału.

3.3. Przygotowanie elektrolitów dla procesu MAO

Do wytworzenia warstw ceramicznych w procesie obróbki mikrołukowej przygotowano różne wodne elektrolity o zróżnicowanym składzie, umożliwiającym wprowadzenie do warstw ceramicznych różnych biododatków. Podczas przygotowywania elektrolitów wykorzystano: wodorotlenek sodu (NaOH, Warchem, Polska), hydroksyapatyt ($Ca_{10}(PO_4)_6(OH)_2$, Sigma-Aldrich), octan cynku ($(CH_3COO)_2Zn$, Warchem, Polska), fosforan sodu dwunastowodny ($Na_2PO_4 \cdot 12H_2O$, Warchem, Polska) oraz nanotlenek cynku (nZnO, Nano3D, Polska). Do przygotowania każdego z elektrolitów stosowano wodę destylowaną (Hydrolab, Polska), a w przypadku niektórych kombinacji niezbędne było użycie alkoholu etylowego (C_2H_5OH, Warchem, Polska). Wszystkie szczegółowe kombinacje elektrolitów zastosowane w pracach [JS2–JS5] zostały przedstawione w metodyce badań zawartej w poszczególnych artykułach.

3.4. Proces wytwarzania ceramicznych warstw w procesie MAO

Proces MAO odbywał się przy wykorzystaniu wysokonapięciowego zasilacza prądu stałego (DC supply, BK PRECISSION , MR 1000020). Układ podczas procesu był układem dwuelektrodowym, gdzie elektrodę ujemną stanowiła elektroda platynowa [JS4, JS5] lub elektroda stalowa [JS2, JS3]. Próbka ze stopu tytanu stanowiła natomiast elektrodę naładowaną dodatnio. Na rys. 1 przedstawiono przykład układu do procesu MAO realizowanego podczas eksperymentów.

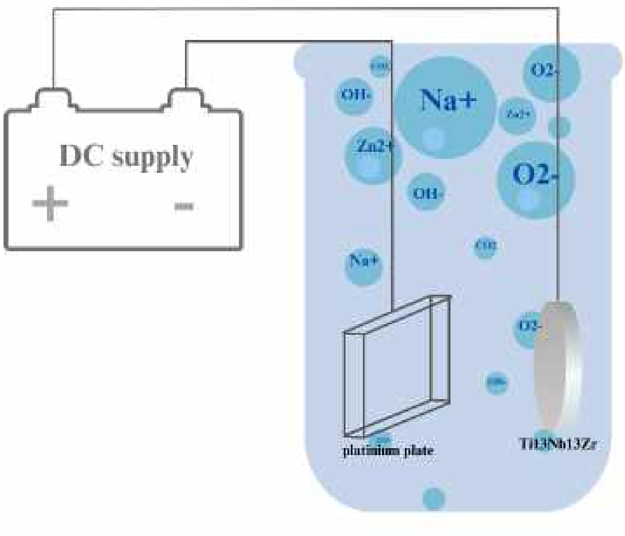

Rysunek 1. Schemat mikrołukowego utleniania dla próbki stopu tyatnu Ti13Nb13Zr

Utlenianiu wysokonapięciowemu z mirko wyładowaniami poddawany był tylko wybrany obszar okrągłego dysku. Próbki umieszczane były w specjalnych uchwytach wytworzonych z polimerów z elementami stalowymi i miedzianym drutem, który pozwalał na prawidłowe dostarczenie prądu do próbki. Próbka była umieszczana w uchwycie, a nakrętka zamykająca układ wyznaczała obszar poddawany modyfikacji. Dla każdej z prac [JS2-JS5] podczas prowadzenia doświadczeń, dla każdej z modyfikowanych próbek, każdorazowo wymieniano elektrolit tak, żeby proces zachodził w jednakowych warunkach, w kontrolowanej temperaturze. 23 °C.

3.5. Badania zmodyfikowanych hybrydowo materiałów stopów tytanu

Bio-stopy tytanu: Ti13Nb13Zr oraz komercyjnie stosowany Ti6Al4V, po przeprowadzonych modyfikacjach z wykorzystaniem techniki laserowego przetapiania laserem Nd:YAG oraz procesu wytwarzania warstw ceramicznych wzbogacanych jonami, o potencjalnym zastosowaniu biomedycznym, zostały przebadane pod względem ich właściwości funkcjonalnych, skupiając się na morfologii powierzchni, charakterze zmodyfikowanych materiałów, składzie chemicznym wynikającym z modyfikacji, a także odporności na korozję, odpowiedzi biologicznej i wybranych właściwościach mechanicznych.

Podstawową techniką wykorzystaną do obserwacji zmodyfikowanych powierzchniowo stopów tytanu była skaningowa mikroskopia elektronowa (SEM), przeprowadzana na każdym etapie prowadzonych doświadczeń. Technika obrazowania, zastosowana do oceny jakościowej wytwarzanych warstw bezpośrednio po hybrydowej modyfikacji, pozwoliła na ocenę jednorodności, obecności pęknięć, uszkodzeń, a także — po dodatkowej obróbce — porowatości materiału. Obrazowanie SEM wykorzystano również po przeprowadzeniu badań zanurzeniowych [JS4]. Zdjęcia wykonywano przy różnych powiększeniach, w zależności od potrzeb szczegółowego przedstawienia cech charakterystycznych powierzchni po modyfikacji. W celu określenia porowatości materiału wykorzystano obrazy SEM, które zostały poddane analizie w oprogramowaniu ImageJ, umożliwiającym pomiar porowatości zmodyfikowanej powierzchni.

Dzięki dodatkowej przystawce w urządzeniu SEM w postaci spektroskopii dyspersji energii (EDS) możliwe było ustalenie składu chemicznego warstwy wierzchniej zmodyfikowanych stopów tytanu; wykonano także analizy składu chemicznego na przekrojach poprzecznych [JS2].

W pracy wykorzystano również– mikroskop optyczny (Olympus UC50), który posłużył do oceny mikrostruktury próbek referencyjnych zmodyfikowanych wyłącznie przy użyciu lasera Nd:YAG ([JS2], [JS4], [JS5]) oraz próbek poddanych podwójnej modyfikacji w pracy [JS2].

Dodatkowo urządzenie to służyło do oceny strefy wpływu ciepła (HAZ – heated affected zone).

Na potrzeby identyfikacji wiązań chemicznych występujących w zmodyfikowanym materiale przy wykorzystaniu hybrydowej modyfikacji laser–MAO [JS2–JS5], MAO–laser [JS2], wykorzystano spektroskopię w podczerwieni z transformatą Fouriera [JS3–JS4] w zakresie 400–4000 cm^{-1} z rozdzielczością 2 cm^{-1} (FTIR, moduł ATR, Perkin Elmer Frontier, USA; Shimadzu Corp., Japonia).

Do identyfikacji faz występujących w modyfikowanych warstwach wierzchnich użyto spektroskopu z wykorzystaniem promieniowania rentgenowskiego (XRD, Philips X'Pert Pro, Almelo, Holandia). Pomiar prowadzono w zakresie $2\theta = 10–90°$ (Cu Kα, $\lambda = 0,1554$ nm).

Stan energetyczny oraz stopień utlenienia poszczególnych pierwiastków chemicznych występujących w zmodyfikowanych materiałach [JS4] określono przy użyciu metody spektroskopii fotoelektronów rentgenowskich – XPS. Do tego celu wykorzystano zaawansowany multispektrometr Escalab 250Xi firmy ThermoFisher Scientific, wykorzystujący precyzyjną plamkę AlKα o średnicy 250 µm promieniowania rentgenowskiego o energii przejścia 20 eV. Niskoenergetyczne bombardowanie elektronami i jonami Ar^+ zastosowano w celu skutecznego zanegowania potencjalnych ładunków powierzchniowych, z końcową kalibracją piku przy użyciu węgla C 1s przy 284,6 eV. Oprogramowanie Advanced Advantage v5.9921 (ThermoFisher Scientific) zostało użyte do dokładnej analizy danych uzyskanych z pomiarów.

Proponowane modyfikacje [JS3, JS4, JS5] zostały zbadane pod względem potencjalnego wzrostu odporności na korozję. Dla badań wstępnych dwóch wskazanych kombinacji modyfikacji przeprowadzono podstawowe testy odporności korozyjnej (potencjostat AtlasCorr, Gdańsk, Polska), skupiające się na określeniu stabilności układu poprzez wykreślenie wykresów zależności potencjału obwodu otwartego (OCP) w czasie jednej godziny w temperaturze 37°C oraz rejestrację krzywych potencjodynamicznych w zakresie od –1 V do +1 V, przy szybkości skanowania 1 mV/s. Uzyskane dane umożliwiły wyznaczenie charakterystycznych parametrów: gęstości prądu korozyjnego (Icorr) oraz potencjału korozyjnego (Ecorr)

Badania prowadzono w środowisku roztworu symulowanych płynów ustrojowych (PBS), z użyciem układu trójelektrodowego, składającego się z kalomelowej elektrody odniesienia, platynowej elektrody pomocniczej oraz elektrody roboczej – próbki stopu tytanu Ti13Nb13Zr poddanej różnym modyfikacjom powierzchniowym.

Dalsza część prac skupiła się wyłącznie na modyfikacji w kombinacji laser–MAO. Dla tej konfiguracji, przy optymalnych parametrach pracy lasera, lecz różnych środowiskach prowadzenia procesu MAO, przeprowadzono analizę odporności na korozję i degradację przy zastosowaniu elektrochemicznej spektroskopii impedancyjnej (EIS, potencjostat Metrohm Autolab PGSTAT302N), w warunkach testu zanurzeniowego w roztworze Hanksa przez 168 godzin.

Warunki badania obejmowały zastosowanie układu trójelektrodowego, w którym próbka pełniła rolę elektrody roboczej, platynowy drut – elektrody pomocniczej, natomiast elektroda odniesienia stanowiła elektroda Ag/AgCl.

Pomiary EIS wykonano w zakresie częstotliwości od 10^5 do 10^{-2} Hz oraz przy zakresie polaryzacji ±10 mV względem potencjału obwodu otwartego (E_OCP), rejestrując 10 punktów na każdą dekadę częstotliwości. Uzyskane dane pozwoliły na wykreślenie wykresów OCP, krzywych Bodego oraz wykresów Nyquista

Na potrzeby określenia zachowania zmodyfikowanego materiału w środowisku nasyconego roztworu PBS, symulującego płyny ustrojowe człowieka, przeprowadzono test zanurzeniowy trwający 14 dni. Zmodyfikowane próbki, przygotowane przy wykorzystaniu dwóch kombinacji: laser–MAO oraz MAO–laser, umieszczono w zamkniętych pojemnikach z 50 ml cieczy PBS i przechowywano w stałych warunkach temperaturowych (cieplarko-suszarka) w temperaturze 37°C.

Podczas testu zanurzeniowego monitorowano zmiany wartości pH oraz masy próbek w dniach 0, 3, 5, 7, 10 i 14. Jak wskazano wcześniej, próbki zostały poddane obserwacjom SEM przed i po teście. W celu oceny potencjalnej degradacji naniesionej warstwy ceramicznej na materiale Ti13Nb13Zr wykonano badania spektroskopii mas atomowych roztworów, w których inkubowano próbki. Przy użyciu spektrometru emisyjnego z plazmą mikrofalową (4210 MP-AES, Agilent) oznaczono zawartość jonów sodu na określonych długościach fal. Z kolei do oznaczenia jonów wapnia zastosowano fotometr płomieniowy BWB-XP (BWB Technologies UK LTD).

Ważnym aspektem w zakresie badań biomateriałów jest określenie charakteru ich powierzchni pod względem chropowatości i zwilżalności. Badania chropowatości wykonano przy wykorzystaniu dwóch urządzeń. W pierwszym etapie zastosowano profilometr stykowy Hommel Etamic Waveline (JENOPTIK), gdzie test przeprowadzono w zakresie pomiarowym 400 µm, przy prędkości przesuwu 0,5 mm/s. Podczas pomiaru zastosowano filtr zgodny z normą ISO 11562. W tym badaniu [JS2] uzyskano wartości takich parametrów jak: Ra (średnia arytmetyczna wysokości chropowatości), Rp (maksymalna wysokość wzniesienia profilu) oraz Wt (całkowita falistość).

Szczegółowe badania charakterystyki powierzchni przeprowadzono dla finalnej kombinacji modyfikacji laser–MAO [JS4], przy użyciu bezkontaktowego profilometru optycznego 3D (Sensofar S Neox, Sensofar Metrology, Terrassa, Hiszpania). Do badań zastosowano technikę mikroskopii konfokalnej, wykorzystując obiektyw Nikon-EPI 20x oraz oprogramowanie SensoSCAN S Neox 7.7. Przeprowadzenie tych badań pozwoliło na ocenę topografii zmodyfikowanego stopu tytanu Ti13Nb13Zr oraz wyznaczenie parametrów chropowatości liniowej, przestrzennej i falistości.

Dla przedstawienia całkowitego obrazu charakteru powierzchni wykonano również badania zwilżalności powierzchni [JS2, JS4, JS5], w tym energię swobodną powierzchni (SFE – surface free energy). Badania zostały wykonane przy wykorzystaniu metody spadającej kropli (sessile drop technique) przy zastosowaniu goniometru kontaktowego (Contact angle goniometer) z wykorzystaniem oprogramowania AttentionOne. Pomiar wykonywano przez 10 sekund od momentu upadku kropli na powierzchnię materiału. W trakcie podstawowego testu zastosowano wodę (ciecz polarna), a do badań energii swobodnej powierzchni zbadano kąt zwilżania dla cieczy niepolarnej – dijodometanu. Swobodną energię powierzchniową obliczono przy użyciu oprogramowania AttentionOne, stosując metodę Owensa, Wendta, Rabela i Kaelble'a (OWRK).

Dla ulepszonego materiału z zaproponowanymi modyfikacjami w cyklu publikacji wykonano przekroje poprzeczne. Materiał przygotowano poprzez przecięcie materiału, a następnie inkludowanie go w żywicy epoksydowej. Następnie próbki zostały wypolerowane (Saphir 330) i poddane trawieniu. Przekroje poprzeczne wykonano przede wszystkim w celu oceny strefy wpływu ciepła modyfikacji laserowej Nd:YAG na stop Ti13Nb13Zr oraz Ti6Al4V [JS2, JS4, JS5]. Dodatkowo, wykonanie przekrojów poprzecznych pozwoliło na ocenę jakości warstw ceramicznych MAO [JS2] oraz zbadanie składu chemicznego techniką EDS [JS3] na przekrojach.

Dla prac wstępnych [JS2] przeprowadzono szereg testów mechanicznych. Wykonano test nanoindentacji NanoTest (Micro Materials, Wielka Brytania), stosując trójścienny diamentowy wgłębnik typu Berkovich, przy założeniu obciążenia testowego 50 mN, które było zwiększane i zdejmowane liniowo przez 15 sekund, z utrzymaniem obciążenia maksymalnego przez 5 sekund. Wykonano 25 powtórzeń dla każdej ze zbadanych próbek.

Test nanoindentacji pozwolił na wyznaczenie wartości zredukowanego modułu Younga. Dla oceny statystycznej istotności badania wykonano analizę wariancji (ANOVA).

Dla próbek pokrytych warstwą ceramiczną MAO [JS2], w celu oceny ich przyczepności do podłoża, przeprowadzono test zarysowania (scratch test) za pomocą urządzenia NanoTest, wykonując 5 powtórzeń dla każdej z badanych próbek, przy obciążeniu 400 mN i długości zarysowania 1000 μm. Test pozwolił na określenie krytycznego obciążenia (Lc – critical load), a także wyznaczenie krzywych emisji akustycznej. Zarysowania po scratch testach były obserwowane pod mikroskopem optycznym (Olympus UC 50).

W aplikacyjnym aspekcie przeprowadzonych modyfikacji hybrydowych laser–MAO [JS4, JS5] kluczowe było wykonanie badań biologicznych. Badania obejmowały ocenę mobilności komórek, jakości DNA, test AlamarBlue oraz ocenę przyczepności komórek (zdjęcia fluorescencyjne), z wykorzystaniem linii C166-GFP – komórek śródbłonka zarodka myszy zainfekowanych genem kodującym zielone białko fluorescencyjne (GFP – Green Fluorescent Protein) oraz C2C12 – linii komórkowej mięśni szkieletowych myszy. Przed przystąpieniem do badań cytokompatybilności konieczne było poddanie zmodyfikowanych próbek standaryzowanemu protokołowi sterylizacji. Próbki zanurzano w 70% roztworze etanolu (C_2H_5OH, Sigma-Aldrich) na 10 minut – proces ten powtarzano trzykrotnie. Następnie próbki płukano, również trzykrotnie, przez 10 minut w roztworze buforu fosforanowego (PBS). Kolejnym etapem było napromieniowanie próbek zanurzonych w 1 ml PBS promieniowaniem UV (UBGI) przez 40 minut. Ekspozycja na promieniowanie UV pozwoliła na uzyskanie jałowości materiału, po czym próbki ponownie przepłukano roztworem PBS przez 10 minut. Następnie próbki kondycjonowano w podłożu Dulbecco's Modified Eagle Medium (DMEM, GIBCO) przez 10 minut, po czym inkubowano je w 1 ml DMEM z dodatkiem 10% surowicy płodowej bydlęcej (FBS, Thermo Scientific) oraz antybiotyków (100 U/ml penicyliny i 100 μg/ml siarczanu streptomycyny, Sigma-Aldrich). Po zakończeniu procedury, próbki stopów tytanu przechowywano przez kolejne 24 godziny w podłożu hodowlanym w temperaturze 37 °C. Każdą z linii komórkowych hodowano zgodnie z zaleceniami producenta, w temperaturze 37 °C, w podłożu DMEM. Przygotowane próbki oraz linie komórkowe wykorzystano do przeprowadzenia testu aktywności metabolicznej (test AlamarBlue, Thermo Fisher) po 24, 72 [JS4] oraz 168 godzinach [JS4]. Dla każdej z modyfikacji prezentowanych w pracach [JS4, JS5] wykonano trzy powtórzenia. Procedura testu AlamarBlue polegała na dodaniu barwnika AlamarBlue w objętości 10% objętości pożywki, a następnie inkubacji przez 90 minut. Pomiar fluorescencji wykonano przy użyciu czytnika mikropłytek BioTek Synergy HT. Ocena ilościowa DNA została wykonana z użyciem niebieskiego fluorochromu Hoechst 33258, zgodnie z zaleceniami producenta (Thermo Fisher, FluoReporter). Ocenę przyczepności komórek i ich namnażania na powierzchni próbek stopów tytanu przeprowadzono przy użyciu mikroskopu fluorescencyjnego Zeiss (Germany).

4. REZULTATY BADAŃ

4.1. Badania wstępne I – Wpływ modyfikacji hybrydowej łączącej technikę wytarzania warstw ceramicznych MAO oraz modyfikację laserową na strukturę bio-stopu tytanu Ti13Nb13Zr [SJS2]

Prace nad podwójną modyfikacją łączącą technikę przetapiania laserowego - laserem Nd:YAG oraz metodę wprowadzenia dodatków do bio stopów tytanu wykorzystując technikę mikrołukowego wytwarzania warstw ceramicznych (MAO) rozpoczęto od zaproponowania dwóch kombinacji tych modyfikacji. W pracy [JS2] wykonano modyfikację w kombinacji modyfikacja laserowa poprzedzająca proces MAO (laser-MAO) oraz w kombinacji, gdzie wytwarzano warstwę ceramiczną przed przetapianiem laserowym (MAO-laser). W pracy zastosowano zmienną moc lasera Nd:YAG (1000 W, 1500 W) przy stałych parametrach posuwu, czasu trwania impulsu lasera oraz częstotliwości dla każdej z kombinacji. W procesie mikrołukowego utleniania zaproponowano stałe parametry osadzania warstwy ceramicznej w zakresie napięcia, natężenia prądu i czasu trwania procesu. Wskazane parametry dobrano na podstawie przeglądu literaturowego oraz prób eksperymentalnych. Proces MAO prowadzony był w środowisku elektrolitu wodnego składającego się z wody destylowanej, wodorotlenku sodu oraz hydroksyapatytu, jako podstawowego składnika budującego kość, co propagować miało wytworzenie warstwy ceramicznej o charakterze aplikacyjnym zgodnym z wymaganiami biomateriałów.

Przeprowadzone badania wykazały, że wszystkie zaproponowane modyfikacje hybrydowe wykazują własności hydrofilowe powierzchni, co jest korzystne ze względy na potencjalne wykorzystanie materiału do celów implantologicznych, ponieważ hydrofilowa powierzchnia stymuluje do zwiększenia przyczepności komórek do materiału.
W pracy wykazano, że kombinacja laser-MAO powoduje zwiększenie chropowatości powierzchni względem materiału rodzimego, ale jest to parametr niższy niż dla kombinacji MAO-laser. Dla obu kombinacji stwierdzić można, co jest zgodne z literaturą, że wyższa moc lasera zwiększa chropowatość powierzchni. Istotnym jest także to, że skład chemiczny

warstwy wierzchniej wpływa na charakter zwilżalności powierzchni oraz żeobecność tlenu zwiększa zwilżalność.

Ważnym aspektem wynikającym z przedstawionych badań wstępnych jest to, że możliwe jest wytworzenie warstwy ceramicznej w procesie MAO bogatej w jony biozgodne, która charakteryzuje się porowatą postacią charakterystyczną dla warstw MAO.
Nie zaobserwowano dla takich warstw zwiększonej liczby pęknięć, szczelin i ubytków. Dla zaprojektowanego elektrolitu wykazano, że warstwa ceramiczna jest zbliżona swoją morfologią do warstwy referencyjnej, co jest dobrym wynikiem ponieważ pre-modyfikacja laserem pozwala na kontrolowaną modyfikację innych własności niż te, które są poprawiane przez wytwarzanie tlenków tytanu. Badania składu chemicznego dla modyfikacji laser-MAO wykazały, że ilość inkorporowanego wapnia dla próbki referencyjnej MAO (P2) jest zbliżona dla modyfikacji laser-MAO (P5), gdzie zastosowano moc lasera 1000W.

Dla modyfikacji w kombinacji laser-MAO wykazano, że moc lasera na poziomie 1500 W, a następnie wytworzenie warstwy ceramicznej jest gorszym typem modyfikacji niż ta sama kombinacja z mocą lasera 1000 W, ponieważ doszło do inkorporowania mniejszej ilości jonów biozgodnych a przyczepność warstwy MAO jest niższa (najniższa wartość parametru Lc – tab. 8 [JS2]). Po teście nanoindentacji wykazano również niższą twardość zmodyfikowanej powierzchni.

Kombinacja modyfikacji MAO-laser spowodowała, że ścieżka wiązki lasera, po badaniu mikroskopem optycznym, jest bardziej wyraźna, co wynika z procesu mieszania się warstwy tlenkowej z materiałem rodzimym. Dodatkowo wykazano, że wytworzenie warstwy ceramicznej MAO prowadzi do zwiększenia strefy wpływu ciepła w materiale,
a zastosowanie modyfikacji laserowej z mocą 1500 W powoduje, że twardość materiału jest niższa. Wykonane przekroje poprzeczne zmodyfikowanych warstw wierzchnich w kombinacji MAO-laser wskazują na bardzo intensywne mieszanie się ceramicznych warstw z materiałem rodzimym. Obserwowana jest wyraźna granica między warstwą wierzchnią a materiałem rodzimym, co nie jest charakterystyczne dla klasycznej modyfikacji laserowej Nd:YAG (P2).

Należy zauważyć, że wykonanie przekrojów poprzecznych dla kombinacji laser-MAO zobrazowało, iż warstwa ceramiczna dopasowuje się do ścieżki wiązki lasera i nie jest ona idealnie odcięta od warstwy wierzchniej materiału rodzimego. Dodatkowo zaobserwowano charakterystyczne kratery dla procesu MAO, co świadczy o występowaniu mirkowyładowań podczas procesu.

Przedstawione badania wstępne wskazują cechy morfologiczne uzyskanych warstw wierzchnich, przedstawiają ich własności mechaniczne, fizyczne w zakresie morfologii, strefy wpływu ciepła, charakteru warstwy pod względem zwilżalności i chropowatości. Kluczowe jest, że zaprezentowane modyfikacje są skrajnie różne od siebie pod względem własności, a szczególną uwagę należy zwrócić na fakt, że nie podjęto się przestawienia wyników EDS dla próbek P7-P8 ze względu na brak obserwowalności dodatków w postaci jonów sodu, czy wapnia w tym badaniu. Może to świadczyć o całkowitym przetopieniu warstwy ceramicznej, co wiąże się bezpośrednio z uzyskaniem mniej rozwiniętej powierzchni, co ze względów aplikacyjnych jest ważne ponieważ w implantologii dąży się do uzyskania powierzchni biomimetycznych.

Istotne dla przedstawionych badań jest to, że:

- Możliwe jest wytworzenie warstwy ceramicznej MAO (P5-P6 [JS2]) na wcześniej przetopionej laserem Nd:YAG powierzchni stopu Ti13Nb13Zr o podobnej ilości inkorporowanych pierwiastków jak warstwy referencyjne (P2). Potwierdzono także możliwość wytworzenia jednorodnej, pozbawionej pęknięć warstwy ceramicznej MAO.
- Przeprowadzenie modyfikacji MAO-laser pozwala uzyskać warstwę wierzchnią stopu Ti13Nb13Zr charakteryzującą się wysoką twardością w wyniku mieszania się materiału rodzimego z ceramiką wytworzoną w procesie mirkrołukowego utleniania.

4.2. Badania wstępne II w zakresie odporności na korozję i składu chemicznego zaproponowanych modyfikacji stopu tytanu Ti13Nb13Zr [JS3]

Badania wstępne zaproponowanych dwóch typów modyfikacji hybrydowej w dwóch kombinacjach zostały rozszerzone o analizy odporności materiału na korozję, badania składu chemicznego oraz identyfikację wiązań występujących w zmodyfikowanych materiałach. Dodatkowo, w celu oceny odporności materiału na degradację korozyjną, przeprowadzono test zanurzeniowy trwający 14 dni.

Analiza wyników spektroskopii w podczerwieni z transformatą Fouriera (FTIR) wykazała obecność wiązań fosforanowych pochodzących od hydroksyapatytu, który był składnikiem elektrolitu użytego w procesie MAO. Stwierdzono również obecność związków tlenków tytanu tworzących warstwę ceramiczną. Dla próbek po podwójnej modyfikacji liczba tych wiązań była większa niż w próbkach referencyjnych, ponieważ zarówno proces laserowy, jak i MAO wiążą się z utlenianiem stopu tytanu.

W przeprowadzonych badaniach EDS na przekroju poprzecznym wykazano, że dla podwójnej modyfikacji w kombinacjach laser–MAO oraz MAO–laser obecne są jony sodu. Natomiast w przypadku jonów wapnia ich obecność nie została potwierdzona w próbkach, w których warstwa ceramiczna MAO została przetopiona wiązką lasera.

Badania składu chemicznego warstwy wierzchniej wykazały, że jony wapnia są obecne w obu kombinacjach, jednak po przeprowadzeniu testu zanurzeniowego (14 dni) nie były one już obserwowane w próbkach, w których warstwa MAO została przetopiona.

Rezultaty testu wskazują, że zmodyfikowany materiał wykazuje bioaktywność, ponieważ na zdjęciach SEM oraz na podstawie analizy EDS zaobserwowano tworzenie się aglomeratów soli na powierzchni materiałów poddanych modyfikacji. Zaobserwowano większe aglomeraty w przypadku modyfikacji w układzie laser–MAO, przy czym największą odpowiedź bioaktywną w teście zanurzeniowym prowadzonym w stężonym buforze fosforanowym (PBS) uzyskano dla modyfikacji laserem o mocy 1000 W.

Bardzo istotnym aspektem aplikacyjnym biomateriałów są badania odporności na korozję. Zostały one przeprowadzone dla każdej z modyfikacji, a ich rezultaty wskazują, że hybrydowa modyfikacja w układzie laser–MAO, z zastosowaniem lasera Nd:YAG o mocy 1000 W, charakteryzuje się najwyższą wartością potencjału korozyjnego Ecorr – na poziomie ok. -212×10^{-3} V. Dla porównania, modyfikacje pojedyncze, zarówno laserowa, jak i z wykorzystaniem powłok ceramicznych MAO, wykazały niższą odporność na korozję niż próbka referencyjna. Zebrane wyniki dostarczają informacji, że zastosowanie podwójnej modyfikacji jest skuteczne w poprawie właściwości funkcjonalnych stopu tytanu Ti13Nb13Zr.

Reasumując, wykonanie badań składu chemicznego na przekrojach poprzecznych materiału, analizy wiązań chemicznych po modyfikacjach oraz oceny odporności korozyjnej pozwoliły na kompleksową ocenę zaproponowanych typów modyfikacji z uwzględnieniem dwóch kombinacji i zmiennych parametrów mocy lasera.

Istotne jest to, że

- Otrzymano warstwy wierzchnie stopu Ti13Nb13Zr wzbogacone o wybrane jony pochodzące ze środowiska elektrolitu zarówno dla kombinacji laser–MAO, jak i MAO–laser. Istotne jest podkreślenie, że przetopienie warstwy ceramicznej znacząco obniża stężenie jonów inkorporowanych podczas procesu MAO, co skutkuje uboższą warstwą wierzchnią materiału. Nie wyklucza to jednak możliwości wzbogacania materiału w wybrane pierwiastki dostosowane do konkretnych wymagań implantologicznych.
- Zastosowanie podwójnej modyfikacji, w której laser został użyty jako wstępny etap przed procesem MAO, okazało się najskuteczniejszym spośród analizowanych podejść w kontekście zwiększenia odporności korozyjnej stopu tytanu Ti13Nb13Zr.

Wykonane badania i ich krytyczna analiza dostarczyły wiedzy na temat wpływu modyfikacji laserowej oraz zastosowania dodatków w postaci jonów inkorporowanych w procesie mikrołukowego utleniania na właściwości funkcjonalne badanego materiału – stopu tytanu Ti13Nb13Zr – w kontekście jego potencjalnych zastosowań biomedycznych.

4.3. Podsumowanie badań wstępnych [JS2], [JS3]

Na podstawie przeprowadzonych badań wstępnych – mechanicznych, chemicznych i fizycznych – dotyczących zaproponowanej modyfikacji stopu tytanu Ti13Nb13Zr, a następnie ich krytycznej analizy, możliwe było wyłonienie najbardziej efektywnej kombinacji dwóch technik modyfikacji powierzchni. Wybrana konfiguracja stanowi podstawę do dalszych badań nad wpływem modyfikacji laserowej (przeprowadzonej z użyciem lasera neodymowo-jagowego Nd:YAG) oraz dodatków wprowadzanych podczas tworzenia warstwy ceramicznej metodą (MAO.

Najlepsze właściwości funkcjonalne uzyskano dla kombinacji, w której pierwszym etapem była modyfikacja laserowa (tzw. pre-treatment), a następnie utlenianie warstwy wierzchniej w procesie MAO. Takie podejście umożliwia nie tylko kontrolowane przetapianie i rozwijanie morfologii powierzchni, lecz także tworzenie porowatej warstwy ceramicznej wzbogaconej jonami o znaczeniu biologicznym, takimi jak jony sodu czy grupy apatytowe, istotnymi w kontekście zastosowań implantologicznych.

Oprócz wskazania kombinacji laser–MAO jako najbardziej perspektywicznej, zidentyfikowano również optymalne parametry pracy lasera Nd:YAG, które umożliwiają uzyskanie jednorodnych warstw ceramicznych MAO na materiale uprzednio poddanym modyfikacji laserowej. Parametry te, wykorzystane w dalszych eksperymentach, to:

I. Moc wiązki lasera Nd:YAG: 1000W
II. Czas trwania impulsu lasera: 2,25 ms
III. Częstotliwość pracy: 25Hz
IV. Posuw lasera: 6 mm/s

4.4. Badania nad nową kombinacją elektrolitów wprowadzających jony cynku do warstw ceramicznych nanoszonych na laserowo zmodyfikowany stop tytanu Ti13Nb13Zr [JS4]

Po przeprowadzeniu kompleksowych badań dla różnych kombinacji modyfikacji dwiema technikami — wysokotemperaturową techniką modyfikacji laserowej laserem Nd:YAG oraz techniką mikrołukowego utleniania warstw— wybrano jedną kombinację do dalszych badań w kolejności modyfikacji laser-MAO. Dla modyfikacji laserowej wybrano tylko jeden parametr pracy urządzenia Nd:YAG. Natomiast w pracy [JS4] skupiono się na skomponowaniu elektrolitu zawierającego jony cynku pochodzące z octanu cynku w połączeniu z NaOH (elektrolit 1), natomiast drugi elektrolit (elektrolit 2) łączył bazę z poprzednich prac [JS2], [JS3] z dodatkiem octanu cynku. Proces MAO prowadzony był dla różnych czasów trwania procesu (7 i 15 minut), przy jednakowym napięciu i natężeniu prądu.

Podstawowe badania jakościowe SEM wykazały, że możliwe jest wytworzenie ceramicznych warstw o charakterystycznej morfologii MAO dla elektrolitu 1 na wcześniej zmodyfikowanym wiązką lasera stopie tytanu Ti13Nb13Zr. Morfologia mikrostruktury jest rozbudowana i nie wykazuje pęknięć, ubytków ani nierówności na powierzchni materiału. Dla podwójnej modyfikacji zaobserwowano dla elektrolitu 1 bardziej regularną powierzchnię niż dla modyfikacji pojedynczej. Dla elektrolitu 2 nie udało się wytworzyć warstwy ceramicznej MAO o charakterystycznej jednorodnej budowie z występującymi regularnymi porami (przykładowo jak w artykułach [17,58,59]). Skomponowany elektrolit 2 nie pozwala uzyskać charakterystycznej budowy warstw MAO, wytworzono ceramiczną warstwę z kraterami, a dla dłuższego czasu osadzania (15 min) zaobserwowano większą porowatość mikrostruktury. Badania grubości warstwy modyfikowanej wykazały, że dla modyfikacji podwójnej dla elektrolitu 1 otrzymano najgrubsze warstwy.

Dla zaproponowanych modyfikacji wykonano szczegółowe badania związane z określeniem stanów energetycznych pierwiastków chemicznych występujących w warstwach MAO oraz wskazano na występujące wiązania.

Badanie XPS pozwoliło określić, że w ceramicznych warstwach cynk występuje w formie tlenku oraz wodorotlenku i tworzy on dwie pary dubletów. Wykazanie obecności tego pierwiastka było bardzo ważne dla przeprowadzonego eksperymentu ze względu na założone wzbogacenie stopu tytanu Ti13Nb13Zr o te jony w celu zwiększenia biokompatybilności i bioaktywności materiału. Istotne jest, że w spektrach XPS zaobserwowano stany energetyczne dla wszystkich pierwiastków obecnych w roztworach wodnych elektrolitu 1 oraz 2. Dla próbek z hydroksyapatytem wykazano także powiązania grup fosforanowych z cynkiem w warstwie ceramicznej MAO (ZnHAp2L – Zn3(PO4)2). Szczegółowe badania FTIR wiązań w warstwach potwierdziły dla modyfikacji przeprowadzanej w elektrolicie 2 występowanie licznych wiązań wskazujących na inkorporację hydroksyapatytu do warstwy ceramicznej. Dodatkowo, zarówno dla elektrolitu 1, jak i 2 wykazano obecność wiązań węglowych pochodzących od octanu wapnia. Wykazano, że dłuższy czas prowadzenia procesu MAO (15 minut) propaguje większą ilość wiązań w materiale, co może świadczyć o bardziej bioaktywnej powierzchni materiału.

Dla przeprowadzonych w pracy [JS4] modyfikacji wykazano, że charakter powierzchni materiału jest hydrofobowy, ponieważ wartość kąta zwilżania waha się dla podwójnych, hybrydowych modyfikacji między 80 a 90°. Uzyskane wartości kąta zwilżania dla próbek wytworzonych w elektrolitach zaprojektowanych na potrzeby pracy [JS4] do wytworzenia warstw ceramicznych na zmodyfikowanej laserowo warstwie różnią się w odniesieniu do charakteru powierzchni w pracy [JS2]. Zmiana wyników może wynikać z obecności jonów cynku, które umożliwiają zmniejszenie zwilżalności powierzchni. Szczegółowe badania chropowatości wykazały, że występują istotne różnice między powierzchniami poddanymi pojedynczej a hybrydowej modyfikacji. Modyfikacja podwójna prowadziła do większego rozwinięcia topografii, wyrażonego wyższymi wartościami parametrów chropowatości (Sa, Sv), co sprzyja osteointegracji poprzez zwiększenie powierzchni kontaktu implantu z tkanką kostną. Jednocześnie zastosowanie obróbki laserowej przed procesem MAO zmniejszało anizotropię i liczbę ostrych wierzchołków na powierzchni, ograniczając tym samym potencjalne mikrouszkodzenia tkanek.

Tak jak w pracy [JS3] skupiono się na odporności korozyjnej zmodyfikowanego materiału stopu Ti13Nb13Zr. W pracy [JS4] wykonano pogłębione badania elektrochemiczne dla przeprowadzonych modyfikacji. Skupiono się na badaniach EIS prowadzonych dla próbek inkubowanych w roztworze Hanksa przez 168 h, gdzie rejestrowano zmiany elektrochemiczne w określonych cyklach. Podstawowym parametrem, który został określony, była wartość potencjału otwartego (OCP). Wykazano, że każda z modyfikacji wykazała wyższą wartość tego potencjału względem próbki referencyjnej stopu tytanu Ti13Nb13Zr, co oznacza, że charakteryzują się one mniejszą skłonnością materiału do korozji. Na podstawie uzyskanych wyników [JS4] wykazano, że wszystkie próbki zawierające w warstwie ceramicznej hydroksyapatyt poprawiają odporność korozyjną, a wydłużony czas trwania procesu dodatkowo poprawia tę właściwość (najlepsze wyniki uzyskano dla próbki hybrydowo zmodyfikowanej, gdzie proces MAO przeprowadzono w elektrolicie 2 przez 15 min). Wykresy przedstawiające pętle pojemnościowe dla badań elektrochemicznej spektroskopii impedancyjnej wykazują, że zastosowanie modyfikacji laserowej przed procesem mikrołukowego utleniania dla stopu tytanu Ti13Nb13Zr poprawia odporność korozyjną.

Ze względu na potencjalne wykorzystanie stopu tytanu Ti13Nb13Zr poddanego modyfikacjom w przemyśle implantologicznym kluczowym było przeprowadzenie wstępnych testów cytokompatybilności i aktywności biologicznej. Dla tej pracy wybrano linię komórkową C166-GFP. Badania mikroskopii fluorescencyjnej wykonane po 24 h od inkubacji komórek na powierzchni zmodyfikowanego materiału wykazały najlepszą odpowiedź komórkową dla próbki zmodyfikowanej tylko laserem Nd:YAG. Początkowe wyniki dla podwójnej modyfikacji wskazywały na komórki w formie kulistej, co mogło sugerować apoptozę, jednakże po upływie 72 h zaobserwowano dla tej modyfikacji hybrydowej obecność żywych komórek. Test AlamarBlue (aktywności metabolicznej komórek) wykazał, że pojedyncza modyfikacja laserowa najlepiej wpływa na aktywność komórek, a także odnotowano najlepsze wyniki dla ilościowego badania DNA. Literatura także potwierdziła, że modyfikacja laserowa ułatwia proliferację i adhezję komórek do materiału. Dla badania ilościowego DNA zanotowano także dobre wyniki dla modyfikacji hybrydowej, przy czym najlepsze wyniki dała próbka poddana modyfikacji podwójnej, gdzie warstwa ceramiczna została wytworzona w środowisku elektrolitu 2 przez 15 min. Stwierdzono, że obecność hydroksyapatytu wpływa na wzrost komórek, dla jonów cynku nie zaobserwowano negatywnego wpływu tego pierwiastka, więc jego stężenie było odpowiednie, co jest także potwierdzone w literaturze, że dobrze dobrane stężenie jonów cynku ułatwia aktywność komórkową i proliferację. Dodatkowo sama obecność warstwy MAO, która jest porowatą strukturą, propaguje dobre zachowanie komórek na powierzchni, ponieważ pory tej warstwy ceramicznej stanowią miejsce zakotwiczenia wypustek cytoplazmatycznych komórek.

Podsumowując, możliwe jest wytworzenie na zmodyfikowanym laserowo stopie tytanu Ti13Nb13Zr warstwy ceramicznej w procesie MAO w środowisku elektrolitów zawierających jony cynku, sodu oraz związek hydroksyapatytu. Morfologia powierzchni dla próbek warstwy ceramicznej MAO dla elektrolitu 1 [JS4] jest morfologią oczekiwaną od warstw MAO, natomiast zbadane właściwości sugerują konieczność stosowania dodatku hydroksyapatytu w celu uzyskania lepszej odporności na korozję, a także biokompatybilności. Obecność jonów cynku w warstwie powoduje zmianę charakteru zwilżalności w kierunku hydrofobowego. Wydłużenie czasu trwania procesu MAO pozwala na uzyskanie grubszych warstw ceramicznych na zmodyfikowanym stopie tytanu Ti13Nb13Zr oraz wpływa pozytywnie na wybrane właściwości funkcjonalne materiału.

Istotnym jest, iż:

- W pracy wytworzono materiał zmodyfikowany hybrydowo przy wykorzystaniu techniki przetapiania laserem Nd:YAG w połączeniu z techniką wytwarzania warstw ceramicznych MAO dla dwóch różnych elektrolitów, przy różnych czasach trwania procesu.
- Stwierdzono, że obecność jonów cynku zmienia charakter zwilżalności powierzchni, a podwójna modyfikacja wpływa na rozbudowę morfologii powierzchni, co ma znaczenie aplikacyjne.
- Zastosowanie modyfikacji laserowej poprawia odporność na korozję, a połączenie techniki przetapiania z techniką MAO daje

jeszcze lepsze wyniki odporności na korozję.

- Wydłużenie czasu trwania procesu MAO pozytywnie wpływa na wybrane właściwości materiału.
- Obecność związków apatytowych sprzyja proliferacji komórek, a także poprawia odporność na korozję.
- Zastosowanie hybrydowej modyfikacji na stopie tytanu Ti13Nb13Zr daje dobre wyniki biokompatybilności materiału, ale wymaga dopracowania składu elektrolitów tak, aby otrzymywane warstwy były jednorodne w swojej budowie.

Przedstawione wyniki dają obiecujące perspektywy dla zastosowań aplikacyjnych. Najważniejszym osiągnięciem tej pracy jest uzyskanie pozytywnej odpowiedzi komórkowej linii C166-GFP dla podwójnej modyfikacji stopu tytanu Ti13Nb13Zr w kombinacji laser-MAO, a także zwiększenie odporności na korozję oraz rozwinięcie morfologii powierzchni materiału.

4.5. Badania zmian własności komercyjnie stosowanego stopu tytanu Ti6Al4V przy zastosowaniu modyfikacji hybrydowej laser MAO

Ostatnia praca z cyklu publikacji [JS5] stanowiła kontynuację modyfikacji z zastosowaniem jonów cynku (nanotlenek cynku), sodu i fosforu inkorporowanych do warstwy ceramicznej MAO na materiale zmodyfikowanym laserem Nd:YAG, jednakże zastosowano tutaj komercyjnie stosowany stop tytanu Ti6Al4V. Kluczowe dla realizacji celów pracy doktorskiej było zbadanie materiału, który jest już wykorzystywany w implantologii. Modyfikację laserową laserem neodymowo-jagowym prowadzono ponownie dla najlepszych parametrów określonych na podstawie prac [JS2] oraz [JS3], natomiast wytwarzanie warstw ceramicznych przebiegało w dwóch elektrolitach o różnym składzie. Elektrolit 1 zawierał fosforan sodu oraz wodorotlenek sodu (czas trwania procesu 10 i 15 min), elektrolit 2 wzbogacony został o proszek nanotlenku cynku (czas trwania procesu MAO 10 min).

Skaningowa mikroskopia elektronowa posłużyła do oceny jakościowej

morfologii powierzchni hybrydowo modyfikowanego stopu tytanu Ti6Al4V. Stwierdzono, że zastosowanie modyfikacji laserowej przed procesem MAO spowodowało uzyskanie bardziej jednorodnych warstw ceramicznych względem pojedynczych modyfikacji referencyjnych. Obecność w elektrolicie nanotlenku cynku poprawiła jednorodność powierzchni, a wydłużenie czasu trwania procesu MAO sprzyjało powstaniu większych porów. Podobnie jak w przypadku wyników kąta zwilżania dla pracy [JS4] wykazano,
że obecność jonów cynku w warstwie ceramicznej wytworzonej na zmodyfikowanej laserowo powierzchni powoduje zmianę zwilżalności na bardziej hydrofobową, natomiast podwójna modyfikacja dla elektrolitu 1 spowodowała zmniejszenie kąta zwilżania, czyli zwiększenie zwilżalności w porównaniu do próbek referencyjnych.

Zbadano także wpływ modyfikacji laserowej laserem Nd:YAG na stop tytanu Ti6Al4V. Określono, że strefa wpływu ciepła ma głębokość 204 μm, co w odniesieniu do głębokości strefy wpływu ciepła dla stopu tytanu Ti13Nb13Zr (głębokość strefy wpływu ciepła = 67,20 μm) jest wartością większą. Wynika to z faktu, że stop zawierający aluminium i wanad jest materiałem mniej twardym niż stop z cyrkonem i niobem.

W celu ustalenia odpowiedzi komórkowej dla zaproponowanych modyfikacji hybrydowych wykorzystano linię komórkową C2C12 do badania mobilności komórek i ich oceny pod mikroskopem fluorescencyjnym. Dla podwójnej modyfikacji wykazano najlepszą odpowiedź komórkową dla modyfikacji, gdzie wytworzono warstwę ceramiczną w elektrolicie 1 w czasie 15 min. Natomiast dla stopu tytanu Ti6Al4V poddanego tylko modyfikacji laserowej zaobserwowano najlepszą odpowiedź komórkową, co potwierdzono zdjęciami fluorescencyjnymi i wynikami testu AlamarBlue. Dla materiału Ti13Nb13Zr w pracy [JS4] również wskazano, że rozwinięta morfologia powierzchni zmodyfikowanej tylko laserowo sprzyja proliferacji i adhezji komórek. Na podstawie obrazów SEM w pracy [JS5] można wnioskować, że wytworzona warstwa MAO charakteryzuje się zbyt małymi porami dla zakotwiczenia cytoplazmatycznych wypustek komórek linii C2C12.

Badania elektrochemiczne EIS w warunkach zanurzeniowych w roztworze Hanksa wykazały, że dla komercyjnego stopu tytanu nie wskazuje się, aby modyfikacja hybrydowa znacząco poprawiała odporność korozyjną. Najwyższe wartości modułu impedancji wykazała próbka stopu tytanu Ti6Al4V, co oznacza najlepsze właściwości antykorozyjne.

Reasumując istotne jest, że:

- Wytworzono ceramiczną warstwę w procesie MAO przeprowadzonym na uprzednio zmodyfikowanej laserowo powierzchni stopu Ti6Al4V.
- Odporność korozyjna dla podwójnej modyfikacji okazała się niższa w porównaniu do pojedynczych modyfikacji.
- Najlepszą odpowiedź komórkową linii C2C12 uzyskano dla próbek po modyfikacji laserowej oraz dla hybrydowo modyfikowanej powierzchni, w której proces MAO prowadzono przez 15 minut.
- Przeprowadzenie modyfikacji hybrydowej, która przynosiłaby więcej korzyści dla zastosowań biomedycznych, wymaga dalszych badań i zaprojektowania bardziej efektywnego środowiska procesu MAO.

PODSUMOWANIE

Przeprowadzone badania wykazały, że możliwe jest zastosowanie dwóch technik modyfikacji, które w połączeniu nadają cechy stopom tytanu, które są wymagane od biomatreiałów. W cyklu publikacji wskazano optymalną kombinację modyfikacji składającej się z techniki przetapiania laserowego laserem Nd:YAG poprzedzającej proces mikrołukowego wywtwarzania warstw ceramicznych na podłożu metalowym. Konfiguracja MAO-laser została odrzucona ze względu na brak znaczących zmian w składzie chemicznym zmodyfikowanej powierzchni, powierzchnia ta jest mniej rozwinięta morfologicznie w porównaniu do wytworzonej warstwy MAO na zmodyfikowanym laserowo materiale.

Badania wstępne pozwoliły na wskazanie najlepszych parametrów modyfikacji laserem Nd:YAG modyfikacji stopu tytanu. Wykazano, że moc wiązki lasera na poziomie 1000 W jest najlepszym parametrem, który pozwoli na wytworzenie jak najlepszej kombinacji technik laser-MAO.

Udowodniono, że warstwa ceramiczna MAO wytworzona na zmodyfikowanej laserowej powierzchni stopu tytanu Ti13Nb13Zr wykazuje większą przyczepność do podłoża w stosunku do wytwarzanej ceramiki na niezmodyfikowanym stopie tytanu.

Wykazano w badaniach wstępnych wpływ hybrydowej modyfikacji na charakter zwilżalności powierzchni i chropowatości. Dalsze badania wykazały, że skład chemiczny warstwy ceramicznej wpływa znacząco na hydrofobowość lub hydrofilowość powierzchni materiału modyfikowanego.

Osiągnięciem dla prowadzonych badań było otrzymanie hybrydowo zmodyfikowanego stopu Ti13Nb13Zr wzbogaconego o bio dodatki inkorporowane w procesie MAO, który wykazał dobrą odpowiedź komórkową podczas badań cytokompatybilności. Optymalną odpowiedź otrzymano dla modyfikacji laser-MAO dla procesu MAO prowadzonego w dłuższym czasie, co oznacza, że dłuższy czas propaguje adhezję komórek do powierzchni. Wykazano, że obecność hydroksyapatytu jest kluczowa dla prawidłowej i intensywnej proliferacji komórek na powierzchni Ti13Nb13Zr.

Wykazano, że wpływ laserowego przetapiania warstwy wierzchniej stopu

Ti6Al4V jest znaczący, ponieważ względem stopu Ti13Nb13Zr strefa wpływu ciepła jest około dwa razy większa. Zaprojektowany elektrolit wykorzystany w procesie MAO dla stopu tytanu Ti6Al4V pozwolił na inkorporowanie jonów cynku do warstwy ceramicznej. Wykazano, że dla tego materiału obecność hydroksyapatytu nie wpłynęła znacząco na odpowiedź komórkową stopu a najlepsze własności biologiczne wykazano tylko dla modyfikacji laserowej oraz dla modyfikacji podwójnej dla elektrolitu wzbogaconego o nanotlenek cynku. W odróżnieniu dla stopu Ti13Nb13Zr przeprowadzone modyfikacje hybrydowe dla Ti6AL4V nie poprawiły odporności na korozję. Wynikać to mogło z bardzo niejednorodnej budowy warstw ceramicznych wytworzonych na modyfikowanych laserowo powierzchniach.

Podsumowując przeprowadzone badania i analiza ich wyników przedstawiona w publikacjach [JS2], [JS3], [JS4], [JS5] pozwoliła na udowodnienie tezy postawionej w pracy. Udowodniono, że zastosowana podwójna modyfikacja łącząca technikę przetapiania laserowego oraz techniki MAO pozwoliła na zwiększenie odporności na korozję stopu tytanu Ti13Nb13Zr, przy czym tak pozytywnego efektu nie odnotowano dla stopu Ti6Al4V. Modyfikacja pozwoliła na rozwinięcie morfologiczne powierzchni, co wpłynęło bezpośrednio na charakter zwilżalności, chropowatość i skład chemiczny stopów tytanu. Udowodniono także, że modyfikacja laserowa wpływa pozytywnie na aktywność komórkową zarówno dla stopu Ti13Nb13Zr i Ti6Al4V, a właściwie skomponowane środowisko prowadzenia procesu MAO pozwala na inkorporowanie dodatków, które także stymulują proliferację i adhezję komórek.

Istotne jest, że przeprowadzone badania i eksperymenty pozwoliły na zrealizowanie wszystkich postawionych celów pracy. Jednocześnie rozwinięty temat modyfikacji hybrydowej łączącej technikę przetapiania powierzchni wiązką lasera Nd:YAG oraz procesu MAO daje dalsze możliwości do poprawiania własności użytkowych stopów tytanu tak aby spełnić wymagania stawiane biomateriałom.

BIBLIOGRAFIA

[1] H.S. Alghamdi, J.A. Jansen, The development and future of dental implants, Dent Mater J 39 (2020) 167–172. https://doi.org/10.4012/dmj.2019-140.

[2] Y. Mooiweer, I. van den Akker-Scheek, M. Stevens, Amount and type of physical activity and sports from one year forward after hip or knee arthroplasty—A systematic review, PLoS One 16 (2021). https://doi.org/10.1371/journal.pone.0261784.

[3] J. Dudley, Implants for the ageing population, Aust Dent J 60 (2015) 28–43. https://doi.org/10.1111/adj.12282.

[4] Informacja o sytuacji osob starszych w Polsce za 2023 r., (n.d.).

[5] Narodowy Fundusz Zdrowia, Realizacja świadczeń endoprotezoplastyki stawowej w 2018 r., (2018) 1–20.

[6] T. Albrektsson, P. Tengvall, L. Amengual, P. Coli, G.A. Kotsakis, D. Cochran, Osteoimmune regulation underlies oral implant osseointegration and its perturbation, Front Immunol 13 (2023). https://doi.org/10.3389/fimmu.2022.1056914.

[7] Y. Liu, B. Rath, M. Tingart, J. Eschweiler, Role of implants surface modification in osseointegration: A systematic review, J Biomed Mater Res A 108 (2020) 470–484. https://doi.org/10.1002/jbm.a.36829.

[8] K. Kong, Y. Chang, Y. Hu, H. Qiao, C. Zhao, K. Rong, P. Zhang, J. Zhang, Z. Zhai, H. Li, TiO2 Nanotubes Promote Osteogenic Differentiation Through Regulation of Yap and Piezo1, Front Bioeng Biotechnol 10 (2022) 1–13. https://doi.org/10.3389/fbioe.2022.872088.

[9] A. Stróż, B. Łosiewicz, M. Zubko, B. Chmiela, K. Balin, G. Dercz, M. Gawlikowski, T. Goryczka, Production, structure and biocompatible properties of oxide nanotubes on Ti13Nb13Zr alloy for medical applications, Mater Charact 132 (2017) 363–372. https://doi.org/10.1016/j.matchar.2017.09.004.

[10] P. Handzlik, K. Gutkowski, Synthesis of oxide nanotubes on Ti13Nb13Zr alloy by the electrochemical method, Journal of Porous Materials 26 (2019) 1631–1637. https://doi.org/10.1007/s10934-019-00759-1.

[11] A. Sharma, J.N. Waddell, K.C. Li, L. A Sharma, D.J. Prior, W.J. Duncan, Is titanium–zirconium alloy a better alternative to pure titanium for oral implant? Composition, mechanical properties, and microstructure analysis, Saudi Dental Journal 33 (2021) 546–553. https://doi.org/10.1016/j.sdentj.2020.08.009.

[12] L.C. Zhang, L.Y. Chen, L. Wang, Surface Modification of Titanium and Titanium Alloys: Technologies, Developments, and Future Interests, Adv Eng Mater 22 (2020) 1–37. https://doi.org/10.1002/adem.201901258.

[13] M. Hatakeyama, N. Masahashi, Y. Michiyama, H. Inoue, S. Hanada, Wear resistance of surface-modified TiNbSn alloy, J Mater Sci 56 (2021) 14333–14347. https://doi.org/10.1007/s10853-021-06213-5.

[14] L. Wang, J. Zhou, J. Liang, J. Chen, Microstructure and corrosion behavior of plasma electrolytic oxidation coated magnesium alloy pre-treated by laser surface melting, Surf Coat Technol 206 (2012) 3109–3115. https://doi.org/10.1016/j.surfcoat.2011.12.040.

[15] Y. Wang, H. Yu, C. Chen, Z. Zhao, Review of the biocompatibility of micro-arc oxidation coated titanium alloys, Mater Des 85 (2015) 640–652. https://doi.org/10.1016/j.matdes.2015.07.086.

[16] M. Shimabukuro, Antibacterial property and biocompatibility of silver, copper, and zinc in titanium dioxide layers incorporated by one-step micro-arc oxidation: A review, Antibiotics 9 (2020) 1–13. https://doi.org/10.3390/antibiotics9100716.

[17] M. Dziaduszewska, M. Shimabukuro, T. Seramak, A. Zielinski, T. Hanawa, Effects of micro-arc oxidation process parameters on characteristics of calcium-phosphate containing oxide layers on the selective laser melted Ti13Zr13Nb alloy, Coatings 10 (2020) 1–24. https://doi.org/10.3390/COATINGS10080745.

[18] B. Makurat-Kasprolewicz, A. Ossowska, Recent advances in electrochemically surface treated titanium and its alloys for biomedical applications: A review of anodic and plasma electrolytic oxidation methods, Mater Today Commun 34 (2023). https://doi.org/10.1016/j.mtcomm.2023.105425.

[19] H. Fujii, K. Takahashi, Y. Yamashita, Application of titanium and its alloys for automobile parts, Nippon Steel Technical Report 02003 (2003) 70–75.

https://doi.org/10.1051/matecconf/202032102003.

[20] A.H. Assari, B. Eghbali, Solid state diffusion bonding characteristics at the interfaces of Ti and Al layers, J Alloys Compd 773 (2019) 50–58. https://doi.org/10.1016/j.jallcom.2018.09.253.

[21] V.M. Tabie, C. Li, W. Saifu, J. Li, X. Xu, Mechanical properties of near alpha titanium alloys for high-temperature applications - a review, Aircraft Engineering and Aerospace Technology 92 (2020) 521–540. https://doi.org/10.1108/AEAT-04-2019-0086.

[22] A.M. Elshazli, R.N. Elshaer, A.H.A. Hussein, S.R. Al-Sayed, Erratum: Elshazli et al. laser surface modification of TC21 (α/β) titanium alloy using a direct energy deposition (DED) process. (Micromachines 2021, 12, 739), Micromachines (Basel) 12 (2021). https://doi.org/10.3390/mi12091078.

[23] A.M. Khorasani, M. Goldberg, E.H. Doeven, G. Littlefair, Titanium in Biomedical Applications — Properties and Fabrication : A Review, 5 (2015) 593–619. https://doi.org/10.1166/jbt.2015.1361.

[24] H. Koizumi, Y. Takeuchi, H. Imai, T. Kawai, T. Yoneyama, Application of titanium and titanium alloys to fixed dental prostheses, J Prosthodont Res 63 (2019) 266–270. https://doi.org/10.1016/j.jpor.2019.04.011.

[25] I. Watanabe, M. McBride, P. Newton, K.S. Kurtz, Laser surface treatment to improve mechanical properties of cast titanium, Dental Materials 25 (2009) 629–633. https://doi.org/10.1016/j.dental.2008.11.006.

[26] F.A. Shah, M.L. Johansson, O. Omar, H. Simonsson, A. Palmquist, P. Thomsen, Laser-modified surface enhances osseointegration and biomechanical anchorage of commercially pure titanium implants for bone-anchored hearing systems, PLoS One 11 (2016) 1–24. https://doi.org/10.1371/journal.pone.0157504.

[27] G.Y. Liu, J. Hu, Z.K. Ding, C. Wang, Bioactive calcium phosphate coating formed on micro-arc oxidized magnesium by chemical deposition, Appl Surf Sci 257 (2011) 2051–2057. https://doi.org/10.1016/j.apsusc.2010.09.050.

[28] Y. Wang, D. Lu, G. Wu, K. Chen, H. Wu, Q. Zhang, J. Yao, Effect of laser surface remelting pretreatment with different energy density on MAO bioceramic coating, Surf Coat Technol 393 (2020) 125815. https://doi.org/10.1016/j.surfcoat.2020.125815.

[29] X. He, X. Zhang, X. Wang, L. Qin, Review of Antibacterial Activity of Titanium-Based Implants' Surfaces Fabricated by Micro-Arc Oxidation, Coatings 7 (2017) 45. https://doi.org/10.3390/coatings7030045.

[30] T. Hanawa, Biocompatibility of titanium from the viewpoint of its surface, Sci Technol Adv Mater 23 (2022) 457–472. https://doi.org/10.1080/14686996.2022.2106156.

[31] M.B. P. Tęczar, B. Majkowska-Marzec, THE INFLUENCE OF LASER ALLOYING OF Ti13Nb13Zr ON SURFACE TOPOGRAPHY AND PROPERTIES, Advances in Material Science 19 (2019) 45–55. https://doi.org/10.2478/adms-2019-0004.

[32] H.D. Nguyen, A. Pramanik, A.K. Basak, Y. Dong, C. Prakash, S. Debnath, S. Shankar, I.S. Jawahir, S. Dixit, D. Buddhi, A critical review on additive manufacturing of Ti-6Al-4V alloy: Microstructure and mechanical properties, Journal of Materials Research and Technology 18 (2022) 4641–4661. https://doi.org/10.1016/j.jmrt.2022.04.055.

[33] K. PIOTROWSKA, M. MADEJ, D. OZIMINA, ASSESSMENT OF TRIBOLOGICAL PROPERTIES OF Ti13Nb13Zr TITANIUM ALLOY USED IN MEDICINE, Tribologia 285 (2019) 97–106. https://doi.org/10.5604/01.3001.0013.5440.

[34] G. Menci, A. Gökhan, D.G. Waugh, J. Lawrence, B. Previtali, A.G. Demir, D.G. Waugh, J. Lawrence, B. Previtali, Laser surface texturing of β-Ti alloy for orthopaedics: Effect of different wavelengths and pulse durations, Appl Surf Sci 489 (2019) 175–186. https://doi.org/10.1016/j.apsusc.2019.05.111.

[35] M. Yadi, H. Esfahani, M. Sheikhi, M. Mohammadi, CaTiO3/α-TCP coatings on CP-Ti prepared via electrospinning and pulsed laser treatment for in-vitro bone tissue engineering, Surf Coat Technol 401 (2020) 126256. https://doi.org/10.1016/j.surfcoat.2020.126256.

[36] J. Sypniewska, M. Szkodo, Influence of Laser Modification on the Surface Character of Biomaterials : Titanium and Its Alloys — A Review, (2022).

[37] P. Navarro, A. Olmo, M. Giner, M. Rodríguez-Albelo, Á. Rodríguez, Y. Torres, Electrical Impedance of Surface Modified Porous Titanium Implants with Femtosecond Laser, Materials 15 (2022). https://doi.org/10.3390/ma15020461.

[38] M. Jażdżewska, B. Majkowska-Marzec, Hydroxyapatite deposition on the laser modified Ti13Nb13Zr alloy, Advances in Materials Science 17 (2018) 5–13. https://doi.org/10.1515/adms-2017-0017.

[39] Q. Wang, H. Wang, Z. Zhu, N. Xiang, Z. Wang, G. Sun, Switchable wettability control of titanium via facile nanosecond laser-based surface texturing, Surfaces and Interfaces 24 (2021) 101122. https://doi.org/10.1016/j.surfin.2021.101122.

[40] H.S. G. Schnell , U. Duenow, Effect of Laser Pulse Overlap and Scanning Line Overlap on Femtosecond Laser-Structured Ti6Al4V Surfaces, Materials 13 (2020) 1–15.

[41] J.I. Kang, M.K. Son, H.C. Choe, W.A. Brantley, Bone-like apatite formation on manganese-hydroxyapatite coating formed on Ti-6Al-4V alloy by plasma electrolytic oxidation, Thin Solid Films 620 (2016) 126–131. https://doi.org/10.1016/j.tsf.2016.07.088.

[42] Z. Lin, T. Wang, X. Yu, X. Sun, H. Yang, Functionalization treatment of micro-arc oxidation coatings on magnesium alloys: a review, J Alloys Compd 879 (2021) 160453. https://doi.org/10.1016/j.jallcom.2021.160453.

[43] J. Baszkiewicz, D. Krupa, J.A. Kozubowski, B. Rajchel, M. Lewandowska-Szumieł, A. Barcz, J.W. Sobczak, A. Kosiński, A. Chróścicka, The effect of sodium-ion implantation on the properties of titanium, J Mater Sci Mater Med 19 (2008) 3081–3091. https://doi.org/10.1007/s10856-008-3431-4.

[44] T.R. Rautray, R. Narayanan, K.H. Kim, Ion implantation of titanium based biomaterials, Prog Mater Sci 56 (2011) 1137–1177. https://doi.org/10.1016/j.pmatsci.2011.03.002.

[45] D. Krupa, J. Baszkiewicz, B. Rajchel, A. Barcz, J.W. Sobczak, A. Biliński, Effect of sodium-ion implantation on the corrosion resistance and bioactivity of titanium, in: Vacuum, 2005: pp. 161–166. https://doi.org/10.1016/j.vacuum.2005.01.020.

[46] E. Anitua, L. Piñas, A. Murias, R. Prado, R. Tejero, Effects of calcium ions on titanium surfaces for bone regeneration, Colloids Surf B Biointerfaces 130 (2015) 173–181. https://doi.org/10.1016/j.colsurfb.2015.04.006.

[47] Sunarso, R. Toita, K. Tsuru, K. Ishikawa, Immobilization of calcium and phosphate ions improves the osteoconductivity of titanium implants,

Materials Science and Engineering C 68 (2016) 291–298. https://doi.org/10.1016/j.msec.2016.05.090.
[48] A. Zastulka, S. Clichici, M. Tomoaia-Cotisel, A. Mocanu, C. Roman, C.D. Olteanu, B. Culic, T. Mocan, Recent Trends in Hydroxyapatite Supplementation for Osteoregenerative Purposes, Materials 16 (2023). https://doi.org/10.3390/ma16031303.
[49] M. Dehestani, E. Adolfsson, L.A. Stanciu, Mechanical properties and corrosion behavior of powder metallurgy iron-hydroxyapatite composites for biodegradable implant applications, Mater Des 109 (2016) 556–569. https://doi.org/10.1016/j.matdes.2016.07.092.
[50] M. Mansoorianfar, M. Mansourianfar, M. Fathi, S. Bonakdar, M. Ebrahimi, E.M. Zahrani, A. Hojjati-Najafabadi, D. Li, Surface modification of orthopedic implants by optimized fluorine-substituted hydroxyapatite coating: Enhancing corrosion behavior and cell function, Ceram Int 46 (2020) 2139–2146. https://doi.org/10.1016/j.ceramint.2019.09.197.
[51] S.V. Kellesarian, M. Yunker, R. Ramakrishnaiah, H. Malmstrom, T.V. Kellesarian, V.R. Malignaggi, F. Javed, Does incorporating zinc in titanium implant surfaces influence osseointegration? A systematic review, n.d.
[52] M. Molenda, J. Kolmas, The Role of Zinc in Bone Tissue Health and Regeneration—a Review, Biol Trace Elem Res 201 (2023) 5640–5651. https://doi.org/10.1007/s12011-023-03631-1.
[53] Y. Liang, J. Xu, J. Chen, M. Qi, X. Xie, M. Hu, Zinc ion implantation-deposition technique improves the osteoblast biocompatibility of titanium surfaces, Mol Med Rep 11 (2015) 4225–4231. https://doi.org/10.3892/mmr.2015.3311.
[54] Z. Wang, X. Wang, Y. Wang, Y. Zhu, X. Liu, Q. Zhou, NanoZnO-modified titanium implants for enhanced anti-bacterial activity, osteogenesis and corrosion resistance, J Nanobiotechnology 19 (2021). https://doi.org/10.1186/s12951-021-01099-6.
[55] G. He, S. Lu, W. Xu, P. Ye, G. Liu, H. Wang, T. Dai, Stable superhydrophobic Zn/ZnO surfaces fabricated via electrodeposition on tin substrate for self-cleaning behavior and switchable wettability, J Alloys Compd 747 (2018) 772–782.

https://doi.org/10.1016/j.jallcom.2018.03.108.
[56] G. Wu, Y. Wang, M. Sun, Q. Zhang, J. Yao, V. Kovalenko, Effect of laser surface melting pretreatment on the growth behavior and mechanical properties of microarc oxidation coating on Ti6Al4V alloy, J Laser Appl 32 (2020) 012013. https://doi.org/10.2351/1.5098000.
[57] S. Abdalla, F. Al-Marzouki, A.A. Al-Ghamdi, A. Abdel-Daiem, Different Technical Applications of Carbon Nanotubes, Nanoscale Res Lett 10 (2015). https://doi.org/10.1186/s11671-015-1056-3.
[58] M. Dziaduszewska, A. Zieliński, Structural and material determinants influencing the behavior of porous Ti and its alloys made by additive manufacturing techniques for biomedical applications, Materials 14 (2021) 1–48. https://doi.org/10.3390/ma14040712.
[59] B. Makurat-Kasprolewicz, M. Wekwejt, A. Ronowska, G. Gajowiec, M. Grodzicka, S. Dzionk, A. Ossowska, Influence of Ultrasound on the Characteristics of CaP Coatings Generated Via the Micro-arc Oxidation Process in Relation to Biomedical Engineering, ACS Biomater Sci Eng 10 (2024) 2100–2115. https://doi.org/10.1021/acsbiomaterials.3c01433.

5. TREŚĆ ARTYKUŁÓW Z OPISEM WKŁADU PRACY DOKTORANTA

5.1. [JS1] Influence of Laser Modification on the Surface Character of Biomaterials: Titanium and Its Alloys—A Review

5.1.1. Wkład pracy doktoranta

Tytuł: Influence of Laser Modification on the Surface Character of Biomaterials: Titanium and Its Alloys—A Review

Autorzy: Joanna Sypniewska, Marek Szkodo

Czasopismo: Coatings 12, 1371.

Rok wydania: 2022

Impact factor: 2.9

Liczba punktów wg MNiSW: 40

DOI: 10.3390/coatings12101371

Procentowy wkład pracy doktoranta: 80

W trakcie pracy nad artykułem zajęłam się opracowaniem przeglądu literatury dotyczącej laserowej modyfikacji tytanu oraz jego stopów, koncentrując się na publikacjach z ostatnich 20-25 lat poprzedzających powstanie manuskryptu. Analizę przeprowadziłam z wykorzystaniem takich baz danych jak GoogleScholar, ScienceDirect, Scopus, Wiley oraz Taylor & Francis. Na podstawie zgromadzonych źródeł przygotowałam wersję całego tekstu. Pełniłam także rolę autorki korespondencyjnej oraz opracowałam odpowiedzi na komentarze recenzentów.

mgr inż. Joanna Sypniewska

5.1.2. Treść artykułu

coatings

MDPI

Review

Influence of Laser Modification on the Surface Character of Biomaterials: Titanium and Its Alloys—A Review

Joanna Sypniewska * and **Marek Szkodo**

Faculty of Mechanical Engineering and Ship Technology, Gdansk University of Technology, Narutowicza, 11/12, 80-233 Gdansk, Poland

* Correspondence: joanna.sypniewska@pg.edu.pl; Tel.: +48-608-458-720

Abstract: Laser surface modification is a widely available and simple technique that can be applied to different types of materials. It has been shown that by using a laser heat source, reproducible surfaces can be obtained, which is particularly important when developing materials for medical applications. The laser modification of titanium and its alloys is advantageous due to the possibility of controlling selected parameters and properties of the material, which offers the prospect of obtaining a material with the characteristics required for biomedical applications. This paper analyzes the effect of laser modification without material growth on titanium and its alloys. It addresses issues related to the surface roughness parameters, wettability, and corrosion resistance, and discusses how laser modification changes the hardness and wear resistance of materials. A thorough review of the literature on the subject provides a basis for the scientific community to develop further experiments based on the already investigated relationships between the effects of the laser beam and the surface at the macro, micro, and nano level.

Keywords: laser modification; titanium; titanium alloys

check for updates

Citation: Sypniewska, J.; Szkodo, M. Influence of Laser Modification on the Surface Character of Biomaterials: Titanium and Its Alloys—A Review. *Coatings* **2022**, *12*, 1371. https://doi.org/10.3390/coatings12101371

Academic Editor: Matic Jovičević-Klug

Received: 21 August 2022
Accepted: 8 September 2022
Published: 20 September 2022

Publisher's Note: MDPI stays neutral with regard to jurisdictional claims in published maps and institutional affiliations.

1. Introduction

Surface modifications of materials provide the base for achieving specific material properties for specific applications. The main advantage of laser surface modification is the ability to improve the properties of different materials [1,2]. In addition, the precision, elasticity, the possibility of parameters control, and the repeatability of this process are indicated as an advantage, as is the small heat-affected zone resulting from the modification [3,4]. Because of the high degree of process sophistication, it is also possible to carry out the process without direct human intervention, thus reducing the risk of negative effects on the body [5].

Researchers mainly use lasers such as a femtosecond laser [6], Nd: YAG laser [7–10], CO_2 laser [11], diode [12,13], and fiber laser [14]. Firstly, they provide the possibility to carry out modification processes by adding a coating of the same or another material. Moreover, they are used for modifications with no further addition of materials [1]. Figure 1 presents a classification of laser machining based on an increase or no increase in material. This article is primarily concerned with laser remelting and texturing, as these two techniques are the most commonly used in the modification of biomaterials. Laser remelting is a technique based on remelting the surface of a material to change its morphology and structure without a specific modification objective, to generally improve the properties affected by a laser beam or, for example, when there is talk of modifying the density of the material or the hardness [7,15–17]. Laser texturing involves melting the material and then cooling it to produce a specific pattern on the surface of the material [18]. A combination of laser hardening and laser texturing is also found in the literature [19]. Laser hardening is a technique aimed at improving the hardness of materials using a laser beam. Furthermore, it has the advantage of being able to increase the wear resistance and improve fatigue properties [20]. Surface modification with no addition of a material, which will be discussed in the following work, directly affects a change in wettability and roughness, corrosion resistance, hardness of the material, and wear resistance. Laser modification is closely related to a change in the surface microstructure and influences the roughness and wettability of materials [21–24]. The advantages of using lasers to modify biomedical materials are the ability to control the effect of heat on the surface structure of the materials due to the local action of a laser pulse on the surface, the small heat-affected zone, and the fact that the process is clean and does not cause material loss [25,26].

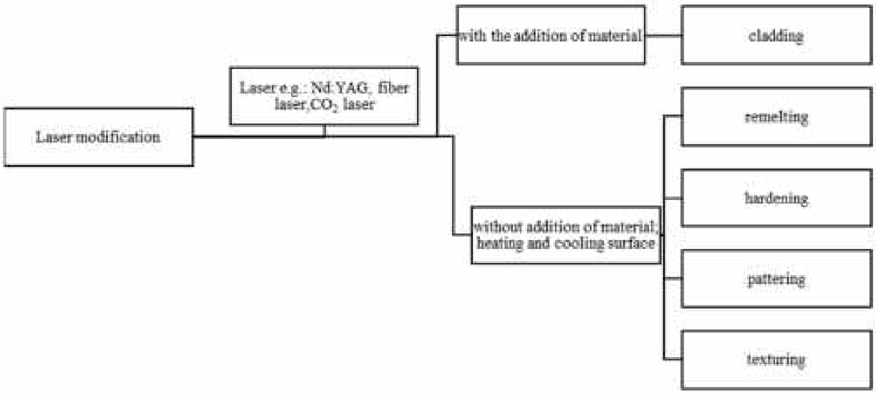

Figure 1. Graphic interpretation of laser modification possibilities based on [1,13,20–22].

The process of the heat treatment of materials by laser is mainly related to the treatment of metallic materials such as aluminum, steel, and its alloys, as well as titanium [2,3,27,28]. Many research efforts are currently focused on gaining a thorough understanding of the properties of titanium and its alloys. Further, efforts are being made to improve these properties to produce a material dedicated to applications.

Titanium and its alloys are widely used in various industries due to their low density. This family of materials has its uses in the manufacture of parts for motorcycles, and sports vehicles to reduce their weight [29,30]. In the aerospace industry, these materials are the third group of materials, after nickel-based materials, in terms of their frequency of use, not only because of their low density, but mainly because of their resistance to corrosion and high temperatures (e.g., alpha alloys and α/β alloys) [31–33]. Considerable attention is given to this material when it comes to medical applications [34,35]. In applications in the field of dental implantology, titanium alloys are used for the production of dental crowns and bridges primarily due to the reduced risk in an allergic reaction and they have a beneficial effect on the process of osseointegration [36,37]. The use of titanium and its alloys is based on its high corrosion resistance, better than steel and cobalt–chromium alloys, owing to the properties of self-assimilation, which are beneficial due to the environment of the body in which the implants are placed [38–41]. In the case of titanium and its alloys, it is said to have little effect on the human body. Pure titanium is a biocompatible material, as are all of its alloys. The alloying elements used to produce titanium alloys, however, do pose a problem, but it should be noted, that titanium and its alloys have hemolytic indices below a value that would indicate the possibility of the formation of embolisms or clots as a result of the presence of this material in the body [42]. Studies by Chen et al. indicate that the presence of vanadium and aluminum in the human body leads to disorders of the nervous system, brain diseases, and circulatory diseases, while also affecting the softening of bone tissue; however, it is indicated that alloys containing aluminum and vanadium (α + β alloys) have mechanical properties on the same level as β alloys. In implantology, aluminum–vanadium alloys are used primarily to produce fracture fixation plates, spinal column components, and connecting elements such as rods, wires, and screws [43]. Review papers over the years related to modifications using laser beams have reported on the benefits of modification for industrial applications (matrix-enhanced laser modification) [44], but they mainly confirm the benefits for biomedical applications [45,46]. Paper [45] focuses on the effect of laser surface texturing on the antimicrobial properties and biological activity of titanium, while a 2005 article [46] provides an overview of the possible types of surface modifications available for various biomaterials and discusses in detail laser modification in the context of the biocompatibility of the modified material. The present review focuses on the mechanical properties of the surface of titanium and its alloys after laser modification. Attention is paid to the properties directly related to the requirements for biomedical materials, such as an adequate material hardness, wear, corrosion resistance, and affinity of the modified surface to bone-forming cells.

A literature review on the effects of laser modification on titanium and its alloys was conducted to present the current state of the art in this field and to highlight the topicality of the problem of the laser modification of titanium and its alloys for biomedical applications due to the requirements that are placed on biomaterials.

2. Methods

This systematic review used the databases: ResearchGate, Science Direct, and Scopus. Google Scholar was also used to analyze the trends in the laser modification of titanium and its alloys. The searching strategy was based on the "laser modification", "laser treatment", "laser remelting", "laser surface modification of titanium and its alloys", and "modification of titanium and its alloys" terms. A bibliography of 175 literature references was collected and extracted from over 200 collected papers. Figure 2 shows the number of articles from each year. The literature review was based mainly on works from 2019 to 2022, which allowed us to discuss issues according to the current state of knowledge on the laser surface modification of titanium and its alloys for selected parameters and properties. The paper discusses the effect of the laser treatment of titanium and its alloys on the surface roughness and wettability, corrosion resistance, and hardness with the indications of micro and macro hardness and wear resistance.

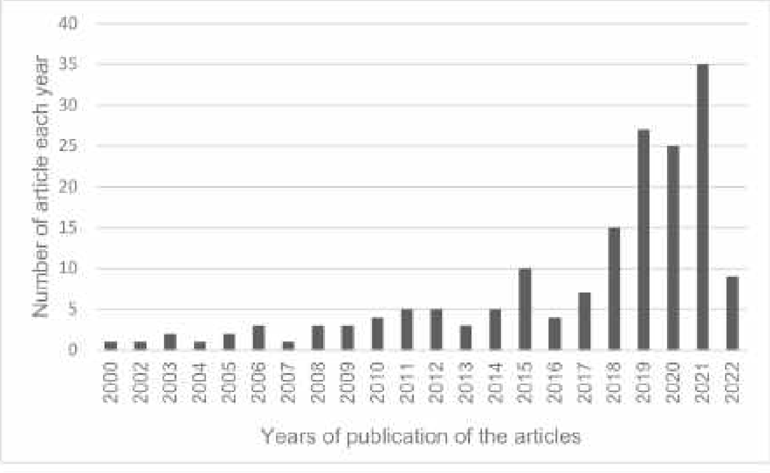

Figure 2. Distribution of the number of articles used per year.

3. Roughness and Wettability

Roughness and surface wettability are very often compared by authors to determine the relationship between these properties [47,48]. The study of these parameters in the case of titanium modifications is very important due to the use of titanium in biomedicine. The evaluation of the roughness parameter is important because an increase in this index has a positive effect on the cell adhesion during osseointegration and on the connection between the bone and an implant [49]. The use of titanium and its alloys in biomedicine is indicated for the manufacture of artificial hip joints, artificial knee joints, bone plates, fracture fixation screws, prosthetic heart valves, pacemakers, and the production of artificial hearts [50,51]. Depending on the area of aspiration of titanium and its alloys, a different surface roughness is required of a biomaterial. For example, heart valve implants, the artificial heart, and other components of the circulatory system must be made of a medium to low-roughness titanium to avoid the formation of areas where blood cells could agglomerate and form blockages, thus stopping the blood flow [52]. In addition, titanium itself possesses anti-thrombogenic properties, and for implant applications, it is necessary to improve the properties of the structure. In the case of osseous dental implants, it is said that components with a high degree of surface roughness are necessary due to the osseointegration process that occurs. An increase in the surface roughness is associated with an increase in the growth surface of osteoblasts and protein polyfusion [53]. Menci et al. [24] point out that laser modification with different types of lasers (e.g., a fiber laser or Nd: YAG laser) is necessary, as the hip implants in question are composed of several elements and each part must have different surface properties. The acetabulum and femoral stem need to be rougher to stimulate bone osseointegration, while the femoral head and distal part of the femoral stem need to be smoother to minimize wear.

In paper [49] it was shown that the roughness of the pore walls created by laser modification was characterized by the roughness parameters, Sa and Sq, with a higher value than on the inter-pore surfaces. The values of Sa and Sq for the inter-pore surfaces were 0.029 μm and 0.04 μm, respectively, while those for the pore walls were 0.126 and 0.149 μm, respectively. The authors concluded from their studies on bone deposition that a higher pore roughness improves the migration of bone-forming cells and also increases the possible surface area for osteoblast attachment to the implant. Furthermore, a high surface roughness is desirable due to increased biointegration and a decreased risk of implant rejection in the body [8].

In papers [8,54–60], an Nd: YAG laser was used to modify titanium alloys and pure titanium. In Table 1, the Nd: YAG laser operating parameters are presented for the literature reviewed subject. In the study, the Nd: YAG laser modification was performed for different laser operating parameters. The effects of varying laser operating parameters on the surface roughness and wettability, which are directly related to the phenomenon of bone cell adhesion, were investigated in a study from 2013, where Györgyey et al. showed [58] a decrease in the R_a roughness parameters using a frequency-doubled Q-switched Nd: YAG laser and a KrF excimer laser. In a 2020 editorial [8] it was observed that the modification of the titanium alloy Ti13Nb13Zr and pure titanium CP-Ti using an Nd: YAG laser caused an increase in the surface roughness. In addition, it was shown that the higher the laser power, the higher the roughness parameters. Additionally, in research work [8] it was pointed out that titanium alloys were rougher than pure titanium before and after laser treatment. Research of [57,61–63] also confirmed that laser modification, regardless of the type of laser, along with increasing the laser parameters, increased the roughness. In paper [57] it was shown that laser processing increased the roughness parameters by approximately 2.8 to 7.5 times at different frequencies relative to the native material. AFM surface texture tests at 10 Hz and 7 Hz successively yielded R_a parameters of 394.35 nm and 279.53 nm, respectively, while this parameter for the reference sample of the Ti6Al4V titanium alloy was 127.20 nm [57].

Table 1. Parameters of Nd: YAG laser modification to improve the roughness of titanium and its alloys.

Laser	Material	Environment	Laser Output Energy	Voltage	Laser Pulse Duration	Irradiation Time	Scanning Speed	Frequency	Average Expansive Area	Fluency/ Power	Shot of Pulses	Roughness Parameters	Reference
Nd: YAG	Ti13Nb13Zr and CP-Ti	air/argon	5; 30 mJ	-	150 ps	5s	-	10 Hz	-	-	50	(Table 2)	[8]
	Ti15Mo and cp Ti grade 2	-	-	-	-	-	0–200 mm/s	20–35 Hz	14 mm^2	1.9 J/cm^2	-	-	[54]
	technically pure VT-1-00 titanium	Air	-	250–400 V	3–10 ms	-	-	1–5 Hz	-	-	1–5	R_a = 3.95 µm R_z = 21.2 µm R_{max} = 29.03 µm S_m = 91 µm	[55]
	Ti6Al4V	-	-	-	-	-	30 mm/min	-	-	200 W	-	R_a = 0.45 µm	[56]
	Ti6Al4V	Argon	-	-	7 ms	-	1 mm/s	1, 3, 5, 7, 10, 15, 20 Hz	-	average power 300 W; peak power 2.1 kW	-	R_a for 10 H z = 0.394 µm R_a for 7 H z = 0.127 R_a µm	
	CP(4) Ti rods	Air	-	-	-	-	-	-	-	1–1.5 J/cm^2	200, 300, 400	-	[58]
	Ti6Al4V	Air	95 mJ	-	-	120 ns	-	10 Hz	-	0.95 W	-	-	[59]
	Ti45Nb	Air, argon, nitrogen	-	-	150 ps	5 ms; 15 s	-	10 Hz	7.1×10^{-4} cm^2	0.13–0.38 J/cm^2	50, 150	(Table 2)	[60]

Table 2. Surface roughness depended on the laser modification environment [8,60].

Sample [60]	**Ti4Nb**											
Laser modification environment	Argon				Air				Nitrogen			
Laser modifications parameters	5 mJ 50 pulses	5 mJ 150 pulses	15 mJ 150 pulses	15 mJ 150 pulses	5 mJ 50 pulses	5 mJ 150 pulses	15 mJ 150 pulses	15 mJ 150 pulses	5 mJ 50 pulses	5 mJ 150 pulses	15 mJ 150 pulses	15 mJ 150 pulses
Surface roughness [µm]	1.026	2.053	1.414	3.062	0.551	0.921	0.884	0.949	0.839	1.148	0.647	0.804
Sample [8]	Ti13Nb13Zr											
Laser modification environment	Air						Argon					
Laser modifications parameters	5 mJ 5 s			30 mJ 5 s			5 mJ 5 s			30 mJ 5 s		
Surface roughness [µm]	0.428			0.988			0.701			1.366		
Sample [8]	CP-Ti											
Laser modification environment	Air						Argon					
Laser modifications parameters	5 mJ 5 s			30 mJ 5 s			5 mJ 5 s			30 mJ 5 s		
Surface roughness [µm]	0.258			0.931			0.927			1.842		

The references state that the laser treatment of titanium surfaces allows for controlling the roughness parameters, R_a, R_z, and R_{max}, in a wide range [55]. The use of a modern fiber laser engraving method [64] allowed the achievement of a surface with a higher roughness than the Ti6Al4V native material. Meanwhile, comparing the results of the roughness measurements at different laser operating parameters, it was observed that with an increase in the laser operating parameters (e.g., groove distance and frequency), there was a decrease in the value of the roughness and an increase in the value of the wetting angle, which was associated with the determination of the surface of the samples as hydrophobic.

Studies [8,60,65] also indicate that the operating environment of the Nd: YAG laser affects the surface roughness and morphologies. The results of EDS [8] have shown that the presence of argon affects the reduction of oxygen molecules for both commercially pure titanium and Ti13Nb13Zr titanium alloy samples; however, the modification carried out in the presence of air caused a strong passivation of the coating and, thus, increased the amount of oxygen on the surface, while the surface roughness for the modified surfaces in the presence of air was lower. Conducting the modification in the presence of argon for each parameter variant results in the roughest surface (Table 2). The laser modification in a nitrogen environment for low power and number of pulses presented in work [60] showed a higher roughness than for the same modification in the presence of air, while in the case of a modification in the presence of argon the modified surfaces—for different laser powers of 5 mJ and 15 mJ and the number of pulses of 50 and 150—were characterized by the highest roughness among all the modified surfaces. The conclusions in [60] are confirmed in [65], where the reason for the lower surface roughness after modification in a nitrogen environment was due to the formation of titanium and nitrogen compounds and the formation of a smaller heat-affected zone. The authors of that article also indicated that for a smaller number of pulses performed, the surface roughness was lower.

Lawrence et al. [56] 2006, presented the idea that laser processing increases the roughness parameters and improves the surface wettability. In Table 3, the literature on the results of the influence of a laser treatment on the character of the surface wettability is summarized. Menci et al. [24] searched for a direct relationship between the contact angle and the Sa parameter for Ti11.5Mo6Zr4.5Sn titanium alloy samples modified by an Nd: YAG laser and fiber laser for different parameters. Wenzel's claim was referred to, which states that increasing the roughness parameter (r) increases the wettability of the surface (where θy is the contact angle of an ideal flat surface and θw is the contact angle of a rough surface) [66]:

$$cos\theta_w = rcos\theta_y$$

The realization of this equation in the work of [24] indicates hydrophilic surface properties because the initial properties of titanium were improved by changing the surface texture (increase in roughness) and there was an increase in droplet diffusion [67].

Table 3. Wettability results on titanium and its alloys observed in the article.

Surface Property	Author, Year, and Reference	Short Conclusion
	Hao et al., 2005 [68]	Observation and study of the surface of laser-modified Ti6Al4V alloy showed an increase in the surface wettability which is beneficial for medical applications of titanium alloys. The increase in the contact angle after laser modification is a result, according to the authors, of an increase in the surface energy of the modified material and an increase in roughness parameters.
	Lawrence et al., 2006 [56]	Lawrence et al. demonstrated that laser treatment improves the surface wettability as a result of a change in the surface energy, an increase in the oxygen content, and an increase in the surface roughness. The cell studies carried out revealed an increase in bone cell adhesion and proliferation for Ti6Al4V titanium alloy samples subjected to laser modification, compared to a titanium alloy without modification.

Table 3. *Cont.*

Surface Property	Author, Year, and Reference	Short Conclusion
Wettability	Cunha, A. et al., 2013 [69]	Obtaining an anisotropic surface by modification is beneficial for controlling the surface wettability and this property is also indicated to improve stem cell adhesion.
	May et al., 2015 [70]	The surface anisotropy of titanium alloy Ti6Al4V subjected to fiber-laser system modification was demonstrated. Wetting angles were smaller for the measurement performed perpendicularly for each laser operating frequency. The formation of contact anisotropy after laser modification was related to the frequency of the laser work, and increasing this parameter decreased the anisotropy.
	Raimbault O. et al., 2016 [71]	The paper focused on the bioactivity of cells towards a femtosecond laser-modified surface but also examined the wettability of the Ti6Al4V titanium alloy, which was determined by measuring the contact angle. It was shown that the storage medium had a great influence on the change of the wettability characteristics of the modified samples. Samples stored in boiling water were slower to change their character to hydrophobic ones due to the slowing down of the passivation process, and the atmospheric environment accelerated these changes.
	Rotella 2017 [72]	The authors used three methods for the surface modification of titanium alloy Ti6Al4V, one of them was a femtosecond laser treatment. The hydrophobic character of the laser-modified samples was observed, but at the same time, it was pointed out that this was not a disadvantage of such a surface because it gives, in a long-term context, a chance for a stronger bonding of the cells with the laser-modified implant.
	Lu et al., 2018 [73]	A laser treatment at different laser fluence values was applied to pure titanium samples and then they were chemically treated. For each of the modification combinations, it was shown that the femtosecond laser modifications decreased the contact angle immediately after the laser treatment, while the contact angle increased after the modification. The possibility to obtain a stable structure with hydrophobic properties was pointed out in the paper as the most important advantage of such a modification.
	Pires et al., 2017 [54]	The Nd: YAG laser treatment produced a superhydrophilic surface. The laser-modified surface consisted of more oxygen, which was one of the factors influencing the change in surface wettability. It was indicated that the use of this type of laser allows for the control of parameters important for bone cells.
	Menci et al., 2019 [24]	In this study, a laser beam modification was performed using two different types of Nd: YAG laser and fiber laser, for different laser wavelengths. It was shown that a fiber laser processing ns 1064 nm produces the highest surface roughness with the greatest reduction in wetting angle. The paper also presents the possibility of using individual lasers with specific parameters to process specific implant components because of the roughness that can be achieved with them.
	Murillo et al., 2019 [74]	It was observed that immediately after the modification of a Ti6Al4V titanium alloy with a UV ns laser and IR-fs pulsed lasers, the surface exhibited hydrophilic properties. In this study, the effect of the sample holding environment of titanium on material aging was investigated.

Table 3. *Cont.*

Surface Property	Author, Year, and Reference	Short Conclusion
	Shaikh et al., 2019 [75]	In this study, a decrease in the contact angle was observed for Ti6Al4V titanium alloy samples which underwent laser modification. It was also observed that the surface of the samples after laser treatment became hydrophilic immediately after the modification; however, during the storage of the material, the contact angle was tested again, and the results showed a change in the surface character toward a hydrophobic one. The authors suggested that this could be due to the oxidation of the modified film as well as contaminants deposited on the sample (the samples were stored in an atmospheric environment).
	Dou et al., 2020 [76]	An increase in hydrophilicity with an increasing laser fluence was observed. The surface hydrophilicity was not stable, and the wettability of the surface changed to hydrophobic properties with time. The need for research on the stability of surface hydrophilicity was indicated.
	Wang et al., 2021 [77]	A 355 mm UV laser modification of commercially pure titanium was carried out. In this study, the possibility of controlling the wettability by light and sample heating was demonstrated. The samples showed a superhydrophilic surface immediately after laser modification.
	Mukherjee et al., 2021 [78]	In this paper, the laser modification of titanium alloy Ti6Al4V using a Yb-doped fiber laser was carried out. It was shown that the surface produced by the laser was anisotropic, which revealed that the contact angle for water was different for a parallel and perpendicular incidence of a drop on the surface. It was shown that in the direction parallel to the laser beam direction, the wetting of the surface was higher as a result of droplet propagation along the corrugation grooves.
	Wang et al., 2021 [79]	A Ti6Al4V titanium alloy was modified with a UV laser at a wavelength of 355 nm. The results of the contact angle measurements were presented for three conditions: for the untreated sample (hydrophilic surface), the sample after laser treatment (superhydrophilic surface), and the sample modified with a laser and additionally subjected to a heat treatment (hydrophobic surface). For the same samples, an erosion test was performed and it was observed that the fastest erosion process occurred for the laser-modified samples and the slowest for those with a hydrophobic surface.
	Singh et al., 2021 [80]	In this study, a CO2 laser modification was carried out on titanium Ti6Al4V alloys. After the modification, the values of the contact angle and surface energy were investigated. It was found that for the laser-modified surface, the contact angle was higher than for the unmodified samples, and the surface energy also increased. It was also found that a decrease in the surface energy resulted in a decrease in the affinity of the modified surface for bacteria, which is beneficial for the potential use of the material in implant production.
	Li et al., 2022 [81]	Pure titanium samples were subjected to laser surface texturing. Wetting angle studies were carried out using distilled water and modified-simulated body fluid (m-SBF). For both fluids, the laser-modified surface showed an increased wettability. It was indicated that the drops on the structure with a higher roughness realized Wenzel's law, which explained the decrease in the contact angle. The wetting angle for the water was higher than for the m-SBF, which gave information that cells would grow better on such a substrate.

The literature identifies four terms for surface wettability: superhydrophilic, hydrophilic, hydrophobic, and superhydrophobic, concerning a drop of water falling on a surface Figure 3 [59].

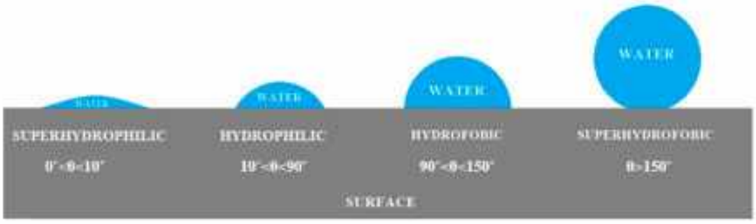

Figure 3. Categories of wettabilitybased on [59,66].

The researchers, Lawrence et al. [56], Menci et al. [24] and Pries et al. [54], treated titanium alloys successively with an Nd: YAG and Yd: YAG laser, and based on contact angle studies, they showed that a laser modification increases the wettability of the sample surface successively for fluids such as human blood, human blood plasma, glycerol and 4-acetanol [56] and water [24]. A decrease in the wetting angle is also shown in Figure 4 for the modification made with the Nd: YAG laser [82]. Pries et al. [54] revealed that the contact angle measured after a laser treatment was 0°. Singh et al. [80] on the other hand, observed that the laser modification of a titanium alloy resulted in a decreased surface roughness, resulting in coatings with a lower wettability than unmodified samples.

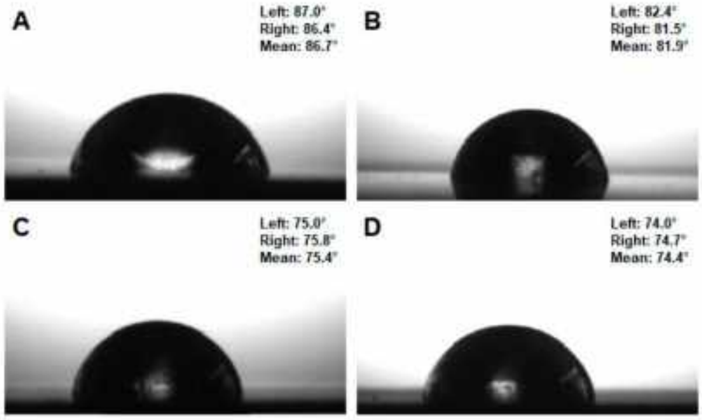

Figure 4. Wettability of material for (**A**) base material Ti13Nb13Zr, (**B**) laser modified sample 700 W, (**C**) laser modified sample 1000 W, and (**D**) laser modified sample 700 + 1000 W [82].

Researchers *Lawrence et al.* [56] *Menci et al.* [24] and *Pries et al.* [54] treated titanium alloys successively with Nd: YAG and Yd: YAG laser, based on contact angle studies they showed that the laser modification increases the wettability of the sample surface successively for fluids such as human blood, human blood plasma, glycerol and 4-acetanol [56] and water [24]. The decrease in wetting angle is also shown in Figure 4 for the modification made with the Nd: YAG laser [82]. *Pries et al.* [54] revealed that the contact angle measured after laser treatment is 0°. *Singh et al.* [80] on the other hand, observed that laser modification of titanium alloy resulted in decreased surface roughness resulting in coatings with lower wettability than unmodified samples.

Conversely, in paper [76], a Ti: sapphire chirped-pulse regenerative amplification laser system with a central wavelength of 800 nm, was used to modify a Ti4Al6V alloy. Initially, the investigated surfaces were characterized by the hydrophilic nature of the modified surface. In the experiment, the contact angle measurements were performed cyclically for up to 155 days after the modification. The observations showed that the effect of the modified surfaces changed from hydrophilic to hydrophobic. Analogous results were also reported in the work of [69,74,75,81,83] for the contact angle for water and for Hank's balanced salt solution (HBSS) for titanium and titanium alloys.

In the research of [73], an alloy was laser-treated with a femtosecond laser, followed by an additional hydrothermal treatment and oxidation. The application of extra modifications did not change the previously established theory that states that with time, the contact angle of laser-modified surfaces increases. Raimbault et al. [71] pointed out that the increase in the contact angle after a certain time after a laser treatment increases due to the increasing passivation of the surface. Moreover, this paper shows that the environment of repository-modified samples is important due to the changing character of the sample wetting. Keeping the laser-modified TA6V samples in an air environment was associated with a faster change in the surface character from hydrophilic to hydrophobic, while an increase in the wetting angle for samples stored in boiling water was smaller. In the study of [72], it is depicted that the change in surface wettability from The decrease in wetting angle is hydrophilic to hydrophobic after a laser treatment does not adversely affect cell adhesion to the material. A better way to illustrate the bonding of a surface to a water droplet is to use the Cassie Baxter model, which takes into account the idea that the contact between a droplet and a surface is affected by air trapped in the irregularities [84]; therefore, an increase in the wetting angle is not uniquely associated with a weakening of the bond between the material and the cells. In addition, the bond is also affected by mechanical stress, which is related to the amount of cracking on the material surface [72].

The references of [62,74,82,83] indicate that laser-modified surfaces can exhibit anisotropic as well as isotropic properties depending on the laser operating parameters [69]. The anisotropy of a surface is more favorable due to its higher wettability than for isotropic surfaces and the contact angles for anisotropic surfaces will be different for parallel and perpendicular directions [70,78,85]. Surface modification resulting in an anisotropic surface is very important for the ability to control the wettability of materials [69], and in addition, due to the medical use of titanium and its alloys, the development of an anisotropic surface is beneficial because of improved osseointegration conditions [47]. It is indicated that the wettability character of laser-modified surfaces can be controlled and changed by external factors such as heat [77,79]. In the study of [77], the hydrophilic properties of a titanium alloy surface were observed immediately after laser modification. It was shown that it was possible to manipulate the character of the surface wettability by using the heating of the samples and UV radiation, which allowed the reversible transformation of the surface from hydrophilic to hydrophobic and the other way around.

4. Corrosion

Titanium and its alloys are characterized by a very high chemical activity. The Pourbaix diagram shows that titanium is a metal that passivates very quickly [86]. The natural, very good corrosion resistance of titanium and its alloys is indicated [87–91]. Additionally, the corrosion behavior is influenced by the presence of β-stabilizing alloying elements and their role in the stability and thickness of the passive layer formed [92]. An important direction of research is the study of the corrosion resistance of titanium bio-alloys [93,94], and to improve this property, it is necessary to limit as far as possible the release of metal ions into the body, since the possibility of adverse health effects due to the presence of, e.g., V or Al in the body has been identified [42,95,96].

It has been shown that titanium and its alloys are stable materials when exposed to environments that react with their surface, but the problem that arises in the root cause of this material is the development of fatigue corrosion, which occurs as a result of the loads on implants. For example, the stress-shielding effect that occurs in implants is due to the greater hardness of titanium than bone. The literature also states that cyclic loads induced by walking affect the corrosion resistance of titanium materials. Moreover, alloying additives in titanium alloys can have negative effects such as vanadium, aluminum, or chromium, whereas alloys with a density of, for example, niobium or tantalum lead to the formation of oxide layers which improve the root resistance of titanium alloys [97].

Laser modification allows the free manipulation of the surface roughness and wettability, which has a significant impact on the corrosion resistance of a material [98,99]. In 2012 [100], corrosion tests on pure titanium and titanium alloy with aluminum and vanadium were performed and based on the corrosion intensity (lA/cm^2), and it was observed that there was a decrease in the corrosion and corrosion-fatigue behavior of the studied materials after laser modification. It was indicated that the reason for the decrease in the corrosion resistance was the presence of residual stresses and small grain sizes in the modified surface, and the resulting microstructure changes differed in potential. The literature indicates that the grain size is affected by the modification of heat [101].

In contrast, the work of [102] cites results from 1984 (Picraux and Pope) 2000 (Suzuki et al.), and 2002 (Yue et al.), which state that laser modification improves the corrosion resistance in, for example, Hank's solution. Travessa et al. [103] showed that laser modification caused significant metallurgical and chemical changes on the surface of an alloy, including the formation of oxides, which resulted in a significant improvement of the corrosion properties compared to metal not subjected to laser treatment. It was also observed, among other things, in the potentiodynamic polarization curves. Navarro [26] showed that a femtosecond laser modification caused changes in the surface of modified samples with different porosities, resulting in an increased impedance (Figure 5). Tests carried out by [103,104] indicated that a thicker oxide or nitride layer formed after laser modification on a material surface, improved the corrosion resistance of a titanium alloy. It was observed that the surface structure after the laser modification, when there were unevenly distributed phase components in it, affected the weakening of the corrosion resistance of the material. The corrosion resistance test carried out in a Ringer's solution Ti6Al4V titanium alloy [105,106], showed an increase in the corrosion resistance in acidic media. Whereas in the papers of [107,108], an increased corrosion resistance of laser-modified samples in Hank's solution and saline solution was shown.

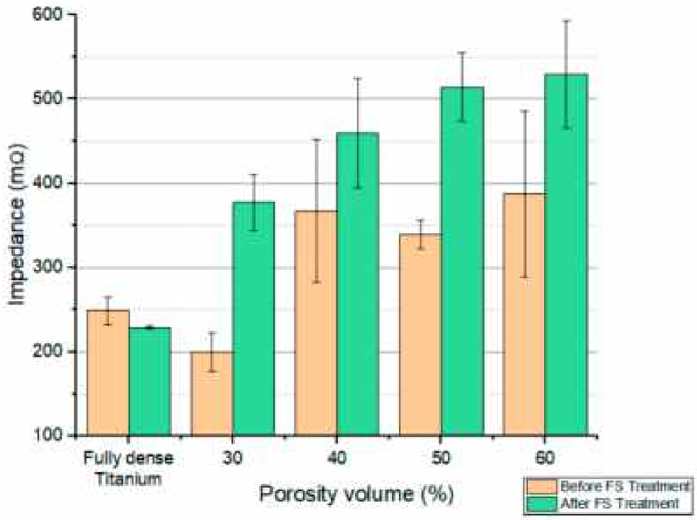

Figure 5. The change of impedance after laser modification for samples with different porosity volume [26].

Researchers in [78,109,110] investigated the effect of laser remelting on pitting and electrochemical corrosion resistance. An analysis of the polarization curves in the work [109] showed an increased resistance to pitting corrosion, which according to the authors was due to a microstructural modification caused by the rapid solidification that occurred during the laser remelting of the surface. Dhara et al. [78] have shown, based on obtained polarization curves, that as a result of the modification, the passive film formed a stable barrier against corrosion. In the paper of [106] it was pointed out that a higher electrochemical resistance was due to the reduction in the volume of the α and β phase, and the thickening of the surface texture. SEM and AFM studies carried out in [108] indicated that the laser modification formed a more reproducible and smoother topography, which increased the corrosion resistance of the material, and a stabilization of the passive layer on the titanium surface was observed, making it less susceptible to further growth [111]. Tests carried out on the chemical composition of the material showed an increase in the presence of nitrides, which acted as a barrier to the ingress of other molecules, and which was considered a condition that could improve the corrosion resistance of a material. An improvement in corrosion resistance by laser ablation was undertaken by [112] in their work, in which they removed the oxide layer, which gave their material a low corrosion resistance, and via the laser ablation, produced a corrosion-resistant oxide layer. This could be observed from an increase in the self-corrosion potential for different energy doses and a decrease in the self-corrosion current, which numerically reflected the corrosion rate of the material; therefore, indicating that the lower the surface corrosion rate the better the corrosion resistance.

5. Hardness

The hardness of titanium and its alloys is reported in the literature to be higher than the hardness of steel on the Vickers scale [113]. For example, titanium alloy Ti6Al4V has a hardness of HV higher (340 HV) than pure titanium (200 HV), which is related to the presence of alloying elements [114,115]. The surface modifications of these materials aim to improve the hardness and mechanical parameters to increase the residence time of an implant in the body [116]. The hardness of the materials used for implants is important because an increase in the material hardness is associated with an increase in the wear resistance [116]. The literature also indicates that the high hardness of a material can adversely affect the behavior of the biomaterial in the body [117]. Laser modification, on the other hand, allows a controlled change in the parameters. Hardness, for example, is widely discussed in the field of orthopedic implants, such as hip and knee implants, because of the need to control the shielding effect of the implant in the bone, and the importance of this parameter, as orthopedic implants are placed under a certain pressure in the body, meaning that the implant must counterbalance this pressure to perform its function properly [118].

A systematic review [119] and research by the authors [10,105,120–122] on the various techniques of the surface modification of titanium have observed an increase in the hardness of materials as a result of laser modification, which has its theoretical basis in [123], where it was indicated that by using a heat source it was possible to control changes in the hardness of materials. Table 4 shows the hardness values obtained for modified titanium alloys and pure titanium using different laser types and parameters. In Figure 6 it is also shown that laser modification improved the nano-hardness of Ti13Nb13Zr alloy samples after a laser modification by an Nd: YAG laser.

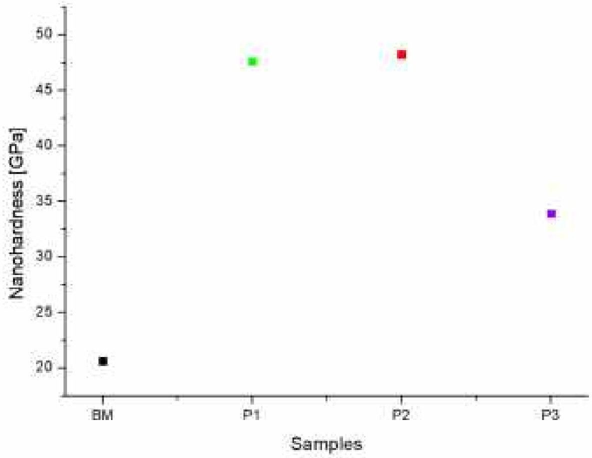

Figure 6. Nano-hardness of laser modified samples. BM: base material, P1: laser modified sample with 800 W and scan rate 60%, P2: laser modified sample with 800 W and scan rate 30%, P3: laser modified sample with 900 W and scan rate 60% [82].

In paper [105], the difference in the hardness value HV between the remelted material and the base material was about 300 HV. The study on the hardness of a titanium alloy was carried out by Khorram et al. [124] which indicated an increase in hardness of 36%. Additionally, Zhang et al. [125] indicated an increase in hardness after laser modification of 60%, while Ushakov et al. [126] determined that the possibility of increasing the Vickers hardness after a laser treatment ranged between 20% and 40%. Moreover, the increase in microhardness was accompanied by an increase in the fracture toughness. The laser modification of porous titanium in the research of [127] resulted in an increase in the hardness at the pore pillars, while an increase in the pore size in the titanium sample resulted in a decrease in the hardness. A significant effect of the pore size on the surface hardening potential by a laser modification was demonstrated.

The change in hardness of samples after laser remelting varies due to the phase transformations occurring during the cooling process [24,109,110]. The increase in material hardness is due to the transformation of the β-phase at high temperatures from about 900 °C to 1050 °C [128], into the α phase and the martensitic α phase, which is hard but very brittle [121,129–131], and the creation of the ω-phase [132,133]. After a laser-induced heat treatment, the formation of a martensitic α-phase was observed as a result of the transformation of the alpha-phase of titanium alloys initially into a beta-phase, and then during the rapid cooling of a material after laser treatment, a martensitic α-phase was formed [134]. Geng et al. [135] indicated that the hardness tests performed after a laser modification of the alloy showed that the measurement of this parameter performed in the β-phase, yielded lower values of hardness than in the α-phase. The results for the β-phase were characterized by large deviations for the elastic modulus due to the small thickness of the β-grains and the presence of α-grains. In studies [136,137] it has been shown that as a result of rapid cooling of a material at the surface after treatment, a martensitic phase with the addition of the β phase is formed, while deep into the material a decrease in the compactness of the martensitic phase is observed, and the α phase tends to become dominant. A comprehensive analysis of the phase transformation in a Ti-64 titanium alloy subjected to an Nd: YAG laser modification was carried out in [138]. The presence of a melted zone and a heat-affected zone after laser treatment were marked and they had different microstructural characteristics. The melted zone was characterized by the presence of martensitic plates throughout, while the heat-affected zone, which was far from the laser source, contained short-rod b particles, martensitic plates and untransformed bulk in its microstructure. It was shown that the change in hardness during laser treatment was influenced by the presence of martensitic plates in the melted zone and a reduction in the grain size. The formation of the martensitic phase limited the diffusion of alloying elements, which directly led to the hardening of the surface structure. The study of [138] presents the preliminary results of values for hardness, using a calculation method and a measurement method. For both methods, the hardness increased with respect to the material without a laser treatment. The hardness for the melted zone was higher than for the heated affected zone and the differences in the hardness values were due to the fact that the calculation method did not take into account the occurrence of coarse α grains in the heated zone, while it was also difficult to take into account the contribution of the individual phases of the material in the zones [138].

The authors of [125] further observed the formation of a large number of dislocations and mesh distortions on the surface of a sample, increasing the hardness of the material. In the melted zone, the formation of nanotwins was observed, which slowed down the dislocation movements, and this had an additional hardening effect on the material [138,139]. It was indicated that reducing the grain size increased the hardness of the material [109]; however, after laser treatment, the grain size of the material increased while the hardness increased, suggesting that the grain size does not significantly affect the hardness as much as the dislocations formed and the phase transformations of the material [140]. In the work of [141], it was indicated that an increase in the amount of oxygen due to a femtosecond laser treatment resulted in an increase in the hardness with a concomitant increase in the brittleness of the material. Applying laser texturing to the surface linearly and performing dimple patterns resulted in an increase in the nano-hardness from 2 GPa for the base material to 4 GPa and 6 GPa, respectively, as tested by nanoindentation. The hardness obtained for each test was dependent on the type of laser selected and the processing parameters chosen. In paper [142], a pulsed laser treatment was performed using two different laser power parameters, and the modified samples were divided into two regions. It was shown that the region of the sample modified with a higher laser power of 3.99 W had a higher hardness than the region modified with a laser power of 1.71 W. In addition, it was shown that for treatment with the lower laser power, no significant difference in the hardness were registered between the remelted layer and the native material. The research of [143] indicated that a laser modification with a low laser power did not increase the hardness of the material as much as in the case of a high laser power, for the reason that a lower power also means less heat and there is not as much formation of the martensitic alpha phase after remelting. A high laser power is directly related to the rapid cooling of the material and as a result the formation of the martensitic alpha phase. In the work of [144], the formation of a TiO_2 rutile and anatase phase was demonstrated, and it was indicated that the amount of oxygen molecules present in the structure depended on the laser modification method, namely, the type of laser and the parameters used. Pan et al. [145], as a result of their conducted research, indicated that the observed increase in the microhardness of the samples subjected to laser treatment was also because with an increase in the laser operating parameters there is an increase in the pressure. It was noted that an overly high value of the laser operating parameters was not able to effectively improve the microhardness of a surface [146], and this was because the yield strength of the titanium alloys had been exceeded [145]. The laser modification primarily increased the microhardness at the surface of the material, and the decrease in the hardness values was a gradient with an increasing test depth [145]. The change of the laser wavelength from 532 nm to 1064 nm showed a huge increase in the surface roughness which had a negative impact on the corrosion properties [147].

Table 4. Microhardness and hardness after laser treatment on titanium and its alloys.

Material	Microhardness and Hardness after Laser Treatment	Laser Parameters								References
		Type of Laser	Energy/Laser Power	Impact Time	Pulse Duration	Frequency	Scan Speed (Mm/S)	Laser Pulses	Environment	
Ti35Nb10Ta	3.8 GPa 3.3 GPa	Nd: YAG	1000 W 1500 W	- -	- -	- -	6.67 mm/s 10 mm/s	- -	Helium	[120]
	untreated material: 3.06 GPa	-	-	-	-	-	-		-	[148]
Ti30Nb4Sn	3.5 GPa 3.3 GPa	Nd: YAG	1000 W 1500 W	-	-	-	the authors 6.67 mm/s 10 mm/s	- -	Helium	[120]
	untreated material 2.44 GPa									[149]
Ti6Al4V	4.9 GPa	Nd: YAG	50 mJ	-	-	10 Hz	-	-	Argon	[105]
	3, 4.01 for 150 μJ, 2.59 GPa for 240 μJ	femtosecond laser	10–240 μJ	-	290 fs	50 kHz	-	-	-	[145]
	3.84 GPa 294 GPa	Nanosecond Laser Shock Peening (LSP	4 J	1 s 3 s	20 ns	1 H	-	-	-	
Ti-5Al-2.5Sn	4.02 GPa	Nd: YAG	165 W	-	-	14 Hz	-	-	-	[124]
Ti6Al4V	2.45–3.43 GPa	-	-	-	-	-	-	500–18,000	-	[146]
Cp-Ti	untreated material: 1.08 GPa 2.59 GPa	Nd: YAG	100 W	-	5 ms	20 Hz	8 mm/s	-	-	[122]

6. Wear Resistance and Fatigue Behavior

An appropriate approach to improving wear resistance at present is to design alloys based on their chemical composition. In parallel, several technologies have been developed to prepare a modified layer with a high wear resistance [150]. The literature indicates that the direct effect on wear resistance is related to the hardness of a material [107,151]. One of the few disadvantages of titanium and its alloys is a low wear resistance [115]. For these materials, the need to improve this property is widely discussed [11,152] because the low wear resistance is a limitation of the various applications. Significant differences in the wear resistance of the various titanium alloys are indicated depending on the α, β, or αβ type [150,153]. The literature points to a low wear resistance, especially in the case of titanium alloys β [92], for example, Ti-5Al-5Mo-5V-1Cr-1Fe [133], Ti–35Nb–7Zr–5Ta [154], and Ti10V2Fe3Al [155].

The literature reports that laser surface modification is a simple method to improve the wear resistance of a material [119,156–159]. In the research by Cheng et al. [133], despite an increased surface hardness after laser modification, no improvement in the wear resistance of the titanium alloy Ti5Al5Mo5V1Cr1Fe was observed.

The papers of [160,161] indicated that laser treatment in a nitrogen environment caused the formation of TiN, which significantly improved the surface hardness and wear resistance of the materials. The increased wear resistance was explained by a decrease in the coefficient of friction [160]. The research of [161] indicated that the relative wear resistance increased by 1.7 times compared to a material without a laser treatment. Moreover, the literature of [158] indicated that a TiN layer formed as a result of remelting in the presence of nitrogen, had a higher hardness and wear resistance than treated titanium alloys.

A study of the effect of laser processing on the wear resistance of pure titanium was carried out in [162], where laser processing was shown to reduce the weight loss of samples during a dry wear test. The study confirmed Archad's theory, that the wear rate is reversely proportional to the hardness [162,163]. The results of [162] for wear resistance indicated that the mass loss for a samples subjected to laser modification was much lower than for material without treatment, and that the wear indices for selected modified samples were practically constant, while for unmodified samples they increased significantly. The samples were subjected to a study of the change in the coefficient of friction during normal loading for increasing loads and the results in the cited work [162] indicated that the pure titanium samples without a modification showed a higher wear and material loss with an increasing normal load, while for modified samples a decrease in the wear was observed with increasing loads. In the work of [164], an increase in the wear resistance was observed in untreated material, while an increase in the load during the experiments lowered the wear resistance. The laser treatment created defects and when the load was applied, the structures were compressed, which increased the wear resistance because the material did not detach from the surface. It was shown that when the maximum temperature reached during the thermal cycle was higher than the melting temperature, a phase change to the martensitic phase occurred, and the fatigue strength and wear resistance of the material were improved; thus, this procedure is also used in the hardening of steels and cast irons [137].

The study results of Zeng et al. [165] also indicated that a laser treatment improved the wear resistance of a material, that the diagram of the dependence of a material loss volume on the wear time for both a non-laser treated and treated material was linear, except for modified samples where a small mass loss was observed, and that it was 37 times lower than the wear of the raw material. The ion release tests carried out showed that the increased wear resistance determined the reduced release of vanadium, which is a toxic element.

In the study of [166], as a result of laser modification, the formation of TiC was observed and it was indicated that the presence of this composite improved the hardness and wear resistance. It was shown that short laser processing times were more advantageous because the melted layer was more homogeneous. Moreover, increasing the laser processing time increased the hardness and surface roughness but the TiC structure was more uneven and hard TiC particles acted as an abrasive tool. The low speed of the laser beam on the material, causing the formation of deeper melts, also had a beneficial effect on increasing the wear resistance of the material.

In paper [167], an XRD study of a Ti834 alloy subjected to modification was carried out, where the fatigue strength (high cycle fatigue) was tested. It was shown that for modified samples there was an increase in the tested strength, which was justified by the formation of compressive stresses after laser shock peening. Jia et al. [168] confirmed that in this type of laser processing, compressive stresses are induced in the sample and increase with an increasing impact time. A 1998 study [169] showed that laser modification combined with previous coating applications allowed for a reduction in the adhesive and abrasive wear.

The researchers of [170,171] compared the treatment of titanium by ion implantation and laser nitriding. It was shown that the use of a CO_2 laser in a nitrogen environment allowed a reduction in the friction between the tested surfaces, with a concomitant decrease in the fatigue strength [171]. Another study [170] evaluated the fretting fatigue behavior of a titanium alloy. It was observed that due to the formation of a heterogeneous, brittle surface after machining during fretting, the surface of the titanium alloy was unable to accept the loads set during fretting. Current literature [172–174] also shows that the use of laser modification is associated with decreasing the fatigue strength in titanium alloys. It is indicated that the fatigue strength is reduced by up to 30% compared to the very good fatigue strength of titanium alloys [172,175]. Additionally, it was indicated that with the increase in surface roughness after laser treatment, the cracks occurring on the surface generate a reduction in the fatigue strength. The resulting surface damage was identified as crack initiation sites [174]. The untreated material had crack initiation sites at the edges of the material, while in the case of the laser-treated material, the initiation site was in the center of the material [173].

7. Conclusions

The literature review focused on the effects of laser modification without material gain on titanium and its alloys. The presented work provides a comprehensive knowledge base on the effects of a fiber laser, Nd: YAG, Yd: YAG laser, and femtosecond laser and the shock peening method on selected properties of the titanium materials used in the medical industry. The paper discusses such properties as the roughness, wettability, resistance to corrosion, wear, and fatigue, as well as the effect of laser modification on material hardness.

1. The first section focused on the surface roughness and wettability, allowing us to assess the impact of laser modification with different types of lasers, which led to the conclusion that the use of this type of modification increases the surface roughness and that it varies depending on the operating parameters of the lasers.
2. The wettability of a surface is a topic that is widely discussed due to the fact that laser modification affects the change in the nature of the surface. Notably, a large impact on the hydrophilicity or hydrophobicity of a surface is the timing of the test in this direction, as well as the environment in which the samples are stored, but depending on the application of the material, there are different requirements, which does not indicate a more advantageous character.
3. Collected publications in the field of corrosion resistance research determine that the action of a laser beam on titanium materials improves the corrosion resistance, which is important because this reduces the release of dangerous elements from the implants.
4. Laser modification alters the micro- and nano-hardness for each type of laser. It is indicated that laser modification allows the process to be carried out in such a way that the hardness obtained after the change is close to that of bone.
5. The effect of laser modification on material wear was presented based on a collection of literature from a wide time range, which allowed the presentation of further opportunities to discuss the selection of optimal laser operating parameters, such as the laser operating power, laser beam density, and pulse duration.

6. In addition, the aspect of wear resistance was discussed, where it was shown that the use of laser modification improves this material property.
7. The presented review of the current literature on the subject provides a theoretical basis for studying the effects of laser processing on titanium and its biostops and for conducting targeted processing in the area where modification is needed to improve implants.
8. The presented review of the current literature related to the effects of laser modification on selected properties of titanium materials and provides a theoretical basis for the researchers' research.
9. The review indicates the need to deepen the research related to the wettability of the surface of titanium materials used in biomedicine, due to the fact that there is no clear indication of which character of the surface is more favorable, and it is necessary to identify the areas of application of a hydrophobic and hydrophilic surface obtained by modification. In addition, it is important to focus on studies related to the durability of materials against wear and fatigue and corrosion because these two properties directly affect the length of stay of an implant in the body.

Author Contributions: Conceptualization, J.S. and M.S.; Methodology, J.S.; Formal analysis, M.S.; Investigation, J.S.; Writing—original draft preparation, J.S.; Writing—review and editing, J.S. and M.S. All authors have read and agreed to the published version of the manuscript.

Funding: This research received no external funding.

Institutional Review Board Statement: Not applicable.

Informed Consent Statement: Not applicable.

Data Availability Statement: Not applicable.

Conflicts of Interest: The authors declare no conflict of interest.

References

1. Bandyopadhyay, A.; Sahasrabudhe, H.; Bose, S. *Laser Surface Modification of Metallic Biomaterials*; Elsevier Ltd.: Amsterdam, The Netherlands, 2016; ISBN 9780081009420.
2. Ardila-Rodríguez, L.A.; Menezes, B.R.C.; Pereira, L.A.; Takahashi, R.J.; Oliveira, A.C.; Travessa, D.N. Surface Modification of Aluminum Alloys with Carbon Nanotubes by Laser Surface Melting. *Surf. Coat. Technol.* **2019**, *377*, 1–11. [CrossRef]
3. Landowski, M. Influence of parameters of laser beam welding on structure of 2205 duplex stainless steel. *Adv. Mater. Sci.* **2019**, *19*, 1–11. [CrossRef]
4. Mao, B.; Siddaiah, A.; Liao, Y.; Menezes, P.L. Laser Surface Texturing and Related Techniques for Enhancing Tribological Performance of Engineering Materials: A Review. *J. Manuf. Process.* **2020**, *53*, 153–173. [CrossRef]
5. Daskalova, A.; Angelova, L.; Carvalho, A.; Trifonov, A.; Nathala, C.; Monteiro, F.; Buchvarov, I. Effect of Surface Modification by Femtosecond Laser on Zirconia Based Ceramics for Screening of Cell-Surface Interaction. *Appl. Surf. Sci.* **2020**, *513*, 145914. [CrossRef]
6. Yang, L.; Ding, Y.; Cheng, B.; He, J.; Wang, G.; Wang, Y. Investigations on Femtosecond Laser Modified Micro-Textured Surface with Anti-Friction Property on Bearing Steel GCr15. *Appl. Surf. Sci.* **2018**, *434*, 831–842. [CrossRef]
7. Temmler, A.; Walochnik, M.A.; Willenborg, E.; Wissenbach, K. Surface Structuring by Remelting of Titanium Alloy Ti6Al4V. *J. Laser Appl.* **2015**, *27*, 1–7. [CrossRef]
8. Laketić, S.; Rakin, M.; Momčilović, M.; Ciganović, J.; Veljović, Đ.; Cvijović-Alagić, I. Surface Modifications of Biometallic Commercially Pure Ti and Ti-13Nb-13Zr Alloy by Picosecond Nd:YAG Laser. *Int. J. Miner. Metall. Mater.* **2021**, *28*, 285–295. [CrossRef]
9. Jażdewska, M.; Kwidzińska, D.B.; Seyda, W.; Fydrych, D.; Zieleiński, A. Mechanical Properties and Residual Stress Measurements of Grade IV Titanium and Ti-6Al-4V and Ti-13Nb-13Zr Titanium Alloys after Laser Treatment. *Materials* **2021**, *14*, 6316. [CrossRef]
10. Majkowska-Marzec, B.; Sypniewska, J. Microstructure and Mechanical Properties of Laser Surface-Treated Ti13Nb13Zr Alloy with MWCNTs Coatings. *Adv. Mater. Sci.* **2021**, *21*, 5–18. [CrossRef]
11. Zieliński, A.; Jażdżewska, M.; Łubiński, J.; Serbiński, W. Effects of Laser Remelting at Cryogenic Conditions on Microstructure and Wear Resistance of the Ti6Al4V Alloy Applied in Medicine. *Trans. Technol. Publ.* **2012**, *183*, 215–224. [CrossRef]
12. Lisiecki, A.; Klimpel, A. Diode Laser Surface Modification of Ti6Al4V Alloy to Improve Erosion Wear Resistance. *Arch. Mater. Sci. Eng.* **2008**, *32*, 5–12.
13. Amaya-Vazquez, M.R.; Sánchez-Amaya, J.M.; Boukha, Z.; Botana, F.J. Microstructure, Microhardness and Corrosion Resistance of Remelted TiG2 and Ti6Al4V by a High Power Diode Laser. *Corros. Sci.* **2012**, *56*, 36–48. [CrossRef]

14. Lisiecki, A. Hybrid Laser Deposition of Composite WC-Ni Layers with Forced Local Cryogenic Cooling. *Materials* **2021**, *14*, 4312. [CrossRef] [PubMed]
15. Lv, F.; Liang, H.; Xie, D.; Mao, Y.; Wang, C.; Shen, L.; Tian, Z. On the Role of Laser in Situ Re-Melting into Pore Elimination of Ti–6Al–4V Components Fabricated by Selective Laser Melting. *J. Alloys Compd.* **2021**, *854*, 156866. [CrossRef]
16. Temmler, A.; Willenborg, E.; Wissenbach, K. Designing Surfaces by Laser Remelting Designing Surfaces by Laser Remelting. In Proceedings of the ICOMM 2012—International Conference on Micromanufacturing, Evanston, IL, USA, 12–14 March 2014. [CrossRef]
17. Szkodo, M.; Bień, A.; Stanisławska, A. Laser Beam as a Precision Tool to Increase Fatigue Resistance in an Eyelet of Undercarriage Drag Strut. *Int. J. Precis. Eng. Manuf.-Green Technol.* **2022**, *9*, 175–190. [CrossRef]
18. Ukar, E.; Lamikiz, A.; Martínez, S.; Arrizubieta, I. Laser Texturing with Conventional Fiber Laser. *Procedia Eng.* **2015**, *132*, 663–670. [CrossRef]
19. Aragaw, E.M.; Gärtner, E.; Schubert, A.; Stief, P.; Dantan, J.; Etienne, A.; Siadat, A. ScienceDirect ScienceDirect Combined Laser Hardening and Laser Surface Texturing Forming Tool 1. 2379 Combined Laser Hardening and Laser Surface Texturing Existing Products for an Assembly Oriented Product Family Identification Methodology to Analyze The. *Procedia CIRP* **2020**, *94*, 914–918. [CrossRef]
20. Balasubramanian, S.; Muthukumaran, V.; Sathyabalan, P. A Study of the Effect of Process Parameters of Laser Hardening in Carbon Steels. *Int. J. Civ. Eng. Technol.* **2017**, *8*, 201–207.
21. Poulon-Quintin, A.; Watanabe, I.; Watanabe, E.; Bertrand, C. Microstructure and Mechanical Properties of Surface Treated Cast Titanium with Nd:YAG Laser. *Dent. Mater.* **2012**, *28*, 945–951. [CrossRef]
22. Xu, Y.; Liu, W.; Zhang, G.; Li, Z.; Hu, H.; Wang, C.; Zeng, X.; Zhao, S.; Zhang, Y.; Ren, T. Friction Stability and Cellular Behaviors on Laser Textured Ti–6Al–4V Alloy Implants with Bioinspired Micro-Overlapping Structures. *J. Mech. Behav. Biomed. Mater.* **2020**, *109*, 1–14. [CrossRef]
23. Braga, F.J.C.; Marques, R.F.C.; de Filho, E.A.; Guastaldi, A.C. Surface Modification of Ti Dental Implants by Nd:YVO 4 Laser Irradiation. *Appl. Surf. Sci.* **2007**, *253*, 9203–9208. [CrossRef]
24. Menci, G.; Gökhan, A.; Waugh, D.G.; Lawrence, J.; Previtali, B. Applied Surface Science Laser Surface Texturing of β-Ti Alloy for Orthopaedics: Effect of Different Wavelengths and Pulse Durations. *Appl. Surf. Sci.* **2019**, *489*, 175–186. [CrossRef]
25. Yadi, M.; Esfahani, H.; Sheikhi, M.; Mohammadi, M. CaTiO3/α-TCP Coatings on CP-Ti Prepared via Electrospinning and Pulsed Laser Treatment for in-Vitro Bone Tissue Engineering. *Surf. Coat. Technol.* **2020**, *401*, 126256. [CrossRef]
26. Navarro, P.; Olmo, A.; Giner, M.; Rodríguez-Albelo, M.; Rodríguez, Á.; Torres, Y. Electrical Impedance of Surface Modified Porous Titanium Implants with Femtosecond Laser. *Materials* **2022**, *15*, 461. [CrossRef]
27. Jażdżewska, M.; Majkowska-Marzec, B. Hydroxyapatite Deposition on the Laser Modified Ti13Nb13Zr Alloy. *Adv. Mater. Sci.* **2018**, *17*, 5–13. [CrossRef]
28. Dywel, P.; Szczesny, R.; Domanowski, P.; Skowronski, L. Structural and Micromechanical Properties of Nd:YAG Laser Marking Stainless Steel (AISI 304 and AISI 316). *Materials* **2020**, *13*, 2168. [CrossRef] [PubMed]
29. Fujii, H.; Takahashi, K.; Yamashita, Y. Application of Titanium and Its Alloys for Automobile Parts. *Nippon Steel Tech. Rep.* **2003**, *02003*, 70–75. [CrossRef]
30. Assari, A.H.; Eghbali, B. Solid State Diffusion Bonding Characteristics at the Interfaces of Ti and Al Layers. *J. Alloys Compd.* **2019**, *773*, 50–58. [CrossRef]
31. Tabie, V.M.; Li, C.; Saifu, W.; Li, J.; Xu, X. Mechanical Properties of near Alpha Titanium Alloys for High-Temperature Applications - a Review. *Aircr. Eng. Aerosp. Technol.* **2020**, *92*, 521–540. [CrossRef]
32. Gomez-Gallegos, A.; Mandal, P.; Gonzalez, D.; Zuelli, N.; Blackwell, P. Studies on Titanium Alloys for Aerospace Application. *Defect Diffus. Forum* **2018**, *385 DDF*, 419–423. [CrossRef]
33. Elshazli, A.M.; Elshaer, R.N.; Hussein, A.H.A.; Al-Sayed, S.R. Erratum: Elshazli et Al. Laser Surface Modification of TC21 (α/β) Titanium Alloy Using a Direct Energy Deposition (DED) Process. *Micromachines* **2021**, *12*, 739. [CrossRef] [PubMed]
34. Khorasani, A.M.; Goldberg, M.; Doeven, E.H.; Littlefair, G. Titanium in Biomedical Applications—Properties and Fabrication: A Review. *J. Biomater. Tissue Eng.* **2015**, *5*, 593–619. [CrossRef]
35. Laska, A. Parameters of the Electrophoretic Deposition Process and Its Influence on the Morphology of Hydroxyapatite Coatings. Review. *Inżynieria Mater.* **2020**, *1*, 20–25. [CrossRef]
36. Watanabe, I.; McBride, M.; Newton, P.; Kurtz, K.S. Laser Surface Treatment to Improve Mechanical Properties of Cast Titanium. *Dent. Mater.* **2009**, *25*, 629–633. [CrossRef] [PubMed]
37. Shah, F.A.; Johansson, M.L.; Omar, O.; Simonsson, H.; Palmquist, A.; Thomsen, P. Laser-Modified Surface Enhances Osseointegration and Biomechanical Anchorage of Commercially Pure Titanium Implants for Bone-Anchored Hearing Systems. *PLoS ONE* **2016**, *11*, e0157504. [CrossRef] [PubMed]
38. Koizumi, H.; Takeuchi, Y.; Imai, H.; Kawai, T.; Yoneyama, T. Application of Titanium and Titanium Alloys to Fixed Dental Prostheses. *J. Prosthodont. Res.* **2019**, *63*, 266–270. [CrossRef]
39. Wierzchoń, T. Modification of Titanium and Its Alloys Implants by Low Temperature Surface Plasma Treatments for Cardiovascular Applications. *Inżynieria Mater.* **2018**, *1*, 4–13. [CrossRef]
40. Manjaiah, M.; Laubscher, R.F. A Review of the Surface Modifications of Titanium Alloys for Biomedical Applications. *Mater. Tehnol.* **2017**, *51*, 181–193. [CrossRef]

41. Yamaguchi, T.; Hagino, H. Formation of Titanium Carbide Layer by Laser Alloying with a Light-Transmitting Resin. *Opt. Lasers Eng.* **2017**, *88*, 13–19. [CrossRef]
42. Piotrowska, K.; Madej, M.; Ozimina, D. Assessment of tribological properties of ti13nb13zr titanium alloy used in medicine. *Tribologia* **2019**, *285*, 97–106. [CrossRef]
43. Chen, Q.; Thouas, G.A. Metallic Implant Biomaterials. *Mater. Sci. Eng. R Reports* **2015**, *87*, 1–57. [CrossRef]
44. Tian, Y.S.; Chen, C.Z.; Wang, D.Y.; Lei, T.Q. Laser surface modification of titanium alloys—A review. *Surf. Eng. Light Alloy. Alum. Magnes. Titan. Alloy.* **2010**, *12*, 398–443. [CrossRef]
45. Sirdeshmukh, N.; Dongre, G. Laser Micro & Nano Surface Texturing for Enhancing Osseointegration and Antimicrobial Effect of Biomaterials: A Review. *Mater. Today Proc.* **2021**, *44*, 2348–2355. [CrossRef]
46. Kurella, A.; Dahotre, N.B. Review Paper: Surface Modification for Bioimplants: The Role of Laser Surface Engineering. *J. Biomater. Appl.* **2005**, *20*, 1–25. [CrossRef]
47. Xue, X.; Ma, C.; An, H.; Li, Y.; Guan, Y. Corrosion Resistance and Cytocompatibility of Ti-20Zr-10Nb-4Ta Alloy Surface Modified by a Focused Fiber Laser. *Sci. China Mater.* **2018**, *61*, 516–524. [CrossRef]
48. Simões, I.G.; dos Reis, A.C.; da Costa Valente, M.L. Analysis of the Influence of Surface Treatment by High-Power Laser Irradiation on the Surface Properties of Titanium Dental Implants: A Systematic Review. *J. Prosthet. Dent.* **2021**, 1–8. [CrossRef]
49. Abdal-hay, A.; Staples, R.; Alhazaa, A.; Fournier, B.; Al-Gawati, M.; Lee, R.S.; Ivanovski, S. Fabrication of Micropores on Titanium Implants Using Femtosecond Laser Technology: Perpendicular Attachment of Connective Tissues as a Pilot Study. *Opt. Laser Technol.* **2022**, *148*, 107624. [CrossRef]
50. Korovessis, P.G.; Deligianni, D.D. Role of Surface Roughness of Titanium Versus Hydroxyapatite on Human Bone Marrow Cells Response. *J. Spinal Disord. Tech.* **2002**, *15*, 175–183. [CrossRef]
51. Elias, C.N.; Lima, J.H.C.; Valiev, R.; Meyers, M.A. Biomedical Applications of Titanium and Its Alloys Biological Materials Science 46-49. *Biol. Mater. Sci.* **2008**, *30*, 46–49.
52. Achneck, H.E.; Jamiolkowski, R.M.; Jantzen, A.E.; Haseltine, J.M.; Lane, W.O.; Huang, J.K.; Galinat, L.J.; Serpe, M.J.; Lin, F.H.; Li, M.; et al. The Biocompatibility of Titanium Cardiovascular Devices Seeded with Autologous Blood-Derived Endothelial Progenitor Cells. EPC-Seeded Antithrombotic Ti Implants. *Biomaterials* **2011**, *32*, 10–18. [CrossRef]
53. Ramesh, S.; Karunamoorthy, L.; Palanikumar, K. Surface Roughness Analysis in Machining of Titanium Alloy. *Mater. Manuf. Process.* **2008**, *23*, 174–181. [CrossRef]
54. Pires, L.C.; Guastaldi, F.P.S.; Nogueira, A.V.B.; Oliveira, N.T.C.; Guastaldi, A.C.; Cirelli, J.A. Physicochemical, Morphological, and Biological Analyses of Ti-15Mo Alloy Surface Modified by Laser Beam Irradiation. *Lasers Med. Sci.* **2019**, *34*, 537–546. [CrossRef] [PubMed]
55. Telegin, S.V.; Lyasnikova, A.V.; Dudareva, O.A.; Grishina, I.P.; Markelova, O.A.; Lyasnikov, V.N. Laser Modification of the Surface of Titanium: Technology, Properties, and Prospects of Application. *J. Surf. Investig.* **2019**, *13*, 228–231. [CrossRef]
56. Lawrence, J.; Hao, L.; Chew, H.R. On the Correlation between Nd:YAG Laser-Induced Wettability Characteristics Modification and Osteoblast Cell Bioactivity on a Titanium Alloy. *Surf. Coat. Technol.* **2006**, *200*, 5581–5589. [CrossRef]
57. Rafiee, K.; Naffakh-Moosavy, H.; Tamjid, E. The Effect of Laser Frequency on Roughness, Microstructure, Cell Viability and Attachment of Ti6Al4V Alloy. *Mater. Sci. Eng. C* **2020**, *109*, 110637. [CrossRef]
58. Györgyey, Á.; Ungvári, K.; Kecskeméti, G.; Kopniczky, J.; Hopp, B.; Oszkó, A.; Pelsöczi, I.; Rakonczay, Z.; Nagy, K.; Turzó, K. Attachment and Proliferation of Human Osteoblast-like Cells (MG-63) on Laser-Ablated Titanium Implant Material. *Mater. Sci. Eng. C* **2013**, *33*, 4251–4259. [CrossRef]
59. Samanta, A.; Wang, Q.; Singh, G.; Shaw, S.K.; Toor, F.; Ratner, A.; Ding, H. Nanosecond Pulsed Laser Processing Turns Engineering Metal Alloys Antireflective and Superwicking. *J. Manuf. Process.* **2020**, *54*, 28–37. [CrossRef]
60. Laketić, S.; Rakin, M.; Momčilović, M.; Ciganović, J.; Veljović, Đ.; Cvijović-Alagić, I. Influence of Laser Irradiation Parameters on the Ultrafine-Grained Ti[Sbnd]45Nb Alloy Surface Characteristics. *Surf. Coat. Technol.* **2021**, *418*, 127255. [CrossRef]
61. Liu, Q.; Liu, Y.; Li, X.; Dong, G. Pulse Laser-Induced Cell-like Texture on Surface of Titanium Alloy for Tribological Properties Improvement. *Wear* **2021**, *477*, 203784. [CrossRef]
62. Zaifuddin, A.Q.; Zulhilmi, F.; Aiman, M.H.; Quazi, M.M.; Ishak, M. Enhancement of Laser Heating Process by Laser Surface Modification on Titanium Alloy. *J. Mech. Eng. Sci.* **2021**, *15*, 8310–8318. [CrossRef]
63. Schnell, U.G.; Duenow, H.S. Effect of Laser Pulse Overlap and Scanning Line Overlap on Femtosecond Laser-Structured Ti6Al4V Surfaces. *Materials* **2020**, *13*, 969. [CrossRef] [PubMed]
64. Eghbali, N.; Naffakh-Moosavy, H.; Sadeghi Mohammadi, S.; Naderi-Manesh, H. The Influence of Laser Frequency and Groove Distance on Cell Adhesion, Cell Viability, and Antibacterial Characteristics of Ti-6Al-4V Dental Implants Treated by Modern Fiber Engraving Laser. *Dent. Mater.* **2021**, *37*, 547–558. [CrossRef] [PubMed]
65. György, E.; Pérez del Pino, A.; Serra, P.; Morenza, J.L. Influence of the Ambient Gas in Laser Structuring of the Titanium Surface. *Surf. Coat. Technol.* **2004**, *187*, 245–249. [CrossRef]
66. El Mogahzy, Y.E. Finishing Processes for Fibrous Assemblies in Textile Product Design. *Eng. Text.* **2009**, 300–326. [CrossRef]
67. Zheng, Q.; Mao, L.; Shi, Y.; Fu, W.; Hu, Y. Biocompatibility of Ti-6Al-4V Titanium Alloy Implants with Laser Microgrooved Surfaces. *Mater. Technol.* **2020**, 1–10. [CrossRef]
68. Hao, L.; Lawrence, J.; Li, L. Manipulation of the Osteoblast Response to a Ti-6Al-4V Titanium Alloy Using a High Power Diode Laser. *Appl. Surf. Sci.* **2005**, *247*, 602–606. [CrossRef]

69. Cunha, A.; Serro, A.P.; Oliveira, V.; Almeida, A.; Vilar, R.; Durrieu, M.C. Wetting Behaviour of Femtosecond Laser Textured Ti-6Al-4V Surfaces. *Appl. Surf. Sci.* **2013**, *265*, 688–696. [CrossRef]
70. May, A.; Agarwal, N.; Lee, J.; Lambert, M.; Akkan, C.K.; Nothdurft, F.P.; Aktas, O.C. Laser Induced Anisotropic Wetting on Ti-6Al-4V Surfaces. *Mater. Lett.* **2015**, *138*, 21–24. [CrossRef]
71. Raimbault, O.; Benayoun, S.; Anselme, K.; Mauclair, C.; Bourgade, T.; Kietzig, A.M.; Girard-Lauriault, P.L.; Valette, S.; Donnet, C. The Effects of Femtosecond Laser-Textured Ti-6Al-4V on Wettability and Cell Response. *Mater. Sci. Eng. C* **2016**, *69*, 311–320. [CrossRef]
72. Rotella, G.; Orazi, L.; Alfano, M.; Candamano, S.; Gnilitskyi, I. Innovative High-Speed Femtosecond Laser Nano-Patterning for Improved Adhesive Bonding of Ti6Al4V Titanium Alloy. *CIRP J. Manuf. Sci. Technol.* **2017**, *18*, 101–106. [CrossRef]
73. Lu, J.; Huang, T.; Liu, Z.; Zhang, X.; Xiao, R. Long-Term Wettability of Titanium Surfaces by Combined Femtosecond Laser Micro/Nano Structuring and Chemical Treatments. *Appl. Surf. Sci.* **2018**, *459*, 257–262. [CrossRef]
74. Huerta-Murillo, D.; García-Girón, A.; Romano, J.M.; Cardoso, J.T.; Cordovilla, F.; Walker, M.; Dimov, S.S.; Ocaña, J.L. Wettability Modification of Laser-Fabricated Hierarchical Surface Structures in Ti-6Al-4V Titanium Alloy. *Appl. Surf. Sci.* **2019**, *463*, 838–846. [CrossRef]
75. Shaikh, S.; Kedia, S.; Singh, D.; Subramanian, M.; Sinha, S. Surface Texturing of Ti6Al4V Alloy Using Femtosecond Laser for Superior Antibacterial Performance. *J. Laser Appl.* **2019**, *31*, 5081106. [CrossRef]
76. Dou, H.Q.; Liu, H.; Xu, S.; Chen, Y.; Miao, X.; Lü, H.; Jiang, X. Influence of Laser Fluences and Scan Speeds on the Morphologies and Wetting Properties of Titanium Alloy. *Optik (Stuttg)* **2020**, *224*, 165443. [CrossRef]
77. Wang, Q.; Wang, H.; Zhu, Z.; Xiang, N.; Wang, Z.; Sun, G. Switchable Wettability Control of Titanium via Facile Nanosecond Laser-Based Surface Texturing. *Surf. Interfaces* **2021**, *24*, 101122. [CrossRef]
78. Mukherjee, S.; Dhara, S.; Saha, P. Enhanced Corrosion, Tribocorrosion Resistance and Controllable Osteogenic Potential of Stem Cells on Micro-Rippled Ti6Al4V Surfaces Produced by Pulsed Laser Remelting. *J. Manuf. Process.* **2021**, *65*, 119–133. [CrossRef]
79. Wang, Z.; Song, J.; Wang, T.; Wang, H. Laser Texturing for Superwetting Titanium Alloy and Investigation of Its Erosion Resistance. *Coatings* **2021**, *11*, 1547. [CrossRef]
80. Singh, I.; George, S.M.; Tiwari, A.; Ramkumar, J.; Balani, K. Influence of Laser Surface Texturing on the Wettability and Antibacterial Properties of Metallic, Ceramic, and Polymeric Surfaces. *J. Mater. Res.* **2021**, *36*, 3985–3999. [CrossRef]
81. Li, H.; Wang, X.; Zhang, J.; Wang, B.; Breisch, M.; Hartmaier, A.; Rostotskyi, I.; Voznyy, V.; Liu, Y. Experimental Investigation of Laser Surface Texturing and Related Biocompatibility of Pure Titanium. *Int. J. Adv. Manuf. Technol.* **2022**. [CrossRef]
82. Tęczar, P.; Majkowska-Marzec, B. The influence of laser alloying of ti13nb13zr on surface topography and properties. *Adv. Mater. Sci.* **2019**, *19*, 45–55. [CrossRef]
83. Ta, D.V.; Dunn, A.; Wasley, T.J.; Kay, R.W.; Stringer, J.; Smith, P.J.; Connaughton, C.; Shephard, J.D. Nanosecond Laser Textured Superhydrophobic Metallic Surfaces and Their Chemical Sensing Applications. *Appl. Surf. Sci.* **2015**, *357*, 248–254. [CrossRef]
84. Liu, K.; Yao, X.; Jiang, L. Recent Developments in Bio-Inspired Special Wettability. *Chem. Soc. Rev.* **2010**, *39*, 3240–3255. [CrossRef] [PubMed]
85. Mukherjee, S.; Dhara, S.; Saha, P. Laser Surface Remelting of Ti and Its Alloys for Improving Surface Biocompatibility of Orthopaedic Implants. *Mater. Technol.* **2018**, *33*, 106–118. [CrossRef]
86. De Oliveira, V.M.C.A.; Aguiar, C.; Vazquez, A.M.; Robin, A.L.M.; Barboza, M.J.R. Corrosion Behavior Analysis of Plasma-Assited PVD Coated Ti-6Al-4V Alloy in 2 M NaOH Solution. *Mater. Res.* **2017**, *20*, 436–444. [CrossRef]
87. Dinu, M.; Franchi, S.; Pruna, V.; Cotrut, C.M.; Secchi, V.; Santi, M.; Titorencu, I.; Battocchio, C.; Iucci, G.; Vladescu, A. *Ti-Nb-Zr System and Its Surface Biofunctionalization for Biomedical Applications*; Elsevier Inc.: Amsterdam, The Netherlands, 2018; ISBN 9780128124567.
88. Supernak-Marczewska, M.; Ossowska, A.; Strąkowska, P.; Zieliński, A. Nanotubular Oxide Layers and Hydroxyapatite Coatings on Porous Titanium Alloy Ti13Nb13Zr. *Adv. Mater. Sci.* **2018**, *18*, 17–23. [CrossRef]
89. Ferdinandov, N.V.; Gospodinov, D.D.; Ilieva, M.D.; Radev, R.H. Structure and Pitting Corrosion of Ti-6al-4v Alloy and Ti-6al-4v Welds. *ICAMS Proc. Int. Conf. Adv. Mater. Syst.* **2018**, 325–330. [CrossRef]
90. Gu, K.X.; Wang, K.K.; Zheng, J.P.; Chen, L.B.; Wang, J.J. Electrochemical Behavior of Ti–6Al–4V Alloy in Hank's Solution Subjected to Deep Cryogenic Treatment. *Rare Met.* **2018**. [CrossRef]
91. Wang, Y.; Tayyebi, M.; Assari, A. Fracture Toughness, Wear, and Microstructure Properties of Aluminum/Titanium/Steel Multi-Laminated Composites Produced by Cross-Accumulative Roll-Bonding Process. *Arch. Civ. Mech. Eng.* **2022**, *22*, 1–14. [CrossRef]
92. Çaha, I.; Alves, A.C.; Rocha, L.A.; Toptan, F. A Review on Bio-Functionalization of β-Ti Alloys. *J. Bio-Tribo-Corrosion* **2020**, *6*, 1–31. [CrossRef]
93. Dias Corpa Tardelli, J.; Bolfarini, C.; Cândido dos Reis, A. Comparative Analysis of Corrosion Resistance between Beta Titanium and Ti-6Al-4V Alloys: A Systematic Review. *J. Trace Elem. Med. Biol.* **2020**, *62*, 126618. [CrossRef]
94. Pawłowski, Ł.; Bartmański, M.; Mielewczyk-Gryń, A.; Zieliński, A. Effects of Surface Pretreatment of Titanium Substrates on Properties of Electrophoretically Deposited Biopolymer Chitosan/Eudragit e 100 Coatings. *Coatings* **2021**, *11*, 1120. [CrossRef]
95. Surma, M.K.; Adach, M.; Dębowska, P.; Turlej, P.S. Projekt i analiza obliczeniowa implantU. *Aktual. Probl. Biomech.* **2019**, 111–122.
96. Bartmański, M.; Pawłowski, Ł.; Zieliński, A.; Mielewczyk-Gryń, A.; Strugała, G.; Cieślik, B. Electrophoretic Deposition and Characteristics of Chitosan-Nanosilver Composite Coatings on a Nanotubular TiO2 Layer. *Coatings* **2020**, *10*, 245. [CrossRef]

97. Manivasagam, G.; Dhinasekaran, D.; Rajamanickam, A. Biomedical Implants: Corrosion and Its Prevention-A Review. *Recent Pat. Corros. Sci.* **2010**, *2*, 40–54. [CrossRef]
98. Boinovich, L.B.; Gnedenkov, S.V.; Alpysbaeva, D.A.; Egorkin, V.S.; Emelyanenko, A.M.; Sinebryukhov, S.L.; Zaretskaya, A.K. Corrosion Resistance of Composite Coatings on Low-Carbon Steel Containing Hydrophobic and Superhydrophobic Layers in Combination with Oxide Sublayers. *Corros. Sci.* **2012**, *55*, 238–245. [CrossRef]
99. Stepanovska, J.; Matejka, R.; Rosina, J.; Bacakova, L.; Kolarova, H. Treatments for Enhancing the Biocompatibility of Titanium Implants. *Biomed. Pap.* **2020**, *164*, 23–33. [CrossRef]
100. Gil, F.J.; Delgado, L.; Espinar, E.; Llamas, J.M. Corrosion and Corrosion-Fatigue Behavior of Cp-Ti and Ti-6Al-4V Laser-Marked Biomaterials. *J. Mater. Sci. Mater. Med.* **2012**, *23*, 885–890. [CrossRef]
101. Tayyebi, M.; Adhami, M.; Karimi, A.; Rahmatabadi, D.; Alizadeh, M.; Hashemi, R. Effects of Strain Accumulation and Annealing on Interfacial Microstructure and Grain Structure (Mg and Al3Mg2 Layers) of Al/Cu/Mg Multilayered Composite Fabricated by ARB Process. *J. Mater. Res. Technol.* **2021**, *14*, 392–406. [CrossRef]
102. Mohammed, M.T.; Khan, Z.A.; Siddiquee, A.N. Surface Modifications of Titanium Materials for Developing Corrosion Behavior in Human Body Environment: A Review. *Procedia Mater. Sci.* **2014**, *6*, 1610–1618. [CrossRef]
103. Nagle Travessa, D.; Vilas Boas Guedes, G.; Capella de Oliveira, A.; Regina Cardoso, K.; Roche, V.; Moreira Jorge, A. The Effect of Surface Laser Texturing on the Corrosion Performance of the Biocompatible β-Ti12Mo6Zr2Fe Alloy. *Surf. Coat. Technol.* **2021**, *405*. [CrossRef]
104. Zeng, C.; Wen, H.; Hemmasian Ettefagh, A.; Zhang, B.; Gao, J.; Haghshenas, A.; Raush, J.R.; Guo, S.M. Reoxidation Process and Corrosion Behavior of TA15 Alloy by Laser Ablation. *Surf. Coat. Technol.* **2020**, *385*, 125397. [CrossRef]
105. Al-Sayed, S.R.; Abdelfatah, A. Corrosion Behavior of a Laser Surface-Treated Alpha–Beta 6/4 Titanium Alloy. *Metallogr. Microstruct. Anal.* **2020**, *9*, 553–560. [CrossRef]
106. Singh, R.; Tiwari, S.K.; Mishra, S.K.; Dahotre, N.B. Electrochemical and Mechanical Behavior of Laser Processed Ti-6Al-4V Surface in Ringer's Physiological Solution. *J. Mater. Sci. Mater. Med.* **2011**, *22*, 1787–1796. [CrossRef] [PubMed]
107. Kumari, R.; Scharnweber, T.; Pfleging, W.; Besser, H.; Majumdar, J.D. Laser Surface Textured Titanium Alloy (Ti-6Al-4V) - Part II - Studies on Bio-Compatibility. *Appl. Surf. Sci.* **2015**, *357*, 750–758. [CrossRef]
108. Kuczyńska-Zemła, D.; Sotniczuk, A.; Pisarek, M.; Chlanda, A.; Garbacz, H. Corrosion Behavior of Titanium Modified by Direct Laser Interference Lithography. *Surf. Coat. Technol.* **2021**, *418*, 127219. [CrossRef]
109. Sun, Z.; Annergren, I.; Pan, D.; Mai, T.A. Effect of Laser Surface Remelting on the Corrosion Behavior of Commercially Pure Titanium Sheet. *Mater. Sci. Eng. A* **2003**, *345*, 293–300. [CrossRef]
110. Xu, Y.; Li, Z.; Zhang, G.; Wang, G.; Zeng, Z.; Wang, C.; Wang, C.; Zhao, S.; Zhang, Y.; Ren, T. Electrochemical Corrosion and Anisotropic Tribological Properties of Bioinspired Hierarchical Morphologies on Ti-6Al-4V Fabricated by Laser Texturing. *Tribol. Int.* **2019**, *134*, 352–364. [CrossRef]
111. Ali, N.; Mustapa, M.S.; Ghazali, M.I.; Sujitno, T.; Ridha, M. Fatigue Life Prediction of Commercially Pure Titanium after Nitrogen Ion Implantation. *Int. J. Automot. Mech. Eng.* **2013**, *7*, 1005–1013. [CrossRef]
112. Liu, B.W.; Mi, G.Y.; Wang, C.M. Reoxidation Process and Corrosion Behavior of TA15 Alloy by Laser Ablation. *Rare Met.* **2021**, *40*, 865–876. [CrossRef]
113. Baxter, J.W.; Bumby, J.R. Fuzzy Control of a Mobile Robotic Vehicle. *Proc. Inst. Mech. Eng. Part I J. Syst. Control. Eng.* **1995**, *209*, 79–91. [CrossRef]
114. Da Rocha, S.S.; Adabo, G.L.; Henriques, G.E.P.; Nóbilo, M.A.D.A. Vickers Hardness of Cast Commercially Pure Titanium and Ti-6Al-4V Alloy Submitted to Heat Treatments. *Braz. Dent. J.* **2006**, *17*, 126–129. [CrossRef] [PubMed]
115. Sharma, A.; Waddell, J.N.; Li, K.C.; A Sharma, L.; Prior, D.J.; Duncan, W.J. Is Titanium–Zirconium Alloy a Better Alternative to Pure Titanium for Oral Implant? Composition, Mechanical Properties, and Microstructure Analysis. *Saudi Dent. J.* **2021**, *33*, 546–553. [CrossRef] [PubMed]
116. Sharan, J.; Lale, S.V.; Koul, V.; Mishra, M.; Kharbanda, O.P. An Overview of Surface Modifications of Titanium and Its Alloys for Biomedical Applications. *Trends Biomater. Artif. Organs* **2015**, *29*, 176–187.
117. Davis, R.; Singh, A.; Jackson, M.J.; Coelho, R.T.; Prakash, D.; Charalambous, C.P.; Ahmed, W.; da Silva, L.R.R.; Lawrence, A.A. *A Comprehensive Review on Metallic Implant Biomaterials and Their Subtractive Manufacturing*; Springer: London, UK, 2022; Volume 120, ISBN 0123456789.
118. Pan, J.; Prabakaran, S.; Rajan, M. In-Vivo Assessment of Minerals Substituted Hydroxyapatite / Poly Sorbitol Sebacate Glutamate (PSSG) Composite Coating on Titanium Metal Implant for Orthopedic Implantation. *Biomed. Pharmacother.* **2019**, *119*, 109404. [CrossRef]
119. Zhang, L.C.; Chen, L.Y.; Wang, L. Surface Modification of Titanium and Titanium Alloys: Technologies, Developments, and Future Interests. *Adv. Eng. Mater.* **2020**, *22*, 1–37. [CrossRef]
120. Rossi, M.C.; Amado, J.M.; Tobar, M.J.; Vicente, A.; Yañez, A.; Amigó, V. Effect of Alloying Elements on Laser Surface Modification of Powder Metallurgy to Improve Surface Mechanical Properties of Beta Titanium Alloys for Biomedical Application. *J. Mater. Res. Technol.* **2021**, *14*, 1222–1234. [CrossRef]
121. Conradi, M.; Kocijan, A.; Klobčar, D.; Godec, M. Influence of Laser Texturing on Microstructure, Surface and Corrosion Properties of Ti-6al-4v. *Metals* **2020**, *10*, 1504. [CrossRef]

122. Chai, L.; Wu, H.; Zheng, Z.; Guan, H.; Pan, H.; Guo, N.; Song, B. Microstructural Characterization and Hardness Variation of Pure Ti Surface-Treated by Pulsed Laser. *J. Alloys Compd.* **2018**, *741*, 116–122. [CrossRef]
123. Pushp, P.; Dasharath, S.M.; Arati, C. Classification and Applications of Titanium and Its Alloys. *Mater. Today Proc.* **2022**. [CrossRef]
124. Khorram, A.; Davoodi Jamaloei, A.; Jafari, A. Surface Transformation Hardening of Ti-5Al-2.5Sn Alloy by Pulsed Nd:YAG Laser: An Experimental Study. *Int. J. Adv. Manuf. Technol.* **2019**, *100*, 3085–3099. [CrossRef]
125. Zhang, T.; Fan, Q.; Ma, X.; Wang, W.; Wang, K.; Shen, P.; Yang, J.; Wang, L. Effect of Laser Remelting on Microstructural Evolution and Mechanical Properties of Ti-35Nb-2Ta-3Zr Alloy. *Mater. Lett.* **2019**, *253*, 310–313. [CrossRef]
126. Ushakov, I.; Simonov, Y. Alterations in the Microhardness of a Titanium Alloy Affected to a Series of Nanosecond Laser Pulses. *MATEC Web Conf.* **2019**, *298*, 00051. [CrossRef]
127. Trueba, P.; Giner, M.; Rodríguez, Á.; Beltrán, A.M.; Amado, J.M.; Montoya-García, M.J.; Rodríguez-Albelo, L.M.; Torres, Y. Tribo-Mechanical and Cellular Behavior of Superficially Modified Porous Titanium Samples Using Femtosecond Laser. *Surf. Coat. Technol.* **2021**, *422*, 127555. [CrossRef]
128. Omoniyi, P.O.; Akinlabi, E.T.; Mahamood, R.M. Heat Treatments of Ti6Al4V Alloys for Industrial Applications: An Overview. *IOP Conf. Ser. Mater. Sci. Eng.* **2021**, *1107*, 012094. [CrossRef]
129. Xu, Y.F.; Yi, D.Q.; Liu, H.Q.; Wang, B.; Yang, F.L. Age-Hardening Behavior, Microstructural Evolution and Grain Growth Kinetics of Isothermal ω Phase of Ti-Nb-Ta-Zr-Fe Alloy for Biomedical Applications. *Mater. Sci. Eng. A* **2011**, *529*, 326–334. [CrossRef]
130. Zafari, A.; Barati, M.R.; Xia, K. Controlling Martensitic Decomposition during Selective Laser Melting to Achieve Best Ductility in High Strength Ti-6Al-4V. *Mater. Sci. Eng. A* **2019**, *744*, 445–455. [CrossRef]
131. El-Hadad, S.; Nady, M.; Khalifa, W.; Shash, A. Influence of Heat Treatment Conditions on the Mechanical Properties of Ti–6Al–4V Alloy. *Can. Metall. Q.* **2018**, *57*, 186–193. [CrossRef]
132. Yao, Y.; Li, X.; Wang, Y.Y.; Zhao, W.; Li, G.; Liu, R.P. Microstructural Evolution and Mechanical Properties of Ti-Zr Beta Titanium Alloy after Laser Surface Remelting. *J. Alloys Compd.* **2014**, *583*, 43–47. [CrossRef]
133. He, B.; Cheng, X.; Li, J.; Tian, X.J.; Wang, H.M. Effect of Laser Surface Remelting and Low Temperature Aging Treatments on Microstructures and Surface Properties of Ti-55511 Alloy. *Surf. Coat. Technol.* **2017**, *316*, 104–112. [CrossRef]
134. Guo, B.; Jonas, J.J. Dynamic Transformation during the High Temperature Deformation of Titanium Alloys. *J. Alloys Compd.* **2021**, *884*, 161179. [CrossRef]
135. Geng, Y.; McCarthy, É.; Brabazon, D.; Harrison, N. Ti6Al4V Functionally Graded Material via High Power and High Speed Laser Surface Modification. *Surf. Coat. Technol.* **2020**, *398*, 126085. [CrossRef]
136. Moura, C.G.; Carvalho, O.; Gonçalves, L.M.V.; Cerqueira, M.F.; Nascimento, R.; Silva, F. Laser Surface Texturing of Ti-6Al-4V by Nanosecond Laser: Surface Characterization, Ti-Oxide Layer Analysis and Its Electrical Insulation Performance. *Mater. Sci. Eng. C* **2019**, *104*, 109901. [CrossRef] [PubMed]
137. Vilar, R.; Almeida, A. *Laser Surface Treatment of Biomedical Alloys*; Elsevier Ltd.: Amsterdam, The Netherlands, 2016; ISBN 9780081009420.
138. Dai, J.; Wang, T.; Chai, L.; Hu, X.; Zhang, L.; Guo, N. Characterization and Correlation of Microstructure and Hardness of Ti–6Al–4V Sheet Surface-Treated by Pulsed Laser. *J. Alloys Compd.* **2020**, *826*, 154243. [CrossRef]
139. Chai, L.; Chen, K.; Zhi, Y.; Murty, K.L.; Chen, L.Y.; Yang, Z. Nanotwins Induced by Pulsed Laser and Their Hardening Effect in a Zr Alloy. *J. Alloys Compd.* **2018**, *748*, 163–170. [CrossRef]
140. Zhang, T.; Fan, Q.; Ma, X.; Wang, W.; Wang, K.; Shen, P.; Yang, J. Microstructure and Mechanical Properties of Ti-35Nb-2Ta-3Zr Alloy by Laser Quenching. *Front. Mater.* **2019**, *6*, 318. [CrossRef]
141. Pfleging, W.; Kumari, R.; Besser, H.; Scharnweber, T.; Majumdar, J.D. Laser Surface Textured Titanium Alloy (Ti-6Al-4V): Part 1 - Surface Characterization. *Appl. Surf. Sci.* **2015**, *355*, 104–111. [CrossRef]
142. Chen, S.; Usta, A.D.; Eriten, M. Microstructure and Wear Resistance of Ti6Al4V Surfaces Processed by Pulsed Laser. *Surf. Coat. Technol.* **2017**, *315*, 220–231. [CrossRef]
143. Chauhan, A.S.; Jha, J.S.; Telrandhe, S.; Srinivas, V.; Gokhale, A.A.; Mishra, S.K. Laser Surface Treatment of α-β Titanium Alloy to Develop a β -Rich Phase with Very High Hardness. *J. Mater. Process. Technol.* **2021**, *288*, 116873. [CrossRef]
144. Kashyap, V.; Ramkumar, P. Improved Oxygen Diffusion and Overall Surface Characteristics Using Combined Laser Surface Texturing and Heat Treatment Process of Ti6Al4V. *Surf. Coat. Technol.* **2022**, *429*, 127976. [CrossRef]
145. Pan, X.; HE, W.; Cai, Z.; Wang, X.; Liu, P.; Luo, S.; Zhou, L. Investigations on Femtosecond Laser-Induced Surface Modification and Periodic Micropatterning with Anti-Friction Properties on Ti6Al4V Titanium Alloy. *Chin. J. Aeronaut.* **2022**, *35*, 521–537. [CrossRef]
146. Rajesh, P.; Muraleedharan, C.V.; Komath, M.; Varma, H. Laser Surface Modification of Titanium Substrate for Pulsed Laser Deposition of Highly Adherent Hydroxyapatite. *J. Mater. Sci. Mater. Med.* **2011**, *22*, 1671–1679. [CrossRef] [PubMed]
147. Ranjith Kumar, G.; Rajyalakshmi, G. Role of Nano Second Laser Wavelength Embedded Recast Layer and Residual Stress on Electrochemical Corrosion of Titanium Alloy. *Mater. Res. Express* **2019**, *6*, 086583. [CrossRef]
148. Utomo, E.P.; Herbirowo, S.; Puspasari, V.; Thaha, Y.N. Characteristics and Corrosion Behavior of Ti–30nb–5sn Alloys in Histidine Solution with Various Nacl Concentrations. *Int. J. Corros. Scale Inhib.* **2021**, *10*, 592–601. [CrossRef]
149. Arrazola, P.J.; Garay, A.; Iriarte, L.M.; Armendia, M.; Marya, S.; Le Maître, F. Machinability of Titanium Alloys (Ti6Al4V and Ti555.3). *J. Mater. Process. Technol.* **2009**, *209*, 2223–2230. [CrossRef]

150. Shao, L.; Du, Y.; Dai, K.; Wu, H.; Wang, Q.; Liu, J.; Tang, Y. β-Ti Alloys for Orthopedic and Dental Applications: A Review of Progress on Improvement of Properties through Surface Modificatio. *Coatings* **2021**, *11*, 1446. [CrossRef]
151. He, D.; Zheng, S.; Pu, J.; Zhang, G.; Hu, L. Improving Tribological Properties of Titanium Alloys by Combining Laser Surface Texturing and Diamond-like Carbon Film. *Tribol. Int.* **2015**, *82*, 20–27. [CrossRef]
152. Kaur, M.; Singh, K. Review on Titanium and Titanium Based Alloys as Biomaterials for Orthopaedic Applications. *Mater. Sci. Eng. C* **2019**, *102*, 844–862. [CrossRef]
153. Faria, A.C.L.; Rodrigues, R.C.S.; Claro, A.P.R.A.; de Mattos, M.G.C.; Ribeiro, R.F. Wear Resistance of Experimental Titanium Alloys for Dental Applications. *J. Mech. Behav. Biomed. Mater.* **2011**, *4*, 1873–1879. [CrossRef]
154. Vishnu, J.; Sankar, M.; Rack, H.J.; Rao, N.; Singh, A.K.; Manivasagam, G. Effect of Phase Transformations during Aging on Tensile Strength and Ductility of Metastable Beta Titanium Alloy Ti–35Nb–7Zr–5Ta-0.35O for Orthopedic Applications. *Mater. Sci. Eng. A* **2020**, *779*. [CrossRef]
155. Qiu, C.; Liu, Q.; Ding, R. Significant Enhancement in Yield Strength for a Metastable Beta Titanium Alloy by Selective Laser Melting. *Mater. Sci. Eng. A* **2021**, *816*, 141291. [CrossRef]
156. Makuch, N.; Kulka, M.; Dziarski, P.; Przestacki, D. Laser Surface Alloying of Commercially Pure Titanium with Boron and Carbon. *Opt. Lasers Eng.* **2014**, *57*, 64–81. [CrossRef]
157. Hatakeyama, M.; Masahashi, N.; Michiyama, Y.; Inoue, H.; Hanada, S. Wear Resistance of Surface-Modified TiNbSn Alloy. *J. Mater. Sci.* **2021**, *56*, 14333–14347. [CrossRef]
158. Zhang, L.C.; Chen, L.Y. A Review on Biomedical Titanium Alloys: Recent Progress and Prospect. *Adv. Eng. Mater.* **2019**, *21*, 1–29. [CrossRef]
159. Salguero, J.; Del Sol, I.; Vazquez-Martinez, J.M.; Schertzer, M.J.; Iglesias, P. Effect of Laser Parameters on the Tribological Behavior of Ti6Al4V Titanium Microtextures under Lubricated Conditions. *Wear* **2019**, *426–427*, 1272–1279. [CrossRef]
160. Wang, H.; Nett, R.; Gurevich, E.L. The Effect of Laser Nitriding on Surface Characteristics and Wear Resistance of NiTi Alloy with Low Power Fiber Laser. *Appl. Sci.* **2021**, *11*, 515. [CrossRef]
161. Jiang, P.; He, X.L.; Li, X.X.; Yu, L.G.; Wang, H.M. Wear Resistance of a Laser Surface Alloyed Ti-6Al-4V Alloy. *Surf. Coat. Technol.* **2000**, *130*, 24–28. [CrossRef]
162. Bahiraei, M.; Mazaheri, Y.; Sheikhi, M.; Heidarpour, A. Mechanism of TiC Formation in Laser Surface Treatment of the Commercial Pure Titanium Pre-Coated by Carbon Using PVD Process. *J. Alloys Compd.* **2020**, *834*, 155080. [CrossRef]
163. Tabrizi, A.T.; Aghajani, H.; Saghafian, H.; Laleh, F.F. Correction of Archard Equation for Wear Behavior of Modified Pure Titanium. *Tribol. Int.* **2021**, *155*, 106772. [CrossRef]
164. Veiko, V.P.; Odintsova, G.V.; Gazizova, M.Y.; Karlagina, Y.Y.; Manokhin, S.S.; Yatsuk, R.M.; Vasilkov, S.D.; Kolobov, Y.R. The Influence of Laser Micro- and Nanostructuring on the Wear Resistance of Grade-2 Titanium Surface. *Laser Phys.* **2018**, *28*. [CrossRef]
165. Zeng, X.; Wang, W.; Yamaguchi, T.; Nishio, K. Characteristics of Surface Modified Ti-6Al-4V Alloy by a Series of YAG Laser Irradiation. *Opt. Laser Technol.* **2018**, *98*, 106–112. [CrossRef]
166. Mohazzab, B.F.; Jaleh, B.; Fattah-alhosseini, A.; Mahmoudi, F.; Momeni, A. Laser Surface Treatment of Pure Titanium: Microstructural Analysis, Wear Properties, and Corrosion Behavior of Titanium Carbide Coatings in Hank's Physiological Solution. *Surf. Interfaces* **2020**, *20*, 100597. [CrossRef]
167. Jia, W.; Hong, Q.; Zhao, H.; Li, L.; Han, D. Effect of Laser Shock Peening on the Mechanical Properties of a Near-α Titanium Alloy. *Mater. Sci. Eng. A* **2014**, *606*, 354–359. [CrossRef]
168. Jia, W.; Zan, Y.; Mao, C.; Li, S.; Zhou, W.; Li, Q.; Zhang, S.; Ji, V. Microstructure Evolution and Mechanical Properties of a Lamellar Near-α Titanium Alloy Treated by Laser Shock Peening. *Vacuum* **2021**, *184*, 109906. [CrossRef]
169. Langlade, C.; Vannes, A.B.; Krafft, J.M.; Martin, J.R. Surface Modification and Tribological Behaviour of Titanium and Titanium Alloys after YAG-Laser Treatments. *Surf. Coat. Technol.* **1998**, *100–101*, 383–387. [CrossRef]
170. Vadiraj, A.; Kamaraj, M. Fretting Fatigue Behavior of Surface Modified Biomedical Titanium Alloys. *Trans. Indian Inst. Met.* **2010**, *63*, 217–223. [CrossRef]
171. Vadiraj, A.; Kamaraj, M.; Kamachi Mudali, U.; Nath, A.K. Effect of Surface Modified Layers on Fretting Fatigue Damage of Biomedical Titanium Alloys. *Mater. Sci. Technol.* **2006**, *22*, 1119–1125. [CrossRef]
172. Campanelli, L.C. A Review on the Recent Advances Concerning the Fatigue Performance of Titanium Alloys for Orthopedic Applications. *J. Mater. Res.* **2021**, *36*, 151–165. [CrossRef]
173. dos Santos, A.; Campanelli, L.C.; Da Silva, P.S.C.P.; Vilar, R.; de Almeida, M.A.M.; Kuznetsov, A.; Achete, C.A.; Bolfarini, C. Influence of a Femtosecond Laser Surface Modification on the Fatigue Behavior of Ti-6Al4V ELI Alloy. *Mater. Res.* **2019**, *22*. [CrossRef]
174. Potomati, F.; Campanelli, L.C.; Da Silva, P.S.C.P.; Simões, J.G.A.B.; de Lima, M.S.F.; Damião, Á.J.; Bolfarini, C. Assessment of the Fatigue Behavior of Ti-6Al-4V ELI Alloy with Surface Treated by Nd:YAG Laser Irradiation. *Mater. Res.* **2019**, *22*, 1–5. [CrossRef]
175. Liu, W.; Liu, S.; Wang, L. Surface Modification of Biomedical Titanium Alloy: Micromorphology, Microstructure Evolution and Biomedical Applications. *Coatings* **2019**, *9*, 249. [CrossRef]

5.2. [JS2] Effect of hybrid modification by ceramic layer formation in MAO process and laser remelting on the structure of titanium bio-alloy Ti13Nb13Zr

5.2.1. Wkład pracy doktoranta

Tytuł: Effect of hybrid modification by ceramic layer formation in MAO process and laser remelting on the structure of titanium bio-alloy Ti13Nb13Zr

Autorzy: Joanna Sypniewska, Marek Szkodo, Beata Majkowska-Marzec, Aleksandra Mielewczyk-Gryń

Czasopismo: Ceramics International Volume 49, Issue 11

Rok wydania: 2023

Impact factor: 5.1

Liczba punktów wg MNiSW: 100

DOI: 10.1016/j.ceramint.2023.02.018

Procentowy wkład pracy doktoranta: 80%

W artykule zajęłam się zaplanowaniem doświadczeń, zaprojektowaniem elektrolitu oraz ustaleniem metodyki badań. Wykonałam prace związane z przygotowaniem próbek do modyfikacji laserowej oraz ich oczyszczaniem po przetapianiu. Wytworzyłam ceramiczne warstwy na stopie tytanu Ti13Nb13Zr. Odpowiadałam za zaplanowanie poszczególnych badań w zakresie morfologii powierzchni, analiz chemicznych, składu fazowego, właściwości mechanicznych oraz zwilżalności. Przeprowadziłam także krytyczną analizę wyników badań i przygotowałam cały manuskrypt. Pełniłam rolę autora korespondencyjnego w kontakcie z czasopismem Ceramics International.

....

mgr inż. Joanna Sypniewska

5.2.2. Treść artykułu

Ceramics International 49 (2023) 16603–16614

Contents lists available at ScienceDirect

Ceramics International

journal homepage: www.elsevier.com/locate/ceramint

Effect of hybrid modification by ceramic layer formation in MAO process and laser remelting on the structure of titanium bio-alloy Ti13Nb13Zr

Joanna Sypniewska [a,*], Marek Szkodo [a], Beata Majkowska-Marzec [a], Aleksandra Mielewczyk – Gryń [b]

[a] Faculty of Mechanical Engineering and Ship Technology, Gdansk University of Technology, Narutowicza, 11/12, 80-233, Gdansk, Poland

[b] Department of Solid State Physics, Gdansk University of Technology, Narutowicza 11/12, 80-233, Gdansk, Poland

ARTICLE INFO

Handling Editor: Dr P. Vincenzini

Keywords:
Laser treatment
Titanium alloy
Ceramics layer
Micro-arc oxidation
Plasma electrolytic oxidation

ABSTRACT

To improve the biological properties of titanium alloy Ti13Nb13Zr, hybrid modifications involving micro-arc oxidation (MAO) and Nd: YAG laser remelting were carried out in two combinations. The first consisted of laser modification before the production of the ceramic layer by the micro-arc oxidation process, and the second combination involved Nd: YAG laser modification after the MAO process. The creation of developed surface morphologies on titanium alloys used in implant manufacturing is currently a widely discussed trend. The modifications used by the authors offer the possibility of obtaining a porous, wettable surface with altered nanohardness.

To investigate the structural properties of the obtained hybrid Nd: YAG-MAO and MAO-laser Nd: YAG modifications, the structure roughness tests were performed with a suitable apparatus and atomic force microscope (AFM) and available software. The surface wettability was evaluated and the surface of the modified Ti13Nb13Zr alloy was subjected to evaluation using a scanning electron microscope (SEM), and an optical microscope. Using available software, chemical composition analysis, porosity analysis, and, adhesion analysis were performed.

Based on the tests carried out, the possibility of carrying out hybrid modification in various combinations was demonstrated. The presence of Na^{+} and Ca^{2+} ions was demonstrated for samples in the combination of laser modification and MAO modification, which is important for biomedical reasons. Each modification allowed changing of the nanohardness, wettability, and roughness in the direction expected, required from biomedical materials. This paper presents an innovative approach to the use of two modifications one using the effect of heat on the matrix and the other focused on the formation of a ceramic coating. Currently, hybrid modifications are desirable in that they allow them to interact positively with each other.

1. Introduction

Laser modification is a technique widely known and discussed in the field of surface modification for various applications. It is a simple and cost-efficient technique that allows control of laser performance throughout the operating time with no heat influence on the material beyond the heat treatment field [1]. Applications of the laser modification technique are indicated for aerospace, automotive, marine, and electronics applications to improve corrosion and erosion resistance [1,2,3]. In the orthopedic implant industry, attention is also given to modifying the structure of the material itself and obtaining a surface with the appropriate roughness, which improves the osseointegration process and the working of the implant components with each other [4]. Furthermore, the possibility of modifying mechanical properties such as hardness and Young's modulus is important due to the need to match the mechanical strength of the inserted implant to the mechanical properties of human bone [5,6]. The use of the Nd: YAG laser has a very extensive spectrum. The use of this type of laser in the military and aerospace industries has been indicated for many years [7] In medicine, it is used to cut soft and hard tissue [8,9] and to modify the surface of implant materials [10]. This type of laser beam is also used in the manufacture of engines in the automotive industry [11]. Characterized by a wavelength of 1064 μm (the laser enables precise operation with limited heat effects on the adjacent structures of the modified component.

* Corresponding author.
E-mail addresses: joanna.sypniewska@pg.edu.pl (J. Sypniewska), marek.szkodo@pg.edu.pl (M. Szkodo), beamajko@pg.edu.pl (B. Majkowska-Marzec), alegryn@pg.edu.pl (A. Mielewczyk – Gryń).

https://doi.org/10.1016/j.ceramint.2023.02.018
Received 22 November 2022; Received in revised form 16 January 2023; Accepted 2 February 2023
Available online 8 February 2023
0272-8842/

A new issue in the world of science is the use of different surface modification techniques for the same material which makes it possible to combine the advantages of different techniques or to reduce the negative effects of one technique with another one. Process micro-arc oxidation known also as plasma electrolytic oxidation [12] is a technique that allows, using micro discharges on the surface of a material, the incorporation of elements present in the electrolyte environment in which the process is carried out, while simultaneously building up a coating on the surface of the material [13]. The technique makes it possible to obtain ceramic coatings that contain specifically determined additives present in the electrolyte medium. This technique is used primarily for magnesium materials [14] and increasingly for titanium alloys [12,13]. The process allows for improving the biocompatibility of the surface due to the possibility to incorporate ions, which are among other things, components of human bone or cause the activation of the osseointegration process. The literature [15] states that strong implant-bone connections are stimulated by the presence of calcium and its phosphates, so the authors of this study chose a process environment in which hydroxyapatite (Ca10(PO4)6(OH)2) was present. Current indications are a combination of micro-arc oxidation and laser modification. The authors will perform this hybrid modification starting with laser modification, followed by micro-arc oxidation [15–17].

The project focuses on a modification that could be used in the medical, dental, and orthopedic implant industries. For this reason, the choice was made to work with the alloy Ti13Nb13Zr, which is an osteoconductive material [18]. Compared to the frequently studied and used titanium alloys with aluminum and vanadium content, Ti13Nb13Zr alloy shows higher biocompatibility and has fewer side effects when implanted, while metallic materials have been shown to have low biocompatibility and low bond strength between bone and implant [19].

The authors of this article focused mainly on the structural properties of hybrid-modified Ti13Nb13Zr titanium alloy in different combinations of the order of use of the Nd: YAG laser and the micro-arc oxidation technique. The authors have devoted considerable attention to the morphology of the surface structure of hybrid-modified Ti13Nb13Zr titanium alloy samples. Wettability and surface roughness are discussed in detail, providing a rich set of information on the properties of the surface and, as pointed out in the literature, this is an area that receives little attention but is an important aspect in the field of implantology for the intrinsic integrity of the implant [20]. What's more basic investigations were carried out to evaluate changes such as porosity, nanohardness, Young modulus of the coatings, and adhesion from scratch test resulting from the double modification.

The need for surface modification due to the demands placed on biomaterials is indicated. The human body defines all elements introduced into its interior as something that may pose a risk, in the case of elements that do not exhibit biocompatibility and appropriate characteristics for tissue binding, element rejection may occur. It is therefore of great benefit to use modifications that build ceramic coatings to build a layer that is compatible with the human body, and the use of laser modification allows a controlled modification of the material to obtain the correct value of mechanical parameters and surface structure [21].

The research provides a basis for considering the application of the presented hybrid modification and the order in which the various modifications should be carried out. In addition, the modification technique used represents a novelty in the field of surface modification for biomedical applications and provides ample opportunity for further work to advance knowledge in this area.

2. Materials and surface treatment

The research used Ti13Nb13Zr titanium bi-alloy specimens. The samples were circular with a height of approximately 5 mm and a diameter of 19 mm. The samples were cut from homogeneous bar-shaped material, the cut is made across the length of the bar. The chemical composition of the bar is given in Table 1. The alloy was chosen for its good properties to the requirements for biomedical applications such as high biocompatibility and good mechanical properties.

Table 1
Chemical composition of Ti13Nb13Zr by weight.

Element	Ti	C	H	O	N	Fe	Nb	Zr
Wt. [%]	71.38	0.8	0.015	0.016	0.05	0.25	14	13.5

Samples were mechanically prepared using a Saphire 330 polishing and grinding machine and 400/800/1200 silicate abrasive paper. The specimens were also cleaned in an ultrasonic cleaner and then washed with isopropanol (99.7%. POCH. Gliwice. Poland).

The study assumed that two combinations of surface modifications were performed on the Ti13Nb13Zr alloy (Fig. 1). The first of the combinations were assumed to perform an initial remelting using an Nd: YAG laser of the surface for two different device power parameters. with constant parameters of laser beam travel speed, frequency, and laser pulse duration. The modification was carried out in a 98% pure argon environment to reduce oxidation during the modification. The next laser modification step was to perform micro-arc oxidation also at constant parameters(Table 2.), at 23°C.

The second combination consisted of a micro-arc oxidation process followed by laser modification of the applied ceramic coating. All oxidations in both combinations took place under the same parameters.

The micro-arc oxidation process was carried out with a DC power supply (BK PRECISION, MR 1000020). The Ti13Nb13Zr titanium alloy samples were machined and cleaned in isopropanol before the process was performed and then placed in an ultrasonic cleaner in distilled water for 10 min. The electrodes in the system were the Ti13Nb13Zr titanium alloy sample on which the MAO process took place - it was the anode (Fig. 2). The opposite electrode, the cathode, was a stainless steel basket (Fig. 2).

To execute the process, a liter of electrolyte was prepared, containing $Na+$ and $Ca2+$ ions derived from 0.7348 g/mol NaOH and 0.0497 g/mol of hydroxyapatite Ca10(PO4)6(OH)2. The process was carried out with constant parameters for each of the modified samples, with no change in values depending on the order of modifications carried out. The parameters for the process carried out are shown in Table 2. As heat energy is released during the MAO process, the authors used a magnetic stirrer and placed the vessel in which the process took place in water at a constant room temperature of 20°C to maintain a constant temperature.

Eight samples modified appropriately were subjected to property tests. The treatment of the individual samples is shown in Table 3. In this paper, the authors will use the names in Table 3.

3. Surface characterization

3.1. Wettability test

To measure the contact angle 3 measurements were taken for each sample using the falling drop method with a goniometer (Contact angle goniometer. Zeiss. Ulm. Germany). The liquid dropped on the surface of the samples was water, and the measurement lasted 10 s for each measurement at room temperature.

3.2. Roughness test

Roughness profile tests were carried out three times on all of the samples (P1–P8), taking into account parameters such as Ra (arithmetic average height), Rp (maximum profile peak height), and Wt (total waviness). The measurements were made with a Hommel Etamic Waveline (JENOPTIK). The test was performed in a measurement range of 400 μm, at a speed of 0.5 mm/s. During the test, an ISO11562 filter was used.

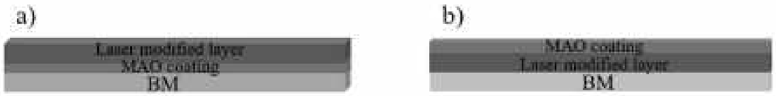

Fig. 1. Scheme of two combinations of the modification Ti13Nb13Zr titanium alloy a) for laser modification before MAO treatment, b) for laser modification after MAO treatment.

Table 2
Parameters of laser modification and micro-arc oxidation.

Laser modification Nd: YAG			
Power	Scan rate	Duration of the laser pulse	Frequency
1000 W 1500 W	0.6 mm/s	2.25 ms	25 Hz
Micro-arc oxidation process			
Voltage	Density $\left[\frac{A}{m^2}\right]$	Time of the process [min]	
300	10.20	15	

3.3. Nanoindentation test

The nanoindentation test was carried out by NanoTest™ Vantage (Micro Materials, Great Britain using a Berkovich three-sided pyramidal diamond. The maximum test load was 50 mN. The load was increased from 0 to 50 mN in 15 s and the unloading time was also 15 s. The number of indentations was 25 with 5s dwell at maximum load.

As a result of the nanoindentation test, values of reduced Young's modulus were obtained using the Oliver-Pharr method. The reduced Young's modulus values obtained were used to calculate Young's modulus using a constant Poisson's ratio of 0.35, formula 1

$$E^{*} = \frac{E}{1-\nu^{2}}, \text{ where } \nu \text{ is a Possion's ratio.} \quad (1)$$

Using the ANOVA statistical method, an analysis of variance was performed on the nanoindentation test results obtained.

3.4. Scratch test of MAO coatings

The scratch test was estimated by NanoTest^{TM}Vantage (Micro Materials, Great Britain) using Berkovich three-sided pyramidal diamond. The load was 400 mN, the scratch length was 1000 μm, and the examination was taken 5 times. Samples with coatings obtained by the MAO process (P2, P5, P6) on Ti13Nb13Zr titanium alloy were subjected to a scratch. The scratch test allowed an indication of the critical load LC, which was determined from the acoustic emission curves. The obtained scratches on the surface of the coatings were observed under an optical microscope (Olympus UC 50).

3.5. Microstructure observation via optical microscope and scanning electron microscope

Laser-modified samples P3, P4, and double-modified samples P7, and P8, where the laser modification was the second modification of the material, were subjected to the observation of the microstructure of the surface using an optical microscope (Olympus UC 50). Examination of the microstructure took place at lens magnifications of x5.

For samples P2 to P8, metallographic samples were taken. The samples were placed in epoxy resin after being cut transversely, then polished and etched. The specimens, in the form of metallographic specimens, were subjected to optical microscopy to evaluate the heat-affected zones, and scanning electron microscopy to assess changes in the microstructure of the hybridised Ti13Nb13Zr alloy.

3.6. Scanning electron microscope (SEM), X-ray diffraction (XRD), and atomic force microscope (AFM) observation – roughness, phase, and chemical composition, and porosity test

The samples modified during the MAO process (P2) and those modified in a combination of laser modification, and micro-arc oxidation process (P5, P6) were subjected to observation under a SEM (Edax Inc., Mahwah, NJ, U.S.A.) and, using an EDS (Energy Dispersive X-Ray Spectroscopy) attachment to the device, X-ray microanalysis was performed, which also enables the analysis of the chemical composition of the sample surface. In addition, the samples were subjected to atomic

Table 3
Samples and their modifications.

Sample	Modification
P1	Mechanically prepared Ti13Nb13Zr titanium alloy
P2	Ti13Nb13Zr modified by the micro-arc oxidation process
P3	Laser modified Ti13Nb13Zr by 1000 W
P4	Laser modified Ti13Nb13Zr by 1500 W
P5	Laser modification of Ti13Nb13Zr by 1000 W + MAO process
P6	Laser modification of Ti13Nb13Zr by 1500 W + MAO process
P7	Ti13Nb13Zr modified by MAO process + laser modification by 1000 W
P8	Ti13Nb13Zr modified by MAO process + laser modification by 1500W

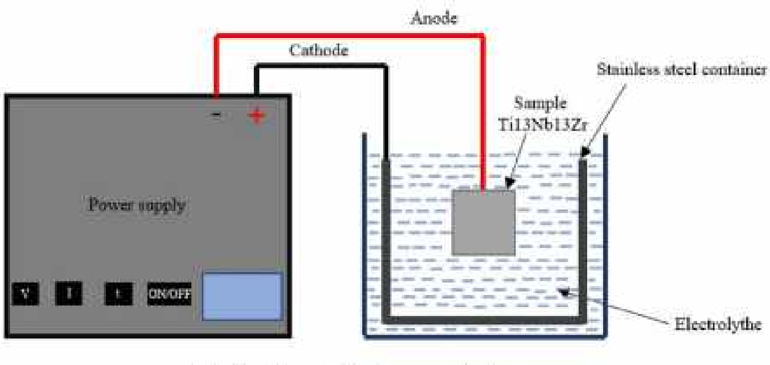

Fig. 2. Scheme of the micro-arc oxidation process.

Table 4
Parameters of profilograph test, wettability measurement, and nanoindentation test.

Sample	Parameters of profilograph test			Contact angle [°]	Reduced Young modulus [GPa]	Young modulus [GPa]
	Ra [μm]	Rp [μm]	Wt [μm]			
P1	0.20 ± 0.01	0.80 ± 0.04	3.42 ± 1.14	73.69 ± 4.27	61.04 ± 9.14	56.57 ± 8.47
P2	0.40 ± 0.01	1.49 ± 0.08	1.25 ± 0.44	69.23 ± 13.32	79.39 ± 24.02	74.85 ± 22.65
P3	0.72 ± 0.02	1.70 ± 0.10	4.74 ± 0.49	64.44 ± 2.15	23.45 ± 0.83	21.01 ± 0.74
P4	1.84 ± 0.10	3.29 ± 0.26	8.44 ± 1.18	61.04 ± 14.74	13.36 ± 0.34	11.88 ± 0.30
P5	1.05 ± 0.02	2.94 ± 0.14	5.02 ± 0.49	61.35 ± 3.40	85.97 ± 22.20	81.55 ± 2.08
P6	2.25 ± 0.24	4.70 ± 0.65	7.67 ± 0.42	59.57 ± 3.25	70.04 ± 26.93	65.45 ± 1.89
P7	4.72 ± 0.24	11.30 ± 0.08	17.33 ± 1.97	32.26 ± 4.00	96.58 ± 26.64	92.54 ± 25.53
P8	3.78 ± 0.02	8.71 ± 0.19	9.87 ± 1.87	52.19 ± 6.30	98.70 ± 22.44	94.76 ± 21.54

force microscopy (AFM; NaniteAFM, Nanosurf AGLiestal, Switzerland) observation, which allowed images to be obtained of the topography of the MAO-modified surfaces. In addition, using SEM images and MultiScan software, pore size and porosity were examined for samples P2, P5, and P6.

The XRD, X-ray diffraction method (Phillips X'Pert Pro, Almelo, Netherlands)was used to determine phases in modified samples. The method was applied by a diffractometer (Cu Kα, λ = 0.1554 nm) in the range 10–90° of 2θ. The measurements were taken at an interval of 0.02 for 2s of measurement per point, the process taking place at ambient temperature.

The entire set of samples (P1–P8) was subjected to AFM observation to obtain the 3D surface roughness parameter Sa, that is, the arithmetic means deviation of the surface roughness from the reference plane over an area of 50 μm × 50 μm.

4. Results and discussion

Using the roughness parameters obtained in the profile graph study presented in Table 4 and taking into account Fig. 3 presenting example contact angles for the tested samples of modified titanium alloy Ti13Nb13Zr as well as roughness and waviness diagrams, it can be indicated that the application of laser modification (P3, P4), carrying out the MAO process (P2) and the application of hybrid modifications (P5–P8) changes the surface roughness of titanium alloy Ti13Nb13Zr. It is indicated from the results that there is an increase in the roughness and a decrease in the contact angle relative to the base material of the Ti13Nb13Zr alloy. Concerning the modifications that were carried out, it should be pointed out that carrying out a single laser modification and a modification using the micro-arc oxidation process produced a rougher surface for the laser-modified sample, which is associated with an increase in surface wettability. These results are in line with the conclusions presented in the literature [6,10,22,23].

Taking into account the core modifications for the presented work, i. e. hybrid laser Nd: YAG-MAO and MAO-laser Nd: YAG modifications, an

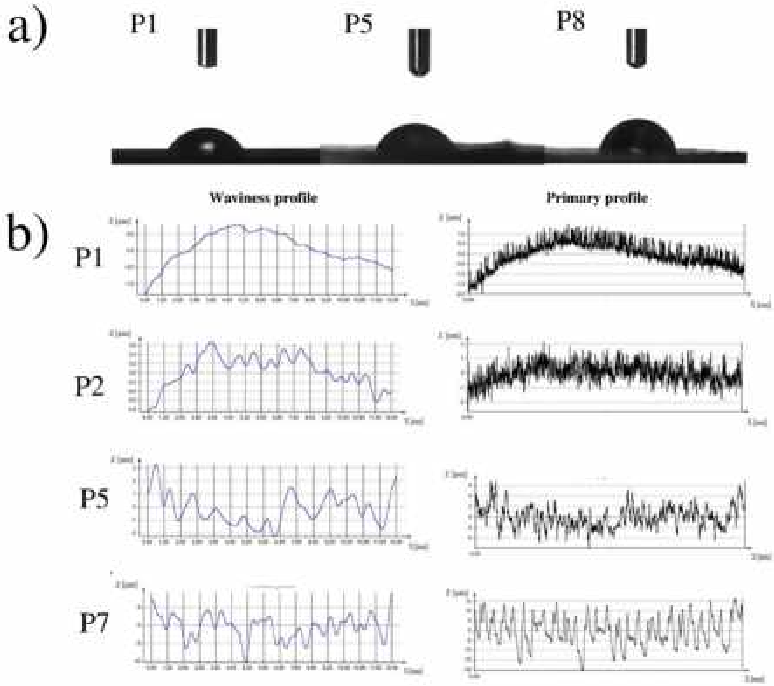

Fig. 3. a) Contact angle for P1- base material and P5 - the lowest contact angle value, P8- the higher contact angle value; b) Presentation of depth and waviness profiles for P1- base material, P2 - base material with MAO coating, P5 – sample with hybrid modification laser 1000 W-MAO, P7 sample with hybrid modification MAO-laser 1000 W.

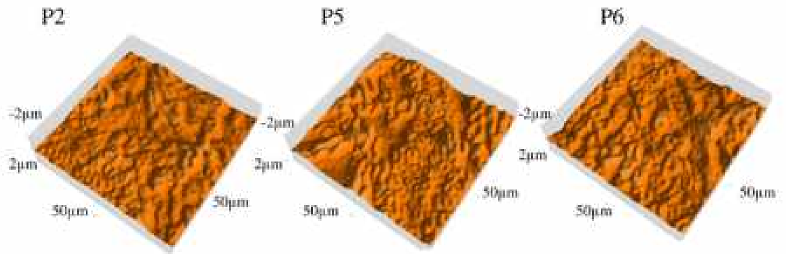

Fig. 4. Atomic force microscopy (AFM) topography of the Ti13Zr13Nb substrate A – P2, B – P5, C – P6

increase in roughness and a decrease in contact angle for the native material is visible. It is observable that the use of a higher laser power of 1500 W for machining, where the laser modification was performed first and then the MAO technique is applied, increases the roughness parameters R_a, R_p, and W_t. This relationship was also confirmed by the determination of the surface roughness parameter S_a, where it was shown that the application of laser modification before carrying out the MAO process affects the roughness by increasing its parameter values (Fig. 4). The literature [15,24,25] indicates that the use of laser modification and increasing the operating parameters, and laser power, results in increased roughness, which is reflected in this work.

However, the opposite situation occurs in the case of hybrid modification of P7 and P8 samples, wherein the first stage of modification MAO coating was deposited and then laser modification was applied on Ti13Nb13Zr titanium alloy samples, here a decrease in roughness is indicated for the P8 sample, where higher laser power was applied. Based on the surface roughness tests carried out, it can be indicated that the MAO-laser modification (P7, P8) allows for obtaining a rougher surface structure than the laser-MAO modification (P5, P6). The Ra parameter value for these modifications varies from 60 to 450 % depending on the Nd: YAG laser power used. The present results are in agreement with the conclusions of the authors of papers [15,26], where it was shown that the deposition of MAO on a smooth surface generates an increase in surface roughness, as MAO coatings are highly porous coatings, while the deposition of MAO coatings on rough surfaces (P5, P6) results in the filling of previously formed depressions and protrusions, which makes the surface less rough. In contrast, work [27] shows that increasing the laser power increases the surface roughness.

Analyzing the test results for specimens P2, P5, and P6 it should be pointed out (Table 4) that the influence on increasing the roughness parameters and decreasing the contact angle for the modified titanium alloy Ti13Nb13Zr is also due to the altered oxygen content obtained from the chemical composition analysis. The resulting oxides on the surface of the samples improve the wettability of the surface [28], and there was an increase in surface roughness Taking into account the current state of the literature, it is indicated that it is more beneficial for biomedical applications to produce a rougher coating with better wettability properties, as this improves the osseointegration process. Bone cells on a rough surface with a high affinity for water are more easily activated, which speeds up the process of bonding between implant and bone. The literature shows that the appropriate range of contact angle values for implant materials should be between 40° and 60° [29,30] or 35° to 85° [31] which was achieved for the modifications carried out in this work. In the case of bone cells, an optimum value for the contact angle is indicated at 55° [31], the closest contact angle to this value was received for sample P6 subjected to hybrid laser Nd: YAG-MAO modification. At the same time, it is pointed out that achieving lower roughness parameters is also advantageous because in implant design it is necessary to create both smooth and rough surfaces, even within the same implant [4]. The literature indicates that the roughness and wettability of the surface to be characterized by the material depends particularly on the type of tissues that will surround

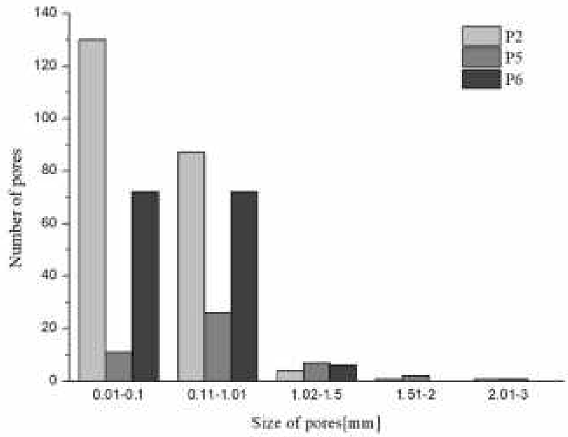

Fig. 5. Size distribution of pores in 5 different compartments for samples P2, P5, P6

the implant, which involves a very individual approach to this issue [32].

Images of the surface structure of the P2, P5, and P6 samples allowed the porosity of the samples to be assessed, on which Nd: YAG laser modification was applied followed by the MAO process. Using MultiScan software, the image was converted into a binary image, which allowed the structure to be analyzed. The number of pores present on the banded area of the half using the SEM was obtained. The pores ranged in size from 0.01 μm to 3 μm. In addition, it was possible to show that the porosity for each of the samples P2, P5, and P6, expressed in %, was respectively: 6.55%, 3.74%, and 6.79% (Fig. 5). The study shows that higher laser power increases surface porosity. The surface of sample P5 has larger pores than samples P2 and p6, but at the same time has the smallest number of pores in the entire area. The coating of sample P2 is characterized by the smallest number of pores, which may indicate that by the previously cited literature [15,26] the MAO coating completed the rough surface after the laser beam and the surface became less rough. The pores produced by the hybrid modification are small, relatively too small if one were to focus on a specific optimal pore size in the literature [33], but at the same time, it is indicated that the absence of hydroxyapatite in implants with an optimal pore size negatively affected the integration of bone into the implant. In the present follow-up, the presence of hydroxyapatite in the fabricated laser-MAO surface is indicated [34]. In addition, it should be noted that the surfaces are rich in terms of their morphology. The SEM images make it possible to note, apart from the pores, the undulations present. on the surface, Such a developed surface of the modified specimens is advantageous for bone cells developing on it because it improves the process of integration of the cells into the implant surface. It is indicated that such a surface is a

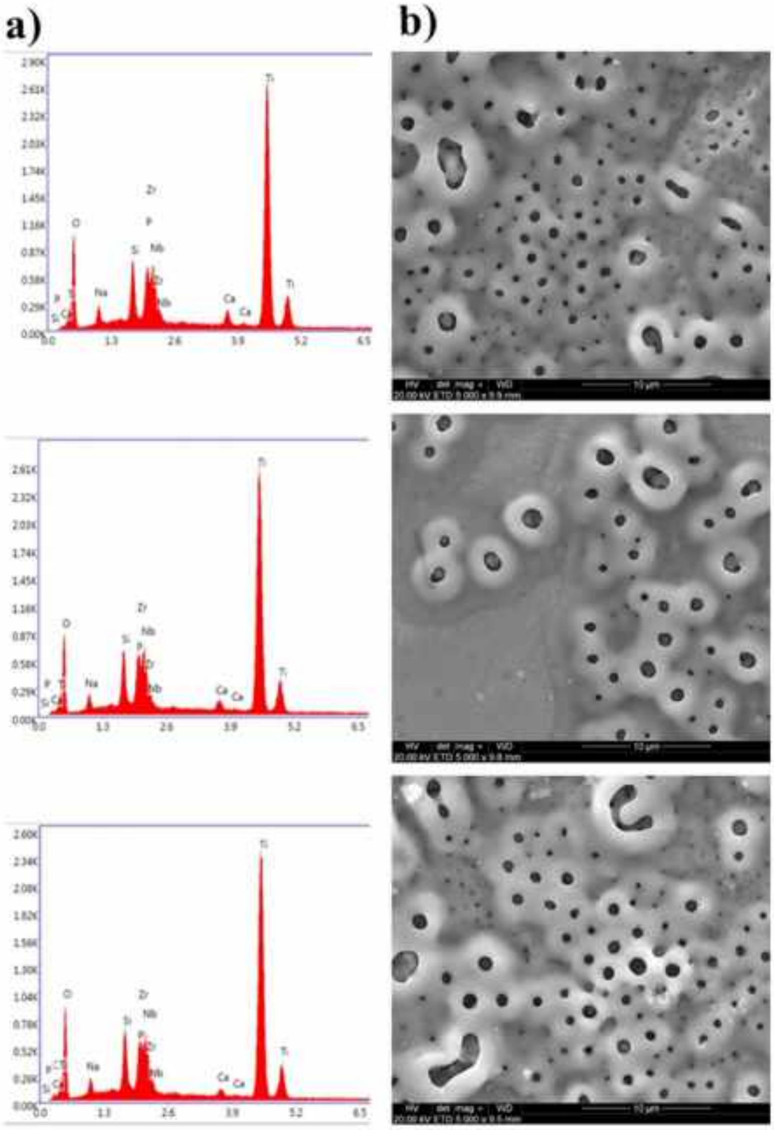

Fig. 6. SEM scanning results a) Results of the EDS analysis of P2, P5, and P6 samples b) surface structure topography of the samples P2, P5, P6

biomimetic surface, i.e. it mimics the naturally occurring bone structure in the body. [35], which is important because such conditions allow the body to react to the material as if it were an integral part of it.

The researchers in this study used an electrolyte whose components were hydroxyapatite and sodium hydroxide, these two components were chosen due to the orientation of the modification to biomedical applications, sodium and calcium derived from hydroxyapatite are elements involved in the process of osseointegration of the bone with the implant, but above all, they are part of the bone-building elements, which allows for increased biocompatibility of the modified biomedical material. Due to the nature of the surface of the modified specimens, it was decided to carry out an SEM + EDS study for the P2, P5, and P6 modifications. The SEM study, during which an EDS analysis of the chemical composition was possible, allowed the percentage composition

Table 5
Composition of P2, P5, P6 samples by weight %.

	O	Na	Si	P	Zr	Nb	Ca	Ti	C
P2	37.9 ± 5.23	3.68 ± 1.38	3.45 ± 0.62	1.24 ± 0.15	5.89 ± 0.90	6.23 ± 0.33	1.37 ± 0.59	39.36 ± 0.56	0.73 ± 0.31
P5	33.72 ± 9.01	3.07 ± 1.79	3.49 ± 1.06	0.63 ± 0.18	6.81 ± 1.24	6.43 ± 1.10	1.21 ± 0.44	44.44 ± 9.73	0.16 ± 0.01
P6	40.49 ± 1.74	4.12 ± 0.71	3.69 ± 0.44	0.70 ± 0.17	6.48 ± 1.12	5.81 ± 0.40	0.80 ± 0.24	36.87 ± 1.71	1.29 ± 0.65

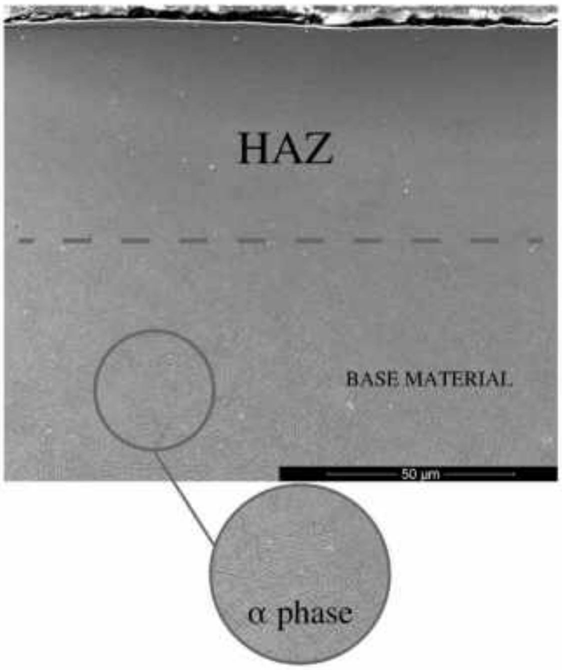

Fig. 7. SEM cross-section of P3 sample with focus on HAZ and base material phase.

of the analyzed samples to be examined(Fig. 6, Table 5). It is important to consider that, according to the theoretical assumptions of the MAO process, the elements present in the electrolyte are incorporated into the surface of the material undergoing modification. Therefore, the analysis aimed to record the presence of Na^{+} and Ca^{2+} ions. The presence of these ions was demonstrated for each of the analyzed samples P2, P5, and P6, which indicates that the process was carried out correctly and additionally indicates that the application of laser modification before coating in the micro-arc oxidation process does not adversely affect the process. It was shown that more sodium ions were incorporated into the surface of the samples than calcium ions. The presence of laser modification in the case of sodium ions resulted, for samples modified with a 1000 W Nd: YAG laser, in a decrease in the % of sodium ions relative to the control sample P2, while there was an increase in the % of sodium ions in the sample previously modified with a 1500 W power. In the case of calcium ions, a clear relationship is observable that the presence of the laser modification and the increase in the laser parameters results in a decrease in the amount of % Ca^{2+} ions in the sample. The change in the percentage of oxygen in the sample is also significant. Titanium, because it is a self-assembling material, has a very high affinity for oxygen and, in addition, surface oxidation occurs during the MAO process; additionally, an increase in oxygen can be generated minimally by the laser treatment. It can be seen that for sample P6 relative to sample P2, a higher percentage of oxygen is observed in the composition, for sample P5 there is less oxygen, while the result for this sample and this element is subject to a high standard deviation. For each of the samples, the proportion of silicon ions was also observed, indicating that the presence of this element is related to the mechanical treatment during the preparation of the samples for testing, as they are subjected to mechanical grinding by silicate papers.

For specimens P3 and P4, the outlined heat-affected zone was very clearly observed; to illustrate the heat-affected zone, an image is shown where the heat-affected zone is indicated and a Fig. 7 of the parent

Table 6
The depht of the heat-affected zone measured by optical microscope software.

Sample	Depth of the heat-affected zone [μm]
P3	67.20
P4	302.60
P5	92.7
P6	289.0
P7	216.12
P8	403.52

material of the Ti13Nb13Zr alloy, which consists of alpha phase martensitic needles. The remelted zone is characterized by the absence of a significant number of needles, there has been a remodeling of the structure and it has become fragmented.. The use of higher laser power for the 1500 W P4 sample resulted in an increase in the heat-affected zone (Table 6), which is also observable in other work using lasers for surface modification indicates with increasing laser power there is an increase in the heat-affected zone [6,10].

Scanning electron microscope (Fig. 8) imaging studies allowed the evaluation of the change in the microstructure of the MAO coating and the effect of the presence of two hybrid treatments on the heat-affected zone and coating behaviour. Sample P2 in cross-section does not show significant porosity, its structure is quite composite. Agglomeration of the coating structure is observed.

For sample P5, a heat-affected zone of the same depth is observed as for sample P3, that due to the use of the same Nd: YAG laser power value. In the case of the applied MAO coating on the laser-modified surface, a higher adhesion of the MAO coating to the Ti13Nb13Zr surface is observed because a more integrated coating is observed than in the case of sample P2, where the metallographic deposit process has detached part of the coating (Fig. 8). In the photograph of sample P5 (b) of Fig. 8), the transverse surface and the outer surface with visible pores of the coating are observable, which indicates that the metallographic specimen preparation process did not damage the coating and it can be observed in its entirety. It is also observed that the micro-arc oxidation process proceeded correctly due to the noticeable incorporation of the coating into the surface of the laser-modified material. For sample P6, a thicker MAO coating is observed to be deposited and it is less porous, few larger protrusions are observed compared to sample P5 this may be due to the substrate as it is rougher due to the higher laser modification power of 1500 W, and it is indicated in the literature [15,26] that a rougher substrate for the MAO process results in a less rough surface. craters can be observed on sample P5 as a result of the MAO process discharge. A heat-affected zone can be observed on the sample, the depth of which is similar to that for sample P4.

Sample P7 and P8 are characterised by an increased heat affected zone a compared to samples P3, P4 and P5, P6 (Table 6). The increase in the HAZ for samples P7, P8 may be related to the fact that the deposited oxide layer caused the activation of the remelting process, which is a factually correct statement because in works [36,37] he presence of oxygen and deprivation of the argon laser modification environment caused an increase in the occurrence of craters on the surface of the material and an increase in the roughness of the material. It is interesting to note that a separate layer is present on the surface of the modified hybrid material using first MAO deposition and then Nd:YAG laser modification, indicating the mixing of the oxygen layer of MAO and the native Ti13Nb13Zr material. EDS studies showed that, in addition to the elements of the native material, calcium-specific maxima were observed, the presence of which is justified because the MAO process environment contained Ca^{2+} ions. Martensite needles are visible in agglomerations of the mixed material, indicating a dynamic transformation activated by the heat of the Nd:YAG laser (Fig. 8).

Fig. 9 presents the XRD spectrum for samples P1 – Ti13Nb13Zr without any modification, P2 with MAO layer, P5, P6, P7, P8 samples modified in a hybrid way. The samples were tested by XRD to show the

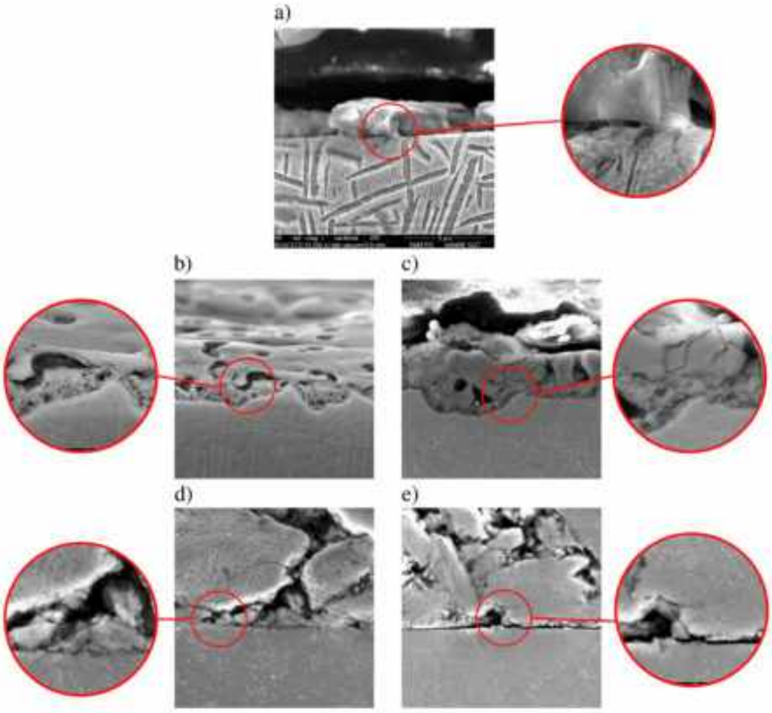

Fig. 8. SEM cross-section images for the same condition as sample a)P2, bb) for P5, c) P6, d) P7, e) P8.The images were taken under the same conditions as sample a) HV: 10 000 kV, mag 10 000, the image in the circle HV 10 000 kV, mag 25 000.

changes in titanium phases after hybrid modifications and to check out the presence of some chemical components from the MAO process environment.

The XRD test did not show the presence of compounds derived from hydroxyapatite or compounds in which Na + ions would be present for samples P2, P5, P6, P7, and P8. Other published studies state that the XRD test does not detect the presence of compounds with ions present in the micro-arc oxidation environment, which does not mean that they are not present as the EDS chemical composition studies indicate the presence of Na^{+}, and Ca^{2+} ions (Table 5). It is indicated that additional phases indicating the presence of ions incorporated in the XRD process may appear in the amorphous structure [23], which is present in the XRD results (Fig. 9). In addition, it is indicated that the absence of compounds from the MAO process is related to the under-concentration of these elements compared to titanium or oxygen [15], n the XRD spectra for samples P2, P5, P6, P7, P7 which have undergone MAO modification P2and hybrid modification in various combinations, the presence of titanium telnide occurring as anatase and rutile is observed. It is indicated in Fig. 9 that for the samples subjected to hybrid modification, the intensity of the maxima for anatase and rutile is higher with the exception of the maximum occurring at 25 indicating the presence of anatase, where it is shown that this form of titanium oxide is absent for the laser modification after MAO coating. The literature indicates that a rutile phase is given for the materials after surface modifications. The study shows an increase in the rutile phase of titanium oxide.

Hybrid-modified samples, where a higher-power Nd:YAG laser was used, show higher intensities of maxima. The presence of titanium oxides indicates the good ability of the Ti13Nb13Zr titanium alloy For each sample, maxima originating from the material substrate are indicated, justified by the structure of the applied MAO coating, which has a porous structure that reveals the Ti13Nb13Zr parent material. For sample P1, the individual phases of the titanium alloy Ti13Nb13Zr, which is an α-β alloy, are indicated. On the basis of the analyzed XRD results(Fig. 9) and nanohardness results (Fig. 10), it can be indicated that rutile-related maxima and, at the same time, higher hardness are observed for the hybrid-modified samples at 100 W laser mod (P5, P7) than for the hybrid-modified samples P6, P8 at 1500 W Nd:YAG laser mod. Based on the theory in the field of anatase and rutile structure and properties, rutile shows a higher Mosh scale hardness, while at the same time being a more stable phase that anatase [38]. However, the literature states that the presence of rutile phase and anatase TiO2 in different ratios does not affect the hardness [39].

The nanoindentation test allowed to obtain values for reduced Young's modulus, and nanohardness and also to calculate Young's modulus, the data of which are presented in Table 4 and Figs. 10 and 11. Based on the data collected, it is fair to say that the modification leads to a change in the material's hardness and Young's modulus. The reference sample, P1, is characterized by good mechanical properties, but the hybrid Laser-MAO and MAO-Laser modifications changed these properties, with an increase in nanohardness and Young's modulus for each parameter. In the work [17] it was indicated that the MAO treatment applied on the laser-modified sample increases the microhardness of the sample, in the work presented also such a relationship was obtained between the control samples and samples P5, and P6. On the other hand, sample P8 of titanium alloy Ti13Nb13Zr achieved the highest values for each Young's modulus, these values were almost 70% higher than the values of this parameter for the native material.

In contrast, sample P7 showed the highest nanohardness. An increase in the hardness of the samples after using the MAO-Nd: YAG laser combination was also demonstrated in the work [40]. In this work, two different modifications were evaluated, which are not widely discussed in the literature; however, it is indicated from the results obtained that the modification in the order of MAO-Nd: YAG laser caused the greatest increase in the parameters analyzed. Both for the modification pair P5,

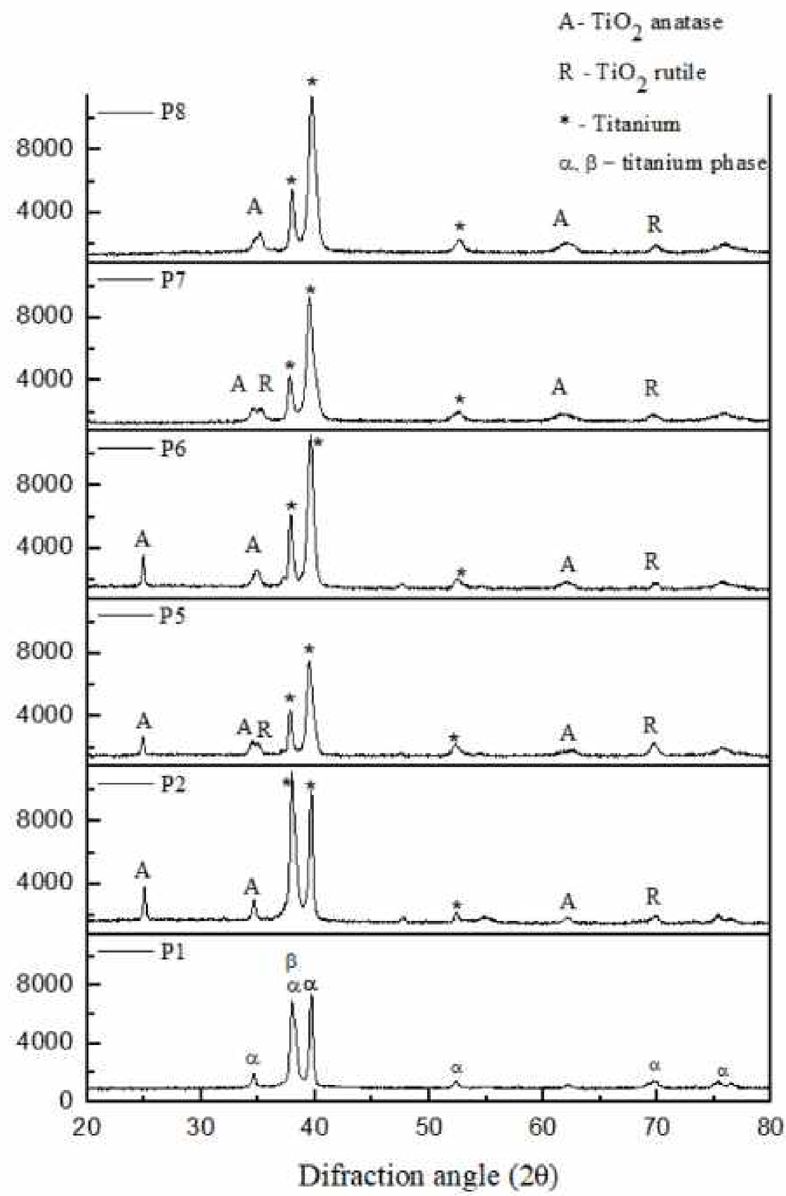

Fig. 9. X-ray diffractograms of samples P1, P2, P5, P6, P7, P8 samples.

P6, and P7, P8, the Ti13Nb13Zr samples modified at a laser operating power of 1000 W showed a higher hardness; at the same time, it should be pointed out that the same relation occurred for the samples P3, P4, which were subjected to a single modification as control samples. The reduced Young modulus of the samples and the lower value of Young modulus for Ti13Nb13Zr samples modified at the lower laser operating power of P4, P6, and P8 may be because, at high laser operating parameters (1500 W), longer martensitic laths are formed as a result of the long cooling process, and these generate a lower hardness of the material [41]. In addition, it has been noted that micropores are formed during the solidification process after laser treatment, which is a result of the retention of gas bubbles during the solidification process of the material [42]. In the case of the single MAO modification, there was an improvement in nanohardness relative to the native material, but this was lower than for the hybrid modified samples (P5–P8). Based on the nanoindentation test, it was shown that modification in the order of MAO-Nd: YAG laser increases the surface nanohardness of the modified material.

An analysis of variance was carried out for the hardness results. The results of the analysis are summarised in Table 7. The analysis conducted allows us to conclude that the differences in hardness between the different surface treatments are significantly different, with a p-value of less than 0.001. The ANOVA analysis also showed that there are strong differences in hardness after the different modifications of the surface

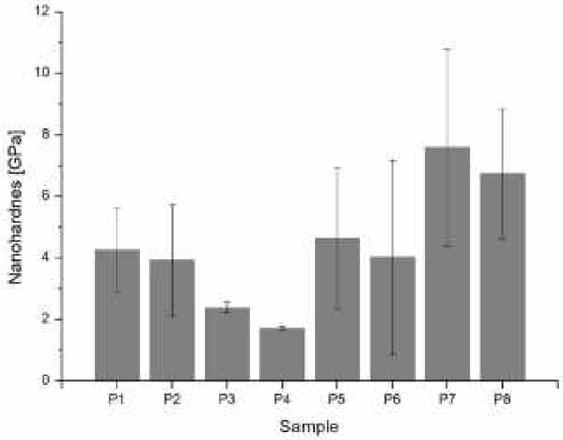

Fig. 10. Nanohardness of all samples P1–P8.

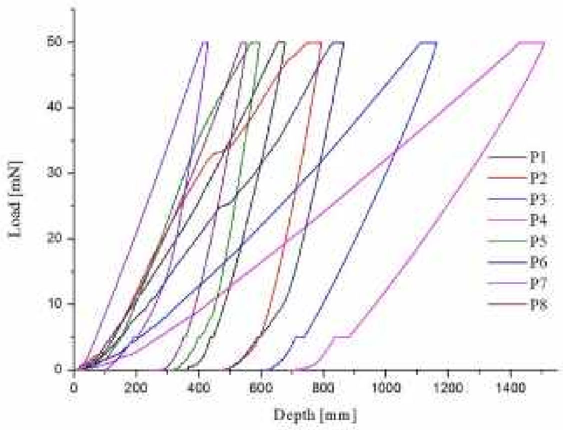

Fig. 11. Hysteresis plots of load-deformation for all samples from P1 to P8. Hysteresis plot made as a median of 25 curves based on measurements taken.

Table 7
ANOVA analysis of nanohardness results.

	The sum of squares SS	df	average square AS	F	p	η^2
among groups	684.35	7	97.74			
within groups	839.83	192	4.37	22.35	<0.0001	0.45
Total	1524.18	199				

layer of the TiZr13Nb13 alloy, as indicated by the η2 value, which is significantly greater than 0.14.

Fig. 12 shows the dependence of the frictional force on the normal force and the acoustic emission, in addition, the average critical force Lc is plotted for the specimens on which the MAO coating was the outer layer of modifications P2, P5, P6 (Table 8). The determination of the critical force L_c is important as it represents the minimum load at which the first coating failure occurs. It is indicated that L c is related to the first deflection of the acoustic emission curve, which is the shock wave that causes the initial microcracking [23,43–45]. The collected data indicated that the coating obtained on the previously modified Nd: YAG laser surface of titanium alloy Ti13Nb13Zr had the highest adhesion. The weakest adhesion to the surface of the MAO coating is characterized by the P6 sample, which was modified with an Nd: YAG laser at a high laser operating power of 1500 W before the MAO process. The difficulty in depositing a stable coating may have been due to the earlier modification because when such a high power is applied, a thicker and harder material surface is produced, as can be seen in the work where there was an increase in the heat-affected zone as the laser power operation increased [10].

The authors decided to analyze the microstructural images obtained with an optical microscope to compare the quality of the melts on samples with a single 1000 W and 1500 W laser modification and samples subjected to laser modification after micro-arc oxidation. Based on Fig. 13, prior micro arc oxidation modificatmicro-arcd the paths of the Nd: YAG laser beam to be more visible, and not so many cracks were observed as in the case of Ti13Nb13Zr titanium alloy modified only with the laser beam. The presence of the MAO coating, however, affected the noticeable extrusions at different stages of the laser beam path which is related to the remelting and mixing of the native material with the applied coating during modification, which improves the microstructure of the coatings [33]. The use of higher laser power for both P4 and P8 samples resulted in fewer cracks and structural damage being observed in the laser beam path, which is associated with more extensive surface remelting [46].

5. Conclusion

On the strength of the author's research, it can be concluded that the application of two different surface modification combinations influences basic material parameters such as wettability, surface roughness, porosity, and coating adhesion, as well as the chemical composition of the applied coatings and hardness and Young's modulus, and the nature of the surface were also evaluated.

The hybrid MAO-laser and laser-MAO modifications represent new modification combinations for titanium alloy Ti13Nb13Zr. Such treatment was intended to complement the mutual modifications and improve the properties of the investigated matrix. Based on the tests carried out, it was found that the application of the hybrid modification results in an increase in the surface roughness values and a decrease in the wetting angle, with the application of the MAO technique before the Nd: YAG laser modification generating the greatest increase in wettability and roughness parameters. It was shown that the 1500 W high-power laser modification (P6) achieves higher surface porosity than micro-arc oxidation alone. In addition, it is important that the authors were able to achieve a coating with the Nd: YAG laser-MAO combination that is rich in calcium and sodium ions, which is important as these ions are naturally present in the chemical composition of bone.

In the case of nanohardness and Young's modulus values, it was shown that the application of the hybrid modification increases the values of these parameters, while the modification with the combination of MAO-laser Nd: YAG significantly increases the values of nanohardness and Young's modulus. A scratch test showed that the coating of sample P5 exhibited higher adhesion to the substrate than that obtained with a single MAO modification (P2). In addition, it was shown that the MAO-laser Nd: YAG hybrid modification influences the nature of the laser beam path, minimizing the number of cracks on the surface.

In conclusion, the use of hybrid modification for two different combinations of MAO-laser Nd: YAG and Nd: YAG laser-MAO is advantageous in that such a surface treatment offers the possibility to produce rich, developed morphologies, which is advantageous in that the selected Ti13Nb13Zr material is used for the manufacture of implants, is used in a multitude of scientific studies conducted towards the future use of this alloy in the production of implants, which are required to have biomimetic properties to improve the intrusion of the material into bone. Surface modification activities stimulate bone-forming cells

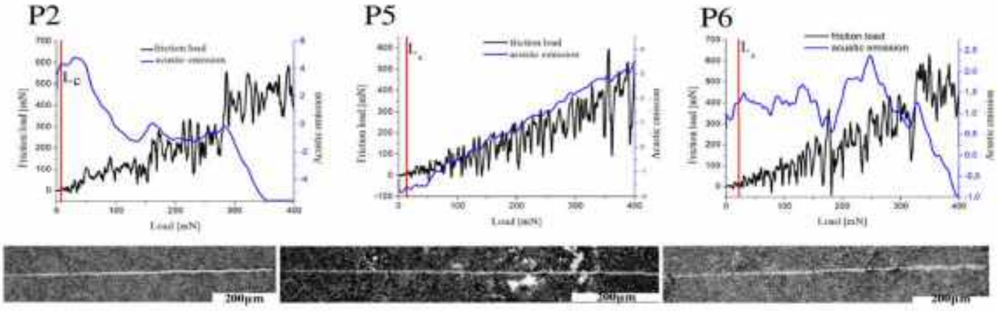

Fig. 12. Scratch test runs with shown scratch (bottom) and marked critical load Lc, acoustic emission, and friction load.

Table 8
Value of critical load Lc [mN] for samples P2, P5, P6

P2	P5	P6
16.52 ± 8.12 mN	18.01 ± 7.77 mN	9.11 ± 5.44 mN

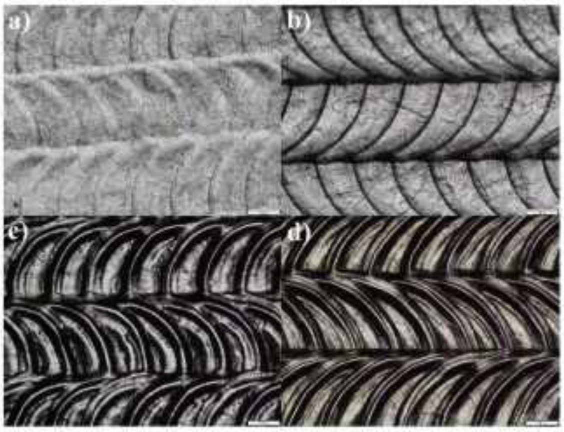

Fig. 13. Microstructure of laser modified samples Ti13Nb13Zr and samples with dual modification MAO-laser modification Ti13Nb13Zr A – laser modified sample; 1000 W (P3), B – laser modified sample 1500 W (P4), C – MAO and laser modified sample (P7); 1000 W, D – MAO as laser modified sample; 1500W (P8).

to grow and, in addition, the presence of calcium and sodium ions increases the biocompatibility of the matrix. In further work on the two types of modification, it is necessary to delve into the mechanical properties of the obtained coatings in their cross-sections, to study the corrosion properties and to improve the porosity aspect of the modifications presented by the authors.

Declaration of competing interest

The authors declare that they have no known competing financial interests or personal relationships that could have appeared to influence the work reported in this paper.

References

[1] Q. Wang, P. Zhou, S. Liu, S. Attarilar, R.L.W. Ma, Y. Zhong, L. Wang, Multi-scale surface treatments of titanium implants for rapid osseointegration: a review, Nanomaterials 10 (2020) 1–27, https://doi.org/10.3390/nano10061244.

[2] C.T. Kwok, Laser Surface Modification of Alloys for Corrosion and Erosion Resistance, 2012. https://doi.org/10.1016/B978-0-85709-015-7.50014-2.

[3] P. Fabbri, M. Messori, Surface Modification of Polymers: Chemical, Physical, and Biological Routes, Elsevier Inc., 2017, https://doi.org/10.1016/B978-0-323-44353-1.00005-1.

[4] G. Menci, A. Gökhan, D.G. Waugh, J. Lawrence, B. Previtali, Applied Surface Science Laser surface texturing of β-Ti alloy for orthopaedics : effect of different wavelengths and pulse durations, Appl. Surf. Sci. 489 (2019) 175–186, https://doi.org/10.1016/j.apsusc.2019.05.111.

[5] J. Pan, S. Prabakaran, M. Rajan, In-vivo assessment of minerals substituted hydroxyapatite/poly sorbitol sebacate glutamate (PSSG) composite coating on titanium metal implant for orthopedic implantation, Biomed. Pharmacother. 119 (2019), 109404, https://doi.org/10.1016/j.biopha.2019.109404.

[6] J. Sypniewska, M. Szkoda, Influence of Laser Modification on the Surface Character of Biomaterials : Titanium and its Alloys — A Review, 2022.

[7] T.J. Rockstroh, Application of slab-based Nd:YAG lasers at GE aircraft engines, LIA (Laser Inst. Am. 71 (1991) 132–140, https://doi.org/10.2351/1.5058358.

[8] T.D. Myers, J.D. McDaniel, The pulsed Nd:YAG dental laser: review of clinical applications, J. Calif. Dent. Assoc. 19 (1991) 25–30.

[9] S.K. Ghaly, D.F. Ghoneim, S.A. Ahmed, A.M. Abdel-Salam, Histological evaluation of retina after photo disruption for vitreous humor by Q-switched neodymium-doped yttrium aluminium garnet (Nd: YAG) laser, J. Laser Med. Sci. 4 (2013) 190–198.

[10] B. Majkowska-Marzec, J. Sypniewska, Microstructure and mechanical properties of laser surface-treated Ti13Nb13Zr alloy with MWCNTs coatings, Adv. Mater. Sci. 21 (2021) 5–18, https://doi.org/10.2478/adms-2021-0021.

[11] N. Pavel, M. Tsunekane, T. Taira, Nd : YAG/Cr 4 + : YAG monolithic micro-laser with multiple-beam output for engine ignition, Opt Express 19 (2011) 1831–1833.

[12] J.I. Kang, M.K. Son, H.C. Choe, W.A. Brantley, Bone-like apatite formation on manganese-hydroxyapatite coating formed on Ti-6Al-4V alloy by plasma electrolytic oxidation, Thin Solid Films 620 (2016) 126–131, https://doi.org/10.1016/j.tsf.2016.07.088.

[13] Y. Wang, H. Yu, C. Chen, Z. Zhao, Review of the biocompatibility of micro-arc oxidation coated titanium alloys, Mater. Des. 85 (2015), https://doi.org/10.1016/j.matdes.2015.07.086.

[14] Z. Lin, T. Wang, X. Yu, X. Sun, H. Yang, Functionalization treatment of micro-arc oxidation coatings on magnesium alloys: a review, J. Alloys Compd. 879 (2021), 160453, https://doi.org/10.1016/j.jallcom.2021.160453.

[15] Y. Wang, D. Lu, G. Wu, K. Chen, H. Wu, Q. Zhang, J. Yao, Effect of laser surface remelting pretreatment with different energy density on MAO bioceramic coating, Surf. Coating. Technol. 393 (2020), 125815, https://doi.org/10.1016/j.surfcoat.2020.125815.

[16] L. Wang, J. Zhou, J. Liang, J. Chen, Microstructure and corrosion behavior of plasma electrolytic oxidation coated magnesium alloy pre-treated by laser surface melting, Surf. Coating. Technol. 206 (2012) 3109–3115, https://doi.org/10.1016/j.surfcoat.2011.12.040.

[17] G. Wu, Y. Wang, M. Sun, Q. Zhang, J. Yao, V. Kovalenko, Effect of laser surface melting pretreatment on the growth behavior and mechanical properties of microarc oxidation coating on Ti6Al4V alloy, J. Laser Appl. 32 (2020), 012013, https://doi.org/10.2351/1.5098000.

[18] F. Marini, E. Luzi, S. Fabbri, S. Ciuffi, S. Sorace, I. Tognarini, G. Galli, R. Zonefrati, F. Sbaiz, M.L. Brandi, Osteogenic differentiation of adipose tissue-derived mesenchymal stem cells on nanostructured Ti6Al4V and Ti13Nb13Zr, Clin. Cases Miner. Bone Metab. 12 (2015) 224–237, https://doi.org/10.11138/ccmbm/2015.12.3.224.

[19] A. Laska, Parameters of the electrophoretic deposition process and its influence on the morphology of hydroxyapatite coatings, Review, Inżynieria Mater. 1 (2020) 20–25, https://doi.org/10.15199/28.2020.1.3.

[20] F. Rupp, R.A. Gittens, L. Scheideler, A. Marmur, B.D. Boyan, Z. Schwartz, J. Geis-Gerstorfer, A review on the wettability of dental implant surfaces I: theoretical and experimental aspects, Acta Biomater. 10 (2014) 2894–2906, https://doi.org/10.1016/j.actbio.2014.02.040.

[21] K.K.A. Mosas, A.R. Chandrasekar, A. Dasan, A. Pakseresht, D. Galusek, Recent advancements in materials and coatings for biomedical implants, Gels 8 (2022), https://doi.org/10.3390/gels8050323.

[22] P. Pachauri, L.R. Bathala, R. Sangur, Techniques for dental implant nanosurface modifications, J. Adv. Prosthodont. 6 (2014) 498–504, https://doi.org/10.4047/jap.2014.6.6.498.

[23] M. Dziaduszewska, M. Shimabukuro, T. Seramak, A. Zielinski, T. Hanawa, Effects of micro-arc oxidation process parameters on characteristics of calcium-phosphate containing oxide layers on the selective laser melted Ti13Zr13Nb alloy, Coatings 10 (2020) 1–24, https://doi.org/10.3390/COATINGS10080745.

[24] M. Jażdżewska, D.B. Kwidzińska, W. Seyda, D. Fydrych, A. Zieleiński, Mechanical Properties and Residual Stress Measurements of Grade IV Titanium and Ti-6Al-4V and Ti-13Nb-13Zr Titanium Alloys after Laser Treatment, 2021.

[25] M.B.P. Tęczar, B. Majkowska-Marzec, THE INFLUENCE OF LASER ALLOYING OF Ti13Nb13Zr ON SURFACE TOPOGRAPHY AND PROPERTIES, Adv. Mater. Sci. 19 (2019) 45–55, https://doi.org/10.2478/adms-2019-0004.

[26] W.B. Dai, L.X. Yuan, C.Y. Li, D. He, D.W. Jia, Y.M. Zhang, The effect of surface roughness of the substrate on fatigue life of coated aluminum alloy by micro-arc oxidation, J. Alloys Compd. 765 (2018) 1018–1025, https://doi.org/10.1016/j.jallcom.2018.06.290.

[27] S. Amruthaluru, H. Sampatirao, M. Palanivel, R.K. Lingamaneni, R. Nagumothu, Effect of laser treatment on morphology and corrosion behaviour of the plasma electrolytic oxidation coatings developed on aluminized steel, Surf. Coating. Technol. 394 (2020), 125888, https://doi.org/10.1016/j.surfcoat.2020.125888.

[28] T. Arunnellaiappan, N. Kishore Babu, L. Rama Krishna, N. Rameshbabu, Influence of frequency and duty cycle on microstructure of plasma electrolytic oxidized AA7075 and the correlation to its corrosion behavior, Surf. Coating. Technol. 280 (2015) 136–147, https://doi.org/10.1016/j.surfcoat.2015.08.043.

[29] B. Majkowska-Marzec, B. Bartosewicz, P. Tęczar, M. Bartmański, J.B. J, Mechanical and corrosion properties of laser surface-treated Ti13Nb13Zr alloy with, Materials 13 (2020) 1–22, https://doi.org/10.3390/ma13183991.

[30] S. Heise, C. Forster, S. Heer, H. Qi, J. Zhou, S. Virtanen, T. Lu, A.R. Boccaccini, Electrophoretic deposition of gelatine nanoparticle/chitosan coatings, Electrochim. Acta 307 (2019) 318–325, https://doi.org/10.1016/j.electacta.2019.03.145.

[31] L. Cordero-Arias, S. Cabanas-Polo, H. Gao, J. Gilabert, E. Sanchez, J.A. Roether, D. W. Schubert, S. Virtanen, A.R. Boccaccini, Electrophoretic deposition of nanostructured-TiO2/chitosan composite coatings on stainless steel, RSC Adv. 3 (2013) 11247–11254, https://doi.org/10.1039/c3ra40535d.

[32] K.L. Menzies, L. Jones, The impact of contact angle on the biocompatibility of biomaterials, Optom. Vis. Sci. 87 (2010) 387–399, https://doi.org/10.1097/OPX.0b013e3181da863e.

[33] J. Mateos, J.M. Cuetos, R. Vijande, E. Fernández, Tribological properties of plasma sprayed and laser remelted 75/25 Cr3C2/NiCr coatings, Tribol. Int. 34 (2001) 345–351, https://doi.org/10.1016/S0301-679X(01)00023-8.

[34] M.J. DanM, J. CrossG, J.RogerJ. Spycher, 7 - Cementless Fixation Techniques and Problems, Jt. Replace. Technol. third ed., 2021, pp. 185–211.

[35] B. Bhushan, Y.C. Jung, Natural and biomimetic artificial surfaces for superhydrophobicity, self-cleaning, low adhesion, and drag reduction, Prog. Mater. Sci. 56 (2011) 1–108, https://doi.org/10.1016/j.pmatsci.2010.04.003.

[36] S. Laketić, M. Rakin, M. Momčilović, J. Ciganović, D. Veljović, I. Cvijović-Alagić, Surface modifications of biometallic commercially pure Ti and Ti-13Nb-13Zr alloy by picosecond Nd:YAG laser, Int. J. Miner. Metall. Mater. 28 (2021) 285–295, https://doi.org/10.1007/s12613-020-2061-9.

[37] S. Laketić, M. Rakin, M. Momčilović, J. Ciganović, Veljović, I. Cvijović-Alagić, Influence of laser irradiation parameters on the ultrafine-grained Ti{sbnd}45Nb alloy surface characteristics, Surf. Coating. Technol. 418 (2021), https://doi.org/10.1016/j.surfcoat.2021.127255.

[38] D.A.H. Hanaor, C.C. Sorrell, Review of the anatase to rutile phase transformation, J. Mater. Sci. 46 (2011) 855–874, https://doi.org/10.1007/s10853-010-5113-0.

[39] B.B. Topuz, G. Gündüz, B. Mavis, Ü. Çolak, The effect of tin dioxide (SnO2) on the anatase-rutile phase transformation of titania (TiO2) in mica-titania pigments and their use in paint, Dyes Pigments 90 (2011) 123–128, https://doi.org/10.1016/j.dyepig.2010.12.013.

[40] F. Wang, Y. Wang, B. Hou, H. Liu, M. Lian, Characteristics of micro-arc oxidation and laser melting modified compound film on Ti alloy surface, Emerg. Mater. Res. 4 (2015) 223–228, https://doi.org/10.1680/emr.15.00003.

[41] S.R. Al-Sayed, A. Abdelfatah, Corrosion behavior of a laser surface-treated alpha–beta 6/4 titanium alloy, Metallogr. Microstruct. Anal. 9 (2020) 553–560, https://doi.org/10.1007/s13632-020-00667-w.

[42] M.C. Rossi, J.M. Amado, M.J. Tobar, A. Vicente, A. Yañez, V. Amigó, Effect of alloying elements on laser surface modification of powder metallurgy to improve surface mechanical properties of beta titanium alloys for biomedical application, J. Mater. Res. Technol. 14 (2021) 1222–1234, https://doi.org/10.1016/j.jmrt.2021.07.037.

[43] M. Bartmański, Ł. Pawłowski, Properties of chitosan/CuNPs coatings electrophoretically deposited on TiO2 nanotubular oxide layer of Ti13Zr13Nb alloy, Mater. Lett. 308 (2022) 9–12, https://doi.org/10.1016/j.matlet.2021.130982.

[44] Ł. Pawłowski, M. Bartmański, A. Mielewczyk-Gryń, A. Zieliński, Chitosan/poly(4-vinylpyridine) coatings formed on AgNPs-decorated titanium, Mater. Lett. 319 (2022), https://doi.org/10.1016/j.matlet.2022.132293.

[45] I. Aydin, A.I. Bahçepinar, M. Kirman, M.A. Çipiloglu, HA coating on Ti6Al7Nb alloy using an electrophoretic deposition method and surface properties examination of the resulting coatings, Coatings 9 (2019), https://doi.org/10.3390/COATINGS9060402.

[46] G.E. Romanos, H. Everts, G.H. Nentwig, Effects of diode and Nd:YAG laser irradiation on titanium discs: a scanning electron microscope examination, J. Periodontol. 71 (2000) 810–815, https://doi.org/10.1902/jop.2000.71.5.810.

5.3. [JS3] Exploring the composition and corrosion resistance in hybrid-modified Ti13Nb13Zr alloy

5.3.1. Wkład pracy doktoranta

Tytul: Exploring the composition and corrosion resistance in hybrid-modified Ti13Nb13Zr alloy

Autorzy: Joanna Sypniewska, Marek Szkodo, Beata Majkowska-Marzec, Aleksandra Mielewczyk-Gryń

Czasopismo: MRS Communications, Volume 14, pages 1439–1445

Rok wydania: 2024

Impact factor: 2.2

Liczba punktów wg MNiSW: 100

DOI: 10.1557/s43579-024-00663-z

Procentowy wkład pracy doktoranta: 80

W niniejszym artykule zajęłam się przygotowaniem materiału do badań. Sposób przygotowania próbek oraz skład elektrolitu były tożsame jak w artykule [JS2] opublikowanym w Ceramics International. W pracy przeprowadziłam badania korozyjne, zanurzeniowe oraz analizę i dyskusję uzyskanych wyników w zakresie składu chemicznego oraz uwalniania jonów do roztworu po badaniach zanurzeniowych. Przygotowałam cały manuskrypt, w tym część merytoryczną wstępu, opis metodyki oraz dyskusję wyników. Nadzorowałam również proces publikacyjny jako autorka korespondencyjna.

mgr inż. Joanna Sypniewska

5.3.2. Treść artykułu

MRS Communications (2024) 14:1439–1445

https://doi.org/10.1557/s43579-024-00663-z

MRS Communications Research Letter

Exploring the composition and corrosion resistance in hybrid-modified Ti13Nb13Zr alloy

Joanna Sypniewska, Marek Szkodo, and Beata Majkowska-Marzec, Institute of Manufacturing and Materials Technology, Faculty of Mechanical Engineering and Ship Technology, Gdańsk University of Technology, Gdansk, Poland
Aleksandra Dorota Mielewczyk-Gryń, Institute of Nanotechnology and Materials Engineering, Faculty of Applied Physics and Mathematics, and Advanced Materials Centre, Gdańsk University of Technology, Gdańsk, Poland
Address all correspondence to Joanna Sypniewska at **joanna.sypniewska@pg.edu.pl**

(Received 25 March 2024; accepted 3 October 2024; published online: 18 October 2024)

Abstract
Hybrid modification, combining Nd: YAG laser and micro-arc oxidation, enhances biomaterials like titanium alloys by improving biocompatibility and corrosion resistance. This study investigates the chemical composition of modified surfaces and their performance in corrosion tests, with implications for implantology. Results show that hybrid treatment improves ion implantation efficiency and corrosion resistance compared to MAO alone, offering promising benefits for the Ti13Nb13Zr alloy. For instance, the Nd: YAG (1000W)-MAO modification exhibits superior corrosion resistance compared to other methods.

Introduction
In material modification, the goal is to enhance material properties in a consistent, uncomplicated, and cost-effective manner. The laser modification method and micro-arc oxidation technique enable the creation of a hybrid-modified surface on the titanium alloy Ti13Nb13Zr. These modifications have been found to significantly impact the mechanical properties of the titanium alloy Ti13Nb13Zr, including its hardness, alterations in Young's modulus, surface roughness, and the hydrophobic/hydrophilic nature of the surface. Currently, the primary focus of research lies in enhancing the corrosion resistance of metallic materials.[1,2] Another critical aspect is the augmentation of the biocompatibility of implant materials to reduce the occurrence of implant failures.[3]

Laser beam modification is widely employed for surface modification due to its reproducibility, safety, and cost effectiveness. Various types of lasers are utilized in this process, including Nd:YAG lasers,[4] erbium lasers,[5] and diode lasers.[6] It is reported that laser techniques influence the surface morphology and increase the surface hardness and mechnaic strength of the layer.[7] Laser modification is a technique that allows increased bioactivity, verified by the rate of hydroxypatite deposition, of cell differentiation.[7,8] The combination of this laser modification method with the micro-arc oxidation technique offers distinct advantages. Unlike the commonly used EPD technique, micro-arc oxidation allows for the incorporation of elements found in the processing environment. These elements can be appropriately doped to suit the material's intended application. In the literature, several studies indicate the incorporation of elements such as sodium ions, phosphorus ions, calcium ions, and zinc ions into materials intended for biomedical applications.[9,10] Calcium ions are frequently incorporated into an electrolyte containing hydroxyapatite, a compound composed of phosphates responsible for bone formation and directly influencing its mechanical strength. Calcium ions are also responsible for the recruitment of cells involved in osseointegration, and they saturate surface Binding Integrin Receptors (RGD).[11]

The modifications presented in this study are innovative because they involve the integration of heat treatment technology with a ceramic layer generation technique. There is currently limited research exploring the feasibility of implementing such modifications in the realm of biomedical applications. This concept is straightforward yet promising, as it capitalizes on the strengths of both these surface modification techniques to potentially yield favorable outcomes.

Methodology and materials

Materials and their preparation for modification
The titanium alloy Ti13Nb13Zr (composition: Ti—reminder, Nb—13.02%, Zr—13.22%, Fe—0.008%, C—0.007%, N—0.021%, O—0.07%, H—0.006%) was chosen for the hybrid modification. The specimens were prepared from a rod of this alloy cut and then ground with 200, 400, and 800 grit sandpaper. The specimens were then ultrasonic cleaned before laser modification and micro-arc oxidation. Eight samples were prepared.

Methods of the modifications
For the modification in this experiment, two methods of modification were used. Laser modification was made by Nd:YAG laser. The process was taken under the same conditions in scan

rate on the level of 60%, duration of the laser pulse at 2.25 ms, and the frequency 25 Hz; the power of the laser was changeable: 1000 W or 150 W. During whole process of laser modification, technically pure argon gas was used (99,9999%) to protect the sample against the oxidation of the surface.

The second modification was the micro-arc oxidation technique. The modification was taken in the environment of water–electrolyte which contains of 0.7348 g/mol NaOH and 0.0497 g/mol of hydroxyapatite $Ca_{10}(PO4)_6(OH)_2$ In the micro-arc oxidation process, there is a DC supply (BK PRECISION, MR 1000020). Density of the current was 20 mA, the voltage on the level was 300 V, and time of the MAO process for all of the samples was 15 min.

Table I shows the description of the examined samples. The tests were taken for eight samples including reference and hybrid-modified samples. The hybrid modification is based on two combinations. The first modification consisted of laser modification at two different laser powers followed by micro-arc oxidation (P5, P6). The second type of modification consisted of depositing an MAO ceramic coating and subsequent melting with an Nd:YAG laser at two different laser powers (P7, P8). Authors used this parameters on the previous work.[12]

FTIR analyze

Fourier transform infrared spectroscopy (FTIR) is employed to analyze the spectra of solids, liquids, and gases, measuring their absorption, emission, and photoconductivity characteristics.[13] This technique is particularly valuable for detecting nanoparticles[14] within samples, all the while offering cost effectiveness and rapid testing.[15] In this study, an FTIR spectrometer (ATR mode), specifically the Perkin Elmer Frontier model, was utilized to investigate the chemical composition of the modified titanium alloy samples (Ti13Nb13Zr). The instrument facilitated the acquisition of data concerning the wavelengths of radiation absorption. FTIR analysis was conducted on each sample, and the resulting FTIR spectra were recorded across the range from 4000 to 400 cm^{-1}.

Corrosion test

Samples P1-P8 were subjected to corrosion resistance testing in phosphate-buffered saline (PBS) pH 7.2. This buffer allows the pH to remain constant. The concentration of ions in the resulting solution and the osmoticity of the solution determine the isotonicity of the solution, which is the same for the human body. Electrochemical measurements were based on the determination of the open-circuit potential (OCP) for a system consisting of a calomel reference electrode, a platinum counter-electrode and a working electrode—titanium alloy sample Ti13Nb13Zr subjected to various surface modifications. The OCP determination process was carried out at 37°C for one hour in PBS solution. Another measurement performed was the potentiodynamic corrosion test. Corrosion curves were performed from − 1 V to 1 V for a scan rate of 1 mV/s.

Table I. Samples and their modification.

Sample	Modification
P1	Native matreial Ti13Nb13Zr
P2	Ti13Nb13Zr modified by MAO technique
P3	Ti13Nb13Zr modified by laser Nd:YAG 1000W
P4	Ti13Nb13Zr modified by laser Nd:YAG 1500W
P5	Ti13Nb13Zr hybrid-modified laser1000W-MAO
P6	Ti13Nb13Zr hybrid-modified laser1500W-MAO
P7	Ti13Nb13Zr hybrid midfied MAO-laser1000W
P8	Ti13Nb13Zr hybrid midfied MAO-laser1500W

Immersion test

The test was conducted at a constant temperature of 37℃, which approximates the average temperature found in the human body,[16,17] and is within the range of temperature fluctuations observed in a PBS-saturated solution according to the literature.[18] The samples were placed inside sealed containers filled with a prepared 50 ml solution. Each sample immersed in the PBS solution underwent a 14-day incubation period, as recommended,[19] at a constant temperature. At specific intervals, namely on days 0, 3, 5, 7, 10, and 14, the pH of the solution was monitored using a pH meter. In addition, the weight of each sample was recorded during these intervals to observe the accumulation of degradation products.

Before and after the immersion test, the samples were examined using a scanning electron microscope, and their chemical composition was analyzed with EDS (Energy Dispersive Spectroscopy). For samples P2, P5, P6, P7, and P8, atomic mass spectroscopy was conducted to determine the presence of sodium and calcium ions in the solution, which could potentially be released from the coatings of the modified samples. The equipment used included the 4210 MP-AES from Agilent, a Flame photometer BWB-XP obtained from BWB Technologies UK LTD, and the Millipore Milli-Q Water Purification System from the USA. The determination of sodium in the tested samples was performed using atomic emission spectrometry with microwave plasma atomization (MP-AES) at specific wavelengths, while the determination of calcium was carried out using the Flame photometer BWB-XP.

Cross-sectional EDS analysis

Samples P2–P8 were prepared to evaluate the chemical composition of the fabricated layers in cross section. The process involved cutting the samples, followed by encapsulating them in polymer resin. After encapsulation, the samples were meticulously polished and etched. Subsequently, they were examined using a scanning optical microscope equipped with EDS (Energy Dispersive X-Ray Spectroscopy) analysis software to analyze their chemical composition.

Results and discussion

FTIR analysis was conducted on all samples, including those subjected to single modifications and hybrid modifications in the order of MAO-Nd:YAG laser and Nd:YAG laser-MAO. In Fig. 1(a), the FTIR spectrum for sample P2 is presented, along with a theoretical interpretation of the FTIR spectrum results. Each spectrum is divided into two distinct sections. The figure illustrates areas specific to each sample, which act as a fingerprint revealing the precise chemical composition of the sample, as well as regions indicative of single and double bonds within the sample.

Figure 1(b) displays a series of spectra for samples P2, P5, P6, P7, and P8. For each of the substrate material modifications, the peaks appear at identical wavenumber values, with variations primarily observed in their transmittance levels. An analysis of the FTIR spectrum allowed for the identification of a wavenumber range spanning from 690 cm^{-1} to 820 cm^{-1}, indicative of oxygen bonding with titanium (O–Ti–O).[20,21] Additionally, the range from 400 to 700 cm^{-1} is recognized as the region where titanium–oxygen bonds occur.[22,23] Notably, within the spectrum generated by the FTIR study, peaks in the region around 632 cm^{-1} are characteristic of the O–H group, associated with the presence of hydroxyapatite. Peaks at 1450 and 1421 are also characteristic of carboxyl groups associated with hydroxyapatite molecules. In the range of 962–1003 cm^{-1}, there is a possible indication of the P–O bond derived from hydroxyapatite.[24] High transmittance signifies a low density of bonds within the sample that absorb visible light, whereas low transmittance indicates a high density of bonds with vibrational energies resonant with the incident light.[25]

The corrosion resistance test carried out allowed the open-circuit potential (OCP) and potentiometric curves to be plotted, as shown in Fig. 1(c), (d). It is clear that any modification leads to an improvement in corrosion properties, in line with findings in the literature.[10,26–28] The data in Table II show the values of key parameters determined during the test, assessing

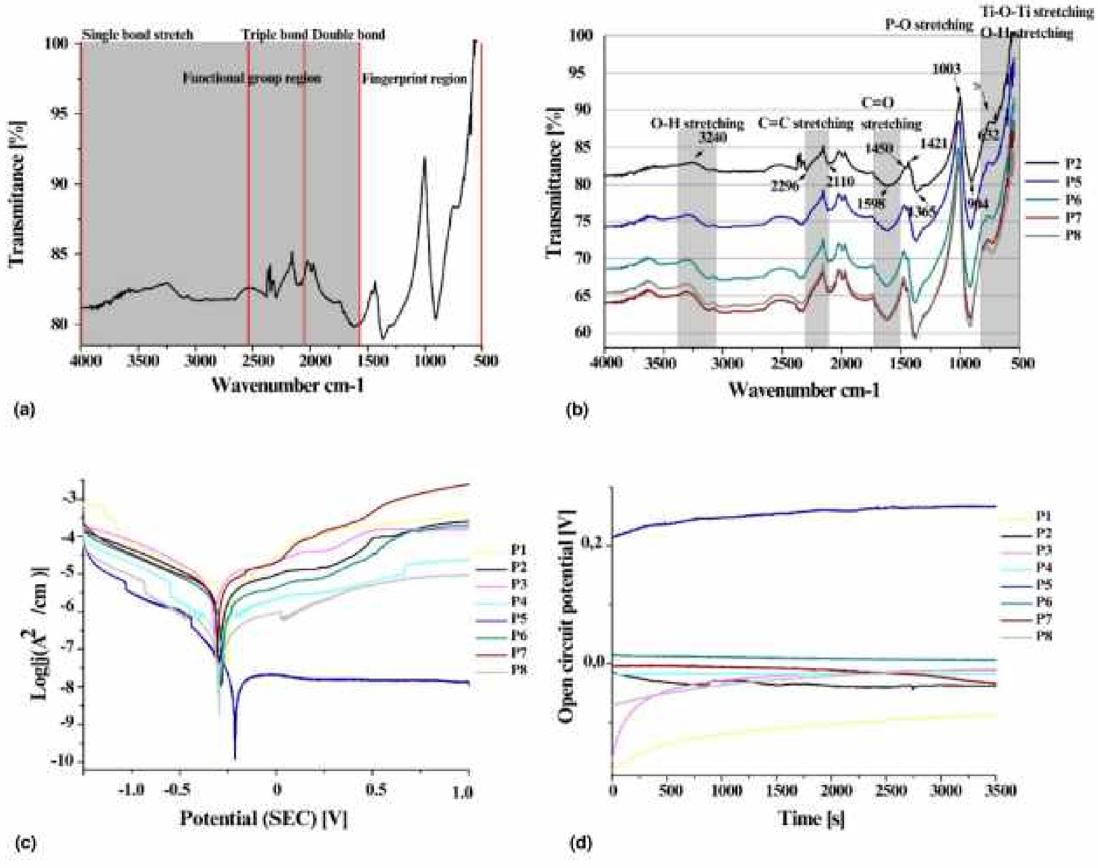

Figure 1. (a) FTIR fingerprint (b) The FTIR results for P2–P8 samples (c) polarization curves for all of the samples (d) OCP curves for all of the samples P1–P8.

Table II. Corrosion test results for P1-P8 samples of Ti13Nb13Zr.

Parameter	P1	P2	P3	P4	P5	P6	P7	P8
Icorr [A/cm2]	3.87×10^{-6}	7.80×10^{-6}	19.30×10^{-6}	8.98×10^{-6}	18.98×10^{-6}	3.31×10^{-6}	6.19×10^{-6}	2.04×10^{-6}
Ecorr [V]	-246.11×10^{-3}	-283.15×10^{-3}	-320.36×10^{-3}	-293.28×10^{-3}	-212.53×10^{-3}	-274.83×10^{-3}	-290.48×10^{-3}	-292.94×10^{-3}

the corrosion resistance of the modified Ti13Nb13Zr alloy. It should be noted that the corrosion potential does not directly determine the corrosion rate but rather indicates the susceptibility of metals to corrosion.[29] Of the group of samples tested, the highest corrosion potential was observed in sample P5, which was subjected to laser modification followed by MAO ceramic coating. This suggests the best corrosion resistance, as in this case, the material oxidizes more slowly and accumulates electrons instead of losing them. The worst corrosion resistance is shown by the sample individually modified with the P3 micro-arc oxidation technique, the E_{corr} value being the lowest for this sample, possibly due to the non-donorogenicity of the layer.[30] The results confirm the validity of the hybrid modification, in line with the literature indicating that single laser modification and the application of an MAO ceramic coating increase corrosion resistance. Furthermore, the use of a double modification in a specific laser-MAO combination effectively combines the advantages of these modifications, ultimately resulting in a material with a surface characterized by improved corrosion resistance.

The EDS chemical composition test confirmed the presence of salt ions on the surface, as shown in Table 3A and illustrated in Fig. 2(b). The presence of salt accumulations on the surface suggests good adhesive properties of the modified surfaces. Importantly, no damage was observed in SEM images resulting from the immersion of samples in concentrated PBS solution for 14 days, as shown in Fig. 2(a). The largest salt agglomeration was observed for the singly modified sample P2—MAO 1000 W. In the case of hybrid modification, sample P5 (laser-MAO) exhibited the highest amount of surface salts after the immersion test. The mass of the samples before and after the immersion test was documented, and no significant mass changes were observed [Fig. 2(c), (b)]. Furthermore, pH measurements at various intervals (0, 3, 5, 7, 10, and 14 days) indicated that pH remained within the acceptable range, fluctuating between 7.34 and 7.40, which is considered neutral for the human body. Based on these findings, there is no evidence suggesting material degradation for either types of modification. Atomic mass spectroscopy was used to determine the amount of sodium and calcium ions in samples P2, P5, P6, P7, and P8, as shown in Fig. 2(c), (a). The results obtained from EDS and atomic mass spectroscopy suggest that calcium ions were released into the electrolyte environment during the immersion test, leading to significant sodium salt accumulation on

Table III. A) The chemical composition of hybrid-modified samples before and after immersion test B) Chemical composition of a cross section of the hybrid-modified samples of Ti13Nb13Zr.

A

Sample	Chemical composition of hybrid-modified samples by weight[%]					
	Before immersion test			After immersion test		
	Na	Ca	O	Na	Ca	O
P2	0.41	0.44	32.71	7.99	0.26	24.58
P5	1.03	0.74	33.03	5.72	0.66	25.29
P6	0.73	0.66	32.49	4.98	0.49	27.21
P7	0.15	0.21	–	0.61	–	3.83
P8	0.23	0.06	–	9.49	–	5.59

B

Sample	Chemical composition of a cross section of the hybrid-modified samples of Ti13Nb13Zr by weight [%]					
	Ti	Nb	Zr	Na	Ca	O
P2	31.46	5.15	6.91	2.47	2.12	45.06
P5	44.45	8.17	8.61	1.08	0.77	33.74
P6	40.44	6.67	8.77	2.33	0.82	64.20
P7	70.82	12.64	12.91	–	0.22	2.80
P8	70.93	12.45	12.92	–	0.32	2.73

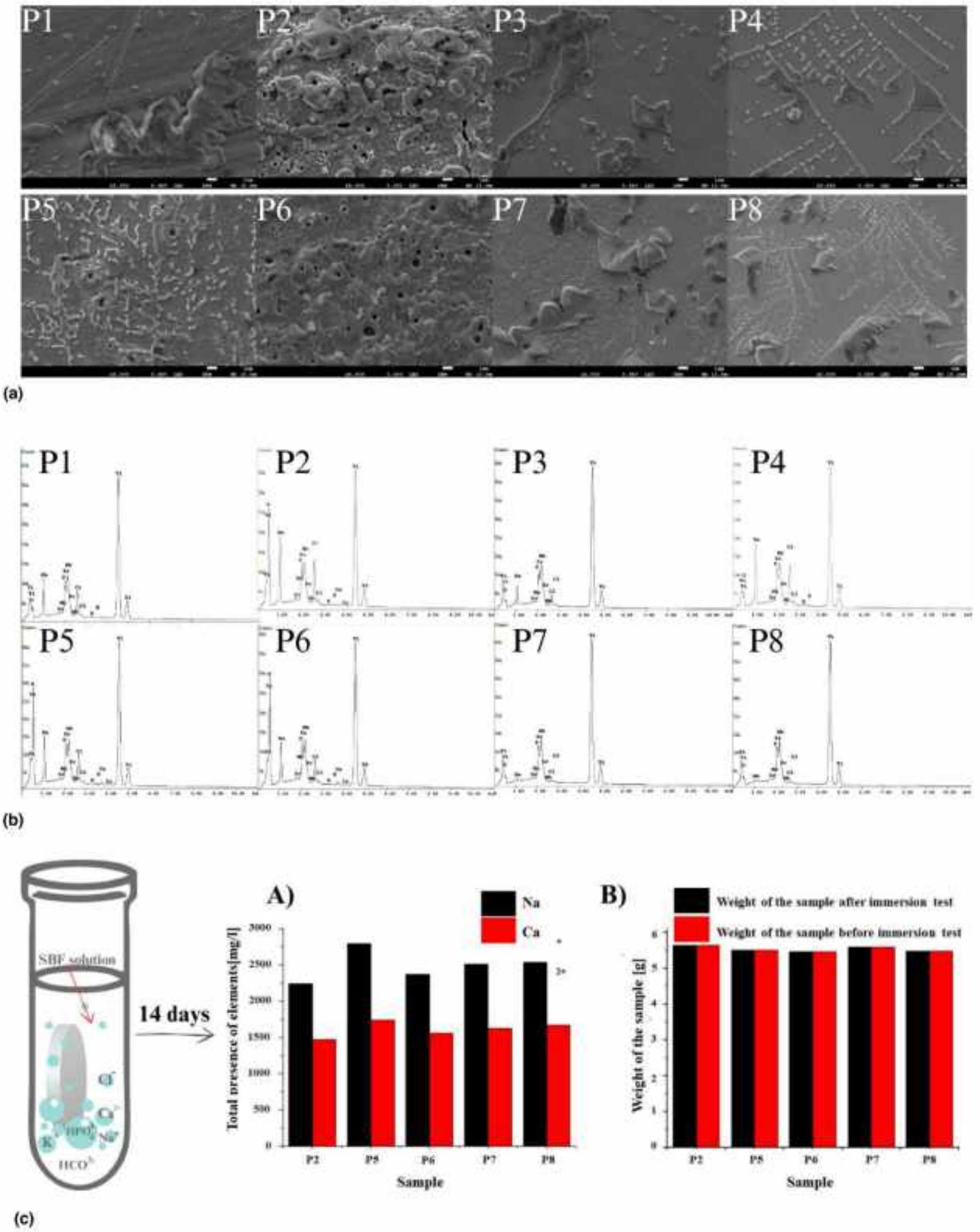

Figure 2. The SEM and EDS example of the investigation (a) SEM images of all of the samples P1–P8 after immersion test (b) The EDS results of all of the samples P1–P8 after immrsion test (c) (a)Column graph of the amout of the Na and Ca particles in immersion test solutions for P2–P8 samples. (b) Column graph of the weight of the samples before and after 14 days of immersion test for P2–P8 samples.

the surface of modified sample structures P2–P8. Specifically, for key hybrid modifications, sample P6 exhibited the best salt adhesion due to the continuous presence of Ca^{2+} ions, indicating coating stability and increased sodium presence on the surface. Sodium present in the PBS solution during the immersion test caused the release of calcium ions into the solution, particularly noticeable in samples P7 and P8, where the initial concentration of calcium ions dropped to zero. Simultaneously, the salts formed on the surface contained sodium ions, which constitute about 0.5–0.8 wt% in human bones.[31]

Table IIIB displays the EDS results on cross sections of samples P2 and hybrid-modified samples P5–P8. These results indicate that for hybrid modifications P5 and P6, the presence of Na^{+} and Ca^{2+} ions is at similar levels to that observed for the surface modification by MAO coating (P2). However, it is confirmed that the combination of modifications involving laser remelting of the MAO coating destroys the coating, with mixing occurring with the native material. In such cases, no elemental ions are observed that could potentially aid the osseointegration process. This finding provides clarity regarding the validity of this modification. Unfortunately, the use of MAO-laser modification samples is disadvantageous because it does not allow for the exploitation of the potential benefits of the produced coating after it has been melted with a very high laser power of 1000 W and 1500 W. Conversely, the modification involving remelting the material's surface beforehand and then applying the MAO ceramic coating (P5, P6) yields much better results, indicating an increased presence of sodium ions compared to sample P2 (Table II).

Conclusion

Based on hybrid modification studies carried out using a combination of micro-arc oxidation and laser modification techniques, it was concluded that the combination of these techniques in an appropriate combination allows the enrichment of TIi13Nb13Zr alloy with beneficial ions and the improvement of selected properties.

FTIR studies have shown that the laser-MAO combination modification yields good results in terms of the presence of titanium–oxygen bonds and the expected functional groups indicative of hydroxyapatite. These results confirm the effectiveness of the laser-MAO combination. The corrosion resistance tests showed that single and dual surface modification techniques improve the corrosion resistance, but that the best properties are obtained with sample P5. Immersion tests in PBS solution showed no change in the weight of the samples, with the pH remaining at the same level throughout the test. SEM images showed that the salts were agglomerated on the surface of the samples, with the best bioactivity values obtained for samples P2 and P5. Atomic mass spectroscopy showed the release of fall ions into the environment. EDS analyses of the hybridized samples showed the presence of sou and calcium ions incoporated by micro-arc oxidation, with the exception of samples P7 and P8, where only the presence of calcium was recorded.

An examination of the chemical composition on the surface showed that the immersion test resulted in an accumulation of salts with calcium ions, and here, an increase of up to nine times that of Na ions was observed.

In conclusion, the method of Nd:YAG laser modification of the surface before MAO ceramic coating, as applied to samples P5 and P6, yielded the best results. This method resulted in increased presence of beneficial ions and improved surface properties, suggesting its potential in the development of biomaterials for applications requiring enhanced corrosion resistance and stability. The results highlight the promise that hybrid modification techniques hold in improving the performance and durability of titanium-based biomaterials.

Author contributions

Joanna Sypniewska: Conceptualization, Methodology, Formal analysis, Formal analysis, Writing—Original Draft, Visualization, and Project administration. Marek Szkodo: helped supervise the project, and Writing—Review & Editing. Beata Majkowska-Marzec: Methodology and Writing—Review & Editing. Aleksandra Mielewczyk Gryń: FTIR Investigation.

Funding

Not applicable.

Data availability

Not applicable.

Declarations

Competing interest

Not applicable.

References

1. M. Bartmański, Ł. Pawłowski, Properties of chitosan/CuNPs coatings electrophoretically deposited on TiO_2 nanotubular oxide layer of Ti13Zr13Nb alloy. Mater. Lett. (2022). https://doi.org/10.1016/j.matlet.2021.130982
2. M. Nica, B. Cretu, D. Ene, I. Antoniac, D. Gheorghita, R. Ene, Failure analysis of retrieved osteosynthesis implants. Materials (2020). https://doi.org/10.3390/ma13051201
3. F. Accioni, J. Vázquez, M. Merinero, B. Begines, A. Alcudia, Latest trends in surface modification for dental implantology: innovative developments and analytical applications. Pharmaceutics (2022). https://doi.org/10.3390/pharmaceutics14020455
4. B. Majkowska-Marzec, J. Sypniewska, Microstructure and mechanical properties of laser surface-treated Ti13Nb13Zr alloy with MWCNTs coatings. Adv. Mater. Sci. **21**, 5–18 (2021). https://doi.org/10.2478/adms-2021-0021
5. S. Il Shin, H.K. Min, B.H. Park, Y.H. Kwon, J.B. Park, Y. Herr, S.J. Heo, J.H. Chung, The effect of Er:YAG laser irradiation on the scanning electron microscopic structure and surface roughness of various implant surfaces: an in vitro study. Lasers Med. Sci. **26**, 767–776 (2011). https://doi.org/10.1007/s10103-010-0819-4
6. M.R. Amaya-Vazquez, J.M. Sánchez-Amaya, Z. Boukha, F.J. Botana, Microstructure, microhardness and corrosion resistance of remelted TiG2 and Ti6Al4V by a high power diode laser. Corros. Sci. **56**, 36–48 (2012). https://doi.org/10.1016/j.corsci.2011.11.006
7. M. Jażdżewska, B. Majkowska-Marzec, R. Ostrowski, J.M. Olive, Influence of surface laser treatment on mechanical properties and residual stresses of titanium and its alloys. Adv. Sci. Technol. Res. J. **17**, 27–38 (2023). https://doi.org/10.12913/22998624/172981
8. H. Yao, X. Zou, S. Zheng, Y. Hu, S. Zhang, C. Liang, H. Zhou, D. Wang, H. Wang, L. Yang, Q. Li, Femtosecond laser-induced nanoporous layer for enhanced osteogenesis of titanium implants. Mater. Sci. Eng. C (2021). https://doi.org/10.1016/j.msec.2021.112247
9. J.P. O'Connor, D. Kanjilal, M. Teitelbaum, S.S. Lin, J.A. Cottrell, Zinc as a therapeutic agent in bone regeneration. Materials **13**, 1–22 (2020). https://doi.org/10.3390/ma13102211
10. M. Dziaduszewska, M. Shimabukuro, T. Seramak, A. Zielinski, T. Hanawa, Effects of micro-arc oxidation process parameters on characteristics of calcium-phosphate containing oxide layers on the selective laser melted Ti13Zr13Nb alloy. Coatings **10**, 1–24 (2020). https://doi.org/10.3390/COATINGS10080745
11. T. Albrektsson, B. Chrcanovic, M. Jacobsson, A. Wennerberg, Osseointegration of implants—a biological and clinical overview. JSM Dent. Surg. **2**, 1022 (2017)
12. J. Sypniewska, M. Szkodo, B. Majkowska-Marzec, A. Mielewczyk-Gryń, Effect of hybrid modification by ceramic layer formation in MAO process and laser remelting on the structure of titanium bio-alloy Ti13Nb13Zr. Ceram. Int. (2023). https://doi.org/10.1016/j.ceramint.2023.02.018
13. D. Guo, Y. Yang, J. Wu, B. Zhao, H. Zhao, H. Su, Y. Lu, Structure of the oxide film on Ti-6Ta alloy after immersion test in 8 mol/L boiling nitric acid medium. J. Electron Spectros. Relat. Phenomena **189**, 122–126 (2013). https://doi.org/10.1016/j.elspec.2013.08.013
14. K. Torres-Rivero, J. Bastos-Arrieta, N. Fiol, A. Florido, Metal and metal oxide nanoparticles: An integrated perspective of the green synthesis methods by natural products and waste valorization: applications and challenges, in *Biosynthesized Nanomaterials*, 1st edn. (Elsevier, Amsterdam, 2021)
15. K.A. Abd-Elsalam, R. Periakaruppan, S. Rajeshkumar, Biosynthesis of silver nanoparticles: synthesis, mechanism, and characterization. Agri-Waste Microbes Prod. Sustain. Nanomater. (2022). https://doi.org/10.1016/C2019-0-04608-0
16. I. Marco, A. Myrissa, E. Martinelli, F. Feyerabend, R. Willumeit-Römer, A.M. Weinberg, O. Van der Biest, In vivo and in vitro degradation comparison of pure MG, MG-10GD and MG-2AG: A short term study. Eur. Cell Mater. **33**, 90–104 (2017). https://doi.org/10.22203/eCM.v033a07
17. F.R. García-Galvan, S. Fajardo, V. Barranco, S. Feliu, Experimental apparent stern–geary coefficients for AZ31B Mg alloy in physiological body fluids for accurate corrosion rate determination. Metals (Basel) **11**, 1–21 (2021). https://doi.org/10.3390/met11030391
18. Y. Honda, M. Inuzuka, S. Nakamura, K. Yamashita, Hydroxyapatite coating and sbf immersion test of surface modified titanium by wet chemical method. Phosphorus Res. Bull. (2004). https://doi.org/10.3363/prb1992.17.0_254
19. A. Liber-Kneć, S. Łagan, *Wydawnictwo politechniki krakowskiej Metody badań biomateriałów i tkanek : wstęp do ćwiczeń laboratoryjnych* (Wydawnictwo PK, Kraków, 2020)
20. M. Al-amin, S.C. Dey, T.U. Rashid, S. Shamsuddin, Solar assisted photocatalytic degradation of reactive azo dyes in presence of anatase titanium dioxide solar assisted photocatalytic degradation of reactive azo dyes in presence of anatase titanium dioxide. Int. J. Latest Res. Eng. Technol. **2**, 14–21 (2016)
21. V.A. Zeitler, C.A. Brown, C.A. Brown, The infrared spectra of some Ti-O-Si, Ti-O-Ti and Si-O-Si compounds. J. Phys. Chem. D **61**, 1174–1177 (1957)
22. O. Kierat, A. Dudek, L. Adamczyk, The effect of the corrosion medium on silane coatings deposited on titanium grade 2 and titanium alloy ti13nb13zr. Materials **14**, 1–14 (2021). https://doi.org/10.3390/ma14216350
23. V.G. Nguyen, H. Thai, D.H. Mai, H.T. Tran, D.L. Tran, M.T. Vu, Effect of titanium dioxide on the properties of polyethylene/TiO_2 nanocomposites. Compos. B Eng. **45**, 1192–1198 (2013). https://doi.org/10.1016/j.compositesb.2012.09.058
24. C. Wen, X. Zhan, X. Huang, F. Xu, L. Luo, C. Xia, Characterization and corrosion properties of hydroxyapatite/graphene oxide bio-composite coating on magnesium alloy by one-step micro-arc oxidation method. Surf. Coat. Technol. **317**, 125–133 (2017). https://doi.org/10.1016/j.surfcoat.2017.03.034
25. P. Bhuyar, N.A. Tamizi, M.H. Rahim, G.P. Maniam, N. Govindan, Effect of ultraviolet light on the degradation of low-density and high-density polyethylene characterized by the weight loss and FTIR. Maejo Int. J. Energy Environ. Commun. **1**, 26–31 (2019). https://doi.org/10.54279/mijeec.v1i2.244915
26. X.J. Dai, X.C. Li, C. Wang, S. Yu, Z.T. Yu, X.R. Yang, Effect of MAO/Ta_2O_5composite coating on the corrosion behavior of Mg–Sr alloy and its in vitro biocompatibility. J. Mater. Res. Technol. **20**, 4566–4575 (2022). https://doi.org/10.1016/j.jmrt.2022.08.132
27. M. Dziaduszewska, A. Zieliński, Structural and material determinants influencing the behavior of porous Ti and its alloys made by additive manufacturing techniques for biomedical applications. Materials **14**, 1–48 (2021). https://doi.org/10.3390/ma14040712
28. J. Sypniewska, M. Szkodo, Influence of laser modification on the surface character of biomaterials : titanium and its alloys: a review. Coatings (2022). https://doi.org/10.3390/coatings12101371
29. Sankara Papavinasam, *Electrochemical polarization techniques for corrosion monitoring* (Woodhead Publishing, Sawston, 2021)
30. M. Bartmanski, A. Zielinski, B. Majkowska-Marzec, G. Strugala, Effects of solution composition and electrophoretic deposition voltage on various properties of nanohydroxyapatite coatings on the Ti13Zr13Nb alloy. Ceram. Int. **44**, 19236–19246 (2018). https://doi.org/10.1016/j.ceramint.2018.07.148
31. O.F. Yasar, W.C. Liao, R. Mathew, Y. Yu, B. Stevensson, Y. Liu, Z. Shen, M. Edén, The carbonate and sodium environments in precipitated and biomimetic calcium hydroxy-carbonate apatite contrasted with bone mineral: structural insights from solid-state NMR. J. Phys. Chem. C **125**, 10572–10592 (2021). https://doi.org/10.1021/acs.jpcc.0c11389

5.4. [JS4] Hybrid laser-micro-arc oxidation techniques for enhanced biocompatibility and surface modification of Ti13Nb13Zr alloy in biomedical applications

5.4.1. Wkład pracy doktoranta

Tytuł: Hybrid laser-micro-arc oxidation techniques for enhanced biocompatibility and surface modification of Ti13Nb13Zr alloy in biomedical applications

Autorzy: Joanna Sypniewska, Marek Szkodo, Beata Majkowska-Marzec, Łukasz Pawłowski, Aleksandra Mirowska, Jacek Ryl, Aleksandra Mielewczyk-Gryń, Łukasz Gaweł, Enrique Martínez Campos, Juan Pablo Fernández Hernán

Czasopismo: Applied Surface Science, Volume 698, 30 July 2025, 163136

Rok wydania: 2025

Impact factor: 6.3

Liczba punktów wg MNiSW: 140

DOI: 10.1016/j.apsusc.2025.163136

Procentowy wkład pracy doktoranta: 65%

Podczas tworzenia artykułu zajęłam się zaprojektowaniem nowego elektrolitu do procesu osadzania mikrołukowego, zawierającego jony cynku oraz hydroksyapatyt. Nadzorowałam prace związane z przetapianiem laserowym za pomocą lasera Nd:YAG, zgodnie z optymalnymi parametrami wskazanymi na podstawie publikacji [JS2] oraz [JS3]. Podjęłam się zaplanowania badań umożliwiających ocenę wytworzonych hybrydowych modyfikacji. Przeprowadziłam badania zwilżalności powierzchni, badania elektrochemiczne, analizy aktywności biologicznej oraz ocenę warstwy wierzchniej i przekroju poprzecznego próbek stopu tytanu Ti13Nb13Zr zmodyfikowanych laserowo. Zweryfikowałam grubość wytworzonych warstw, a także przeprowadziłam analizę, ocenę i dyskusję wyników badań chemicznych i fazowych (EDS, XRD, FTIR, XPS) oraz badań morfologii powierzchni (SEM). Nadzorowałam prace nad manuskryptem i współtworzyłam jego całość, przygotowując część merytoryczną wstępu, opis metodyki oraz dyskusję. Pełniłam rolę autora korespondencyjnego.

Joanna Sypniewska
mgr inż. Joanna Sypniewska

5.4.2. Treść artykułu

Applied Surface Science 698 (2025) 163136

Contents lists available at ScienceDirect

Applied Surface Science

journal homepage: www.elsevier.com/locate/apsusc

Full Length Article

Hybrid laser-micro-arc oxidation techniques for enhanced biocompatibility and surface modification of Ti13Nb13Zr alloy in biomedical applications

Joanna Sypniewska [a,*], Marek Szkodo [a], Beata Majkowska-Marzec [a], Łukasz Pawłowski [a], Aleksandra Mirowska [a], Jacek Ryl [b], Aleksandra Mielewczyk-Gryń [b], Łukasz Gaweł [c], Enrique Martínez Campos [d], Juan Pablo Fernández Hernán [e]

[a] Institute of Manufacturing and Materials Technology, Faculty of Mechanical Engineering and Ship Technology, Gdańsk University of Technology, Gdansk, Poland
[b] Institute of Nanotechnology and Materials Engineering, Faculty of Applied Physics and Mathematics, and Advanced Materials Centre, Gdańsk University of Technology, Gdańsk, Poland
[c] Department of Electrochemistry Corrosion and Materials Engineering, Faculty of Chemistry, Gdansk University of Technology, 11/12 Narutowicza Street, 80-233, Gdansk, Poland
[d] Group of Organic Synthesis and Bioevaluation, Instituto Pluridisciplinar, Universidad Complutense de Madrid (UCM), Associated Unit to the ICTP-IQM-CSIC, Paseo Juan XXIII, n° 1, 28040 Madrid, Spain
[e] Department of Materials Science and Engineering, Escuela Superior de Ciencias Experimentales y Tecnología, Universidad Rey Juan Carlos (URJC), C/ Tulipán s/n, 28933 Móstoles, Spain

ARTICLE INFO

Keywords:
Micro-arc oxidation
Laser modification
Hybrid modification
Titanium alloy
Surface modification
Ceramics layer

ABSTRACT

The research conducted in this paper focuses on an innovative hybrid surface modification technique for Ti13Nb13Zr alloys, combining an Nd: YAG laser treatment process with a micro-arc oxidation (MAO) technique. The work aimed to increase biocompatibility and improve surface properties, crucial for biomedical applications. By introducing zinc and sodium ions into the ceramic films and manipulating the duration of the MAO process, significant improvements in surface morphology, corrosion resistance, and cytocompatibility were achieved. Surface topography analyses showed a dual modification effect, increasing roughness, isotropy, and wettability properties, which are important for improving osteointegration and cell proliferation. Corrosion resistance tests confirmed a clear increase in corrosion resistance for hybrid-modified samples, especially those with a hydroxyapatite-enriched MAO ceramic layer. Cytocompatibility tests showed increased cell adhesion and proliferation, highlighting the benefits of combining laser and MAO techniques. These results indicate the great potential of the hybrid method in terms of improving the functionality and durability of bone and dental implants.

1. Introduction

The materials used for implants require adequate biocompatibility, corrosion resistance, and biological activity [1,2]. Biological, chemical, and physical modifications are used for this purpose, very often resulting in scientists producing layers and coatings that improve the initial properties of the parent material. Titanium alloy Ti13Nb13Zr is currently new alloy, as its initial properties are much better than those of vanadium-aluminium alloys and pure titanium materials [3]. Improving corrosion properties and bioactivity is an aspect that constantly requires development. To this end, coating and layering methods such as electrophoretic deposition [4,5], anodising [6] or plasma electrolytic oxidation. PEO, is known as microarc oxidation [7]. Furthermore, thermal techniques, particularly laser modifications, are widely employed to alter biomaterials. Lasers including Nd:Er, fiber lasers, CO_2 lasers, and nanosecond diode lasers are frequently utilized for this purpose [8–12]. In addition to the various types of laser, there are also various laser modification techniques: laser cladding, remelting, hardening, etc. [8,9].

Current literature reports [13,14] state that, in addition to magnesium or magnesium-rich materials and Fe-rich materials, zinc shows promise for biomedical applications. Zinc, whether in pure or alloyed form or as an additive in the form of ions, can be used to produce implants [15]. In the human body, zinc primarily exists as Zn^{2+} ions, with

* Corresponding author.
E-mail address: joanna.sypniewska@pg.edu.pl (J. Sypniewska).

https://doi.org/10.1016/j.apsusc.2025.163136
Received 4 February 2025; Received in revised form 21 March 2025; Accepted 30 March 2025
Available online 31 March 2025

approximately 60 % located in muscles, 30 % in bones, and the remaining 10 % distributed across the liver, skin, kidneys, and brain [16,17]. Deficiency of this ion in the body can already cause growth retardation in fetal development, abnormal development of the fetal skull bones, and homeostatic disorders [18,19]. Zinc also plays a critical role in bone regeneration, serving as an activator of chondrocyte and osteoblast functions [19].

Laser modification offers a stable and easily programmable process, with consistent power parameters, laser beam size, and scan rate [8]. On the other hand, the mico-arc oxidation process is characterized by several successive reactions, where meticulous control of the process and electrolyte saturation is necessary to maintain quality ceramic layers. [20]. The MAO/PEO technique differs from conventional anodic oxidation primarily in the voltage applied; in MAO, the voltage ranges from several to several hundred volts. The high voltage generates plasma, leading to high-temperature and high-pressure discharges during the process [21].

Modifications involving the use of heat modification techniques in combination with micro-arc oxidation (MAO/PEO) techniques are becoming increasingly popular. A study has been published in 2024 [22] modification based on laser treatment at different speeds combined with a micro-arc oxidation process. It was shown that the use of such a composite coating resulted in an improved quality of the deposited ceramic layer, the spaces between successive ceramic layers in the MAO coating were eliminated, the adhesion of the layer to the substrate was increased and an increase in biocompatibility was observed [22]. Work published in earlier years indicates that the use of laser treatment before micro-arc oxidation on titanium and its alloys also has the effect of enriching ceramic layers with bio-additives developing the surface (changing the contact angle and surface roughness) and improving their tribological properties [23,24]. It is known that these surface features (amongst others) affect also cell behavior, especially in terms of early cell adhesion, proliferation, or differentiation (including matrix secretion) [25,26]. In a paper [27] the combination of two modification techniques has been shown to increase cell proliferation and enhance the corrosion resistance of the material.

This study introduces a novel hybrid modification technique combining Nd:YAG laser treatment and micro-arc oxidation. The Ti13Nb13Zr titanium alloy was enriched with zinc and sodium ions, and this combined approach expanded the surface morphology, creating a conducive environment for cell growth. The ongoing development of bone and dental implants is increasingly crucial due to the aging population and rising patient awareness, making the exploration of new modification techniques essential to meeting the evolving demands on biomaterials.

2. Methodology

2.1. Material

The study used Ti13Nb13Zr titanium alloy specimens (JIANGSU GANGYA METAL PRODUCTS LIMITED) with a diameter of 12 mm. The specimens were polished on a polishing machine (Saphir 330, ATM GmbH, Mammelzen, Germany) before each modification—single and double with papers of a gradation of 60 to 2000.

2.2. The environment of the mao process

The chemical composition of the electrolytes was based on the literature review [23,28] and preliminary experiments. Water-based electrolyte without hydroxyapatite was mixed using a magnetic stir at 50 °C for 3 h hours before the MAO treatment, the ingredients of the solution were presented in Table 1 and the parametres of all of the modifications shown in Table 2. Electrolyte with hydroxyapatite was mixed using magnetic stir for 3 h hours at room temperature in two different solutions 960 ml water with NaOH, $Zn(C_4H_6O_4)_2$ and 40 ml C_2H_5OH with hydroxyapatite.

Table 1
Electrolyte: The element of the solution.

1l Electrolyte nr. 1	1 l water-alcohol electrolyte 2
3.48 g NaOH 1.75 g $Zn(C_4H_6O_4)_2$	1.74 g NaOH 0.875 g $Zn(C_4H_6O_4)_2$
–	0.25 g hydroxyapatite

Table 2
Names and parameters of the modifications for Ti13Nb13Zr samples.

Samples	Modification
R	Reference
RL	Laser modified by 1000 W reference
NaZn1 – MAO7	MAO reference – electrolyte 1 by 7 min process
NaZn2 – MAO15	MAO reference – electrolyte 1 by 15 min process
ZnHAP1 HAP7	MAO reference – electrolyte 2 by 7 min process
ZnHAP2 HAP15	MAO reference – electrolyte 2 by 15 min process
NaZn1L MAO7L	Hybrid modified sample – laser modified by 1000 W and MAO process in electrolyte 1 by 7 min
NaZn2L MAO15L	Hybrid modified sample – laser modified by 1000 W and MAO process in electrolyte 1 by 15 min
ZnHAP1L HAP7L	Hybrid modified sample – laser modified by 1000 W and MAO process in electrolyte 2 by 7 min
ZnHAP2L HAP15L	Hybrid modified sample – laser modified by 1000 W and MAO process in electrolyte 2 by 15 min

2.3. MAO process

Micro-arc oxidation process (scheme of this process on Fig. 1A) was taken under two different time conditions The process was taken under the intensity of current 0,170 A for two different times of the process 7 and 15 min. For both types of electrolytes achieved a voltage on the level of 300 V Two different time conditions were taken for the two types of electrolytes. During the process, the temperature was measured and fluctuated between 22–27 °C.

2.4. Nd:YAG laser pre-treatment

The Nd:YAG (TruLaser Station 5004, TRUMPF, Germany) laser treatment process (Fig. 1B) took place under controlled conditions in the presence of argon (99.99 % pure). The laser power was set at 1000 W, the pulse duration of the laser beam was 2.25 ms and the scan rate was at 60 %. The samples were remelted according to the designed program.

3. Description of the modified samples of TI13NB13ZR

3.1. Wettability and roughness tests

A goniometer (Contact angle goniometer, Zeiss, Ulm, Germany) with AttentionOne software was used to measure contact angle. Measurements were taken 10 s. During the test, water (polar), and diiodomethane (is non-polar liquid) were to examine contact angle and surface free energy. The wetting angle was tested using the falling drop method. The wetting angle was studied using water, for 10 s. The surface free energy was calculated using the AttentionOne software, using the method of Owens, Wendt, Rabel, and Kaelble (WORK). To carry out the surface free energy analysis, it was necessary to measure the contact angle for polar and non-polar liquids: water and diiodomethane.

The obtained surfaces were examined with the use of a non-contact 3D optical profilometer (Sensofar S Neox, Sensofar Metrology, Terrassa, Spain). The confocal microscopy technique was applied for the study. A Nikon-EPI 20x objective was used with SensoSCAN S Neox 7.7

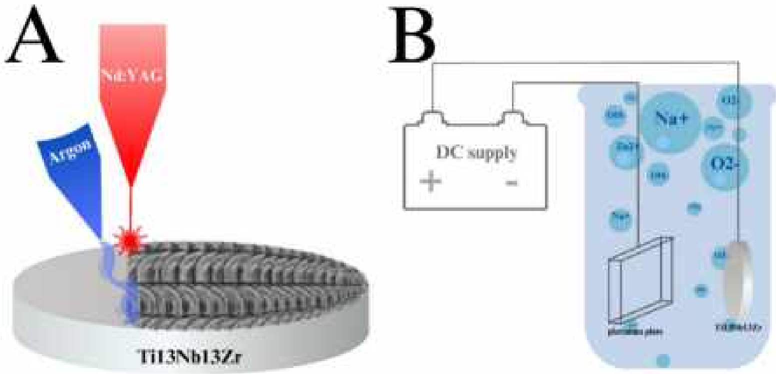

Fig. 1. A) Laser modification of Ti13Nb13Zr by Nd:YAG laser B) Scheme image of micro-arc oxidation process for Ti13NbZr.

software. A pixel size was equal to 0.69 μm. Three randomly chosen areas of 1.34 x 1.60 mm were measured within each sample. In order to calculate the required roughness parameters, a methodology in accordance with the standards ISO 25178 and ISO 21920 was used.

3.2. Examination of microstructure, morphology, thickness, and chemical composition

Observation of the microstructure of modified samples was taken by high-resolution scanning electron microscope (SEM, JEOL JSM-7800F, JEOL Ltd., Tokyo, Japan) with an acceleration voltage of 5 kV and magnifications 5000 to 1000. The energy dispersive X-ray spectroscopy was used to examine chemical composition (EDS, Edax Inc., Pleasanton, CA, USA).

The thickness of the ceramic layer was tested using a FMP10-20 dual-band meter (SN100146594, Helmut Fischer GmbH, Germany)z. Ten measurements were taken for each sample and the mean of the results and standard deviation are presented.

To study the chemical bonds formed in the ceramics layer on Ti13Nb13Zr by MAO, the Fourier-transform infrared spectroscopy (FTIR; Perkin Elmer Frontier, Waltham, MA, USA) was used in the range of 400–4000 cm-1 and the resolution was 2 cm-1.

To examine the changes in phases in Ti13Nb13Zr was used X-ray diffraction method (Phillips X'Pert Pro, Almelo, Netherlands). The temperature was ambient. XRD method was applied using a diffractometer (Cu Kα, λ = 0.1554 nm) in the range 10–90° of 2θ.

X-ray photoelectron spectroscopy (XPS) was used to determine the composition and surface chemistry of the ceramics layer. The analysis was performed in the core-level binding energy range for Na 1 s, Zn 2p, P 2p, and Ca 2p. ThermoFisher Scientific's advanced Escalab 250Xi multispectroscope was used for this purpose, using AlKα X-rays with a precise spot diameter of 250 μm and a pass energy of 20 eV. Low-energy electron and Ar^+ ion bombardment were used to effectively negate potential surface charges, with a final peak calibration using adventitious carbon C 1 s at 284.6 eV Advanced Advantage v5.9921 software (ThermoFisher Scientific) was used to accurately analyse the data obtained from the measurements, allowing peak deconvolution and calibration.

3.3. Electrochemical tests for corrosion evaluation

Electrochemical tests were performed for the evaluation of the corrosion behavior of the Ti13Nb13Zr samples with different surface treatments. A total surface of 0.28 cm^2 of the sample was exposed to 7 mL of Hanks' balanced salt solution for up to 168 h at a temperature of 37 °C for *in vitro* simulation of physiological conditions. Evolution of the open circuit potential (E_{OCP}), linear polarization resistance, and electrochemical impedance spectroscopy (EIS) were conducted using a Metrohm Autolab PGSTAT302N potentiostat. Three-electrode cell configuration was used, with the sample acting as the working electrode, a Pt wire acting as the counter electrode, and the Ag/AgCl reference electrode. EIS was developed applying a frequency range from 10^5 to 10^{-2} Hz and a polarization range of ± 10 mV concerning the open circuit potential (E_{OCP}), acquiring 10 points per decade. Linear polarization resistance was performed by the application of a potential range of ± 10 mV for the open circuit potential. Electrochemical tests were performed after 1 h of stabilization time.

Scanning electron microscopy (SEM Hitachi S-3400 N) and energy dispersive X-ray spectroscopy (EDS Bruker AXS Xflash Detector 5010) were used for the morphological and compositional evaluation of the surface of the different samples after immersion in the Hanks' solution during the electrochemical corrosion tests.

3.4. Bioactivity tests

3.4.1. Sample preparation

Before cytocompatibility evaluation, all coated specimens underwent a standardized sterilization protocol. Initially, the samples were immersed in 70 % ethanol for 10 min, with this procedure repeated three times to ensure thorough decontamination. Subsequently, the specimens were rinsed three times in phosphate-buffered saline (PBS), with each rinse lasting 10 min. The samples were then transferred to multiwell plates containing 1 mL of PBS and subjected to ultraviolet germicidal irradiation (UVGI) for 40 min to achieve sterilization. Following UVGI exposure, the samples were rinsed again in PBS for 10 min. To enhance preparation, the specimens were subsequently immersed in Dulbecco's Modified Eagle Medium (DMEM, GIBCO) for 10 min. Lastly, the samples were incubated in 1 mL of DMEM supplemented with 10 % fetal bovine serum (FBS, Thermo Scientific) and antibiotics (100 U/mL penicillin and 100 μg/mL streptomycin sulfate, Sigma-Aldrich). As a final step, the samples were maintained in the complete culture medium at 37 °C for 24 h before testing.

3.4.2. Cell culture

Endothelial C166-GFP cell line was chosen as a cytocompatibility model due to their autofluorescence and adherent proliferation. Cells were incubated at 37 °C in supplemented DMEM as described above.

3.4.3. Metabolic activity and DNA quantification analyses

The metabolic activity of cell cultures was assessed using the AlamarBlue assay (Thermo Fisher), performed at 24 and 72 h of culture. This non-toxic method leverages the reducing power of cellular machinery to quantify mitochondrial activity in viable cells. For each time point, three samples were analyzed. The procedure involved adding

AlamarBlue dye to the culture medium of each sample at a concentration of 10 % relative to the medium volume. The samples were then incubated for 90 min, and fluorescence was subsequently measured using a BioTek Synergy HT microplate reader.

3.4.4. DNA quantification

DNA content was determined using the blue-fluorescent Hoechst 33,258 nucleic acid stain, in accordance with the manufacturer's instructions (Thermo Fisher, FluoReporter). This assay was conducted after 72 h of culture, with fluorescence measurements obtained using a BioTek Synergy HT microplate reader.

4. Results and discussion

4.1. SEM

Fig. 2 shows the modified surfaces of the Ti13Nb13Zr alloy. Fig. 2 presents the results of single modifications. The MAO process carried out in electrolyte 1, with two different process parameters, resulted in the formation of a ceramic layer with a characteristic structure typical for the mixed oxidation process. Pores are visible, distributed in a regular pattern, with similar sizes. No material discontinuities are observed. SEM images show small protrusions, indicating a developed surface morphology. A similar qualitative result was obtained for the samples modified by laser and then coated with MAO ceramic (NaZn1L, NaZn2L). The laser modification did not disrupt the continuity of the ceramic surface. The main change was in the size of the pores, which are larger compared to the single modification [29,30].

In the case of electrolyte 2, surfaces obtained by applying the MAO process to the ZnHAp1 and ZnHAp2 samples show a very irregular ceramic layer, with numerous gaps, height differences in the layer, and an uneven distribution of pores. Many holes with irregular, elongated shapes are observed. Additionally, the ceramic formed in this electrolyte is very thin, as grinding marks on the Ti13Nb13Zr samples are visible in the images. For the ZnHAp1L and ZnHAp2L samples, the surface is more regular compared to the single modification. Although a uniform, characteristic ceramic layer is not observed, the pores formed are of similar shapes and sizes. No visible laser beam tracks are seen, which indicates complete coverage of the surface with ceramic in this modification.

For the samples made in electrolyte 2, regardless of the process duration and modification combinations, it cannot be stated that the resulting ceramic is of sufficient quality. A positive result is that the laser modification slightly improved the homogeneity of the layers, though discontinuities remain in the structure.

4.2. Thickness of the coatings

The film thickness measurements show that the laser modification improves the efficiency of the mirco-arc oxidation process by stimulating the formation of a thicker layer. Table 3 presents measuremnets of the thickness of the coatings. The films with the smallest thicknesses were those where hydroxyapatite was added to the electrolyte environment. It is also confirmed by SEM analysis that these layers are of the worst quality. The extended duration of the MAO process resulted in the formation of thicker ceramic layers with bio-additives, which is in line with the trend in the literature [31,32].

4.3. XPS

Fig. 3 presents the X-ray photoelectron spectra (XPS) obtained for the following samples: reference, laser-modified, and those subjected to

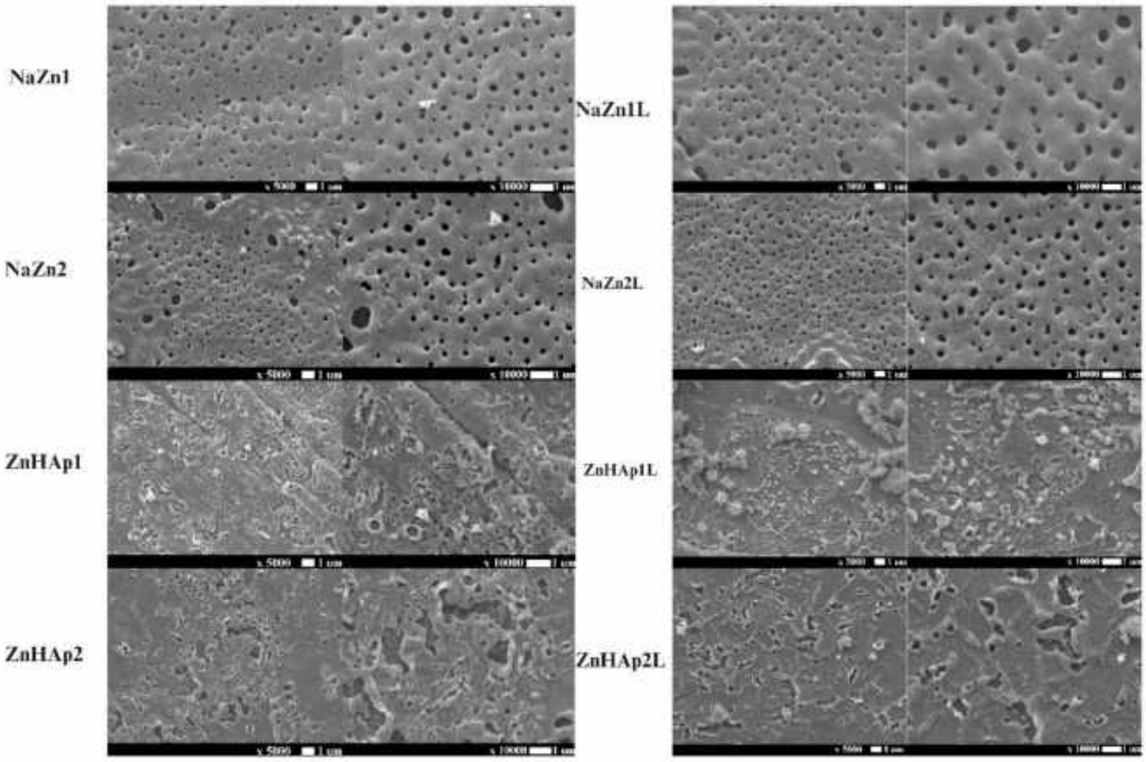

Fig. 2. SEM images for modified samples by micro-arc oxidation process and double modification laser-MAO.

Table 3
Thickness of the coatings for all of the modified samples.

NaZn1	NaZn2	ZnHAp1	ZnHAp2	NaZn1L	NaZn2L	ZnHAp1L	ZnHAp2L	L	
2,09	3,05	0,544	0,997	3,71	4,14	2,04	1,39	1,75	Average
0,2424	0,3659	0,2799	0,6227	0,645	1,119	0,6118	0,4624	0,7091	Deviation

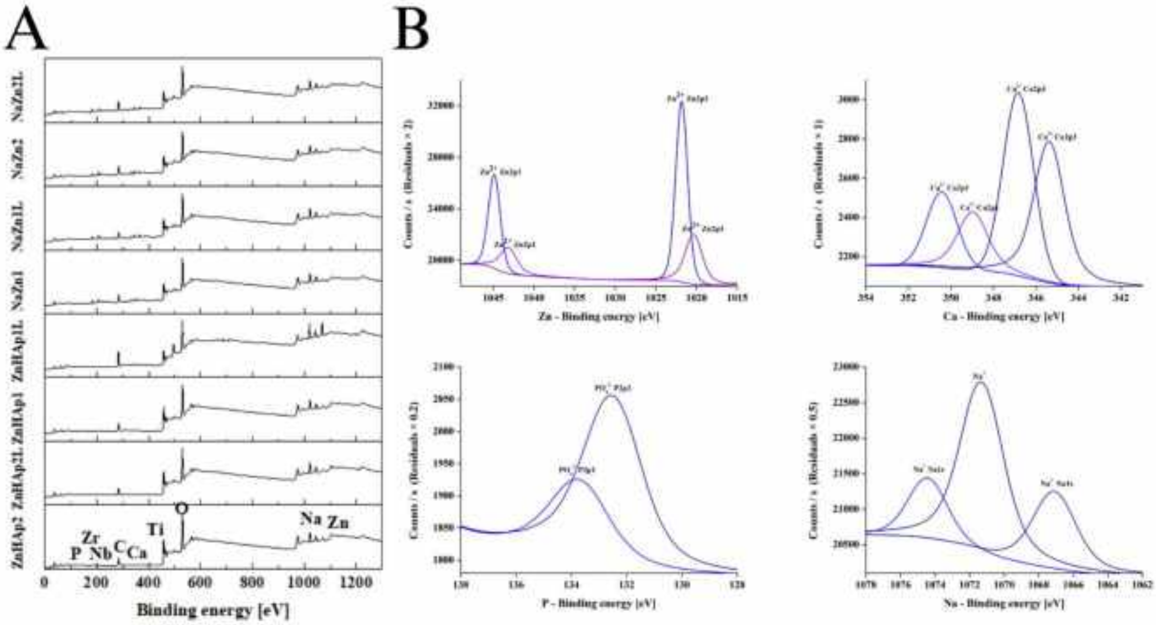

Fig. 3. A) All of the survey spectra for XPS of modified samples b)Example of XPS spectra presentation for ZnHAp2L.

dual modificationFor laser-modified samples, the maxima originating from carbon are higher than for other modifications without laser treatment. All key dopants were detected for samples modified using the hybrid laser-MAO technique, verifying the successful incorporation of elements during the micro-arc oxidation (MAO) process.

The spectra for dopants such as Ca, Zn, Na, and P are shown in Fig. 3 (A and B) for the dual-modified sample (ZnHAp2L). In the case of zinc, two doublets were identified. At a binding energy of approximately 1022 eV, the presence of Zn in the form of zinc oxide (ZnO) was confirmed [33] Furthermore, literature reports confirm the presence of Zn^{2+} ions associated with two compounds—ZnO and $Zn(OH)_2$—at binding energies ranging from 1022 to 1024 eV [33]. The doublets with $Zn2p_{3/2}$ indicate the presence of Zn in the form of $Zn_3(PO_4)_2$, with phosphate groups (PO_4^{3-}) derived from hydroxyapatite. This confirms that Zn is present predominantly in the Zn^{2+} state [34]. Similarly, a study on PEO-modified surfaces also detected phosphorus and zinc ions at binding energy values consistent with the results of the present study Phosphorus is incorporated into the ceramic layer in the form of PO_4^{3-} ions, as revealed by the P2p energy peak [33]. During the process, Ca^{2+} ions migrate towards the anode via diffusion, with a similar migration behavior observed for Zn^{2+} ions [35,36]. For calcium, binding energies around 347 eV and 351 eV both correspond to bonds in $Ca_3(PO_4)_2$, characteristic of hydroxyapatite, which was included in electrolyte 2 [33,37]. The XPS spectra also showed characteristic peaks for sodium. Due to small binding energy differences in sodium bonds, this element may form bonds with both oxygen and titanium [38].

4.4. FTIR

FTIR spectrum presented in Fig. 4. A maximum at 1462 cm^{-1} suggests the presence of carbon bonding within the hydroxyapatite crystal structure in the form of CO_3^{2-} ions [39]. The maximum at 3642 cm^{-1} corresponds to a hydroxyl group (O–H), indicating the presence of hydroxyapatite, confirming this compound in samples ZnHAp1, ZnHAp2, ZnHAp1L, and ZnHAp2L. Distinct maxima originating from titanium oxide bonds O-Ti-O are also clearly visible in the range of 400–700 cm^{-1} [40]. The maximum at 872–876 cm^{-1} is characteristic of zinc oxide and was observed in all samples with a ceramic coating formed in an electrolyte containing zinc acetate dihydrate; the absence of this maximum in RL samples further supports its presence. It is also noteworthy that ceramic layers containing hydroxyapatite exhibit shifts around the wavelength range of 800–1100 cm^{-1}, characteristic of PO_4^{3-} bonds in hydroxyapatite [41,42]. Such shifts were observed in samples subjected to the MAO process for 15 min, both for single and double modification. Literature indicates that shifts in the range of 1915–2382 cm^{-1} occur for P-H bonds in apatite; samples subjected to dual laser-MAO modification in electrolyte 2 exhibit shifts in this region, consistent with the presence of bone-forming compounds [43]. Maxima at 2350 cm^{-1} denote carbon triple bonds C≡C. Maxima in the range of 2850–2950 cm^{-1} are characteristic of carbon-hydrogen bonds C–H [44]. Maxima at 1654 cm^{-1} and 1740 cm^{-1} indicate double bonds between oxygen and carbon C=O [45].

4.5. Wettability

Fig. 5 presents graphs showing the change in contact angle values for

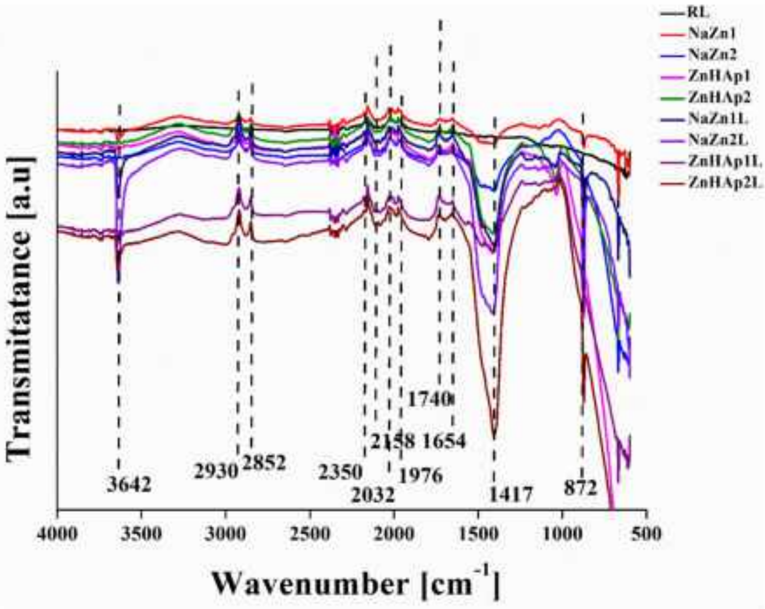

Fig. 4. The FTIR results for modified samples of Ti13Nb13Zr.

each modification and the base material, measured with two liquids: water and diiodomethane. The obtained contact angle results allowed for the determination of total surface free energy, as well as its polar and dispersive components.

Surfaces are classified as hydrophilic when the contact angle ranges from 0° to 90°, while surfaces are considered hydrophobic when the contact angle exceeds 90° [46]. Contact angle analysis is crucial for potential biomedical applications, as the surface-to-water interaction affects the implant's behavior with body fluids, bacterial cells, and proteins within the human body [47]. According to Fig. 5A, the lowest contact angle for water was observed for the unmodified base material, and contact angles increased (wettability decreased) with each modification. Contact angle values for each of the double modifications ranged around 80°-90°, which may indicate a tendency toward a hydrophobic surface character. Extending the duration of the MAO process for hybrid modifications, both with and without hydroxyapatite, resulted in surfaces with the highest contact angles. It is notable that laser modification prior to micro-arc oxidation deposition reduced wettability.

A decrease in contact angle is advantageous, as it enhances surface propagation for cells, improving adhesion to the substrate. However, it is also suggested that an increased contact angle has positive effects, as it can improve resistance to bacterial colonization by reducing bacterial adhesion. A higher contact angle also reduces the risk of negative biofilm formation on the implant surface.

Fig. 5B presents the results for surface free energy values. Sample R, representing the base material Ti12Nb13Zr titanium alloy, exhibits the highest surface free energy due to its high polar component value. Modified samples, whether single or double modifications, show lower surface free energy than the base material. Except for sample NaZn2, the remaining modifications display similar surface energy values, with all samples having a dispersive component value higher than the polar component."

4.6. Roughness

Fig. 6 presents obtained topography maps for the investigated samples. Also, peaks and valleys distributions histograms, and line profiles of the surfaces are presented. The topographies indicate the characteristic laser-treated surfaces associated with the laser path. For these surfaces, the histograms are wider, meaning that multiple valleys and peaks were prominent on the surface. On ground surfaces, after the MAO process and after electrophoretic deposition, the histograms are narrower and the surfaces are more uniform. For a quantitative description of the obtained topographies, the average values of the area roughness (Sa) and line roughness (Ra) were calculated. In addition, parameters such as root mean square deviation of a surface profile (Sq) and line profile (Rq), maximum height of a surface profile (Sz) and linear profile (Rz), maximum peak height (Sp) and valley depth (Sv), skewness (Ssk) and kurtosis (Sku) were determined. Also, functional volume parameters such as material volume (Vm), void volume (Vv), dale void volume (Vvv) and core void volume (Vvc) were evaluated. The results of these calculations are shown in Table 4.

The most commonly used linear parameter Ra and surface parameter Sa clearly indicate that the smoothest surface was exhibited by the sample R, subjected only to the grinding process. Considering bone tissue regeneration applications, it is important to remember that rougher surfaces provide a larger contact area between the implant and bone, which promotes better bone tissue growth on the implant surface [48]. This improves implant stability and long-term implant placement [49]. Smooth surfaces have less ability to form a bond with bone, which can lead to a longer healing process and less stable integration. Each surface treatment proposed in this study resulted in an increase in average roughness compared to the ground sample. In the case of the MAO-treated surfaces, it can be observed that Ra and Sa parameters increase with increasing MAO process time. In addition, samples subjected to prior laser modification show several times higher values of Ra and Sa parameters compared to their non-laser-treated analogs. This means that laser processing generally increases surface roughness, which can contribute to better osteointegration [8]. The average roughness Sa of the surfaces subjected to only MAO processing ranged from ~ 0.19 to ~ 0.35 μm, while in the case of samples previously laser processed the values of Sa ranged from ~ 1.18 to ~ 1.34 μm. It should be remembered that Ra/Sa parameters can be useful as a basic indicator of roughness, but do not fully capture the complexity of surface structure. As an

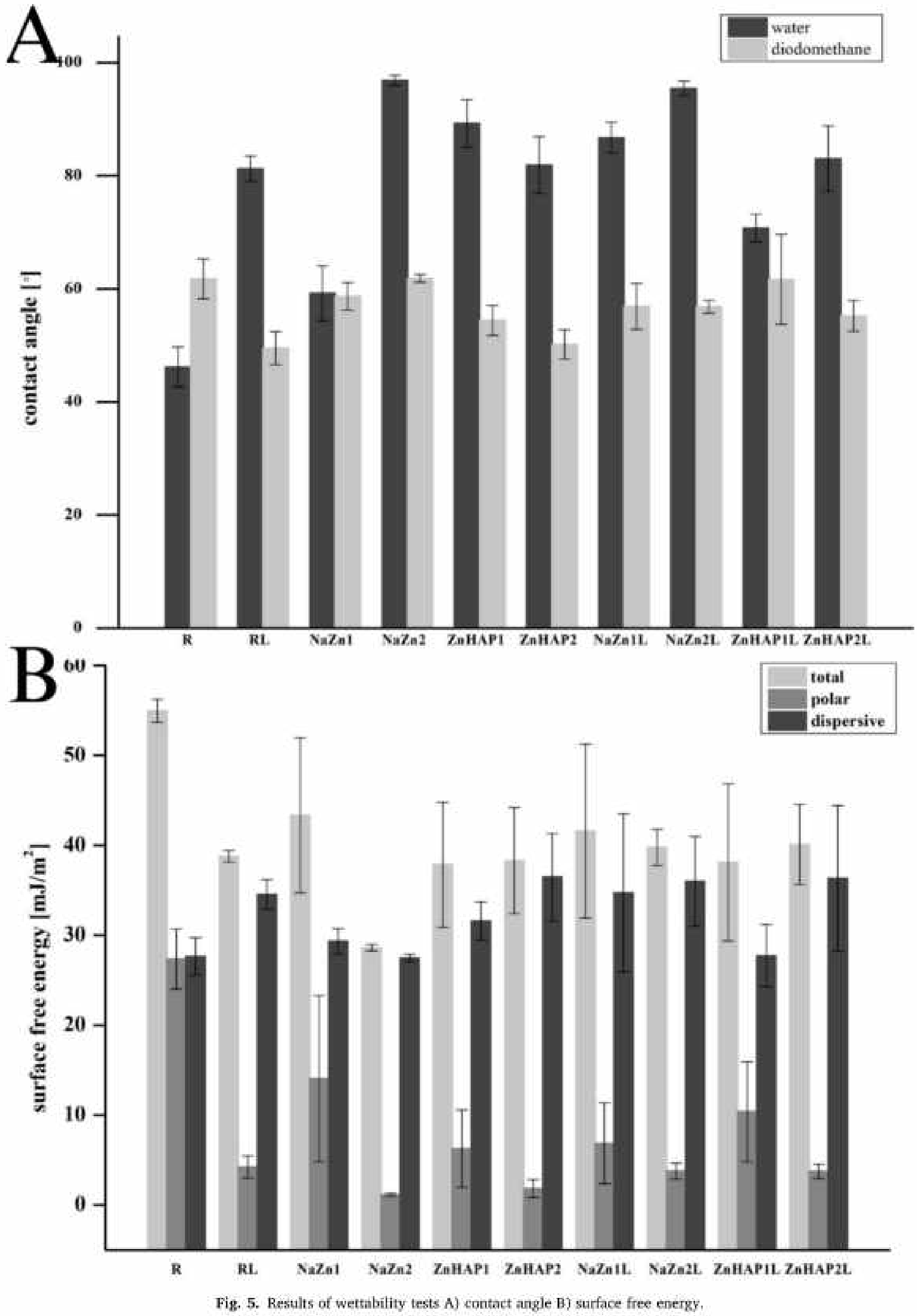

Fig. 5. Results of wettability tests A) contact angle B) surface free energy.

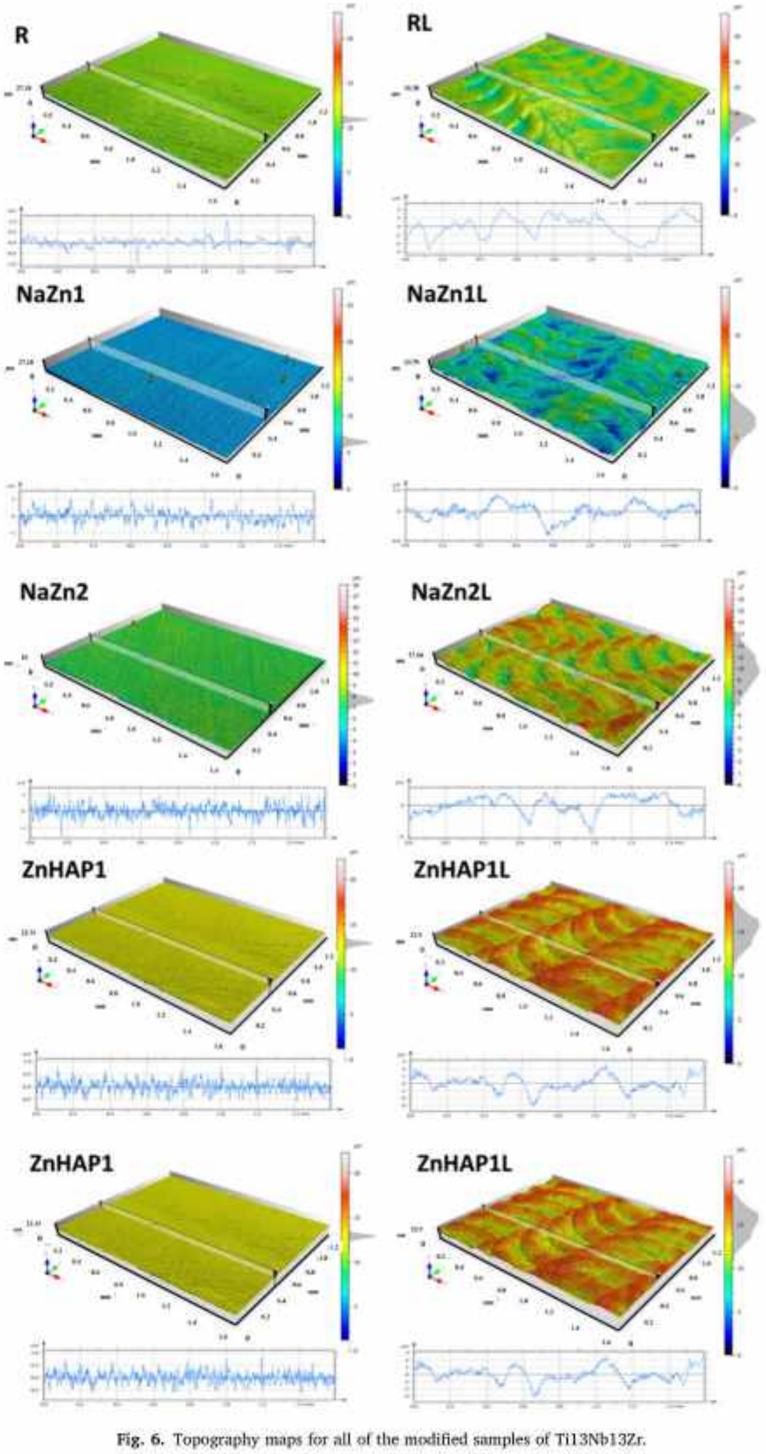

Fig. 6. Topography maps for all of the modified samples of Ti13Nb13Zr.

Table 4
Selected roughness parameters of the investigated samples calculated according to the ISO 25178 and ISO 21920 standards.

	R	RL	NaZn1	NaZn2	ZnHAP1	ZnHAP2	NaZn1L	NaZn2L	ZnHAP1L	ZnHAP2L
Ra [μm]	0.14 ±0.01	0.92 ±0.08	0.25 ±0.01	0.25 ±0.01	0.16 ±0.01	0.21 ±0.01	0.80 ±0.08	1.00 ±0.20	0.80 ±0.11	1.19 ±0.13
Rq [μm]	0.18 ±0.01	1.11 ±0.10	0.32 ±0.02	0.33 ±0.02	0.20 ±0.01	0.28 ±0.01	1.03 ±0.04	1.23 ±0.19	0.98 ±0.09	1.46 ±0.10
Rz [μm]	1.33 ±0.32	4.64 ±0.43	2.16 ±0.20	2.48 ±0.25	1.27 ±0.05	2.65 ±0.63	5.44 ±0.20	5.63 ±0.12	4.67 ±0.48	6.35 ±0.55
Sa [μm]	0.17 ±0.01	1.26 ±0.18	0.27 ±0.01	0.35 ±0.06	0.19 ±0.01	0.23 ±0.01	1.18 ±0.16	1.27 ±0.02	1.31 ±0.02	1.34 ±0.03
Sq [μm]	0.25 ±0.01	1.58 ±0.21	0.49 ±0.07	0.45 ±0.08	0.26 ±0.01	0.31 ±0.02	1.47 ±0.21	1.56 ±0.02	1.61 ±0.01	1.64 ±0.04
Sp [μm]	11.66 ±1.79	20.10 ±1.46	23.54 ±6.74	8.13 ±1.99	7.43 ±2.44	10.10 ±2.88	13.30 ±5.48	11.08 ±2.40	9.83 ±2.76	9.03 ±0.59
Sv [μm]	9.47 ±1.10	16.77 ±2.72	7.80 ±2.42	7.94 ±0.40	13.47 ±3.11	13.27 ±0.77	8.05 ±1.47	10.59 ±0.48	14.04 ±1.87	9.64 ±1.06
Sz [μm]	21.14 ±1.85	36.87 ±2.16	31.34 ±9.16	16.07 ±2.05	20.90 ±5.19	23.37 ±3.65	21.34 ±6.94	21.67 ±2.84	23.87 ±0.94	18.66 ±1.65
Ssk [-]	1.40 ±0.88	−0.46 ±0.06	14.97 ±7.38	0.47 ±0.28	−0.53 ±0.45	−0.98 ±0.14	−0.15 ±0.05	−0.12 ±0.03	−0.23 ±0.06	−0.20 ±0.04
Sku [-]	137.98 ±40.69	3.16 ±0.13	53.71 ±34.61	7.68 ±4.02	33.37 ±8.26	27.79 ±1.26	3.21 ±0.28	2.70 ±0.07	2.62 ±0.07	2.55 ±0.05
Vm [10^{-5} mm^3/mm^2]	1.24 ±0.01	5.51 ±0.68	2.78 ±0.33	2.18 ±0.17	1.27 ±0.01	1.64 ±0.01	5.93 ±0.36	5.93 ±0.01	5.82 ±0.25	5.66 ±0.32
Vv [10^{-5} mm^3/mm^2]	26.80 ±0.82	193.30 ±25.40	44.30 ±2.00	56.80 ±9.11	31.00 ±0.39	37.10 ±2.50	191.70 ±28.00	206.00 ±2.50	207.70 ±3.77	218.00 ±6.48
Vvv [10^{-5} mm^3/mm^2]	3.01 ±0.13	21.60 ±3.32	3.79 ±0.09	5.44 ±1.13	3.14 ±0.16	3.82 ±0.36	17.80 ±2.94	17.40 ±0.45	18.40 ±0.97	18.80 ±0.37
Vvc [10^{-5} mm^3/mm^2]	23.80 ±0.68	172.00 ±22.10	40.50 ±1.98	51.40 ±7.98	27.80 ±0.22	33.20 ±2.12	174.30 ±25.20	188.30 ±2.49	189.30 ±4.71	199.00 ±6.48

example, the Ra and Sa parameters consider peaks and valleys equally. In the context of bone implants, the presence of more valleys may be more favorable for tissue ingrowth, while the presence of peaks may lead to micro-damage to tissue. In applications such as bone implants, more detailed roughness parameters and surface texture analysis are needed to accurately assess their impact on osteointegration and other biological functions [50]. In the context of the Sv parameter, which describes the depth of the valleys, which is particularly important in the implant application of the material [51], it should be noted that in the case of the native ground material, laser treatment significantly increases the Sv value, but for all MAO- and laser-modified samples the Sv values are similar. It is important to note that the time of the MAO process does not significantly affect the obtained Sv parameters. On samples previously subjected to laser treatment, no significant effect of this treatment on the depth of valleys was also observed. The Ssk parameter is another important indicator describing the asymmetry of the surface roughness profile, particularly relevant in the context of implant materials, as it affects how the surface interacts with surrounding tissues, body fluids, and cells. In the context of materials for implants, lower Ssk values, which imply an advantage of valleys over peaks, will be preferred. Surfaces with positive obliquity, i.e., those with more peaks than valleys, can generate greater point pressures on the tissue, which can lead to microdamage and delayed integration [52]. The analyses carried out showed that all surfaces on which laser treatment was carried out take negative Ssk values. That again indicates the beneficial effect of laser treatment. Bone implants must promote osteointegration or integration of the implant into the bone. A surface with extreme peaks and valleys (high Sku kurtosis values) can lead to point pressure on the tissue, which can cause micro-injury and inflammation, delaying healing and integration into the bone. Laser treatment effectively reduces surface kurtosis for all samples tested. The highest Sku values were observed for the ground sample. In addition, it was noted that the time of the MAO process influences the reduction of the Sku parameter which can also have a beneficial effect from the perspective of implant applications. On samples subjected only to the MAO process, kurtosis values ranged from − 7.68 to − 53.71, while if they were also subjected to laser treatment the range was − 2.55 to − 3.21. For advanced analysis of surface topography, the functional parameters – Vv and Vm – were analyzed. High Vv values mean that the surface has deeper valleys or more space available below the midline. In the context of implants, valleys can act as storage spaces for body fluids, which promotes the osteointegration process by providing nutrients and enabling cell transport. High values of the Vm parameter can increase the coefficient of friction, which can be beneficial for mechanical stability in the initial stages after implantation, but at the same time can lead to surface wear if it is too high. It can be clearly observed that performing laser treatment causes an increase in both Vm and Vv parameters. However, no significant effect of electrolyte composition and MAO time on the values of these parameters was observed. Fig. 7 stands for isotropy for all of the samples. There are three groups depending on the percentage of isotropy. A value of less than 20 percent indicates an anisotropic surface, between 20 and 80 percent, and a mixed structure I of more than 80 percent indicates an isotropic surface [51,53]. For the

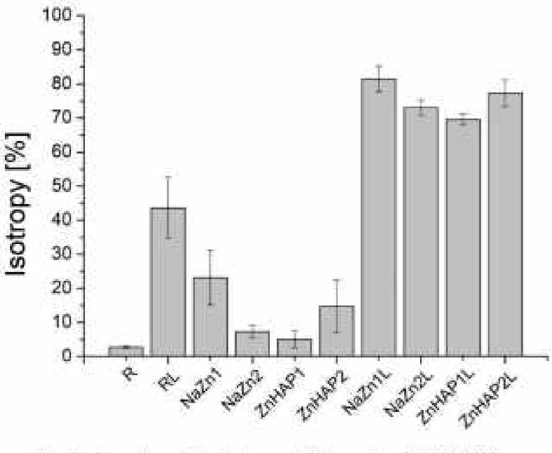

Fig. 7. Isotrophy of alla of the modified samples of Ti13Nb13Zr.

single-modified samples, isotropy was greater than that of the native material, with only the RL sample and NaZn1 reaching the level to determine the mixed structure. The remaining single-modified samples show an anisotropic surface. For the double modification, all surfaces were determined as mixed structures, with the highest values achieved for samples NaZn1L and ZnHAP2L, indicating a more isotropic surface. The mixed surface combines the advantages of an isotropic surface, which is close to the natural bone structure, and an anisotropic surface, which promotes antibacterial properties [51,54].

4.7. Corrosion behaviour

Fig. 8 shows the evolution of the open circuit potential (E_{OCP}) for the different samples over the immersion time. Higher values for the E_{OCP} indicate a lower tendency to suffer corrosion as the materials behave more cathodically. As shown, all the samples that were surface-modified achieved significantly higher E_{OCP} values than those for the reference sample. Thus, all the surface treatments were able to reduce the likelihood of the metallic substrate suffering from corrosion compared to the reference sample.

Fig. 9 shows the linear polarization resistance values obtained for all the conditions. The values for the reference sample (R) could not be obtained because the system did not remain sufficiently stable to achieve the linear behavior required in the small polarization range around E_{OCP}. This may indicate that surface-level processes affecting system stability were occurring in the reference sample, even at a small scale. On the other hand, these phenomena seemed to be reduced in the samples with different surface treatments, where sufficient stability was achieved to obtain valid polarization resistance measurements.

Assessing the evolution of polarization resistance for the different surface treatment conditions, it is noted that the presence of the laser treatment by itself, as well as a pretreatment for a MAO coating, appears to improve the polarization resistance of the samples, compared to those samples without a laser treatment. In general, for all conditions, the polarization resistance values remain constant throughout the immersion time, although a decrease is generally observed for all the samples from 1 h to 24 h of immersion. However, from 24 h onwards, the value remains stable, indicating a high anticorrosion behaviour of the samples. Among all of them, samples treated with laser and the hydroxyapatite MAO coating for 15 min (ZnHAp2L) show polarization resistance values that are significantly superior compared to the rest of the conditions. On the other hand, samples treated only with MAO coatings generated after 7 and 15 min and without a laser pretreatment (NaZn1 and NaZn2) showed the highest decrease in polarization resistance during the first 24 h of immersion, as well as the lowest polarization resistance values all over the immersion time.

These results show that samples treated with MAO coatings with hydroxyapatite present, in all cases and all over the experimentation time, had higher polarization resistance values than samples with the MAO coatings without hydroxyapatite, regardless of the coating generation time (7 or 15 min). On the other hand, focusing on the differences between samples with and without the application of the laser treatment previous to the generation of the regular MAO and the HAp MAO coatings, data show that the application of the laser promotes, in all cases, an increase in the polarization resistance of the samples treated with both MAO and HAp MAO coatings regardless of the coating generation time (7 or 15 min). Thus, based on these data, the sample that presents the best performance in terms of corrosion resistance is the one treated with a combination of laser followed by the generation of a HAp MAO coating generated for 15 min (ZnHAp2L).

Electrochemical impedance spectroscopy data show the evolution and the changes in the corrosion behavior of the samples treated with the different coating conditions, as well as the evolution of their impedance values over the immersion time. Nyquist curves (Fig. 10) show the response of the system to the sinusoidal excitation of ± 10 mV amplitude at a frequency range from 105 to 10–2 Hz. For short immersion times at high frequencies (Fig. 10Ab), all samples, except samples R, RL, and ZnHAp2L, presented two capacitive loops. This morphology of the Nyquist curves has been described in the literature for metallic substrates coated with porous coatings [55,56] The presence of only one capacitive loop in the Nyquist diagrams can be related to the presence of a single compact layer coating the surface of the metallic

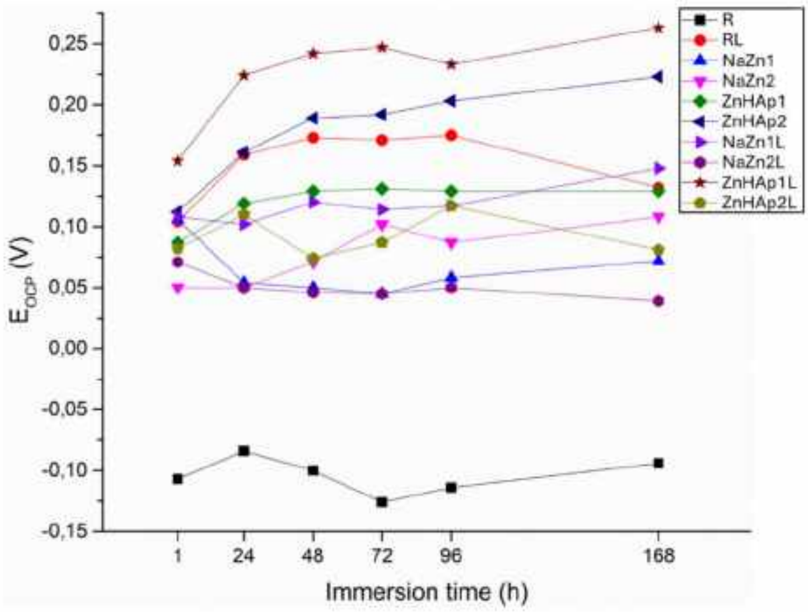

Fig. 8. Evolution of the open circuit potential for the different conditions immersed in Hanks' solution.

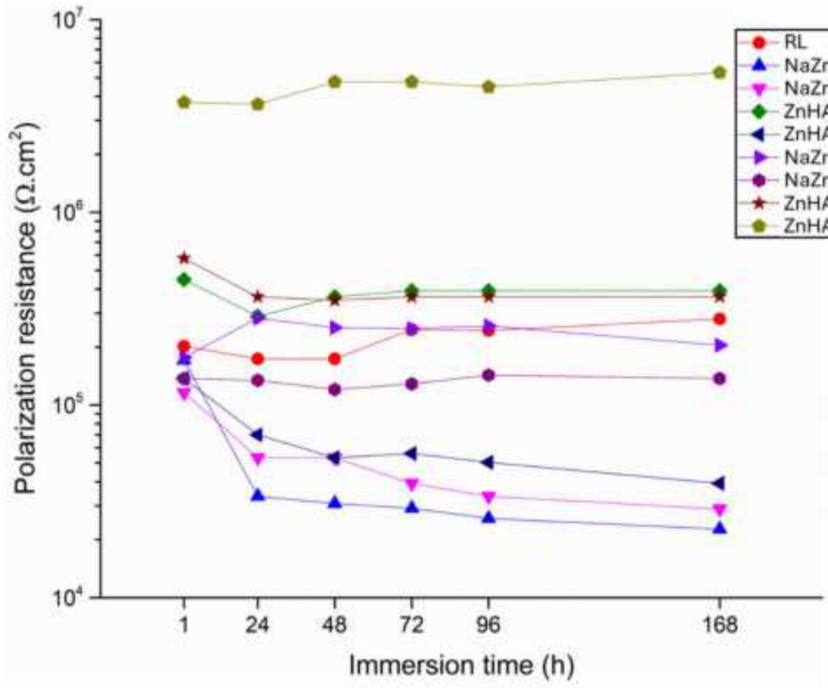

Fig. 9. Evolution of the polarization resistance values for the surface-modified samples.

substrate [57].

Samples with MAO coatings without previous laser treatment (NaZn1, NaZn2, ZnHAp1, and ZnHAp2) presented the lowest diameters for their capacitive loops at high frequencies likely related to the presence of electrolyte inside the coating due to the porosity of these coatings letting the intake of Hanks' solution during immersion, that reduces the protective behavior of the coatings. In fact, the diameter of the capacitive loops at high frequencies for these samples decreases along the immersion time, indicating a reduction in the protective behavior of these samples, especially in the case of samples NaZn1 and NaZn2. Thus, the application of the laser treatment prior to the generation of the MAO coatings seems to improve the corrosion resistance of the samples.

On the other hand, samples R, RL, and ZnHAp2L present one capacitive loop throughout the immersion time, indicating the presence of a compact coating on the surface of those samples. In the case of samples R and RL, these coatings can be composed of nanometric oxide layers that form spontaneously after immersion in the electrolyte. These samples were made from an alloy composed of valve metals, which promote the generation of protective oxide layers on a nanometric scale [58] These spontaneously generated oxide layers protect the metallic substrate by acting as protective barriers, preventing more aggressive corrosion processes. However, the diameter of the capacitive loops at low frequencies of samples R and RL decreased as the immersion time increased, probably due to a partial dissolution of the oxide layer [59], but that was not the case for the ZnHAp2L sample, whose curve remained almost constant throughout the experimentation time. At low frequencies, the samples that showed the best behavior against corrosion were ZnHAp1, ZnHAp1L, and ZnHAp2L, with the latter showing the best anticorrosion performance, following the results from the polarization resistance tests. Thus, HAp-containing MAO coatings performed better against corrosion than MAO coatings without hydroxyapatite.

The Bode diagrams (supplementary file Fig. 9), illustrate the evolution of impedance for the samples with different coating conditions. The impedance value at low frequencies indicates the protective capacity of the different treatments. The uncoated sample (R) and the sample with laser treatment (RL) show impedance values that remain constant throughout the immersion time, likely due to the presence of a protective thin oxide coating on their surface. This behavior is repeated for coatings that are more compact and less porous, which offer high protection to the metallic substrate and show impedance values that remain constant throughout the immersion time. On the other hand, for the rest of the samples, especially those with more porous coatings, the impedance value fluctuates and decreases over time as the electrolyte penetrates the coatings through their pores. From the Bode diagrams, it can be concluded that the samples with the best corrosion resistance were those treated with ZnHAp1, ZnHAp1L, and ZnHAp2L coatings, especially the ZnHAp2L coating that showed impedance values that were one or two orders of magnitude higher than the rest of the samples at low frequencies. On the other hand, the samples with the worst performance were NaZn1 and NaZn2. These results are consistent with those obtained in the polarization resistance tests. From the electrochemical corrosion tests, it can be concluded that the combination of laser treatment with hydroxyapatite-containing MAO coatings provided the best anticorrosion performance.

After immersion in Hanks' solution during 168 h for corrosion tests, SEM and EDS were used on the surface of the different samples (Figs. 11 and 12) for the evaluation of the corrosion process. In the case of the reference Ti13Nb13Zr sample (R), slight differences in terms of corrosion damage were found between the non-immersed zone (Fig. 11a) and the immersed zone (Fig. 11b) of the surface of the sample. However, the damage on the zone of the surface that was immersed in the Hanks' solution was not widespread. As previously exposed, this alloy is composed of valve metals that promote the formation of nanometric oxide layers that protect it from corrosion. Also, isolated accumulations of NaCl and KCl crystals precipitated from the electrolyte were found at some points of the immersed zone (Fig. 11c).

In the case of the Ti13Nb13Zr samples treated with laser (RL), SEM micrographs show the marks of the laser treatment as aligned rounded

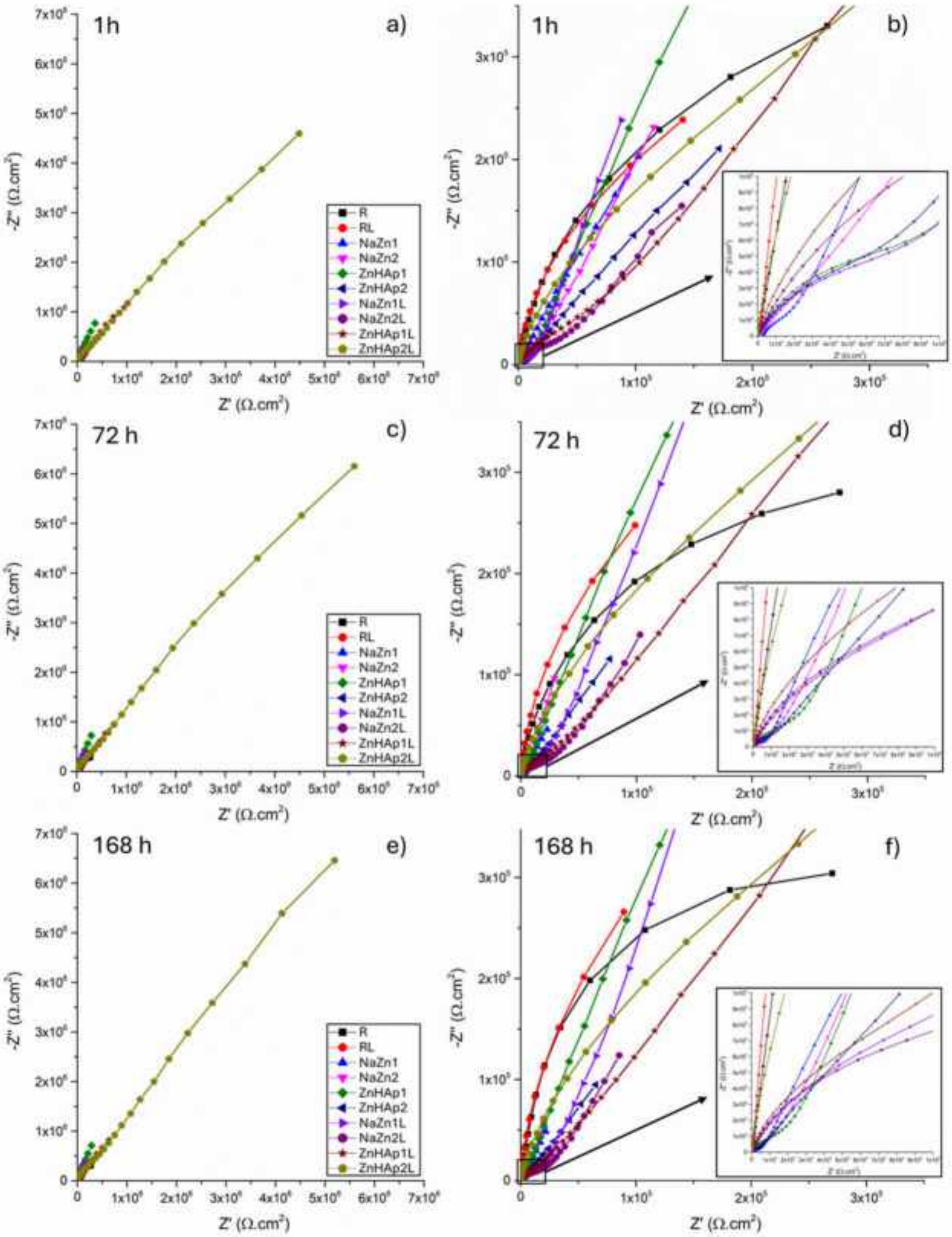

Fig. 10. A) Nyquist plots for the different conditions after 1 h (a, b), 72 h (c, d), and 168 h (e, f) of immersion in Hanks' solution; B) Bode plots for the different conditions after 1 h, 72 h and 168 h of immersion in Hanks' solution at 37 °C.

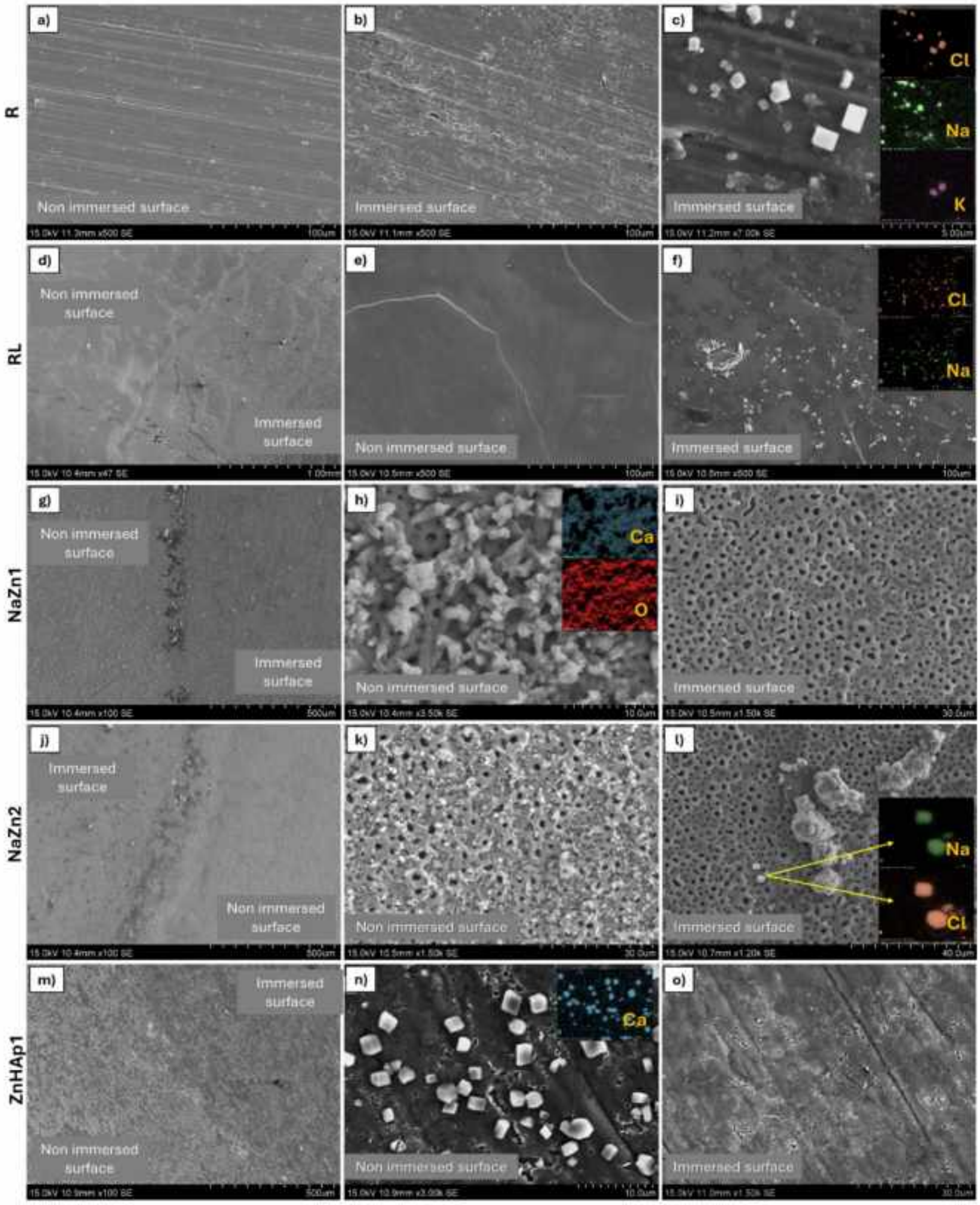

Fig. 11. SEM micrographs after immersion in Hanks' solution for the following samples: R ((a), non-immersed zone, (b) immersed zone, (c) detail of immersed zone), RL ((d) boundary between immersed and non-immersed zone, (e) non-immersed zone, (f) immersed zone), NaZN1 ((g) boundary between immersed and non-immersed zone, (h) non-immersed zone, (i) immersed zone), NaZn2 ((j) boundary between immersed and non-immersed zone, (k) non-immersed zone, (l) immersed zone with sodium chloride deposits from the electrolyte), ZnHAp1 ((m) boundary between immersed and non-immersed zone, (n) non-immersed zone, (o) immersed zone.

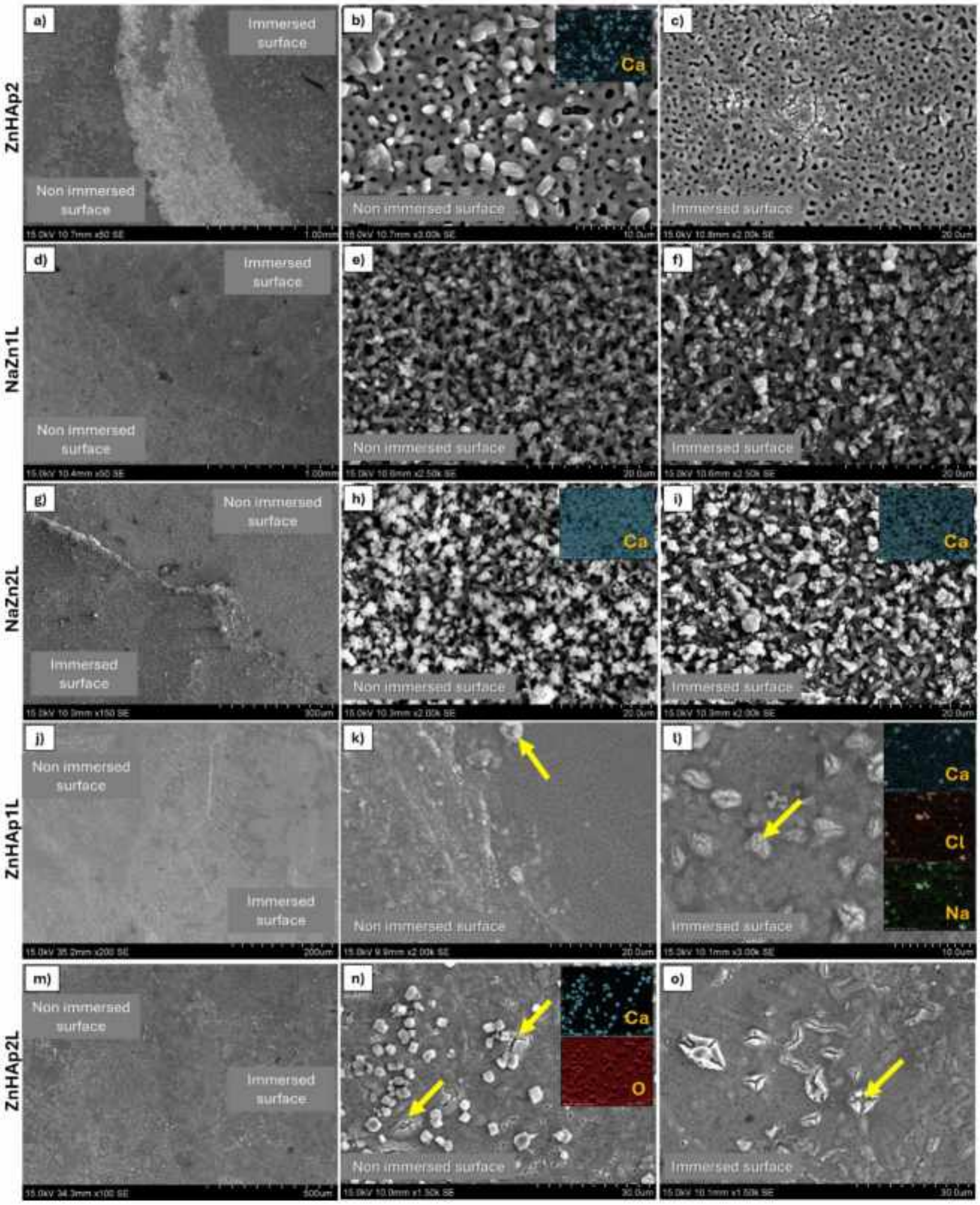

Fig. 12. SEM micrographs after immersion in Hanks' solution for the following samples: ZnHAp2 ((a) boundary between immersed and non-immersed zone, (b) non-immersed zone, (c) immersed zone), NaZn1L ((d) boundary between immersed and non-immersed zone, (e) non-immersed zone, (f) immersed zone), NaZN2L ((g) boundary between immersed and non-immersed zone, (h) non-immersed zone, (i) immersed zone), ZnHAp1L ((j) boundary between immersed and non-immersed zone, (k) non-immersed zone, (l) immersed zone with sodium chloride and calcium deposits), ZnHAp2L ((m) boundary between immersed and non-immersed zone, (n) non-immersed zone, (o) immersed zone with calcium deposits.

marks (Fig. 11d). Fig. 11e shows a closer view of the non-immersed zone of the RL sample, where it was possible to observe how the surface of the sample was modified by the action of the laser due to melting and solidification processes. For the immersed zone (Fig. 11f), as in the case of the reference sample, NaCl precipitates were found all over the surface. However, no significant damage due to corrosion was found on the immersed surface of this sample. Probably, the formation of a thin oxide layer on the surface of the sample during immersion in the Hanks' solution offered protection against corrosion to the metallic substrate.

In the case of NaZn1 and NaZn2 samples, where MAO coatings were generated using electrolyte 1, no significant differences were observed at low magnification between the non-immersed and the immersed zones (Fig. 11g and 11j). Nevertheless, at higher magnification, an accumulation of calcium microparticles was found all over the surface of the non-immersed zone (Fig. 11A.h and 11A.k), likely formed during the MAO coating generation. However, these particles were removed from the surface of the immersed zone during corrosion tests. Some of the particles could have dissolved in the Hanks' solution, and some could have been dragged to the limit between the non-immersed and the immersed zones. Regarding the corrosion process, no signs of coating degradation or corrosion of the Ti13Nb13Zr substrate were found for these samples (Fig. 11i and 11l). However, these samples presented the worst anticorrosion behavior in the electrochemical test, especially as they suffered the most significant decrease in polarization resistance and impedance during the first 24 h of immersion in the Hanks' solution. This behavior could be explained by two factors. First, the presence of the Ca microparticles could influence the corrosion behavior of these samples as, at the beginning of the immersion, part of the pores of the coatings were occluded by the particles, hindering the intake of electrolyte through the coating. As the immersion time increased, the Ca particles were removed from the surface, thus opening the pores and allowing the electrolyte to penetrate the coating, consequently decreasing the barrier effect that it provides. Secondly, it is important to note that the pores of the MAO coatings generated on these samples (Fig. 11i and 11l) appear larger than the pores of the rest of the MAO coatings generated in this research. This would negatively affect their capacity to provide an effective barrier, allowing higher electrolyte intake inside the coating and reducing their protective behavior, as previously concluded from the electrochemical corrosion tests.

ZnHAp1 samples (Fig. 11m) were among the best performers against corrosion. MAO coatings were generated on these samples from electrolyte 2 with the addition of hydroxyapatite. Consequently, calcium microparticles from hydroxyapatite were found all over the non-immersed zone (Fig. 11n), formed during the generation of the coating. This finding could indicate improved biocompatibility of these coatings. However, these calcium microparticles were removed from the surface of the immersed zone due to the action of the Hanks' solution used as an electrolyte during the corrosion tests (Fig. 11o). Regarding corrosion behavior, no signs of corrosion or coating degradation were observed after immersion. Moreover, and perhaps the most important feature of these coatings, the amount and size of pores were dramatically reduced (Fig. 11o) compared with the previous NaZn1 and NaZn2 samples (Fig. 11i and 11l), reducing the possibility and volume of electrolyte intake during immersion. Thus, the barrier effect provided by these coatings was significantly enhanced, as concluded from electrochemical test data.

The appearance of the ZnHAp2 samples (Fig. 12a) significantly differed from that of the ZnHAp1 samples (Fig. 11m), yet the only difference between these two conditions was the time used for the MAO coating process, which was 15 min for the ZnHAp2 and 7 min for the ZnHAp1. As in the case of the ZnHAp1 samples, Ca microparticles from the hydroxyapatite added to the electrolyte were found on the surface of the non-immersed zone of the ZnHAp2 samples (Fig. 12), but these microparticles presented an irregular morphology contrary to what was found for the ZnHAp1 samples (Fig. 11n), likely due to the more prolonged MAO process that could degrade Ca microparticles to some extent, making them losing their cubic morphology. Also, no Ca microparticles were found on the surface of the zone that was immersed in Hanks' solution (Fig. 12). However, the main difference between ZnHAp2 and ZnHAp1 samples was found in the morphology of the coatings. While ZnHAp1 coatings presented low porosity and the pore size was significantly reduced (Fig. 11o), ZnHAp2 coatings showed a porosity level (Fig. 12) similar to that found in the NaZn1 and NaZn2 samples (Fig. 11i and 11l). Thus, in terms of corrosion resistance, ZnHAp2 behaved more like NaZn1 and NaZn2 samples, making these three conditions the ones that worst performed against corrosion as concluded from the electrochemical tests data.

Samples NaZn1L and NaZn2L (Fig. 12.d and 12.g) were treated with laser and then coated with MAO coatings from electrolyte 1 with different processing times. As in the case of the NaZn1 and NaZn2 samples that did not undergo the laser treatment prior to the MAO process, the surfaces of the non-immersed zones were covered by Ca microparticles (Fig. 12e and 12 h), precipitated during the MAO process. However, the main difference that these samples present, compared with the rest of the conditions, is that after immersion during the electrochemical tests, Ca microparticles were not totally removed from the surface of the immersed zones for both conditions (Fig. 12f and 12i). Under the Ca microparticles, MAO coatings present a porosity level similar to that of NaZn1 and NaZn2 samples (Fig. 11i and 11l). However, looking at the electrochemical test data, NaZn1L and NaZn2L showed a medium performance against corrosion among all the samples, but better than NaZn1 and NaZn2 samples without the laser treatment. This behavior could be explained by the presence of the Ca microparticles that were not removed during immersion in Hanks' solution from the surface of these samples. Thus, the Ca microparticles blocking part of the porosity of the coatings could help to decrease the intake of electrolyte into the coatings, increasing the barrier effect that they provided and, therefore, enhancing the corrosion resistance of these samples.

Finally, the surfaces of samples ZnHAp1L and ZnHAp2L, treated with a laser followed by the generation of MAO coatings from electrolyte 2 with the addition of hydroxyapatite, were evaluated. In the case of the ZnHAp1L sample, no significant differences were be observed at low magnification (Fig. 12j) between the zone that was immersed in the Hanks' solution during the electrochemical tests and the non-immersed zone. However, for the ZnHAp2L sample, at low magnification (Fig. 12m), the non-immersed zone appears dotted with white microparticles which, at higher magnification (Fig. 12n), were identified as Ca microparticles, probably precipitated during the MAO process from the hydroxyapatite added to the electrolyte, as in the case of the ZnHAp1 sample (Fig. 11n). Nevertheless, after immersion in the Hanks' solution for the electrochemical tests, the Ca microparticles were removed from the surface of the ZnHAp2L samples (Fig. 12o). Interestingly, not all the white dots that can be appreciated at low magnification for both conditions (Fig. 12j and 12 m) were identified as Ca microparticles. At higher magnification, cracked structures were found on the surface of both samples, marked with arrows in Fig. 12k, 12 l, 12n, and 12o. These structures were found only on the surface of ZnHAp1L and ZnHAp2L samples, both for the immersed and the non-immersed zones, indicating that they were generated during the MAO coating process. However, the presence of these cracks does not seem to negatively affect the anticorrosion performance of these coatings, as these cracked structures are surface defects rather than defects that extend through the entire thickness of the coating. In fact, these coatings presented the best performance in terms of anticorrosion protection, as can be inferred from the electrochemical test data, where sample ZnHAp2L performed the best against corrosion. This behavior can be related to the fact that these samples exhibit the least porosity of all the coatings generated in this research, providing the best barrier effect to protect the Ti13Nb13Zr substrates.

4.8. Cytocompatibility

Cytocompatibility studies were conducted on selected samples with potentially optimal properties for the application, as well as on reference samples, including the pure titanium alloy Ti13Nb13Zr (R) and laser-modified alloy (RL). Additionally, samples subjected to single MAO modification for 15 min in two different electrolytes (NaZn2, ZnHAp2) and samples with dual laser-MAO modification (NaZn2L, ZnHAp2L) were analyzed. In this sense, an endothelial autofluorescent C166-GFP was selected to evaluate their cytocompatibility.

Fluorescence microscopy images (Fig. 13) indicate that laser modification (RL) allowed early cell adhesion and promote cell growth on the surface. After a period of 24 h for each modification, cell growth was observed, the strongest again for the laser-only modification. After 24 h for the NaZn2L and ZnHAp2L double modification, many cells with spherical morphology were observed, which could indicate limited cell adhesion or even apoptosis, but after 72 h the presence of viable cells was observed. The Results from the fluorescence microscopy assessment were confirmed by the results from the cell metabolic activity test (Fig. 14A) using Alamar Blue over 72 h, where laser modified samples achieved the highest score. The DNA quantification test (Fig. 14B) also yielded the best results for this modification. Studies on laser modification of the surface indicate that changing the topography of the matrix promotes increased cell adhesion and proliferation [60,61]. Samples subjected to hybrid modifications demonstrated a good capacity for cell proliferation on their surface, with a significant difference observed between the base material (R) and the dual modifications (NaZn2L, ZnHAp2L). DNA quantification results are higher than those for single MAO modification; however, the cell metabolic activity test indicated very similar results for both single and dual modifications. In the study [27] research was also conducted on the dual modification of titanium using various lasers and the PEO (MAO) technique. The results indicate that for laser-ceramic combinations, increased cell adhesion and proliferation are observed. The protrusions formed as a result of the MAO technique provide anchoring areas for cytoplasmic processes, simultaneously enhancing cell stability. This is attributed to the increased values of wettability angle and surface roughness [27,62]. Such surfaces were described as synergistic, featuring a roughened, leveled, and porous morphology [27].

The presence of zinc in the ceramic coating did not negatively affect cell viability it doesn't negatively affect the cell growth. The literature indicates that the presence of zinc positively influences bone tissue metabolism, increases cell proliferation, and promotes tissue regeneration, but only at low concentrations of this bioadditive. Excessive zinc concentrations can have adverse effects, which is why its optimal concentration is crucial for achieving these benefits. Studies confirm that zinc plays an important role in cellular processes related to bone growth and repair, but its effects are dose-dependent [63,64]. It is worth noting that an excessive amount of zinc in modified layers can cause apoptosis. The presence of hydroxyapatite in the doubly modified ZnHAp2 sample also positively influenced cell growth, which is visible in Fig. 14A and 14B, hydroxyapatite is a phosphate of the fallow I clinically used and has demonstrated bioactive, osteoconductive properties [65,66].

DNA quantification tests allow the assessment of cellular patterning and DNA synthesis by measuring the total DNA content on the modified surface [67]. The results of quantitative DNA analysis for the studied samples are presented in Fig. 14B. Based on the conducted research, it can be concluded that the highest DNA content was observed in samples modified with laser treatment. The hybrid modification (Nd:YAG laser-MAO) yielded very promising results compared to single modifications involving only the ceramic layer deposited through the MAO process. The presence of laser modification promotes the formation of a morphologically developed surface, creating more favourable conditions for the cells [68]. These favourable outcomes suggest improved cell proliferation, and indicate that the increased DNA content may reflect the proper functioning of bioactive agents present on the surface (zinc, sodium, hydroxyapatite). Modified surfaces with higher DNA content potentially enhance bioinclusion, which, in turn, could reduce the risk of resection.

5. Conclusion

The study confirmed the effectiveness of hybrid surface modification of Ti13Nb13Zr alloy using laser treatment (Nd:YAG) and micro-arc oxidation (MAO). The MAO process carried out in the presence of zinc ions, sodium ions and hydroxyapatite allowed to obtain ceramic layers with developed topography and increased isotropy, which positively influenced the biological and mechanical properties of the surface.

FTIR and XPS analyses provided important information about the chemical composition and structure of the ceramic layers. FTIR spectra revealed the presence of bonds typical of titanium oxides (O-Ti-O), hydroxyapatite (PO_4^{3-} groups) and carbonates (CO_3^{2-}) in the layer structure. The presence of hydroxyapatite was confirmed by characteristic peaks at 3642 cm^{-1} (O–H bonds) and 872–876 cm^{-1} (ZnO bonds). On the other hand, XPS studies showed effective incorporation of Zn^{2+}, Na^{+}, Ca^{2+} ions and phosphate groups into the ceramic layer. Characteristic Zn peaks at bond energies of 1022–1045 eV indicate the presence of zinc oxide (ZnO) and zinc phosphate ($Zn_3(PO_4)_2$), confirming the efficiency of the modification process. In addition, the presence of hydroxyapatite was found to promote the migration of Ca^{2+} ions and their integration into the film structure as $Ca_3(PO_4)_2$, which positively affects the bioactivity of the surface.

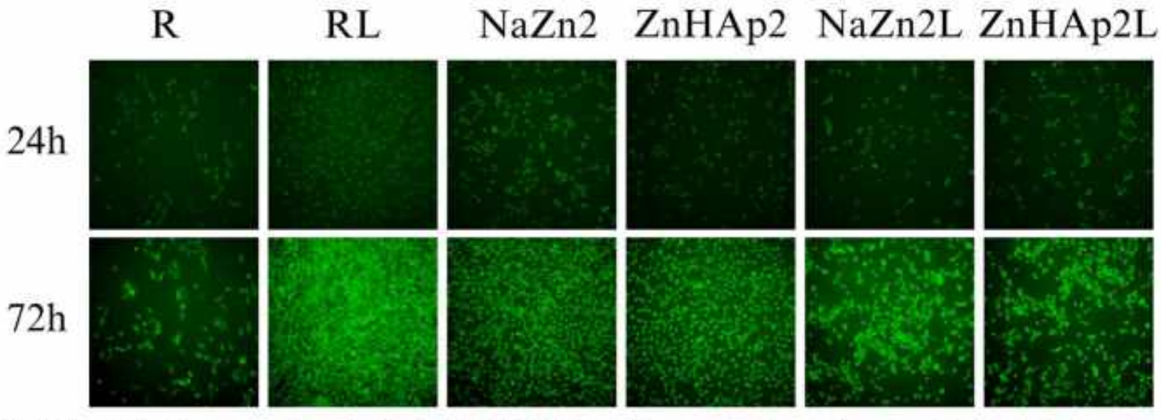

Fig. 13. Presentation of fluorescence micrographs of the Endothelial C166-GFP cell cultures grown on various coating surfaces after 24 and 72 h of incubation.

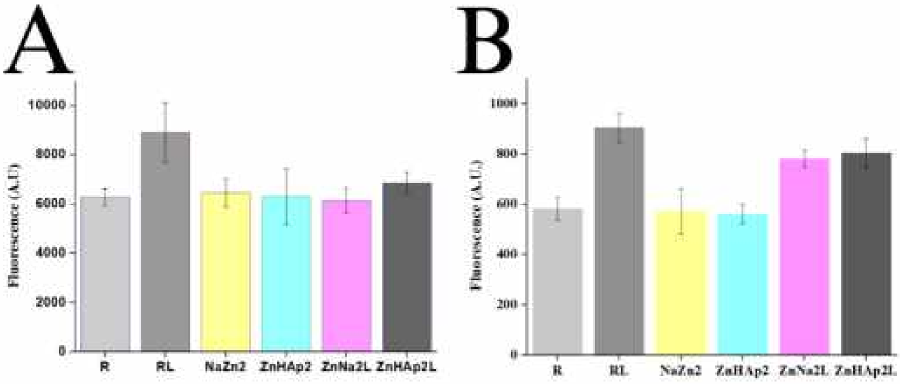

Fig. 14. A) Quantification of cell metabolic activity using Alamar blue assay after 72 h B) DNA quantification for Ti13Nb13Zr samples with and without modifications.

Morphological analyses showed significant differences between surfaces subjected to single and hybrid modification. The double modification led to a greater development of topography, expressed in higher values of roughness parameters (Sa, Sv), which favors osteointegration by increasing the implant's contact area with bone tissue. At the same time, the use of laser prior to the MAO process reduced anisotropy and the number of sharp peaks on the surface, thus limiting potential tissue microdamage.

Electrochemical tests showed a significant improvement in corrosion resistance for all modified samples, especially for the hybrid samples where the ceramic layers contained hydroxyapatite. The weakest polarization resistance results, particularly within the first 24 h, were observed for samples subjected only to single MAO modification using electrolyte 1. Laser modification must improve the stability of electrochemical parameters, which is crucial for the potential application of the material in implants with stringent corrosion resistance requirements.

Cytocompatibility tests revealed significant differences in cell adhesion and proliferation. The hybrid surfaces, especially those with the addition of hydroxyapatite, showed higher cell metabolic activity and DNA quantification values compared to unmodified surfaces and those subjected to single modification. The weakest results were observed for the NaZn2L sample after 24 h, where spherical-shaped cells indicating apoptosis were noted, although the situation improved after 72 h. The presence of zinc and hydroxyapatite had a positive effect on cell growth, confirmed by increased metabolic activity. The hybrid modification combines the advantages of both techniques, enhancing surface bioactivity, and making the ZnHAp2L sample the most promising for biomedical implant applications.

In conclusion, the study confirmed that the combination of laser treatment with the MAO process allows obtaining ceramic layers with optimised mechanical, biological and electrochemical properties. The application of this technique can significantly contribute to improving the functionality and durability of bone and dental implants, meeting the growing demands in the field of biomaterials.

CRediT authorship contribution statement

Joanna Sypniewska: Writing – original draft, Validation, Resources, Project administration, Methodology, Conceptualization. **Marek Szkodo:** Writing – review & editing. **Beata Majkowska-Marzec:** Writing – review & editing, Validation, Methodology. **Łukasz Pawłowski:** Writing – review & editing, Methodology, Investigation. **Aleksandra Mirowska:** Investigation. **Jacek Ryl:** Writing – review & editing, Methodology. **Aleksandra Mielewczyk-Gryń:** Investigation. **Łukasz Gaweł:** Writing – review & editing, Methodology, Investigation. **Enrique Martínez Campos:** Writing – review & editing, Supervision, Methodology. **Juan Pablo Fernández Hernán:** Writing – original draft, Validation, Supervision, Investigation, Conceptualization.

Declaration of competing interest

The authors declare that they have no known competing financial interests or personal relationships that could have appeared to influence the work reported in this paper.

Acknowledgments

This work was supported by the Gdańsk University of Technology under the Aurum Supporting International Research Team Building – 'Excellence Initiative – Research University' [grant number: 2/2021/IDUB/II.1.3].1

Appendix A. Supplementary data

Supplementary data to this article can be found online at https://doi.org/10.1016/j.apsusc.2025.163136.

Data availability

Data will be made available on request.

References

[1] S. Prasad, M. Ehrensberger, M.P. Gibson, H. Kim, E.A. Monaco, Biomaterial properties of titanium in dentistry, J. Oral Biosci. 57 (2015) 192–199, https://doi.org/10.1016/j.job.2015.08.001.

[2] S.J. Reinke, G. Gobbi, V.J. Rocha, Y.P. Sousa, T.P. Coutinho, Biomaterial: Concepts and Basics Properties (2020) www.eijst.org.uk.

[3] M. Bartmański, Ł. Pawłowski, A. Belcarz, A. Przekora, G. Ginalska, G. Strugała, B. M. Cieślik, A. Pałubicka, A. Zieliński, The chemical and biological properties of nanohydroxyapatite coatings with antibacterial nanometals, obtained in the electrophoretic process on the TI13ZR13NB alloy, Int. J. Mol. Sci. 22 (2021) 1–16, https://doi.org/10.3390/ijms22063172.

[4] Ł. Pawłowski, M. Bartmański, A. Mielewczyk-Gryń, A. Zieliński, Chitosan/poly(4-vinylpyridine) coatings formed on AgNPs-decorated titanium, Mater. Lett. 319 (2022), https://doi.org/10.1016/j.matlet.2022.132293.

[5] K. Malisz, B. Świeczko-Żurek, J.M. Olive, G. Pecastaings, A. Sionkowska, A. Laska, G. Gajowiec, Research of chitosan coatings deposited by electrophoretic deposition method at various voltage and time parameters, Mater. Chem. Phys. 315 (2024), https://doi.org/10.1016/j.matchemphys.2024.128984.

[6] B. Makurat-Kasprolewicz, A. Ossowska, Recent advances in electrochemically surface treated titanium and its alloys for biomedical applications: A review of anodic and plasma electrolytic oxidation methods, Mater. Today Commun. 34 (2023), https://doi.org/10.1016/j.mtcomm.2023.105425.

[7] Y. Wang, H. Yu, C. Chen, Z. Zhao, Review of the biocompatibility of micro-arc oxidation coated titanium alloys, Mater. Des. 85 (2015) 640–652, https://doi.org/10.1016/j.matdes.2015.07.086.

[8] J. Sypniewska, M. Szkodo, Influence of Laser Modification on the Surface Character of Biomaterials: Titanium and Its Alloys — A Review (2022).

[9] B. Majkowska-Marzec, J. Sypniewska, Microstructure and mechanical properties of laser surface-treated Ti13Nb13Zr alloy with MWCNTs coatings, Adv. Mater. Sci. 21 (2021) 5–18, https://doi.org/10.2478/adms-2021-0021.

[10] C.G. Moura, O. Carvalho, L.M.V. Gonçalves, M.F. Cerqueira, R. Nascimento, F. Silva, Laser surface texturing of Ti-6Al-4V by nanosecond laser: Surface characterization, Ti-oxide layer analysis and its electrical insulation performance, Mater. Sci. Eng. C 104 (2019) 109901, https://doi.org/10.1016/j.msec.2019.109901.

[11] S. Il Shin, H.K. Min, B.H. Park, Y.H. Kwon, J.B. Park, Y. Herr, S.J. Heo, J.H. Chung, The effect of Er:YAG laser irradiation on the scanning electron microscopic structure and surface roughness of various implant surfaces: An in vitro study, Lasers Med. Sci. 26 (2011) 767–776, https://doi.org/10.1007/s10103-010-0819-4.

[12] G.E. Romanos, H. Everts, G.H. Nentwig, Effects of diode and Nd:YAG laser irradiation on titanium discs: a scanning electron microscope examination, J. Periodontol. 71 (2000) 810–815, https://doi.org/10.1902/jop.2000.71.5.810.

[13] H. Kabir, K. Munir, C. Wen, Y. Li, Recent research and progress of biodegradable zinc alloys and composites for biomedical applications: Biomechanical and biocorrosion perspectives, Bioact. Mater. 6 (2021) 836–879, https://doi.org/10.1016/j.bioactmat.2020.09.013.

[14] A.R. Khan, N.S. Grewal, C. Zhou, K. Yuan, H.J. Zhang, Z. Jun, Recent advances in biodegradable metals for implant applications: Exploring in vivo and in vitro responses, Results Eng. 20 (2023), https://doi.org/10.1016/j.rineng.2023.101526.

[15] Y. Liu, T. Du, A. Qiao, Y. Mu, H. Yang, Zinc-based biodegradable materials for orthopaedic internal fixation, J Funct Biomater 13 (2022), https://doi.org/10.3390/jfb13040164.

[16] J.C. King, D.M. Shames, L.R. Woodhouse, Zinc and Health: Current Status and Future Directions Zinc Homeostasis in Humans 1, 2000.

[17] V. Sloup, I. Jankovská, S. Nechybová, P. Peřinková, I. Langrová, Zinc in the animal organism: a review, Sci. Agric. Bohem. 48 (2017) 13–21, https://doi.org/10.1515/sab-2017-0003.

[18] D. Hernández-Escobar, S. Champagne, H. Yilmazer, B. Dikici, C.J. Boehlert, H. Hermawan, Current status and perspectives of zinc-based absorbable alloys for biomedical applications, Acta Biomater. 97 (2019) 1–22, https://doi.org/10.1016/j.actbio.2019.07.034.

[19] J.P. O'Connor, D. Kanjilal, M. Teitelbaum, S.S. Lin, J.A. Cottrell, Zinc as a therapeutic agent in bone regeneration, Materials 13 (2020), https://doi.org/10.3390/ma13102211.

[20] A. Apelfeld, S. Grigoriev, B. Krit, V. Ludin, I. Suminov, D. Chudinov, Improving the stability of the coating properties for group plasma electrolytic oxidation, Manuf. Lett. 33 (2022) 54–59, https://doi.org/10.1016/j.mfglet.2022.08.005.

[21] W. Yao, L. Wu, J. Wang, B. Jiang, D. Zhang, M. Serdechnova, T. Shulha, C. Blawert, M.L. Zheludkevich, F. Pan, Micro-arc oxidation of magnesium alloys: A review, J. Mater. Sci. Technol. 118 (2022) 158–180, https://doi.org/10.1016/j.jmst.2021.11.053.

[22] Y. Meng, P. Liu, X. Chen, Laser remelting combined with micro-arc oxidation coating to improve the biocompatibility of titanium implants, Mater. Lett. 370 (2024), https://doi.org/10.1016/j.matlet.2024.136867.

[23] J. Sypniewska, M. Szkodo, B. Majkowska-Marzec, A. Mielewczyk-Gryń, Effect of hybrid modification by ceramic layer formation in MAO process and laser remelting on the structure of titanium bio-alloy Ti13Nb13Zr, Ceram. Int. 49 (11) (2023) 16603–16614, https://doi.org/10.1016/j.ceramint.2023.02.018.

[24] Y. Qin, D. Xiong, J. Li, Tribological properties of laser surface textured and plasma electrolytic oxidation duplex-treated Ti6Al4V alloy deposited with MoS2 film, Surf. Coat. Technol. 269 (2015) 266–272, https://doi.org/10.1016/j.surfcoat.2014.12.003.

[25] A. Civantos, E. Martinez-Campos, V. Ramos, C. Elvira, A. Gallardo, A. Abarrategi, Titanium coatings and surface modifications: toward clinically useful bioactive implants, ACS Biomater Sci. Eng. 3 (2017) 1245–1261, https://doi.org/10.1021/acsbiomaterials.6b00604.

[26] A. Santos-Coquillat, E. Martinez-Campos, H. Mora Sánchez, L. Moreno, R. Arrabal, M. Mohedano, A. Gallardo, J. Rodriguez-Hernandez, E. Matykina, Hybrid functionalized coatings on metallic biomaterials for tissue engineering, Surf Coat Technol 422 (2021), https://doi.org/10.1016/j.surfcoat.2021.127508.

[27] S.S. Nisar, S. Arun, H.C. Choe, Plasma electrolytic oxidation coatings on femtosecond laser-treated Ti-6Al-4V alloy for bio-implant use, Surf. Coat. Technol. 464 (2023), https://doi.org/10.1016/j.surfcoat.2023.129553.

[28] Q.M. Zhao, L. Cheng, Z.T. Liu, J.J. Zhao, Surface characteristics of Zinc-TiO2 coatings prepared via micro-arc oxidation, Compos Interfaces 21 (2014) 585–593, https://doi.org/10.1080/15685543.2014.914377.

[29] E.R. 1*, T.I. Török, A review of plasma electrolytic oxidation coating characteristics and affecting factors, n.d.

[30] H. Khanmohammadi, S.R. Allahkaram, N. Towhidi, A.M. Rashidfarokhi, Preparation of PEO coating on Ti6Al4V in different electrolytes and evaluation of its properties, Surf. Eng. 32 (2016) 448–456, https://doi.org/10.1179/1743294415Y.0000000083.

[31] H. Huang, X. Wei, J. Yang, J. Wang, Influence of surface micro grooving pretreatment on MAO process of aluminum alloy, Appl. Surf. Sci. 389 (2016) 1175–1181, https://doi.org/10.1016/j.apsusc.2016.08.088.

[32] G. Sundararajan, L. Rama Krishna, Mechanisms underlying the formation of thick alumina coatings through the MAO coating technology, Surf Coat Technol 167 (2003) 269–277, https://doi.org/10.1016/S0257-8972(02)00918-0.

[33] R. Luo, Y. Jiao, S. Zhang, J. Wu, X. Wu, K. Lu, P. Zhang, Y. Li, X. Ni, Q. Zhao, Fabrication, properties and biological activity of a titanium surface modified with zinc via plasma electrolytic oxidation, Front. Mater. 10 (2023), https://doi.org/10.3389/fmats.2023.1202110.

[34] Y. Liu, C. Chen, T. Liang, Y. Wang, R. Zhao, G. Li, C. Bai, Y. Wu, F. Yu, L. Sheng, R. Zhang, Y. Zhao, In vitro long-term antibacterial performance and mechanism of Zn-doped micro-arc oxidation coatings, Colloids Surf. B Biointerfaces 233 (2024), https://doi.org/10.1016/j.colsurfb.2023.113634.

[35] L. Sopchenski, K. Popat, P. Soares, Bactericidal activity and cytotoxicity of a zinc doped PEO titanium coating, Thin Solid Films 660 (2018) 477–483, https://doi.org/10.1016/j.tsf.2018.05.055.

[36] L.P. Qiao, J. Lou, S.F. Zhang, B. Qu, W.H. Chang, R.F. Zhang, The entrance mechanism of calcium and phosphorus elements into micro arc oxidation coatings developed on Ti6Al4V alloy, Surf. Coat. Technol. 285 (2016) 187–196, https://doi.org/10.1016/j.surfcoat.2015.11.041.

[37] D. Wei, Y. Zhou, D. Jia, Y. Wang, Chemical treatment of TiO 2 -based coatings formed by plasma electrolytic oxidation in electrolyte containing nano-HA, calcium salts and phosphates for biomedical applications, Appl. Surf. Sci. 254 (2008) 1775–1782, https://doi.org/10.1016/j.apsusc.2007.07.144.

[38] V. Malinovschi, A. Marin, C. Ducu, V. Andrei, E. Coaca, V. Craciun, M. Lungu, Influence of sodium aluminate concentration and process duration on microstructure, mechanical and electrochemical behavior of PEO coatings formed on CP-Ti, Surf. Coat. Technol. 418 (2021), https://doi.org/10.1016/j.surfcoat.2021.127240.

[39] H. Sahana, D.K. Khajuria, R. Razdan, D.R. Mahapatra, M.R. Bhat, S. Suresh, R. R. Rao, L. Mariappan, Improvement in bone properties by using risedronate adsorbed hydroxyapatite novel nanoparticle based formulation in a rat model of osteoporosis, J. Biomed. Nanotechnol. 9 (2013) 193–201, https://doi.org/10.1166/jbn.2013.1482.

[40] O. Kierat, A. Dudek, L. Adamczyk, The effect of the corrosion medium on silane coatings deposited on titanium grade 2 and titanium alloy ti13nb13zr, Materials 14 (2021) 1–14, https://doi.org/10.3390/ma14216350.

[41] D.A. Torres-Ceron, E. Restrepo-Parra, C.D. Acosta-Medina, D. Escobar-Rincon, R. Ospina-Ospina, Study of duty cycle influence on the band gap energy of TiO2/P coatings obtained by PEO process, Surf. Coat. Technol. 375 (2019) 221–228, https://doi.org/10.1016/j.surfcoat.2019.06.021.

[42] R. Kumari, C. Blawert, J.D. Majumdar, Microstructures and properties of plasma electrolytic oxidized Ti alloy (Ti-6Al-4V) for bio-implant application, Metall. Mater. Trans. A 47 (2016) 788–800, https://doi.org/10.1007/s11661-015-3256-y.

[43] S. Durdu, Ö.F. Deniz, I. Kutbay, M. Usta, Characterization and formation of hydroxyapatite on Ti6Al4V coated by plasma electrolytic oxidation, J. Alloy. Compd. 551 (2013) 422–429, https://doi.org/10.1016/j.jallcom.2012.11.024.

[44] C. Vivek, B. Balraj, S. Thangavel, Structural, optical and electrical behavior of ZnO@Ag core–shell nanocomposite synthesized via novel plasmon-green mediated approach, J. Mater. Sci. Mater. Electron. 30 (2019) 11220–11230, https://doi.org/10.1007/s10854-019-01467-x.

[45] K. Tao, S. Song, J. Ding, H. Dou, K. Sun, Carbonyl groups anchoring for the water dispersibility of magnetite nanoparticles, Colloid Polym. Sci. 289 (2011) 361–369, https://doi.org/10.1007/s00396-011-2380-5.

[46] J. Lisoń-Kubica, A. Taratuta, K. Goldsztajn, M. Antonowicz, W. Walke, A. Dyner, M. Basiaga, Modern methods of surface modification for new-generation titanium alloys, Acta Bioeng. Biomech. 24 (2022) 147–158, https://doi.org/10.37190/ABB-02175-2022-01.

[47] G. Strnad, N. Chirila, C. Petrovan, O. Russu, Contact angle measurement on medical implant titanium based biomaterials, Procedia Technol. 22 (2016) 946–953, https://doi.org/10.1016/j.protcy.2016.01.094.

[48] A. Fukuda, M. Takemoto, T. Saito, S. Fujibayashi, M. Neo, D.K. Pattanayak, T. Matsushita, K. Sasaki, N. Nishida, T. Kokubo, T. Nakamura, Osteoinduction of porous Ti implants with a channel structure fabricated by selective laser melting, Acta Biomater. 7 (2011) 2327–2336, https://doi.org/10.1016/j.actbio.2011.01.037.

[49] R. Krishna Alla, K. Ginjupalli, N. Upadhya, M. Shammas, R. Krishna Ravi, R. Sekhar, Surface Roughness of Implants: A Review, 2011. http://www.sbaoi.org.

[50] A.I. Nicolas-Silvente, E. Velasco-Ortega, I. Ortiz-Garcia, L. Monsalve-Guil, J. Gil, A. Jimenez-Guerra, Influence of the titanium implant surface treatment on the surface roughness and chemical composition, Materials 13 (2020), https://doi.org/10.3390/ma13020314.

[51] B. Makurat-Kasprolewicz, M. Wekwejt, A. Ronowska, G. Gajowiec, M. Grodzicka, S. Dzionk, A. Ossowska, Influence of ultrasound on the characteristics of CaP coatings generated via the micro-arc oxidation process in relation to biomedical engineering, ACS Biomater Sci. Eng. 10 (2024) 2100–2115, https://doi.org/10.1021/acsbiomaterials.3c01433.

[52] N. Kournetas, S. Spintzyk, E. Schweizer, T. Sawada, F. Said, P. Schmid, J. Geis-Gerstorfer, G. Eliades, F. Rupp, Comparative evaluation of topographical data of dental implant surfaces applying optical interferometry and scanning electron microscopy, Dent. Mater. 33 (2017) e317–e327, https://doi.org/10.1016/j.dental.2017.04.020.

[53] N. Barton, E. Quadros, Anisotropy is Everywhere, to See, to Measure, and to Model, Rock Mech. Rock Eng. 48 (2015) 1323–1339, https://doi.org/10.1007/s00603-014-0632-7.

[54] L. Damiati, M.G. Eales, A.H. Nobbs, B. Su, P.M. Tsimbouri, M. Salmeron-Sanchez, M.J. Dalby, Impact of surface topography and coating on osteogenesis and bacterial attachment on titanium implants, J Tissue Eng 9 (2018), https://doi.org/10.1177/2041731418790694.

[55] W.A. Badawy, A.M. Fathi, R.M. El-Sherief, S.A. Fadl-Allah, Electrochemical and biological behaviors of porous titania (TiO2) in simulated body fluids for implantation in human bodies, J. Alloy. Compd. 475 (2009) 911–916, https://doi.org/10.1016/j.jallcom.2008.08.061.

[56] M.E.P. Souza, L. Lima, C.R.P. Lima, C.A.C. Zavaglia, C.M.A. Freire, Effects of pH on the electrochemical behaviour of titanium alloys for implant applications, J. Mater. Sci. - Mater. Med. 20 (2009) 549–552, https://doi.org/10.1007/s10856-008-3623-y.
[57] L. Wang, M. Wang, M. Zhong, X. Li, Z. Cui, Degradation of thermal oxide film on pure titanium in an acidic environment containing fluoride, npj Mater. Degrad. 6 (2022), https://doi.org/10.1038/s41529-022-00275-9.
[58] A. Gutiérrez, M.F. López, J.A. Jiménez, C. Morant, F. Paszti, A. Climent, Surface characterization of the oxide layer grown on Ti-Nb-Zr and Ti-Nb-Al alloys, Surf. Interface Anal. 36 (8) (2004) 977–980, https://doi.org/10.1002/sia.1816.
[59] C.E.B. Marino, L.H. Mascaro, EIS characterization of a Ti-dental implant in artificial saliva media: Dissolution process of the oxide barrier, J. Electroanal. Chem. 568 (2004) 115–120, https://doi.org/10.1016/j.jelechem.2004.01.011.
[60] I. Shivakoti, G. Kibria, R. Cep, B.B. Pradhan, A. Sharma, Laser surface texturing for biomedical applications: A review, Coatings 11 (2021) 1–15, https://doi.org/10.3390/coatings11020124.
[61] T.R. Rautray, R. Narayanan, T.Y. Kwon, K.H. Kim, Surface modification of titanium and titanium alloys by ion implantation, J. Biomed. Mater. Res. B Appl. Biomater. 93 (2010) 581–591, https://doi.org/10.1002/jbm.b.31596.
[62] S. Arun, B.S. Lim, S.G. Ahn, H.C. Choe, Osteoconductive element-doped, porous, and low-elastic-modulus duplex coatings on a Ti-6Al-4 V alloy: A hybrid coating system for accelerating cell growth, J. Alloy. Compd. 943 (2023), https://doi.org/10.1016/j.jallcom.2023.169131.
[63] J. Dornelas, G. Dornelas, A. Rossi, A. Piattelli, N. Di Pietro, T. Romasco, C. F. Mourão, G.G. Alves, The incorporation of zinc into hydroxyapatite and its influence on the cellular response to biomaterials: a systematic review, J Funct Biomater 15 (2024), https://doi.org/10.3390/jfb15070178.
[64] Q.M. Atiyea, F.M. Al-Najar, G.F. Karim, S.S. Al-Salihi, Molecular evaluation of the impact of Nd:YAG laser and static magnetic field on genomic DNA of some bacterial isolates using RAPD-PCR, J. Pure Appl. Microbiol. 16 (2022), https://doi.org/10.22207/JPAM.16.3.62.
[65] D. Kumar, J.P. Gittings, I.G. Turner, C.R. Bowen, A. Bastida-Hidalgo, S.H. Cartmell, Polarization of hydroxyapatite: Influence on osteoblast cell proliferation, Acta Biomater. 6 (2010) 1549–1554, https://doi.org/10.1016/j.actbio.2009.11.008.
[66] S.V. Dorozhkin, Calcium orthophosphate-based biocomposites and hybrid biomaterials, J. Mater. Sci. 44 (9) (2009) 2343–2387, https://doi.org/10.1007/s10853-008-3124-x.
[67] K. Nielsen, H.S. Mogensen, J. Hedman, H. Niederstätter, W. Parson, N. Morling, Comparison of five DNA quantification methods, Forensic Sci. Int. Genet. 2 (2008) 226–230, https://doi.org/10.1016/j.fsigen.2008.02.008.
[68] M.B. da Cruz, J.F. Marques, A.F.S. Marques, S. Madeira, Ó. Carvalho, F. Silva, J. Caramês, A.D.S.P. da Mata, Modification of zirconia implant surfaces by Nd:YAG laser grooves: does it change cell behavior? Biomimetics 7 (2022) https://doi.org/10.3390/biomimetics7020049.

5.5. [JS5] Hybrid laser-micro-arc oxidation techniques for enhanced biocompatibility and surface modification of Ti13Nb13Zr alloy in biomedical applications

5.5.1. Wkład pracy doktoranta

Tytuł: Influence of hybrid modification on functional properties of a commercial bio-titanium alloy Ti6Al4V*

**artykuł pod recenzją w czasopiśmie Materials Letters*

Autorzy: Joanna Sypniewska, Marek Szkodo, Beata Majkowska-Marzec, Łukasz Pawłowski, Enrique Martínez Campos, Juan Pablo Fernández Hernán

Czasopismo: Materials Letters, status: under review

Rok wydania: 2025

Impact factor: 2.7

Liczba punktów wg MNiSW: 70

DOI: 10.1016/j.apsusc.2025.163136

Procentowy wkład pracy doktoranta: 70

W pracy podjęłam się przygotowania nowego elektrolitu wodnego zawierającego nanotlenek cynku, przeznaczonego do zastosowania w procesie modyfikacji komercyjnie stosowanego stopu tytanu Ti6Al4V. Nadzorowałam proces modyfikacji laserowej, zgodnie z optymalnymi parametrami ustalonymi w [JS2] i [JS3]. Przeprowadziłam badania hybrydowej modyfikacji typu laser–MAO, obejmujące analizę morfologii powierzchni (SEM, mikroskop optyczny) oraz składu chemicznego (EDS). Wykonałam także badania głębokości strefy wpływu ciepła dla tego materiału, a także zwilżalności powierzchni po modyfikacji laserowej i po wytworzeniu warstwy ceramicznej wzbogaconej jonami.Dodatkowo, we współpracy z naukowcami z uczelni w Madrycie i Móstoles (Hiszpania), przeprowadziłam badania elektrochemiczne oraz analizy bioaktywności. W ramach pracy przygotowałam cały manuskrypt, obejmujący wprowadzenie merytoryczne, metodykę oraz dyskusję wyników. Byłam również autorką korespondencyjną.

Joanna Sypniewska ....
mgr inż. Joanna Sypniewska

5.5.2. Potwierdzenie recenzji artykułu

Outlook

Your Submission: MLBLUE-D-25-02878

Od em.mlblue.10e6.942818.50fb74c1@editorialmanager.com
<em.mlblue.10e6.942818.50fb74c1@editorialmanager.com>
w imieniu użytkownika
Y.F. Zheng <em@editorialmanager.com>
Data Śr, 18.06.2025 10:02
Do Joanna Sypniewska <joanna.sypniewska@pg.edu.pl>

Dear Miss Sypniewska,

The reviewer(s) and editor have evaluated your manuscript "Influence of hybrid modification on functional properties of a commercial bio-titanium alloy Ti6Al4V" (Miss Joanna Sypniewska). As you will see from the comments below and on https://www.editorialmanager.com/mlblue/, moderate revision has been requested. Given that the requested revisions are moderate the new version is required within **Jul 18, 2025**.

To submit a revision, go to https://www.editorialmanager.com/mlblue/ and log in as an Author. You will find your submission record under Submission(s) Needing Revision. Please note that resubmissions not received within **Jul 18, 2025** may be withdrawn, unless you contact me to extend the deadline.

With your resubmission, explain how and where each point of the reviewer's comments has been incorporated. For this, use submission item "Revision
Notes" when uploading your revision. Also, indicate the changes in an annotated version of the revised manuscript (submission item "Revision, changes marked"). Should you disagree with any part of the reviews, please explain why. To facilitate further review, add line numbers to the text of your manuscript.

Please present any figures, tables etc. as separate files. See the Artwork Guidelines on the home page right menu for further file naming conventions, referencing and format issues. Please upload source files (e.g. Word or LaTeX) of the text and figures. PDF files of the text cannot be handled by the typesetters.

Please strictly follow the formatting requirements as presented in the Guide for Authors at http://www.elsevier.com/locate/mlblue. As regards the figures: The cost for colour printing should be met by the author. In order to reduce the cost you may choose to redraw those figures where colour can be substituted by using different graphical shapes.

I hope that you will find these comments to be of use to you and am looking forward to receiving your revision.

Thank you for submitting your work to this journal.

PLEASE NOTE: Materials Letters would like to enrich online articles by displaying interactive figures that help the reader to visualize and explore your research results. For this purpose, we would like to invite you to upload figures in the MATLAB .FIG file format as supplementary material to our

online submission system. Elsevier will generate interactive figures from these files and include them with the online article on SciVerseScienceDirect. If you wish, you can submit .FIG files along with your revised submission.

Please note that this journal offers a new, free service called AudioSlides: brief, webcast-style presentations that are shown next to published articles on ScienceDirect (see also http://www.elsevier.com/audioslides). If your paper is accepted for publication, you will automatically receive an invitation to create an AudioSlides presentation.

Materials Letters features the Interactive Plot Viewer, see: http://www.elsevier.com/interactiveplots. Interactive Plots provide easy access to the data behind plots. To include one with your article, please prepare a .csv file with your plot data and test it online at http://authortools.elsevier.com/interactiveplots/verification before submission as supplementary material.

Research Elements (optional)
This journal encourages you to share research objects - including your raw data, methods, protocols, software, hardware and more – which support your original research article in a Research Elements journal. Research Elements are open access, multidisciplinary, peer-reviewed journals which make the objects associated with your research more discoverable, trustworthy and promote replicability and reproducibility. As open access journals, there may be an Article Publishing Charge if your paper is accepted for publication. Find out more about the Research Elements journals at https://www.elsevier.com/authors/tools-and-resources/research-elements-journals?dgcid=ec_em_research_elements_email.

Kind regards,

Y.F. Zheng, PH.D
Editor
Materials Letters

5.5.3. Treść artykułu

Materials Letters

Influence of hybrid modification on functional properties of a commercial bio-titanium alloy Ti6Al4V

--Manuscript Draft--

Manuscript Number:	
Article Type:	Short Communication
Keywords:	laser modification, hybrid modification, surface treatment, micro-arc oxidation, plasma-electrolitic oxidation
Corresponding Author:	Joanna Sypniewska, M.D. Gdańsk University of Technology Gdansk, Województwo pomorskie POLAND
First Author:	Joanna Sypniewska, M.D.
Order of Authors:	Joanna Sypniewska, M.D.
	Łukasz Pawłowski, PhD
	Marek Szkodo, Professor
	Beata Majkowska-Marzec, PhD
	Juan Pablo Fernández Hernán, PhD
	Enrique Martínez Campos, PhD
Abstract:	Although Ti6Al4V is widely used, its surface still needs improvement for medical applications. Here alloy was modified by a two-step process: laser treatment followed by micro-arc oxidation (MAO). This aimed to create a rough surface enriched with bioelements such as sodium, phosphorus, and zinc. Zinc ions were introduced into the MAO layer as zinc oxide nanoparticles (nZnO). SEM analysis revealed a complex but uneven surface, suggesting good potential for further hybrid surface development. Laser treatment improved the alloy's stability and corrosion resistance. Wettability tests confirmed full hydrophilicity, a key factor in cell response. Notably, the single- and double-modified samples without nZnO showed the best biological performance, likely due to their high hydrophilicit

Manuscript

Influence of hybrid modification on functional properties of a commercial bio-titanium alloy Ti6Al4V

Joanna Sypniewska[1*], Marek Szkodo[1], Beata Majkowska-Marzec[1], Łukasz Pawłowski[1], Juan Pablo Fernández Hernán[2], Enrique Martínez Campos[3],

*corresponding author: joanna.sypniewska@pg.edu.pl

[1] Institute of Manufacturing and Materials Technology, Faculty of Mechanical Engineering and Ship Technology, Gdańsk University of Technology, Gdansk, Poland ; *corresponding author, joanna.sypniewska@pg.edu.pl

[2] Department of Applied Mathematics, Materials Science and Engineering, and Electronic Technology, Escuela Superior de Ciencias Experimentales y Tecnología, Universidad Rey Juan Carlos

[3] Group of Organic Synthesis and Bioevaluation, Instituto Pluridisciplinar, Universidad Complutense de Madrid (UCM), Associated Unit to the ICTP-IQM-CSIC, Paseo Juan XXIII, nº 1, 28040 Madrid, Spain

ABSTRACT

Although Ti6Al4V is widely used, its surface still needs improvement for medical applications. Here alloy was modified by a two-step process: laser treatment followed by micro-arc oxidation (MAO). This aimed to create a rough surface enriched with bioelements such as sodium, phosphorus, and zinc. Zinc ions were introduced into the MAO layer as zinc oxide nanoparticles (nZnO). SEM analysis revealed a complex but uneven surface, suggesting good potential for further hybrid surface development. Laser treatment improved the alloy's stability and corrosion resistance. Wettability tests confirmed full hydrophilicity, a key factor in cell response. Notably, the single- and double-modified samples without nZnO showed the best biological performance, likely due to their high hydrophilicit

INTRODUCTION

The Ti6Al4V titanium alloy is the most commonly used commercial alloy. It has a lower Young's modulus than pure titanium, which is beneficial in dental and orthopedic applications[1]. It is widely available and less expensive than other titanium alloys. Surface modification of biomedical materials is a major field in biomaterials research. Dual techniques allow precise control of properties and combine advantages from different methods to produce optimized surfaces [2,3].

Laser modification is repeatable and controllable, allowing design of surfaces with desired wettability, roughness, and morphology that support bone cell growth [4,5]. Main and most important advantage of the MAO ability to produce biocompatible ceramic layers with a characteristic elements, resulting from the incorporation of elements into the coating [6,7]. Elemental nanoparticles offer an attractive solution due to their ability to penetrate most cellular organelles, which stimulate faster activation of biological processes. The nZnO exhibit antibacterial properties and promote osseointegration [8]. Sodium and phosphorus ions serve as a valuable source of osteoinductive elements and additionally increase the biocompatibility of the material with the human body [9].

Presented dual modification of Ti6Al4V improves surface roughness and wettability, forming a developed microstructure. Combining both methods gives promising results for reproducible biomaterials with bioadditives that may reduce implant rejection and reoperation risk.

.

MATERIALS AND METHODS

1. Sample preparation

   The samples were made of Ti6Al4V and were ground before Nd:YAG laser remelting. They were then cleaned in an ultrasonic bath using isopropanol. Laser surface modification was performed under fixed parameters: laser power of 1000 W, pulse duration of 2.25 ms, and a scan rate of 60%. After laser treatment, the samples underwent MAO process under constant conditions with a 300 V and a current of 0.123 A (Table 1).

Tab. 1 A) Chemical composition of the MAO electrolyte B) Sample modification

A	
Electrolyte	Composition
Electrolyte 1	$Na_3PO_4 \cdot 12H_2O$ 3g/L NaOH 1g/L
Electrolyte 2	$Na_3PO_4 \cdot 12H_2O$ 3g/L NaOH 1g/L 0,5g of nZnO
B	
Sample	Modification
Ref	Ti6Al4V
Ref_L	Ti6Al4V modified by 1000 W
M_300_10	MAO in electrolyte 1 for 10 minutes
M_300_15	MAO in electrolyte 1 for 15 minutes
Z_300_10	MAO in electrolyte 2 for 10 minutes
ML_300_10	Laser (1000 W) and MAO in electrolyte 1 for 10 minutes
ML_300_15	Laser (1000 W) and MAO in electrolyte 1 for 15 minutes
ZL_300_10	Laser (1000 W) and MAO in electrolyte 2 for 10 minutes

2. Surface morphology

   The samples were analyzed for surface morphology using a high-resolution scanning electron microscope (SEM, JEOL Ltd., Tokyo, Japan) and Ref_L observed with metallurgical microscope. Chemical composition of modified layers was examined using an EDS (TESCAN, Czech Republic). Surface wettability messured by sensile drop method with a goniometer equipped with Attention One software.

3. Biological tests

   Before testing, samples were sterilized using ethanol, PBS (Phosphate-Buffered saline) rinses, UV irradiation, and pre-incubation in supplemented DMEM. C2C12 cells were cultured at 37 °C in standard conditions. Cell viability was evaluated using the Alamar Blue assay after 168 h. Fluorescence was measured using a BioTek Synergy HT reader. Details are provided [2].

4. Corrosion tests

   Samples were immersed in Hank's solution during 168 h to simulate physiological conditions. Corrosion behavior was assessed by electrochemical impedance spectroscopy (EIS), with ±10 mV around open circuit potential, and a frequency range from 10^5 to 10^{-2} Hz.

RESULTS AND DISCUSSION

The surface of Ti6al4V alloy was subjected to dual modification using an Nd:YAG laser and MAO, which enabled the formation of morphologically highly developed structures (Fig. 1a). The use of an electrolyte containing nZnO significantly improved surface uniformity. The use of laser modification improved uniformity of the layer in the case of electrolytes 1 and 2, which indicates that increased substrate roughness promotes the formation of a more homogeneous coating. Prolonging the MAO process promoted the formation of larger pores and the presence of crystalline salt forms. The presented morphology is very similar to the irregular morphology of MAO layers reported in the literature after laser [3].

Contact angle measurements (fig. 1c) showed that each of the modified surfaces exhibited hydrophilic properties. Dual modification promotes the propagation of hydrophobic properties of the material, which was also indicated in previous studies by Sypniewska et al.[2]. From an application perspective, a higher contact angle is advantageous as it minimizes the risk of undesirable tissue adhesion, while, as reported in the literature, it does not impede osteogenic cell development. Particular attention should be paid to achieving a moderately wettable surface [10].

Low standard deviations in contact angle values indicate a relatively regular and uniform structure of modified surface. EDS showed that for MAO layers deposited from electrolyte containing nZnO, the zinc content was approximately 0.1% (fig.1b). In dual modification, only ML_300_10 exhibited an increased sodium ion content compared to other samples, which is significant for potential biomedical applications of this commercial titanium alloy. Microstructural analysis of Ti6Al4V allowed for the evaluation of the quality of laser remelting. Laser treated samples of 1000 W showed consistent laser track patterns, with no observed precipitates, contaminants, or surface cracks. Heat-affected zone (HAZ) for this alloy was approximately 204 μm in depth (fig.1 d, e).

a)

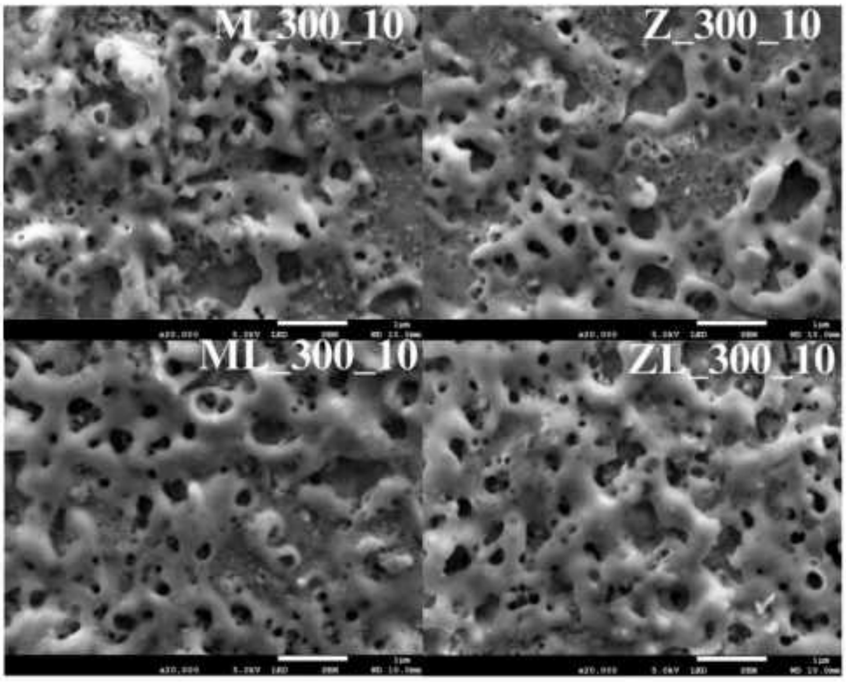

b)

Sample	Chemical composition [%]						
	Ti	Al	V	O	Na	P	Z
M_300_10	59.1	3.2	2.5	34.2	0.1	1.0	
M_300_15	58.7	3.2	2.5	34.6	0.1	1.0	
Z_300_10	58.2	3.0	2.4	35.0	0.2	1.1	0.1
ML_300_10	57.0	3.4	2.5	35.8	0.5	0.9	
ML_300_15	58.9	3.0	2.5	33.7	1.1	0.8	
ZL_300_10	58.2	3.4	2.5	34.8	0.1	0.9	0.1

c)

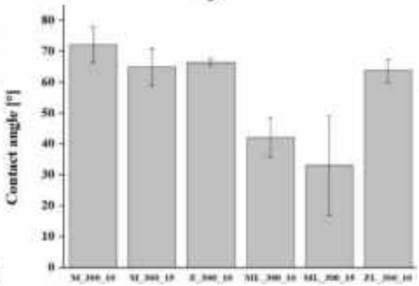

d)

e)

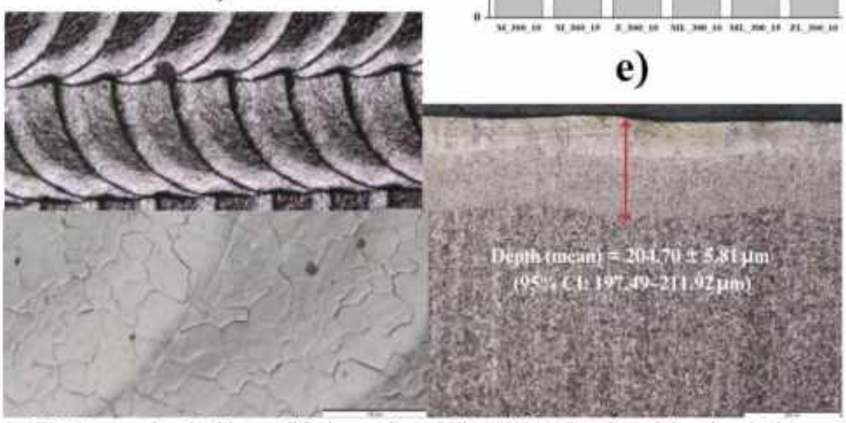

Figure 1. a) SEM images for double-modified samples of Ti6Al4V b) Results of the chemical composition of modified samples (EDS examination) c) contact angle results for all of the modified samples of Ti6Al4V, d) surface morphology of laser modified sample e) cross section image of Ref_L sample and the depth of HAZ

The best cellular response (fig.2) was observed for the laser-modified reference sample and the laser–MAO double-modified sample. Sample ML_300_15 exhibited the lowest contact angle, which can promote optimal cell proliferation. The other samples didn't demonstrate an adequate cellular response. For instance, in the case of sample M_300_15, no cell proliferation was observed; the cells displayed a clustered appearance, although no cytotoxicity of the substrate toward the cells was detected. Based on SEM images, it can be concluded that the pores of the MAO layers are too small for the cells C2C12, as their average size ranges between 100-300 μm [11].

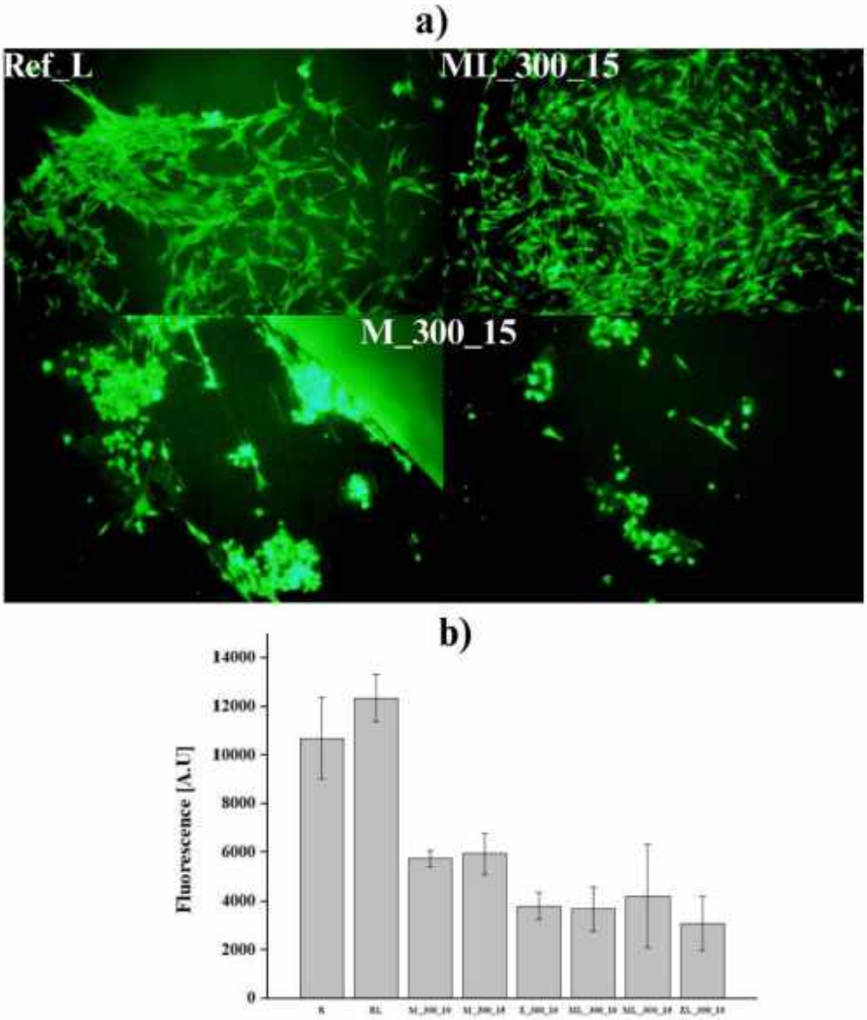

Figure 2. a) Presentation of fluorescence micrographs of the C2C12 cell cultures grown on various coating surfaces after 72 h of incubation b) Quantification of cell metabolic activity using Alamar blue assay after 168 h.

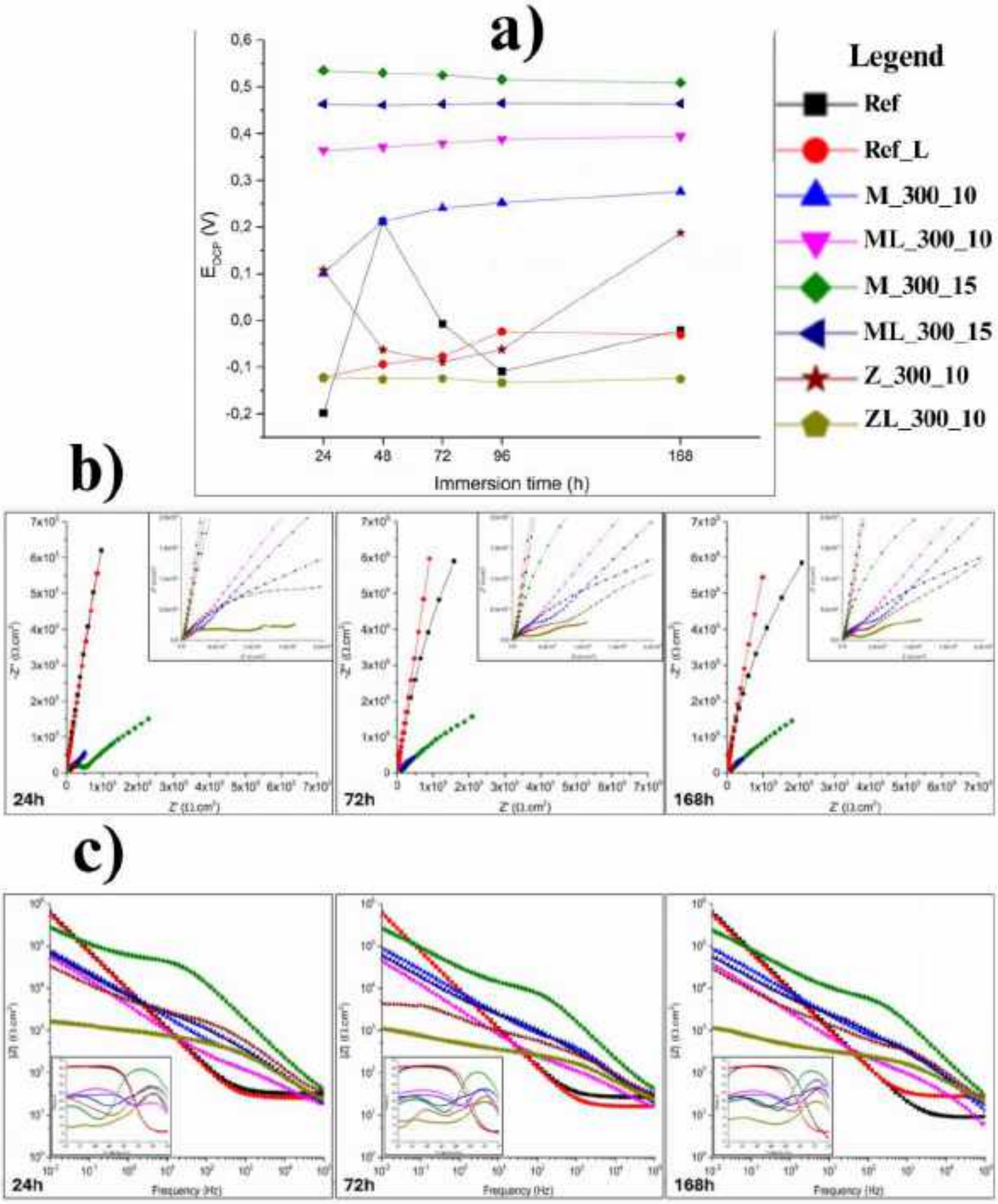

Figure 3. a) Evolution of OCP over immersion time for the different conditions. b) Nyquist plots after 24 h, 72 h and 168 h of immersion. c) Bode plots for impedance modulus after 24 h, 72 h, and 168 h of immersion. Insets show Bode plots for phase angle *Legend is for all samples

The results shown in Figure 3a indicate that the presence of MAO-coated samples, except those containing Zn, leads to an increase in the open circuit potential (OCP), suggesting a shift toward more cathodic behaviour compared to the non-coated samples. However, EIS tests reveal that the Ref_L samples exhibit the highest impedance modulus values and the most effective anticorrosion performance over immersion. The comparatively lower performance of the coated samples may be attributed to the partial degradation of the porous MAO coatings during immersion. These coatings display more than one time constant and fluctuations in phase angle values (Figure 3b and 3c), indicating only partially capacitive behaviour at high frequencies. This results in limited protection and changing protective capacity over time. In contrast, the Ref and Ref_L samples exhibit a single time constant and a transition from nearly pure resistive behaviour at high frequencies to nearly pure capacitive behaviour at low frequencies, likely due to the formation of a stable oxide layer on the surface during immersion. The Ref_L sample shows minimal changes in impedance modulus and phase angle throughout the immersion period, demonstrating the most stable and corrosion-resistant behaviour.

CONCLUSION

It is possible to form a ceramic layer on laser-treated Ti6Al4V. This process allows the introduction of bioactive ions into the ceramic layer. The treated surfaces show a hydrophilic nature. Their shape is irregular but supports cell growth. Good metabolic response was observed in Alamar Blue tests for optimal parameters. Laser treatment improved the corrosion resistance of the alloy to some extent of the Ti6Al4V, making it more stable over time. The key samples in this study were a laser-only reference and ML_300_15, without zinc ions. This work provides a solid foundation for further studies on dual surface treatment. It shows the potential to control the addition of useful ions into the material.

REFERENCES

[1] G.M. Rodriguez, J. Bowen, M. Zelzer, A. Stamboulis, Selective modification of Ti6Al4V surfaces for biomedical applications, RSC Adv 10 (2020) 17642–17652. https://doi.org/10.1039/c9ra11000c.

[2] J. Sypniewska, M. Szkodo, B. Majkowska-Marzec, Ł. Pawłowski, A. Mirowska, J. Ryl, A. Mielewczyk-Gryń, Ł. Gaweł, E.M. Campos, J.P. Fernández Hernán, Hybrid laser-micro-arc oxidation techniques for enhanced biocompatibility and surface modification of Ti13Nb13Zr alloy in biomedical applications, Appl Surf Sci 698 (2025). https://doi.org/10.1016/j.apsusc.2025.163136.

[3] G. Wu, Y. Yin, S. Zhang, Y. Wang, Y. Xiang, L. Li, J. Yao, Effect of laser texturing on the antiwear properties of micro-arc oxidation coating formed on Ti-6Al-4V, Surf Coat Technol 453 (2023). https://doi.org/10.1016/j.surfcoat.2022.129114.

[4] C. Wang, P. Tian, H. Cao, B. Sun, J. Yan, Y. Xue, H. Lin, T. Ren, S. Han, X. Zhao, Enhanced Biotribological and Anticorrosion Properties and Bioactivity of Ti6Al4V Alloys with Laser Texturing, ACS Omega 7 (2022) 31081–31097. https://doi.org/10.1021/acsomega.2c03166.

[5] J. Sypniewska, M. Szkodo, Influence of Laser Modification on the Surface Character of Biomaterials : Titanium and Its Alloys — A Review, (2022).

[6] B. Makurat-Kasprolewicz, A. Ossowska, Recent advances in electrochemically surface treated titanium and its alloys for biomedical applications: A review of anodic and plasma electrolytic oxidation methods, Mater Today Commun 34 (2023). https://doi.org/10.1016/j.mtcomm.2023.105425.

[7] M. Dziaduszewska, M. Shimabukuro, T. Seramak, A. Zielinski, T. Hanawa, Effects of micro-arc oxidation process parameters on characteristics of calcium-phosphate containing oxide layers on the selective laser melted Ti13Zr13Nb alloy, Coatings 10 (2020) 1–24. https://doi.org/10.3390/COATINGS10080745.

[8] Y. Li, Y. Yang, Y. Qing, R. Li, X. Tang, D. Guo, Y. Qin, Enhancing zno-np antibacterial and osteogenesis properties in orthopedic applications: A review, Int J Nanomedicine 15 (2020) 6247–6262. https://doi.org/10.2147/IJN.S262876.

[9] J. Baszkiewicz, D. Krupa, J.A. Kozubowski, B. Rajchel, M. Lewandowska-Szumieł, A. Barcz, J.W. Sobczak, A. Kosiński, A. Chróścicka, The effect of sodium-ion implantation on the properties of titanium, J Mater Sci Mater Med 19 (2008) 3081–3091. https://doi.org/10.1007/s10856-008-3431-4.

[10] Z. Xing, J. Cai, Y. Sun, M. Cao, Y. Li, Y. Xue, A. Finne-Wistrand, M. Kamal, Altered surface hydrophilicity on copolymer scaffolds stimulate the osteogenic differentiation of human mesenchymal stem cells, Polymers (Basel) 12 (2020) 1–15. https://doi.org/10.3390/polym12071453.

[11] C. Ma, X. Gao, Y. Yang, X. Bian, B. Wang, X. Liu, Y. Wang, D. Su, G. Zhang, L. Qu, N. Zhang, The three-dimensional culture of L929 and C2C12 cells based on SPI-SA interpenetrating network hydrogel scaffold with excellent mechanical properties, Front Bioeng Biotechnol 11 (2023). https://doi.org/10.3389/fbioe.2023.1329183.

6. OŚWIADCZENIA

6.1. [JS1] Influence of Laser Modification on the Surface Character of Biomaterial: Titanium and its alloys – A review

OŚWIADCZENIE WSPÓŁAUTORÓW PUBLIKACJI

CO-AUTHORSHIP STATEMENT

Ja niżej podpisany oświadczam, że poniżej przedstawiony podział procentowy przedstawia rzeczywisty wkład autorów w publikację:

J.Sypniewska, M.Szkodo: *Influence of Laser Modification on the Surface Character of Biomaterials: Titanium and Its Alloys - A Review. Coatings*, 2022, 12, 1371. doi.org/10.3390/coatings12101371 (MNiSW 100 pkt.)

Imię i nazwisko autora /Author name and surname	Procentowy wkład autora/ Percented distribution of co-author [%]	Data i podpis autora/ Date and co-author signature
Joanna Sypniewska	80	Joanna Sypniewska 17/06/2025
Marek Szkodo	20	MSzkodo

POLITECHNIKA GDAŃSKA | WYDZIAŁ INŻYNIERII MECHANICZNEJ I OKRĘTOWNICTWA

Gdańsk, 12.06.... 2025

prof. Dr inż. hab. Marek Szkodo
Instytut Technologii Maszyn i Materiałow
Wydział Inżynierii Mechanicznej i Okrętownictwa
Politechnika Gdańska

OŚWIADCZENIE

Oswiadczam, iż mój wkład 20% w publikację:

J.Sypniewska, M.Szkodo; *Influence of Laser Modification on the Surface Character of Biomaterials: Titanium and Its Alloys - A Review*, Coatings, 2022, 12, 1371. https:// doi.org/10.3390/coatings12101371 (MNiSW 100 pkt.)

Obejmował nadzorowanie prac oraz edytowanie draftu manuskryptu.

M.Szkodo
....

Podpis

6.2. [JS2] Effect of hybrid modification by ceramic layer formation in MAO process and laser remelting on the structure of titanium bio-alloy Ti13Nb13Zr

Oświadczenie współautorów publikacji

Niniejszym podaję procentowy wkład autorski w publikację:

Sypniewska, J., Szkodo, M., Majkowska-Marzec, B., & Mielewczyk-Gryń, A. (2023). Effect of hybrid modification by ceramic layer formation in MAO process and laser remelting on the structure of titanium bio-alloy Ti13Nb13Zr. CERAMICS INTERNATIONAL (2022). 49. 16603-16614

Imię i nazwisko współautora	Procentowy wkład autorski	Data i podpis współautora
Joanna Sypniewska	80%	26/06/2023 Joanna Sypniewska
Beata Majkowska-Marzec	10%	Majkowska-Marzec 27.06.2023r.
Marek Szkodo	5%	M. Szkodo
Aleksandra Mielewczyk-Gryń	5%	[illegible]

POLITECHNIKA GDAŃSKA | WYDZIAŁ INŻYNIERII MECHANICZNEJ I OKRĘTOWNICTWA

Gdańsk, 10.06.2025

dr inż. Beata Majkowska-Marzec
Instytut Technologii Maszyn i Materiałow
Wydział Inżynierii Mechanicznej i Okrętownictwa
Politechnika Gdańska

OŚWIADCZENIE

Oswiadczam, iż mój wkład 10% w publikację:

J.Sypniewska, M.Szkodo, B. Majkowska-Marzec, A. Mielewczyk-gryń; *Effect of hybrid modification by ceramic layer formation in MAO process and laser remelting on the structure of titanium bio-alloy Ti13Nb13Zr*; Ceramics international, 2023 https://doi.org/10.1016/j.ceramint.2023.02.018; (MNiSW 100 pkt.)

Obejmował przeprowadzenie modyfikacji laserowej stopu tytanu i nadzór prac nad manuskryptem.

Majkowska-Marzec Beata
Podpis

POLITECHNIKA GDAŃSKA | WYDZIAŁ INŻYNIERII MECHANICZNEJ I OKRĘTOWNICTWA

Gdańsk, 17/06 2025

prof. dr inż. hab. Marek Szkodo
Instytut Technologii Maszyn i Materiałow
Wydział Inżynierii Mechanicznej i Okrętownictwa
Politechnika Gdańska

OŚWIADCZENIE

Oswiadczam, iż mój wkład 5% w publikację:

J.Sypniewska, M.Szkodo, B. Majkowska-Marzec, A. Mielewczyk-gryń; *Effect of hybrid modification by ceramic layer formation in MAO process and laser remelting on the structure of titanium bio-alloy Ti13Nb13Zr*; Ceramics international, 2023 https://doi.org/10.1016/j.ceramint.2023.02.018; (MNiSW 100 pkt.)

Obejmował nadzorowanie prac, przeprowadzenie analizy statystycznej ANOVA oraz edytowanie draftu manuskryptu.

M. Szkodo
....

Podpis

POLITECHNIKA GDAŃSKA | WYDZIAŁ FIZYKI TECHNICZNEJ I MATEMATYKI STOSOWANEJ

Gdańsk, 17/06 2025

dr inż. hab. Aleksandra Mielewczyk-Gryń, prof. PG
Instytut Nanotechnologii i Inżynierii Materiałowej
Wydział Fizyki Technicznej i Matermatyki Stosowanej
Politechnika Gdańska

OŚWIADCZENIE

Oswiadczam, iż mój wkład 5% w publikację:

J.Sypniewska, M.Szkodo, B. Majkowska-Marzec, A. Mielewczyk-gryń; *Effect of hybrid modification by ceramic layer formation in MAO process and laser remelting on the structure of titanium bio-alloy Ti13Nb13Zr*; Ceramics international, 2023 https://doi.org/10.1016/j.ceramint.2023.02.018; (MNiSW 100 pkt.)

Obejmował przeprowadzenie badań dyfrakcji rengenowskiej (XRD – X-ray diffraction) i analizę wyników.

....
Podpis

6.3. [JS3]Exploring the composition and corrosion resistance in hybrid-modified Ti13Nb13Zr alloy

OŚWIADCZENIE WSPÓŁAUTORÓW PUBLIKACJI

CO-AUTHORSHIP STATEMENT

Ja niżej podpisany oświadczam, że poniżej przedstawiony podział procentowy przedstawia rzeczywisty wkład autorów w publikację:

J. Sypniewska, M. Szkodo, B. Majkowska-Marzec, A. Mielewczyk-Gryń, Exploring the composition and corrosion resistance in hybrid-modified Ti13Nb13Zr alloy. MRS Communications (2024). https://doi.org/10.1557/s43579-024-00663-z; (MNiSW 100 pkt.)

Imię i nazwisko autora /Author name and surname	Procentowy wkład autora/ Percented distribution of co-author [%]	Data i podpis autora/ Date and co-author signature
Joanna Sypniewska	80	J. Sypniewska
Marek Szkodo	5	M. Szkodo
Beata Majkowska – Marzec	10	Majkowska-Marzec B.
Aleksandra Mielewczyk-Gryń	5	Mielewczyk

POLITECHNIKA GDAŃSKA | WYDZIAŁ INŻYNIERII MECHANICZNEJ I OKRĘTOWNICTWA

Gdańsk, 17.04... 2025

prof. dr inż. hab. Marek Szkodo
Instytut Technologii Maszyn i Materiałow
Wydział Inżynierii Mechanicznej i Okrętownictwa
Politechnika Gdańska

OŚWIADCZENIE

Oswiadczam, iż mój wkład 5%w publikację:

J. Sypniewska, M. Szkodo, B. Majkowska-Marzec, A. Mielewczyk-Gryń, Exploring the composition and corrosion resistance in hybrid-modified Ti13Nb13Zr alloy. MRS Communications (2024). https://doi.org/10.1557/s43579-024-00663-z; (MNiSW 100 pkt.)

Obejmował nadzorowanie prac oraz edytowanie draftu manuskryptu.

......M. Szkodo......

Podpis

POLITECHNIKA GDAŃSKA | WYDZIAŁ INŻYNIERII MECHANICZNEJ I OKRĘTOWNICTWA

Gdańsk, 10.06.2025

dr inż. Beata Majkowska-Marzec
Instytut Technologii Maszyn i Materiałów
Wydział Inżynierii Mechanicznej i Okrętownictwa
Politechnika Gdańska

OŚWIADCZENIE

Oswiadczam, iż mój wkład 10% w publikację:

J. Sypniewska, M. Szkodo, B. Majkowska-Marzec, A. Mielewczyk-Gryń, *Exploring the composition and corrosion resistance in hybrid-modified Ti13Nb13Zr alloy*. MRS Communications (2024). https://doi.org/10.1557/s43579-024-00663-z; (MNiSW 100 pkt.)

Obejmował przeprowadzenie modyfikacji laserowej stopu tytanu i nadzór prac nad manuskryptem.

Majkowska-Marzec Beata

Podpis

POLITECHNIKA GDAŃSKA | WYDZIAŁ FIZYKI TECHNICZNEJ I MATEMATYKI STOSOWANEJ

Gdańsk, 09.06. 2025

dr inż. hab. Aleksandra Mielewczyk-Gryń, prof. PG
Instytut Nanotechnologii i Inżynierii Materiałowej
Wydział Fizyki Technicznej i Matermatyki Stosowanej
Politechnika Gdańska

OŚWIADCZENIE

Oswiadczam, iż mój wkład 5%w publikację:

J. Sypniewska, M. Szkodo, B. Majkowska-Marzec, A. Mielewczyk-Gryń, *Exploring the composition and corrosion resistance in hybrid-modified Ti13Nb13Zr alloy.* MRS Communications (2024). https://doi.org/10.1557/s43579-024-00663-z; (MNiSW 100 pkt.)

Obejmował przeprowadzenie badań spektroskopii w podczerwieni z transformacją Fouriera (FTIR - Fourier Transform Infrared spectroscopy) i analizę wyników badań.

Podpis

6.4. [JS4] Hybrid laser-micro-arc oxidation techniques for enhanced biocompatibility and surface modification of Ti13Nb13Zr alloy in biomedical applications

OŚWIADCZENIE WSPÓŁAUTORÓW PUBLIKACJI

CO-AUTHORSHIP STATEMENT

Ja niżej podpisany oświadczam, że poniżej przedstawiony podział procentowy przedstawia rzeczywisty wkład autorów w publikację:

I, the undersigned, hereby declare that the percentage distribution presented below accurately reflects the actual contribution of each author to the following publication:

Sypniewska, J., Szkodo, M., Majkowska-Marzec, B. Pawłowski Ł., Mirokwska A., Ryl J., Mielwwczyk-Gryń A., Gawl Ł. Campos E.M., Fernández Hernán J.P., Hybrid laser-micro-arc oxidation techniques for enhanced biocompatibility and surface modification of Ti13Nb13Zr alloy in biomedical applications. Applied Surface Science 698, 163136 (2024) https://doi.org/10.1016/j.apsusc.2025.163136

Imię i naziwsko współautora /Name and surname co-author	Procetowt wkład autora / Percented distribution of co-authors [%]	Data i podpis autora /Date and co-author signature
Joanna Sypniewska	65	
Marek Szkodo	5	
Beata Majkowska – Marzec	5	
Łukasz Pawłowski	3	
Aleksandra Mirowska	3	
Jacek Ryl	3	
Aleksandra Mielewczyk-Gryń	3	
Łukasz Gaweł	3	
Enrique Martínez Campos	5	
Juan Pablo Fernández Hernán	5	

POLITECHNIKA GDAŃSKA | WYDZIAŁ INŻYNIERII MECHANICZNEJ I OKRĘTOWNICTWA

Gdańsk, 17/06..... 2025

prof. dr inż. hab. Marek Szkodo
Instytut Technologii Maszyn i Materiałow
Wydział Inżynierii Mechanicznej i Okrętownictwa
Politechnika Gdańska

OŚWIADCZENIE

Oswiadczam, iż mój wkład 5% w publikację:

Sypniewska, J., Szkodo, M., Majkowska-Marzec, B. Pawłowski Ł., Mirowska A., Ryl J., Mielwwczyk-Gryń A., Gawł Ł. Campos E.M., Fernández Hernán J.P., *Hybrid laser-micro-arc oxidation techniques for enhanced biocompatibility and surface modification of Ti13Nb13Zr alloy in biomedical applications.* Applied Surface Science 698, 163136 (2024) https://doi.org/10.1016/j.apsusc.2025.163136; (MNiSW 140 pkt.)

Obejmował nadzorowanie prac oraz edytowanie draftu manuskryptu.

M. Szkodo
....

Podpis

POLITECHNIKA GDAŃSKA | WYDZIAŁ INŻYNIERII MECHANICZNEJ I OKRĘTOWNICTWA

Gdańsk, 28.06. 2025

dr inż. Łukasz Pawłowski
Instytut Technologii Maszyn i Materiałów
Wydział Inżynierii Mechanicznej i Okrętownictwa
Politechnika Gdańska

OŚWIADCZENIE

Oswiadczam, iż mój wkład 3% w publikację:

Sypniewska, J., Szkodo, M., Majkowska-Marzec, B. Pawłowski Ł., Mirowska A., Ryl J., Mielwwczyk-Gryń A., Gawl Ł. Campos E.M., Fernández Hernán J.P., *Hybrid laser-micro-arc oxidation techniques for enhanced biocompatibility and surface modification of Ti13Nb13Zr alloy in biomedical applications.* Applied Surface Science 698, 163136 (2024) https://doi.org/10.1016/j.apsusc.2025.163136; (MNiSW 140 pkt.)

Obejmował przeprowadzenie badań skaningowym mikroskopem elektronowym (SEM – Scanning Electrone Microscope) oraz analizy składu pierwiastkowego (EDS – Energy Dispersive X-ray Spectroscopy).

Łukasz Pawłowski
....
Podpis

POLITECHNIKA GDAŃSKA | WYDZIAŁ INŻYNIERII MECHANICZNEJ I OKRĘTOWNICTWA

Gdańsk, ..12.06.. 2025

dr inż. Beata Majkowska-Marzec
Instytut Technologii Maszyn i Materiałow
Wydział Inżynierii Mechanicznej i Okrętownictwa
Politechnika Gdańska

OŚWIADCZENIE

Oswiadczam, iż mój wkład 5% w publikację:

Sypniewska, J., Szkodo, M., Majkowska-Marzec, B. Pawłowski Ł., Mirowska A., Ryl J., Mielwwczyk-Gryń A., Gawł Ł. Campos E.M., Fernández Hernán J.P., *Hybrid laser-micro-arc oxidation techniques for enhanced biocompatibility and surface modification of Ti13Nb13Zr alloy in biomedical applications.* Applied Surface Science 698, 163136 (2024) https://doi.org/10.1016/j.apsusc.2025.163136; (MNiSW 140 pkt.)

Obejmował przeprowadzenie modyfikacji laserowej stopu tytanu i nadzór prac nad manuskryptem.

Majkowska-Marzec Beata
Podpis

POLITECHNIKA GDAŃSKA | WYDZIAŁ INŻYNIERII MECHANICZNEJ I OKRĘTOWNICTWA

Gdańsk, 13.06.2025

dr inż. Aleksandra Mirowska
Instytut Technologii Maszyn i Materiałow
Wydział Inżynierii Mechanicznej i Okrętownictwa
Politechnika Gdańska

OŚWIADCZENIE

Oswiadczam, iż mój wkład 3% w publikację:

Sypniewska, J., Szkodo, M., Majkowska-Marzec, B. Pawłowski Ł., Mirowska A., Ryl J., Mielwwczyk-Gryń A., Gawł Ł. Campos E.M., Fernández Hernán J.P., *Hybrid laser-micro-arc oxidation techniques for enhanced biocompatibility and surface modification of Ti13Nb13Zr alloy in biomedical applications.* Applied Surface Science 698, 163136 (2024) https://doi.org/10.1016/j.apsusc.2025.163136; (MNiSW 140 pkt.)

Obejmował przeprowadzenie badań chropowatości i topografii powierzchni oraz analizę tych wyników.

Aleksandra Mirowska
Podpis

POLITECHNIKA GDAŃSKA | WYDZIAŁ FIZYKI TECHNICZNEJ I MATEMATYKI STOSOWANEJ

Gdańsk, 10.06...... 2025

prof. dr hab. inż. Jacek Ryl
Instytut Nanotechnologii i Inżynierii Materiałowej
Wydział Fizyki Technicznej i Matermatyki Stosowanej
Politechnika Gdańska

OŚWIADCZENIE

Oswiadczam, iż mój wkład 3% w publikację:

Sypniewska, J., Szkodo, M., Majkowska-Marzec, B. Pawłowski Ł., Mirowska A., Ryl J., Mielwwczyk-Gryń A., Gawł Ł. Campos E.M., Fernández Hernán J.P., *Hybrid laser-micro-arc oxidation techniques for enhanced biocompatibility and surface modification of Ti13Nb13Zr alloy in biomedical applications.* Applied Surface Science 698, 163136 (2024) https://doi.org/10.1016/j.apsusc.2025.163136; (MNiSW 140 pkt.)

Obejmował opiekę merytoryczna nad analizą wyników badań spektroskopii fotoelektronów w zakresie promieniowania X

....

Podpis

POLITECHNIKA GDAŃSKA | WYDZIAŁ FIZYKI TECHNICZNEJ I MATEMATYKI STOSOWANEJ

Gdańsk, 10.07..... 2025

dr inż. hab. Aleksandra Mielewczyk-Gryń, prof. PG
Instytut Nanotechnologii i Inżynierii Materiałowej
Wydział Fizyki Technicznej i Matermatyki Stosowanej
Politechnika Gdańska

OŚWIADCZENIE

Oswiadczam, iż mój wkład 3% w publikację:

Sypniewska, J., Szkodo, M., Majkowska-Marzec, B. Pawłowski Ł., Mirowska A., Ryl J., Mielwwczyk-Gryń A., Gawł Ł. Campos E.M., Fernández Hernán J.P., *Hybrid laser-micro-arc oxidation techniques for enhanced biocompatibility and surface modification of Ti13Nb13Zr alloy in biomedical applications.* Applied Surface Science 698, 163136 (2024) https://doi.org/10.1016/j.apsusc.2025.163136; (MNiSW 140 pkt.)

Obejmował przeprowadzenie badań dyfrakcji rengenowskiej (XRD – X-ray diffraction) i przeprowadzenie badań spektroskopii w podczerwieni z transformacją Fouriera (FTIR - Fourier Transform Infrared spectroscopy).

AMielewczyk-Gryń..........

Podpis

Gdańsk, 10.06.2025

dr inż. Łukasz Gaweł
Katedra Korozji i Elektrochemii
Wydział Chemiczny
Politechnika Gdańska

OŚWIADCZENIE

Oswiadczam, iż mój wkład 3% w publikację:

Sypniewska, J., Szkodo, M., Majkowska-Marzec, B. Pawłowski Ł., Mirowska A., Ryl J., Mielwwczyk-Gryń A., Gawł Ł. Campos E.M., Fernández Hernán J.P., *Hybrid laser-micro-arc oxidation techniques for enhanced biocompatibility and surface modification of Ti13Nb13Zr alloy in biomedical applications.* Applied Surface Science 698, 163136 (2024) https://doi.org/10.1016/j.apsusc.2025.163136; (MNiSW 140 pkt.)

Obejmował przeprowadzenie i analizę badań spektroskopii fotoelektronów w zakresie promieniowania X a także opis części dyskusji badań.

Łukasz Gaweł
Podpis

CSIC
CONSEJO SUPERIOR DE INVESTIGACIONES CIENTÍFICAS

04.06.2025; Madrid, Spain

UNIVERSIDAD
COMPLUTENSE
MADRID

PhD
Enrique Martínez Campos
Group of Organic Synthesis and Bioevaluation,
Instituto Pluridisciplinar,
Universidad Complutense de Madrid (UCM),
Associated Unit to the ICTP-IQM-CSIC
e-mail: emartinezcampos79@gmail.com

STATEMENT

I declare that my 5% contribution to the publication:

Sypniewska, J., Szkodo, M., Majkowska-Marzec, B. Pawłowski Ł., Mirokwska A., Ryl J., Mielwwczyk-Gryń A., Gawl Ł. Campos E.M., Fernández Hernán J.P., Hybrid laser-micro-arc oxidation techniques for enhanced biocompatibility and surface modification of Ti13Nb13Zr alloy in biomedical applications. Applied Surface Science 698, 163136 (2024) https://doi.org/10.1016/j.apsusc.2025.163136

Consisted of training Joanna Sypniewska in the field of biological testing and conducting the analysis of the obtained results.

....
Co-author's signature

Universidad
Rey Juan Carlos

04.06.2025, Mostoles/Madrid, Spain

Assistant Professor, Phd Eng
Juan Pablo Fernández Hernán
Department of Applied Mathematics,
Materials Science and Engineering,
and Electronic Technology
Rey Juan Carlos University
e-mail: juanpablo.fernandez@urjc.es

STATEMENT

I declare that my 5% contribution to the publication:

Sypniewska, J., Szkodo, M., Majkowska-Marzec, B. Pawłowski Ł., Mirokwska A., Ryl J., Mielwwczyk-Gryń A., Gawl Ł. Campos E.M., Fernández Hernán J.P., Hybrid laser-micro-arc oxidation techniques for enhanced biocompatibility and surface modification of Ti13Nb13Zr alloy in biomedical applications. Applied Surface Science 698, 163136 (2024) https://doi.org/10.1016/j.apsusc.2025.163136

Consisted of training Joanna Sypniewska in the field of electrochemical testing and conducting the analysis of the obtained results.

....
Co-author's signature

6.5. [JS5] Influence of hybrid modification on functional properties on commercial bio-titanium alloy Ti6Al4V

OŚWIADCZENIE WSPÓŁAUTORÓW PUBLIKACJI

CO-AUTHORSHIP STATEMENT

Ja niżej podpisany oświadczam, że poniżej przedstawiony podział procentowy przedstawia rzeczywisty wkład autorów w publikację:

I, the undersigned, hereby declare that the percentage distribution presented below accurately reflects the actual contribution of each author to the following publication:

Sypniewska, J., Szkodo, M., Majkowska-Marzec, B. Fernández Hernán J.P, Campos E.M, .Pawłowski Ł Influence of hybrid modification on functional properties on commercial bio-titanium alloy Ti6Al4V.
Paper in submmision process

Imię i naziwsko autora /Author name and surname	Procetowt wkład autora/ Percented distribution of co-author [%]	Data i podpis autora/ Date and co-author signature
Joanna Sypniewska	70	
Marek Szkodo	5	
Beata Majkowska – Marzec	5	
Juan Pablo Fernández Hernán	5	
Enrique Martínez Campos	5	
Łukasz Pawłowski	5	

POLITECHNIKA GDAŃSKA | WYDZIAŁ INŻYNIERII MECHANICZNEJ I OKRĘTOWNICTWA

Gdańsk, 17/06.... 2025

prof. dr inż. hab. Marek Szkodo
Instytut Technologii Maszyn i Materiałow
Wydział Inżynierii Mechanicznej i Okrętownictwa
Politechnika Gdańska

OŚWIADCZENIE

Oswiadczam, iż mój wkład 5% w publikację:

Sypniewska, J., Szkodo, M., Majkowska-Marzec, B. Fernández Hernán J.P, Campos E.M, .Pawłowski Ł Influence of hybrid modification on functional properties on commercial bio-titanium alloy Ti6Al4V.*

Obejmował nadzorowanie prac oraz edytowanie draftu manuskryptu.

*Artykuł w procesie recenzji.

M. Szkodo
....

Podpis

POLITECHNIKA GDAŃSKA | WYDZIAŁ INŻYNIERII MECHANICZNEJ I OKRĘTOWNICTWA

Gdańsk, 09.06.2025

dr inż. Łukasz Pawłowski
Instytut Technologii Maszyn i Materiałow
Wydział Inżynierii Mechanicznej i Okrętownictwa
Politechnika Gdańska

OŚWIADCZENIE

Oswiadczam, iż mój wkład 5% w publikację:

Sypniewska, J., Szkodo, M., Majkowska-Marzec, B. Fernández Hernán J.P, Campos E.M, .Pawłowski Ł. Influence of hybrid modification on functional properties on commercial bio-titanium alloy Ti6Al4V.*

Obejmował przeprowadzenie badań skaningowym mikroskopem elektronowym (SEM – Scanning Electrone Microscope) oraz analizy składu pierwiastkowego (EDS – Energy Dispersive X-ray Spectroscopy).

*Artykuł w procesie recenzji.

Łukasz Pawłowski

Podpis

04.06.2025; Madrid, Spain

PhD
Enrique Martínez Campos
Group of Organic Synthesis and Bioevaluation,
Instituto Pluridisciplinar,
Universidad Complutense de Madrid (UCM),
Associated Unit to the ICTP-IQM-CSIC
e-mail: emartinezcampos79@gmail.com

STATEMENT

I declare that my 5% contribution to the publication:

Sypniewska, J., Szkodo, M., Majkowska-Marzec, B. Fernández Hernán J.P, Campos E.M, .Pawłowski Ł Influence of hybrid modification on functional properties on commercial bio-titanium alloy Ti6Al4V.
Paper in the submission process

Consisted of training Joanna Sypniewska in the field of biological testing and conducting the analysis of the obtained results.

....

Co-author's signature

POLITECHNIKA GDAŃSKA | WYDZIAŁ INŻYNIERII MECHANICZNEJ I OKRĘTOWNICTWA

Gdańsk, 12/06..... 2025

dr inż. Beata Majkowska-Marzec
Instytut Technologii Maszyn i Materiałow
Wydział Inżynierii Mechanicznej i Okrętownictwa
Politechnika Gdańska

OŚWIADCZENIE

Oswiadczam, iż mój wkład 5% w publikację:

Sypniewska, J., Szkodo, M., Majkowska-Marzec, B. Fernández Hernán J.P, Campos E.M, ,Pawłowski Ł. Influence of hybrid modification on functional properties on commercial bio-titanium alloy Ti6Al4V.*

Obejmował przeprowadzenie modyfikacji laserowej stopu tytanu i nadzór prac nad manuskryptem.

*Artykuł w procesie recenzji.

Majkowska-Marzec Beata
....
Podpis

Universidad
Rey Juan Carlos

04.06.2025, Mostoles/Madrid, Spain

Assistant Professor, Phd Eng
Juan Pablo Fernández Hernán
Department of Applied Mathematics,
Materials Science and Engineering,
and Electronic Technology
Rey Juan Carlos University
e-mail: juanpablo.fernandez@urjc.es

STATEMENT

I declare that my 5% contribution to the publication:

Sypniewska, J., Szkodo, M., Majkowska-Marzec, B. Fernández Hernán J.P, Campos E.M, .Pawłowski L Influence of hybrid modification on functional properties on commercial bio-titanium alloy Ti6Al4V.
Paper in the submission process

Consisted of training Joanna Sypniewska in the field of electrochemical testing and conducting the analysis of the obtained elctrochemical and biological results.

....

Co-author's signature